

The copyright of this thesis rests with the University of Cape Town. No quotation from it or information derived from it is to be published without full acknowledgement of the source. The thesis is to be used for private study or non-commercial research purposes only.

A Pharmacological Investigation of South African
Lichens, Desiccation-tolerant Plants and the
Medicinal Tree, *Warburgia salutaris*

Tracy Kellermann

Thesis Presented for the Degree of

DOCTOR OF PHILOSOPHY

In the Division of Pharmacology
UNIVERSITY OF CAPE TOWN

February 2010

Supervisor: Prof. P.J. Smith

Co-supervisor: Dr W. Campbell

Declaration

A Pharmacological Investigation of South African Lichens, Desiccation-tolerant Plants and the Medicinal Tree, *Warburgia salutaris*

I, Tracy Ann Kellermann, hereby grant the University of Cape Town free licence to reproduce the above thesis in whole or in part, for the purpose of research. I declare that this thesis represents my own unaided work, both in concept and execution, and that apart from the normal guidance from my supervisor, I have received no assistance (except where acknowledgements indicate otherwise) and that neither the substance nor any part of the above thesis has been submitted in the past, or is being, or is to be submitted for a degree at this University or at any other university.

This thesis is presented for examination for the degree of PhD.

SIGNED: _____

DATE: _____

Acknowledgements

I would like to acknowledge the following individuals in the Division of Pharmacology, University of Cape Town:

- my supervisor, Prof Peter Smith, who has shown a huge amount of support and encouragement during the course of this degree, always ready with a calm word of advice.
- my co-supervisor, Dr Bill Campbell, for his support and assistance in deciphering the chemistry side of things.
- Dr Lubbe Wiesner, for introducing me to mass spectrometry and bioavailability studies, and for reviewing those parts of the thesis.
- Dr Carmen Lategan and Mrs Sumaya Salie for assistance with malaria and cytotoxicity assays.
- Ms Alicia Evans for assisting with the intricacies of mass spectrometry, and for allowing me access to her precious API4000.
- Mrs Jennifer Norman for performing the WinNonlin analysis.
- Mr Noor Salie for assistance with the *in vivo* work.
- Mr Trevor Finch for performing the intravenous dosing.
- Mrs Afia Fredericks and Mrs Jean van Dyk for answering countless queries about mass spectrometry.

The following organisations provided financial support during the course of this degree, for which I am extremely grateful:

- The National Research Foundation
- The Carl and Emily Fuchs Foundation
- The Ernst and Ethel Eriksen Trust
- The Lowenstein Trust
- The University of Cape Town

I am indebted to the following people for assistance with plant collections, identification and voucher specimens:

- Dr Ziets Zietsman for collections of desiccation-tolerant plants
- Dr Tassilo Feuerer for genetic identification of the lichens
- Dr Einar Timdal for visual identification of lichens
- Mr Ricket Swanepoel for allowing me to search for lichens in Paarl Nature Reserve
- Mr Ken Seaman (Dad) and Mrs Willene Kellermann (Skoonma) for assisting with lichen collections
- Dr Koos Roux of the Compton Herbarium at Kirstenbosch Botanical Gardens for assistance with identification of *Cheilanthes* species
- Mr Terry Trinder-Smith of the Bolus Herbarium at the University of Cape Town

On a personal note, I would like to express gratitude to my parents, Ken and Marieta Seaman for their encouragement and support, without which I would never even have attempted my first degree. I am also extremely grateful to my husband, Cobus, for being a pillar of strength, our baby daughter Jessica for being the light of my life, as well as our family and friends for all their support.

Abstract

There is an urgent need for new antimicrobial agents as a result of the rapid rate of resistance emergence to available therapies, as well as to combat new and emerging diseases. Natural products still provide a largely untapped resource of chemical entities with the potential for development into useful pharmaceuticals. On this basis, an investigation into the antimicrobial activities of South African lichens, desiccation-tolerant plants and the medicinal tree, *Warburgia salutaris*, was undertaken with the aim of investigating *in vitro* bioactivity. Furthermore, this project aimed to evaluate *in vivo* pharmacokinetic profiles of the most bioactive constituents, as well as to investigate a method for determining lead-like properties earlier on in the drug development process.

The crude acetone extract of the lichen, *Teloschistes chrysophthalmum*, exhibited the most potent activity against any organism, namely *S. aureus* (IC₅₀ of 1.1µg/ml). The lichen metabolite, usnic acid, was identified in several extracts and was shown to have moderate antimalarial activity (IC₅₀ of 15.1µg/ml). Two anti-Staphylococcal compounds, L17-1 and L17-3, were isolated from *T. chrysophthalmum* with IC₅₀'s of 1.1 and 0.7µg/ml respectively against drug-sensitive *S. aureus* and 11.1 and 11.4µg/ml against MRSA. These compounds displayed very little cytotoxicity against the CHO cell line, with IC₅₀'s of 81.0 and greater than 100µg/ml for L17-1 and L17-3 respectively and resultant favourable selectivity indices of 73.6 and greater than 142.9 respectively.

Only two of the thirty extracts of the desiccation-tolerant plants inhibited organism growth at 125µg/ml or less. The methanol extract of *M. flabellifolius* exhibited variable activity against *C. albicans*, initially as potent (<7.8µg/ml), but with a subsequent loss of activity. Exhaustive fractionation failed to yield an active component. Sequential extracts prepared from various parts of commercially cultivated *W. salutaris* showed that the DCM extracts of the bark, stem and twigs

exhibited potent antifungal and moderate antimycobacterial activity. The most active extract, the DCM extract of the bark with an IC_{50} of 4.2 μ g/ml against *C. albicans*, was further fractionated, leading to the isolation of 19 pure or semi-pure compounds, three of which were identified as muzigadial, warburganal and ugandensidial. These compounds and fractions displayed potent cytotoxicity, despite promising activity against *C. albicans*, making them unsuitable for further pharmacological investigation.

The most promising hit compounds from *in vitro* testing were L17-1 and L17-3 from the lichen, *T. chrysophthalmum*. These two compounds were administered to mice together at 10mg/kg each, orally and subcutaneously, to determine which compound presented the best *in vivo* pharmacokinetic profile. A method was developed for the detection of both compounds in a single assay from 10 μ l of mouse whole blood using sensitive LC-MS/MS technology, with the lowest level of detection being 24ng/ml. The results of the initial *in vivo* testing revealed that L17-3 achieved greater levels *in vivo*, with a good C_{max} concentration of 14.5 μ g/ml after oral administration. Subsequent administration of L17-3 alone at 5mg/kg orally, subcutaneously and intravenously revealed that this compound has 40.7 and 41.7% oral and subcutaneous bioavailability respectively. Oral administration of L17-3 resulted in a C_{max} of 2.78 μ g/ml at a T_{max} of 3.4 hours, with a resultant half-life of 2.98 hours. No signs of *in vivo* toxicity were observed after oral or subcutaneous administration at either 5mg/kg or 10mg/kg. L17-3 is an orally bioavailable compound, capable of reaching *in vitro* MIC levels (15.6 μ g/ml) *in vivo*, without toxicity, with the distinct potential to clear a systemic *S. aureus* infection *in vivo*. This project has emphasised the pharmacological potential of the largely unstudied lichen-derived compounds. Furthermore, a method has been suggested for the selection of bioavailable natural product-derived compounds earlier on in the drug development process.

Table of Contents

Declaration	ii
Acknowledgements	iii
Abstract	v
Table of Contents	vii
List of Figures	x
List of Tables	xv
List of Abbreviations	xvii
Chapter 1	1
Introduction.....	1
1.1 Infectious diseases and the need for new drugs	1
1.1.1 <i>Mycobacterium tuberculosis</i>	5
1.1.2 <i>Klebsiella pneumoniae</i>	9
1.1.3 <i>Staphylococcus aureus</i>	12
1.1.4 <i>Candida albicans</i>	13
1.2 Natural products and drug discovery.....	16
1.3 Traditional medicine in drug discovery.....	21
1.4 Lichens as a source of antimicrobials	22
1.5 Desiccation-tolerant plants as a source of antimicrobials	26
1.6 The medicinal plant <i>Warburgia salutaris</i>	29
1.7 Aims and objectives	33
Chapter 2	35
Lichens	35
2.1 Introduction.....	35
2.2 Results.....	35
2.2.1 Bioactivity testing of crude acetone extracts.....	38
2.2.2 Bioactivity testing and profiling of usnic acid	40
2.2.3 Antimicrobial activity of extracts of <i>Xanthopharmelia semiviridis</i> (Eastern Cape)	42
2.2.4 Isolation of compounds from <i>Teloschistes chrysophthalmum</i>	44
2.2.4.1 Bioactivity testing of fractions and compounds from <i>Teloschistes</i> <i>chrysophthalmum</i>	44
2.2.4.2 Comparison of the constituents of the PE and ACN fractions of <i>Teloschistes chrysophthalmum</i> to those of the acetone extract of the growth substrate	49
2.2.4.3 Identification of active compounds from <i>Teloschistes</i> <i>chrysophthalmum</i>	51
2.3 Discussion.....	59
Chapter 3	65
Dessiccation-tolerant plants	65
3.1 Introduction.....	65
3.2 Results: Dessiccation-tolerant plants	65
3.2.1 Antimicrobial activities of crude extracts	65
3.2.2 <i>Myrothamnus flabellifolius</i> fractions	68

3.3 Discussion.....	74
Chapter 4	77
<i>Warburgia salutaris</i>	77
4.1 Introduction.....	77
4.2 Results: <i>Warburgia salutaris</i>	77
4.2.1 Bioactivity of crude extracts	77
4.2.2 Antimicrobial activity of the bark dichlormethane fractions	81
4.2.3 Identification of compounds isolated from <i>W. salutaris</i>	86
4.3 Discussion.....	90
Chapter 5	95
<i>In vivo</i> bioavailability of lichen-derived compounds	95
5.1 Introduction.....	95
5.2 Results.....	96
5.2.1 Assay development.....	96
5.2.2 Initial bioavailability study of L17-1 and L17-3.....	100
5.2.3 Bioavailability study of L17-3 in mice	104
5.2.3.1 Oral	104
5.2.3.2 Subcutaneous	106
5.2.3.3 Intravenous	108
5.3 Discussion.....	112
Chapter 6	123
Conclusion.....	123
Chapter 7	130
Materials and methods	130
7.1 Chemicals and reagents.....	130
7.2 Broth micro-dilution assay.....	130
7.2.1 Antimycobacterial assay	131
7.2.2 Antibacterial assay	133
7.2.3 Antifungal assay	133
7.3 Bio-autography.....	134
7.4 Antimalarial assay	135
7.5 Cytotoxicity assay.....	136
7.6 High performance liquid chromatography.....	137
7.7 Lichen materials and methods	138
7.7.1 Collection of lichen material.....	138
7.7.2 Lichen identification	138
7.7.3 Extract preparation.....	139
7.7.4 HPLC profiles of lichen extracts and precipitates	139
7.7.5 Bioactivity testing	140
7.7.6 Isolation of compounds from <i>Teloschistes chrysophthalmum</i>	140
7.7.6.1 Fractionation of the acetone extract	140
7.7.6.2 HPLC collections	141
7.7.6.3 Nuclear Magnetic Resonance	141
7.7.6.4 Mass spectrometry.....	142
7.7.6.5 Compound identification.....	142
7.7.7 Fractionation of <i>Xanthoparmelia semiviridis</i> (Eastern Cape)	142

7.7.7.1	Preparation of extracts.....	142
7.7.7.2	HPLC evaluation of the active extracts	143
7.8	Materials and methods for desiccation-tolerant plants	143
7.8.1	Plant collection.....	143
7.8.2	Extract preparation.....	143
7.8.3	Bioactivity testing	144
7.8.3.1	Microtitre-plate assays	144
7.8.3.2	Bio-autography.....	145
7.8.4	Fractionation and isolation of compounds from <i>M. flabellifolius</i>	145
7.8.4.1	Dichloromethane extract.....	145
7.8.4.2	Ethyl acetate extract.....	146
7.8.4.3	Methanol extract	147
7.9	Materials and methods: <i>Warburgia salutaris</i>	149
7.9.1	Plant material	149
7.9.2	Extract preparation.....	149
7.9.3	HPLC profiling of crude extracts of <i>W. salutaris</i>	149
7.9.4	Fractionation of dichloromethane bark extract	150
7.9.5	Compound identification.....	151
Chapter 8	152
<i>In vivo</i> materials and methods	152
8.1	Ethics approval.....	152
8.2	Test animals	152
8.3	Assay development for detection of compounds in whole blood	152
8.3.1	Mass spectrometer optimisation	152
8.3.2	Chromatography development	154
8.3.3	Extraction.....	154
8.3.4	Preparation of calibration standards	156
8.4	Initial bioavailability study of lichen compounds administered together in mice	156
8.4.1	Oral dose	157
8.4.2	Subcutaneous dose	157
8.5	Bioavailability study of L17-3 in mice	157
8.5.1	Oral dose	157
8.5.2	Subcutaneous dose	158
8.5.3	Intravenous dose	158
8.5.4	Data analysis.....	158
References	159
Appendix.....	187
A.	Extract yields	187
B.	HPLC chromatograms	189
C.	NMR spectra.....	190
	Lichen NMR.....	190
	<i>Warburgia salutaris</i> NMR.....	202
D.	<i>In vivo</i> bioavailability	205
E.	Lichen genetic sequences.....	208

List of Figures

Figure 1: A schematic of antibiotic sites of action and potential bacterial resistance mechanisms to antimicrobial agents	3
Figure 2: A representation of the selection of resistant organisms by antibiotics ..	4
Figure 3: Countries that have reported XDR-TB cases	6
Figure 4: The geographic distribution of carbapenemase-producing bacteria	11
Figure 5: Furuncle near the knee caused by <i>S. aureus</i> infection.....	12
Figure 6: A timeline depicting the discovery of novel classes of antibiotics and introduction to the market place.....	17
Figure 7: The chemical structures of some lichen metabolites	25
Figure 8: Compounds isolated from <i>Warburgia</i> species.....	29
Figure 9: Electron microscopy pictures of (A) <i>Xanthoparmelia notata</i> , (B) <i>Xanthoparmelia semiviridis</i> , (C) unknown lichen from Eastern Cape (L14), (D) <i>Xanthoparmelia semiviridis</i> from Eastern Cape, (E) <i>Flavoparmelia soredicans</i> and (F) <i>Teloschistes chrysophthalmum</i>	36
Figure 10: Photographs of the investigated lichen species	37
Figure 11: An HPLC chromatogram of usnic acid (Sigma) at 243.5nm.	41
Figure 12: An HPLC chromatogram of the acetone extract of <i>Usnea rubroincta</i> at 248.1nm showing the prominent peak of usnic acid.....	41
Figure 13: An HPLC chromatogram of the petroleum ether extract of <i>Xanthoparmelia semiviridis</i> from the Eastern Cape at 233.1nm with the individual compound absorbance displayed in the insert.	43
Figure 14: An HPLC chromatogram of the dichloromethane precipitate of <i>Xanthoparmelia semiviridis</i> from the Eastern Cape at 254nm	43
Figure 15: A chromatogram of the ACN fraction of the acetone extract of <i>Teloschistes chrysophthalmum</i>	44
Figure 16: The dose response curves of (A) the acetone extract, (B) the ACN fraction, (C) the PE fraction, (D) L17-1 and (E) L17-3 from <i>Teloschistes chrysophthalmum</i> against drug sensitive <i>S. aureus</i> ATCC 12600. Figure F represents the effect of ciprofloxacin.	47
Figure 17: The dose response curves of (A) the ACN fraction, (B) the PE fraction, (C) L17-1 and (D) L17-3 from <i>Teloschistes chrysophthalmum</i> against methicillin-resistant <i>S. aureus</i> ATCC 43300. Figure E represents the effect of ciprofloxacin.	48
Figure 18: The dose-response curves depicting the effect of L17-1 (A) and L17-3 (B) from <i>Teloschistes chrysophthalmum</i> and the drug control, emetine (C) on CHO cells.....	49
Figure 19: An HPLC chromatogram of the acetone extract of the roof tiles at 242.3nm	50
Figure 20: An HPLC chromatogram of the acetonitrile fraction of the acetone extract of <i>Teloschistes chrysophthalmum</i> at 242.3nm.	50
Figure 21: An HPLC chromatogram of the petroleum ether fraction of the acetone extract of <i>Teloschistes chrysophthalmum</i> at 226nm.	51
Figure 22: The ¹ H NMR spectrum of L17-1 isolated from <i>Teloschistes chrysophthalmum</i>	52

Figure 23: The ^{13}C spectrum of L17-1 isolated from <i>Teloschistes chrysophthalmum</i> obtained on a Varian 600MHz instrument	52
Figure 24: The molecular structure of three lichen-derived chlorodepsidones	53
Figure 25: The high-resolution mass spectrum and predicted elemental composition of compound L17-1	54
Figure 26: The product ions of L17-1	55
Figure 27: The ^1H NMR spectrum of L17-3 isolated from <i>Teloschistes chrysophthalmum</i> obtained on a Varian 600MHz instrument	56
Figure 28: The ^{13}C NMR spectrum of L17-3 isolated from <i>Teloschistes chrysophthalmum</i> obtained on a Varian 600MHz instrument	57
Figure 29: The high-resolution mass spectrum and predicted elemental composition of L17-3	57
Figure 30: The product ions of L17-3	58
Figure 31: Pictures of <i>Xerophyta retinervis</i> in flower (A) (R. Botha) and (B) desiccated state at collection (P.C. Zietsman); <i>Myrothamnus flabellifolius</i> in wet (C) and desiccated (D) states (P.C. Zietsman); <i>Selaginella dregei</i> (E) (P.C. Zietsman) and <i>Cheilanthes contracta</i> (F) (T. Kellermann) in their desiccated states.....	66
Figure 33: An example of bio-autographic plates containing <i>M. aurum</i> A+ exhibiting a large zone of inhibition in the ACN fraction on the left (A) and three zones of inhibition in the PE fraction on the right (B) from the DCM extract of <i>M. flabellifolius</i>	70
Figure 34: The dose response curves of (A) compound 21c (pure) and (B) fraction 21d from the third HPLC fraction of the methanol extract of <i>M. flabellifolius</i> against <i>S. aureus</i> ATCC 12600. Figure (C) illustrates the effect of ciprofloxacin on <i>S. aureus</i>	73
Figure 35: The dose response curve of the dichloromethane extract of <i>Warburgia salutaris</i> bark against <i>Candida albicans</i> ATCC 90028.....	78
Figure 36: A chromatogram of the acetonitrile fraction of the dichloromethane extract of the leaves of <i>Warburgia salutaris</i> at 210nm.	79
Figure 37: A chromatogram of the dichloromethane extract of the bark of <i>Warburgia salutaris</i> at 210nm.	79
Figure 38: A chromatogram of the dichloromethane extract of the stems of <i>Warburgia salutaris</i> at 210nm.	80
Figure 39: A chromatogram of the dichloromethane extract of the twigs of <i>Warburgia salutaris</i> at 210nm.	80
Figure 40: The HPLC chromatogram of fraction WSBD3 from the acetonitrile fraction of the dichloromethane extract of the bark of <i>Warburgia salutaris</i> at 244nm.	83
Figure 41: The HPLC chromatogram of fraction WSBD4 from the acetonitrile fraction of the dichloromethane extract of the bark of <i>Warburgia salutaris</i> at 244nm.	83
Figure 42: A chromatogram at 229nm of fraction six originating from the HPLC separation of the acetonitrile fraction of the dichloromethane extract of <i>Warburgia salutaris</i>	87

Figure 43: The chemical structures of muzigadial (4), warburganal (5) and ugandensidial (6) isolated from the bark of <i>Warburgia salutaris</i> .	87
Figure 44: Chromatogram of the LC-MS method for the detection of L17-1 and L17-3	96
Figure 45: The relative quantities of L17-1 and L17-3 extracted from mouse whole blood using pH3 to pH11 Universal buffer.	97
Figure 46: A chromatogram depicting the lowest level of quantification of L17-3, 24.4ng/ml, on an API4000 LC-MS/MS	99
Figure 47: A representative calibration curve for L17-3 obtained on an API 4000 LC-MS/MS	100
Figure 48: Levels of L17-1 in mouse whole blood after the administration of 10mg/kg by oral and subcutaneous dosing.	102
Figure 49: Levels of L17-3 in mouse whole blood after the administration of 10mg/kg by oral and subcutaneous administration.	103
Figure 50: Blood levels of L17-3 in 5 individual mice after oral administration of 5mg/kg.	105
Figure 51: Blood levels of L17-3 in the 5 individual mice after subcutaneous administration of 5mg/kg	107
Figure 52: Blood levels of L17-3 in the 5 individual mice after intravenous administration of 5mg/kg	109
Figure 53: The levels of L17-3 after oral, subcutaneous and intravenous dosing at 5mg/kg over 96 hours.	111
Figure 54: The HPLC profile at 210nm of the active TLC band originating from the DCM fraction of the ethyl acetate extract of <i>M. flabellifolius</i> . Eight fractions were collected, as indicated on the diagram.	147
Figure 55: The HPLC chromatogram at 254nm of the ethyl acetate fraction of the methanol extract of <i>Myrothamnus flabellifolius</i> run at 2ml/min over a gradient of 18 to 30% ACN in 30 minutes and the seven fractions collected.	148
Figure 56: The HPLC profile of the subsequent collections from fraction 21 (semi-preparative HPLC) of the ethyl acetate fraction of the methanol extract of <i>M. flabellifolius</i> .	149
Figure 57: A chromatogram at 210nm depicting the eight collected fractions originating from the ACN fraction of the DCM bark extract of <i>W. salutaris</i> .	151
Figure 58: A flow diagram of the extraction method for L17-1 and L17-3 from mouse whole blood	155
Figure 59: The HPLC chromatogram of the liquid-liquid petroleum ether fraction of <i>W. salutaris</i> bark dichloromethane extract (WSBD1) at 229.9nm.	189
Figure 60: The HPLC chromatogram of the liquid-liquid petroleum ether fraction of <i>W. salutaris</i> bark dichloromethane extract (WSBD2) at 238.8nm	189
Figure 61: The GHMBC spectrum from L17-1 isolated from <i>Teloschistes chrysophthalmum</i>	190
Figure 62: The GHMBC spectrum from L17- isolated from <i>Teloschistes chrysophthalmum</i>	191
Figure 63: The GCOSY spectrum from L17-1 isolated from <i>Teloschistes chrysophthalmum</i>	192

Figure 64: The GHSQC spectrum of L17-1 isolated from <i>Teloschistes chrysophthalmum</i>	193
Figure 65: The DEPT spectrum of L17-1 isolated from <i>Teloschistes chrysophthalmum</i>	194
Figure 66: The ^1H NMR spectrum of L17-3 from <i>T. chrysophthalmum</i> obtained on a 900mHz instrument.....	194
Figure 67: An expansion of the region from 2.25 to 2.7ppm on the ^1H NMR spectrum of L17-3 derived from <i>T. chrysophthalmum</i> obtained on a 900mHz instrument.	195
Figure 68: The ^{13}C spectrum of L17-3 derived from <i>T. chrysophthalmum</i>	195
Figure 69: The ^{13}C spectrum of L17-3 derived from <i>T. chrysophthalmum</i>	196
Figure 70: The ^{13}C spectrum of L17-3 derived from <i>T. chrysophthalmum</i>	196
Figure 71: The ^{13}C spectrum of L17-3 derived from <i>T. chrysophthalmum</i>	197
Figure 72: The GCOSY correlations of L17-3 derived from <i>T. chrysophthalmum</i>	197
Figure 73: The GCOSY correlations of L17-3 derived from <i>T. chrysophthalmum</i>	198
Figure 74: The GHMBC correlations of L17-3 derived from <i>T. chrysophthalmum</i>	198
Figure 75: The GHMBC correlations of L17-3 derived from <i>T. chrysophthalmum</i>	199
Figure 76: The GHMBC correlations of L17-3 derived from <i>T. chrysophthalmum</i>	199
Figure 77: The GHMQC correlations of L17-3 derived from <i>T. chrysophthalmum</i>	200
Figure 78: The GHMQC correlations of L17-3 derived from <i>T. chrysophthalmum</i>	200
Figure 79: The DEPT spectra of L17-3 derived from <i>T. chrysophthalmum</i>	201
Figure 80: The ^1H NMR spectrum of muzigadial isolated from the dichloromethane extract of the bark of <i>Warburgia salutaris</i>	202
Figure 81: The ^{13}C spectrum of muzigadial isolated from the dichloromethane extract of the bark of <i>Warburgia salutaris</i>	202
Figure 82: The ^1H NMR spectrum of warburganal isolated from the dichloromethane extract of the bark of <i>Warburgia salutaris</i>	203
Figure 83: The ^{13}C NMR spectrum of warburganal isolated from the dichloromethane extract of the bark of <i>Warburgia salutaris</i>	203
Figure 84: The ^1H NMR spectrum of ugandensidal isolated from the dichloromethane extract of the bark of <i>Warburgia salutaris</i>	204
Figure 85: The ^{13}C NMR spectrum of ugandensidal isolated from the dichloromethane extract of the bark of <i>Warburgia salutaris</i>	204
Figure 86: The <i>in vivo</i> concentration of L17-1 in each of three mice after oral administration at 10mg/kg in combination with L17-3.	205
Figure 87: The <i>in vivo</i> concentration of L17-1 in each of three mice after subcutaneous administration at 10mg/kg in combination with L17-3.	205
Figure 88: The <i>in vivo</i> concentration of L17-3 in each of three mice after oral administration at 10mg/kg in combination with L17-1.	206

Figure 89: The <i>in vivo</i> concentration of L17-3 in each of three mice after subcutaneous administration at 10mg/kg in combination with L17-1 .	206
Figure 90: The genetic sequence of <i>Xanthoria parietina</i> (L1)	208
Figure 91: The genetic sequence of <i>Xanthoparmelia notata</i> (L8)	208
Figure 92: The genetic sequence of <i>Xanthoparmelia semiviridis</i> (WC) (L11)	208
Figure 93: The genetic sequence of an unknown lichen species L14, possibly a <i>Parmotrema</i> sp.	208
Figure 94: The genetic sequence of <i>Xanthoparmelia semiviridis</i> (EC) (L15)	209
Figure 95: The genetic sequence of <i>Flavoparmelia soledicans</i> (L16)	209
Figure 96: The genetic sequence of <i>Teloschistes chrysophthalmum</i> (L17)	209
Figure 97: The genetic sequence of an unknown lichen (L18)	209
Figure 98: The genetic sequence of <i>Thamnolia subuliforme</i> (L19)	210
Figure 99: The genetic sequence of <i>Usnea rubrotincta</i> (L20)	210

University of Cape Town

List of Tables

Table 1: Compounds with bioactivity isolated from various <i>Warburgia</i> species ..	31
Table 2: The collection details of the ten investigated lichen species	36
Table 3: The <i>in vitro</i> antimicrobial activities of ten lichen acetone extracts in µg/ml.	39
Table 4: The antimicrobial activity of usnic acid and antimicrobial control drugs.	40
Table 5: The activity of <i>Xanthoparmelia semiviridis</i> (Eastern Cape) extracts and precipitates against four organisms.	42
Table 6: The activity of fractions and pure compounds originating from the lichen <i>Teloschistes chrysophthalmum</i> against drug-sensitive and –resistant reference strains of <i>Staphylococcus aureus</i> , as well as the toxicity of the two active compounds against CHO cells.	46
Table 7: The NMR chemical shift values and two-dimensional correlations for L17-1	53
Table 8: The NMR chemical shift values and two-dimensional correlations for L17-3	56
Table 9: The antimicrobial activity of four South African desiccation-tolerant plants.	67
Table 10: The bioactivity of fractions originating from the dichloromethane and ethyl acetate extracts of <i>Myrothamnus flabellifolius</i>	71
Table 11: The MIC's (µg/ml) of the seven fractions resulting from the semi- preparative HPLC separation of the ethyl acetate fraction of the methanol extract of <i>Myrothamnus flabellifolius</i>	72
Table 12: The activity of <i>Warburgia salutaris</i> extracts against <i>Staphylococcus aureus</i> , <i>Klebsiella pneumoniae</i> , <i>Candida albicans</i> and <i>Mycobacterium aurum</i>	78
Table 13: The cytotoxicity of the four most active crude extracts from <i>Warburgia salutaris</i>	81
Table 14: The effect of the fractions of the dichloromethane extract of the bark of <i>Warburgia salutaris</i> on <i>Candida albicans</i> and <i>Mycobacterium aurum</i>	82
Table 15: The effect of eight HPLC fractions isolated from WSBDA, the acetonitrile fraction of the dichloromethane extract of the bark of <i>Warburgia salutaris</i> , on <i>Candida albicans</i> and <i>Mycobacterium aurum</i>	84
Table 16: The bioactivity of seven HPLC fractions and pure compounds isolated from fraction six of the acetonitrile fraction of <i>Warburgia salutaris</i> bark dichloromethane extract.	85
Table 17: The activity of the fractions/compounds isolated from the HPLC fractions 4 and 7 of the acetonitrile fraction of the dichloromethane extract of <i>Warburgia salutaris</i> bark against <i>Candida albicans</i> and <i>Mycobacterium aurum</i>	86
Table 18: The resonances of the ¹³ C NMR spectra of muzigadial, warburganal and ugandensidial isolated from the bark of <i>Warburgia salutaris</i>	88
Table 19: The resonances of the ¹ H NMR spectra of muzigadial, warburganal and ugandensidial isolated from the bark of <i>Warburgia salutaris</i>	89

Table 20: A representative table to illustrate the lowest level of quantification for L17-3 as being 781ng/ml on an API 2000 mass spectrometer.	98
Table 21: A representative table to illustrate the lowest level of quantification for L17-3 as being 24ng/ml on an API 4000 mass spectrometer.	99
Table 22: The pharmacokinetic parameters of L17-1 after oral administration at 10mg/kg to three mice in combination with L17-3.	101
Table 23: The pharmacokinetic parameters of L17-1 after subcutaneous administration at 10mg/kg to three mice in combination with L17-3.	101
Table 24: The pharmacokinetic parameters of L17-3 after oral administration at 10mg/kg to three mice in combination with L17-1.	103
Table 25: The pharmacokinetic parameters of L17-3 after subcutaneous administration at 10mg/kg to three mice in combination with L17-1.	103
Table 26: The pharmacokinetic parameters as obtained by WinNonlin analysis for the oral dosing of five mice with L17-3 at 5mg/kg.	106
Table 27: The pharmacokinetic parameters as obtained by WinNonlin analysis for the subcutaneous dosing of five mice with L17-3 at 5mg/kg.	106
Table 28: The pharmacokinetic parameters as obtained by WinNonlin analysis for the intravenous dosing of five mice with L17-3 at 5mg/kg.	108
Table 29: The average pharmacokinetic parameters of L17-3 after intravenous, oral and subcutaneous dosing at 5mg/kg.	110
Table 30: The TLC conditions applied and the bioactivity tested for using the bioautography method.	145
Table 31: ESI settings for compounds L17-1 and L17-3 on an API 2000 LC-MS/MS.	153
Table 32: MS/MS settings for compounds L17-1 and L17-3 on an API 2000 LC-MS/MS.	154
Table 33: The percentage yields of the acetone extracts of ten lichen species	187
Table 34: The percentage yield of extracts of <i>Xanthopharmelia semiviridis</i> (L15) from the Eastern Cape	187
Table 35: The percentage yields of desiccation-tolerant plants	188
Table 36: The percentage yield of <i>Warburgia salutaris</i> dichloromethane and ethyl acetate extracts	189
Table 37: The measured levels of L17-3 in five mice after oral administration at 5mg/kg. Values are in µg/ml. The LLOQ for L17-3 was determined to be 0.0244µg/ml.	207
Table 38: The measured levels of L17-3 in five mice after subcutaneous administration at 5mg/kg. Values are in µg/ml. The LLOQ for L17-3 was determined to be 0.0244µg/ml.	207
Table 39: The measured levels of L17-3 in five mice after intravenous administration at 5mg/kg. Values are in µg/ml. The LLOQ for L17-3 was determined to be 0.0244µg/ml.	207

List of Abbreviations

Ac	acetone
ACN	acetonitrile
AFB	acid-fast bacilli
AmBD	amphotericin B deoxycholate
AUC	area under the curve
BCG	bacilli Calmette-Guérin
CFU	colony-forming units
CHO	Chinese hamster ovarian
Cip	ciprofloxacin
CLQ	chloroquine
CM	complete medium
CO ₂	carbon dioxide
DCM	dichloromethane
DMSO	dimethylsulfoxide
DNA	deoxyribonucleic acid
EA	ethyl acetate
EHT	electron high tension
ESBL	extended-spectrum β -lactamase
ESI	electron spray ionization
FDA	Federal Drug Administration
GPS	global positioning system
HIV	human immunodeficiency virus
$t_{1/2z}$	half-life (elimination)
HPLC	high pressure liquid chromatography
HR-MS	high resolution mass spectrometry
INH	isoniazid
INT	<i>p</i> -iodonitrotetrazolium salt
IV	intravenous
LC-MS/MS	liquid chromatography/tandem mass spectrometer
LJ	Lowenstein-Jensen
L-L	liquid-liquid
LLOQ	lowest limit of quantification
MBC	minimum bactericidal concentration
MDR-TB	multi-drug resistant tuberculosis
MeOH	methanol
MFC	minimum fungicidal concentration
MIC	minimum inhibitory concentration
MRSA	methicillin-resistant <i>Staphylococcus aureus</i>
MTT	3-[4,5-Dimethylthiazol-2-yl]-2,5-diphenyltetrazolium bromide
Mw	molecular weight
NBT	nitro blue tetrazolium salt
Nys	nystatin
OADC	oleic acid, albumin, dextrose, catalase

PD	pharmacodynamic
PE	petroleum ether
PK	pharmacokinetic
pLDH	parasite lactate dehydrogenase assay
RNA	ribonucleic acid
rpm	revolutions per minute
SDA	soubaroud-dextrose agar
SI	selectivity index
TB	tuberculosis
TFA	trifluoroacetic acid
TMS	tetramethyl silane
TLC	thin layer chromatography
TSA	tryptone soya agar
TSB	tryptone soya broth
WHO	World Health Organization
XDR-TB	extensively drug-resistant tuberculosis

Chapter 1

Introduction

1.1 Infectious diseases and the need for new drugs

Infectious diseases are responsible for an enormous amount of global morbidity and mortality. Infection with the human immunodeficiency virus (HIV) has had a major impact on the occurrence and treatment of infectious diseases, particularly in southern Africa (Fauci, 2001; Madhi *et al.*, 2000). Compounding this problem has been the emergence of drug resistance, particularly in developing countries with high rates of infectious diseases and large populations living in crowded and unhygienic environments (Kunin, 1993). In the case of respiratory infections, the organisms most frequently responsible are *Mycobacterium tuberculosis*, *Moraxella catarrhalis*, *Haemophilus influenzae*, *Streptococcus pneumoniae* and *Staphylococcus aureus*, *Mycoplasma pneumoniae*, *Bordetella pertussis*, *Klebsiella pneumoniae*, *Pseudomonas aeruginosa* and *Proteus mirabilis* (Ehrhardt and Russo, 2001; Porras, 1996).

Infectious diseases are still regarded as neglected diseases, as there is still a lack of safe, affordable and effective treatments available. Drug companies no longer invest as much money into antibacterial drug development due to poor profit margins in comparison to chronic medication (Talbot *et al.*, 2006; Projan, 2003). Furthermore, for most bacterial diseases, more than one type of drug is available for treatment in the case of drug resistance, and few organisms have become resistant to all the available drugs. Nowadays, for a drug to be approved, it needs to show improved efficacy over currently available therapies, but this could be dangerous if the disease-causing organisms become resistant to a broad range of drugs thereby reducing the number of potential second-line drugs on the market (Projan, 2003). In comparison to the 20 years between

1983 to 1987, the approval of new antibiotics by the Federal Drug Administration (FDA) decreased by 56% from 1998 to 2002 (Spellberg *et al.*, 2004).

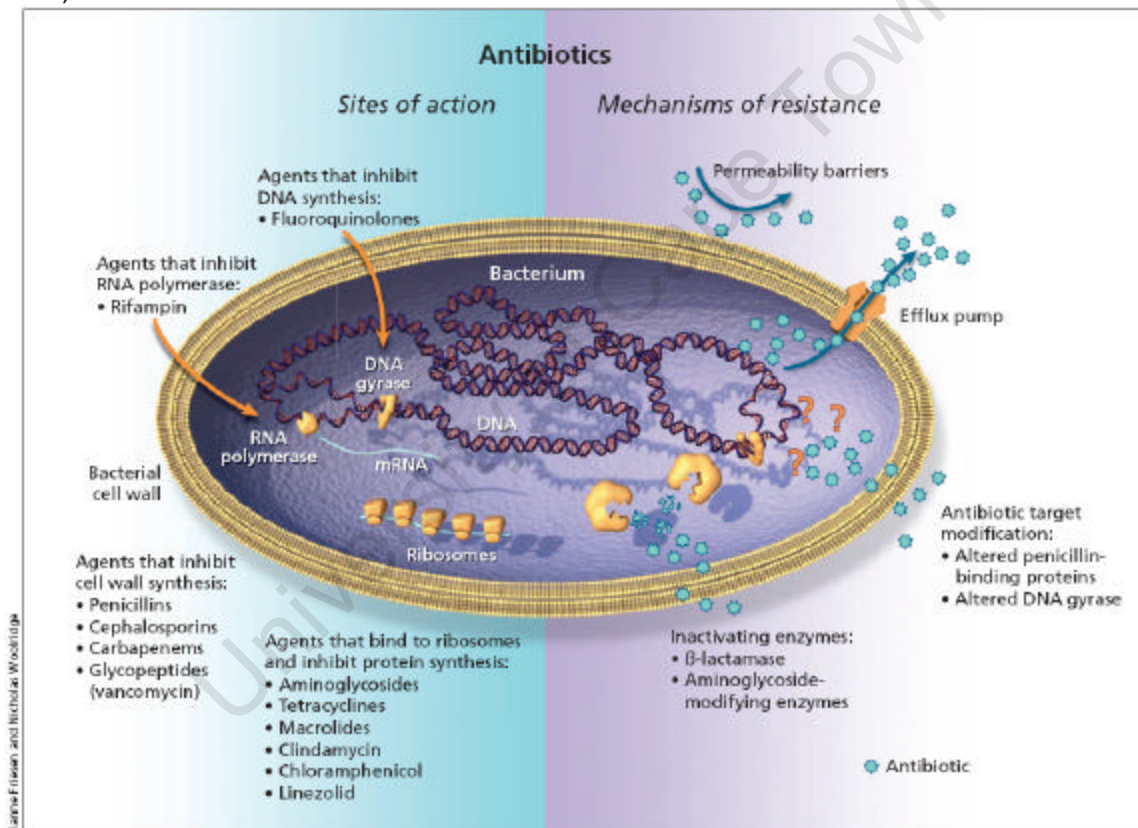
Trouiller *et al.* (2002) found that of the 1393 new chemical entities marketed between 1975 and 1999, only sixteen were for tropical diseases and tuberculosis, all with public sector involvement. These chemicals have all been included in the World Health Organization (WHO) Essential Drug List as they represent a definite therapeutic benefit. A further impediment to the development of a new antimicrobial drug is the prohibitive cost, which is estimated to be about US\$403 million, and if taken to the point of marketing approval, those costs rise to US\$802 million (DiMasi *et al.*, 2003).

There is an urgent need for new antimicrobial agents, due to the emergence of multi-drug resistance in common pathogens, the rapid emergence of new infections and the possibility that these organisms may be used in a military capacity (Spellberg *et al.*, 2004; Bradley *et al.*, 2007). Emerging resistance to currently available antimicrobial agents is a growing problem as the laboratory detection of emerging phenotypes is difficult and empiric therapies need to be altered by clinicians. Drug resistance also leads to longer and more expensive treatment and increased morbidity and mortality (Mulvey and Simor, 2009). Several factors contributing to increasing antimicrobial resistance are misuse of antibiotics, more immunocompromised hosts, poor hygiene and a greater number of invasive procedures (File, 1999; Owens and Rice., 2006; Kunin, 1993). There is a direct link between the rate at which organisms become resistant and exposure to the drug (Tenover, 2001).

A review by Andersson (2003) shows that if high levels of resistant organisms are present within the community they are likely to remain there for some time. A contributor to the evolution of antibiotic resistant organisms in man is the use of antibiotics in agricultural animal feed over the last four decades as growth promoters and prophylactically for disease-prevention. This can create a serious health problem, especially where the same classes of antimicrobials are being

used in human-based therapy (Wegener, 2003; File, 1999; Tenover and Hughes, 1996). Compounding this problem is the fact that human (and animal) commensal gut anaerobic bacteria have developed the ability to acquire and disseminate a broad range of mobile deoxyribonucleic acid (DNA) transfer factors, including genes encoding resistance to antibiotics. This horizontal DNA transfer has been shown to occur between unrelated bacterial species (between Gram-positive and Gram-negative bacteria) (Vedantum and Hecht, 2003).

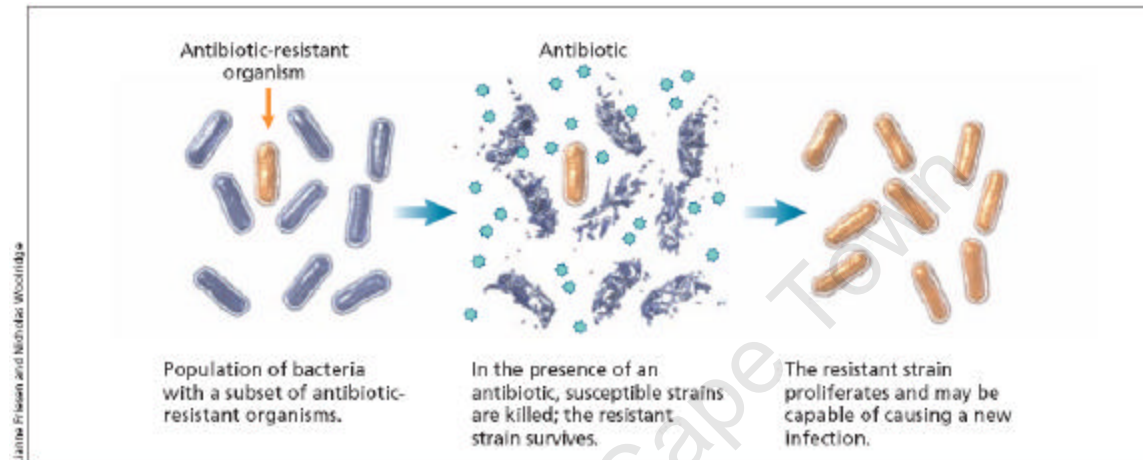
Figure 1: A schematic of antibiotic sites of action and potential bacterial resistance mechanisms to antimicrobial agents (Mulvey and Simor, 2009; modified from the original diagram by Neu, 1992)



Researchers have come to realise that the development of antibiotic resistant organisms is inevitable. Bacteria have evolved several ways in which to survive inhibition or killing by antibiotics, as shown in Figure 1. These include enzymatic inactivation of the agent, active removal of the agent from the cell by efflux pumps, reducing the binding efficiency of drugs by target mutation and by simply

decreasing the uptake of antibiotics (Singh and Barrett, 2006; File, 1999; Mulvey and Simor, 2009; Piddock, 2006; Paulsen, 2003). Furthermore, the emergence and dispersion of resistant strains are likely to result from antibiotic selection pressure (Mulvey and Simor, 2009), as shown in Figure 2.

Figure 2: A representation of the selection of resistant organisms by antibiotics (Mulvey and Simor, 2009)



With regards to the development of new antibiotics, efforts have largely been focused on improving the efficacy of existing classes of drugs, as well as agents that when co-administered with current antibiotics, reverse the organism resistance (for example, β -lactamase inhibitors such as clavulanic acid) (Singh and Barrett, 2006). Apart from the need for new antibiotics, measures need to be put in place for the prudent use of currently available and new drugs to increase the lifespan of the available drugs (Andersson, 2003; File, 1999; Owens and Rice., 2006; Fendrick *et al.*, 2001; Murray, 1994). Disease-causing pathogens have the ability to evade established treatments which means that not only are new classes of antimicrobials required, but a better understanding of host-microbe interactions (Courvalin and Davies, 2003). With the rate at which international travel is increasing, one can expect the spread of drug resistant bacteria to spread as well. Constant and efficient surveillance is required to document and detect the spread of resistant organisms, new mechanisms of

resistance and the mechanisms of resistance development (Verhoef and Fluit, 2006).

For the purpose of this project, early drug discovery was aimed at four classes of pathogenic organisms, namely mycobacteria, Gram-positive bacteria, Gram-negative bacteria and yeast. The representative organisms in each class are *Mycobacterium tuberculosis*, *Staphylococcus aureus*, *Klebsiella pneumoniae* and *Candida albicans*.

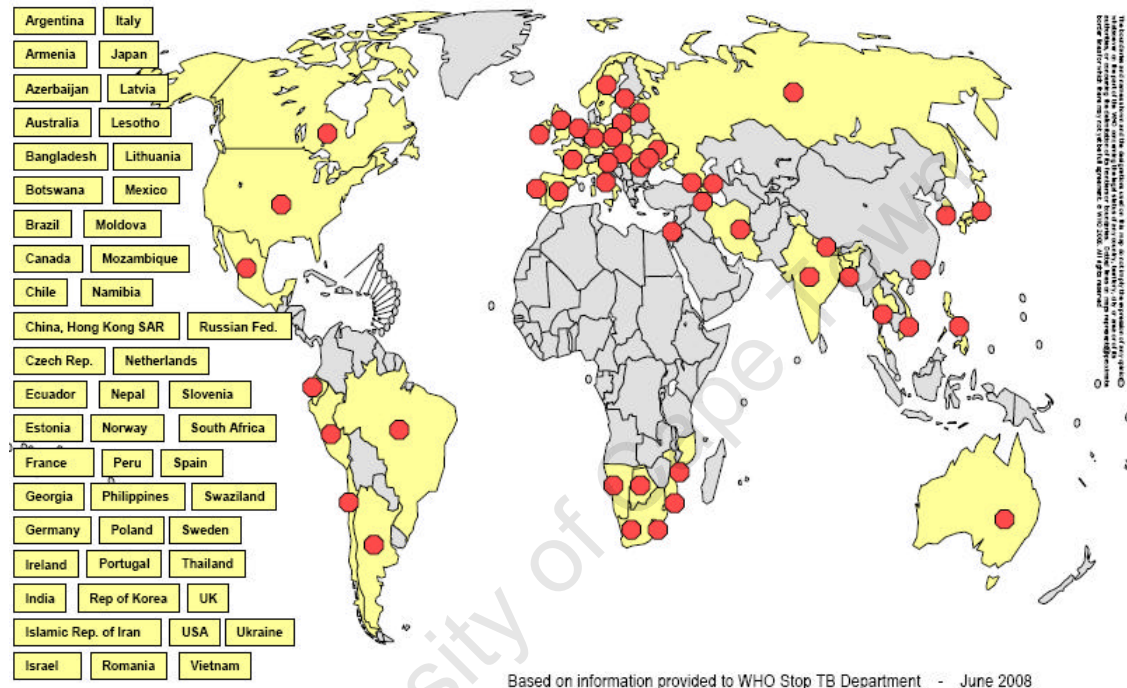
1.1.1 *Mycobacterium tuberculosis*

The WHO reported that tuberculosis (TB), the cause of much morbidity and mortality globally, was responsible for 9.2 million new cases and 1.6 million deaths in 2006 (WHO, 2008). Tuberculosis is diagnosed by sputum smear microscopy, a rapid and low cost method for detecting acid-fast bacilli (AFB) in sputum (Trébucq, 2004). Current treatment regimens are based on a six to eight month course of multi-drug therapy, which leads to high rates of patient nonadherence and subsequent increases in mortality and development of drug resistant strains (O'Brien and Nunn, 2001). Multi-drug resistant TB (MDR-TB) is classified as TB resistant to at least two of the front-line drugs, rifampicin and isoniazid. Extensively drug resistant TB (XDR-TB) is MDR-TB that is also resistant to at least three of the six classes of second-line drugs, therefore making it more expensive and difficult to treat and it is subsequently associated with very high mortality rates (Duncan, 2003; WHO, 2008). 45 countries have reported XDR-TB cases, as is represented in Figure 3. The only prevention against TB infection has been the BCG (bacilli Calmette-Guérin) vaccine, the effectiveness of which is controversial (Maes, 1999).

HIV infection has had a major impact on TB. The WHO (2008) estimates that in 2006, 0.7 million cases and 0.2 million deaths resulting from TB were in HIV-positive people. In South Africa alone, 44% of people with TB are also HIV-positive (WHO, 2008). A study in Zambia showed that 49% of patients with

confirmed TB infection were HIV positive and these patients often had irregular chest X-ray presentations and negative sputum smears, despite testing culture positive for TB (Elliott *et al.*, 1990). Furthermore, simultaneous infection with HIV and TB is associated with increased mortality and drug toxicity (Wallis *et al.*, 1996).

Figure 3: Countries that have reported XDR-TB cases (WHO, 2008)



The complete genome sequence of *M. tuberculosis* H37Rv shows that the organism differs substantially from other bacteria in that many genes are directed towards the production of enzymes involved in lipogenesis and lipolysis as well as proteins that may allow antigenic variation (Cole *et al.*, 1998). The mycobacterial cell wall plays a large role in its intrinsic resistance to antibiotic agents. Its low permeability can be attributed to the few porins in the cell wall slowing down the movement of hydrophilic agents across the cell wall and the thick lipid bilayer also hinders the movement of lipophilic agents (Jarlier and Nikaido, 1994). This complex cell wall structure unique to mycobacteria is viewed as a major target for novel drug development (Chatterjee, 1997; Wheeler and Anderson, 1996). For example, two enzymes, FAS I and FAS II, are

responsible for fatty acid synthesis, some of which form precursors for the mycolic acids in the cell wall. The FAS II system in particular is unique to microbes (Mdluli and Spigelman, 2006). Apart from this permeability barrier which slows down the movement of antibiotic agents into the cell, the organism also uses efflux pumps, antibiotic modifying, degrading and target-modifying enzymes to nullify the effects of some antibiotics.

Despite the resemblance to Gram-negative bacteria in its ability to provide selective permeability and sharing of orthologous genes for energy production (Fu and Fu-Liu, 2002), mycobacteria do not appear to gain antibiotic resistance by means of transmissible genetic elements, such as plasmids (Nguyen and Thompson, 2006). Furthermore, outside of the cell wall and plasma membrane is a capsule composed primarily of polysaccharide and protein. This layer has been shown to aid in the organism's adhesion to and penetration of host cells, contain toxic lipids and contact-dependent lytic substance, as well as providing a passive barrier to diffusion of molecules, thereby aiding the pathogenicity of the organism (Daffé and Etienne, 1999).

No new novel compound for the treatment of TB has been developed in many years, particularly due to the high cost of new drug development in comparison to the TB market size. Furthermore, the price at which these drugs can be sold needs to be kept low to accommodate their use in poor countries (O'Brien and Nunn, 2001). The TB Structural Genomics Consortium was established to obtain more structural and functional information on proteins produced by *M. tuberculosis* that are essential to its growth and virulence. This information can further be applied to the identification of new drug targets and the development of new anti-tuberculosis agents (Goulding *et al.*, 2002). As a result of the elucidation of the complete genome sequence of *M. tuberculosis*, new drug targets have been identified and high throughput screening needs to be employed, together with rational drug design, followed by optimization of the candidates into drug-like compounds (Duncan, 2003).

Most anti-tuberculosis drug development has been based on the production of derivatives of existing drugs. An example is the rifamycin derivative, KRM-1648, which inhibits bacterial RNA polymerase (Fujii *et al.*, 1995). An ethambutol analogue, SQ109, developed from a combinatorial approach, displays similar activity to INH *in vitro*, and promising *in vivo* activity with good tissue distribution, despite its low oral bioavailability (Jia *et al.*, 2005; Hampton, 2005). The introduction of the rifampicin derivative, rifapentine, into treatment regimens can enable an increase in the dosing interval as a result of its long half life compared to rifampicin. Its use in the treatment of MDR-TB, however, is limited, due to cross resistance with rifampicin-resistant strains (Chaulet, 1998; Tam, 1998).

Ballell *et al.* (2005) reviewed small synthetic molecules with antimycobacterial activity, of which the most promising tuberculosis-specific leads appeared to be the diarylquinolones R207910 and PA-824. The diarylquinolones represent a new class of compounds potentially effective against TB. In particular, R207910, has been shown to be particularly potent and specific to mycobacteria, with *in vitro* MIC's of 0.03 to 0.12 µg/ml against reference and antibiotic susceptible strains of *M. tuberculosis*. This compound appears to have a unique mode of action, ensuring that cross resistance with current anti-TB drugs should not be a problem. Furthermore, this compound has been shown to have more potent *in vivo* bactericidal activity than INH or rifampicin. *In vivo* murine and human pharmacokinetic studies have shown good oral absorption, long plasma half-life, high penetration into the tissues associated with TB infection and lack of obvious toxicity (Andries *et al.*, 2005). Several fluoroquinolones, particularly gatifloxacin and moxifloxacin, are also currently in various stages of clinical evaluation (O'Brien, 2003).

A series of nitroimidazopyran compounds have also shown potent bactericidal activity against actively growing and dormant TB bacilli, as well as MDR-TB. They have a unique mechanism of action, inhibiting a step in the production of

cell wall mycolates. Furthermore, these small molecules are orally bioavailable and can be easily manufactured on a large-scale, making them an ideal drug candidate for further clinical trials (Stover *et al.*, 2000). The genome sequence of *M. tuberculosis* led to the cloning, expression and purification of MT CYP51, a protein that is similar to the drug targets, CYP51 isozymes, in fungi. The authors subsequently demonstrated the antimycobacterial activity of several anti-mycotic azole drugs against *M. bovis* and *M. smegmatis* after showing that they bind to MT CYP51 with high affinity (Guardiola-Diaz *et al.*, 2001).

A new class of antituberculosis drug should ideally be able to shorten the duration of treatment, be able to treat latent TB, and be effective against drug resistant strains (O'Brien and Nunn, 2001; Duncan, 2003; Iseman, 2002; Ballell *et al.*, 2005). However, there is agreement among researchers that any new agent, however effective, introduced into a poorly managed treatment programme will still result in the development of drug resistant strains.

1.1.2 *Klebsiella pneumoniae*

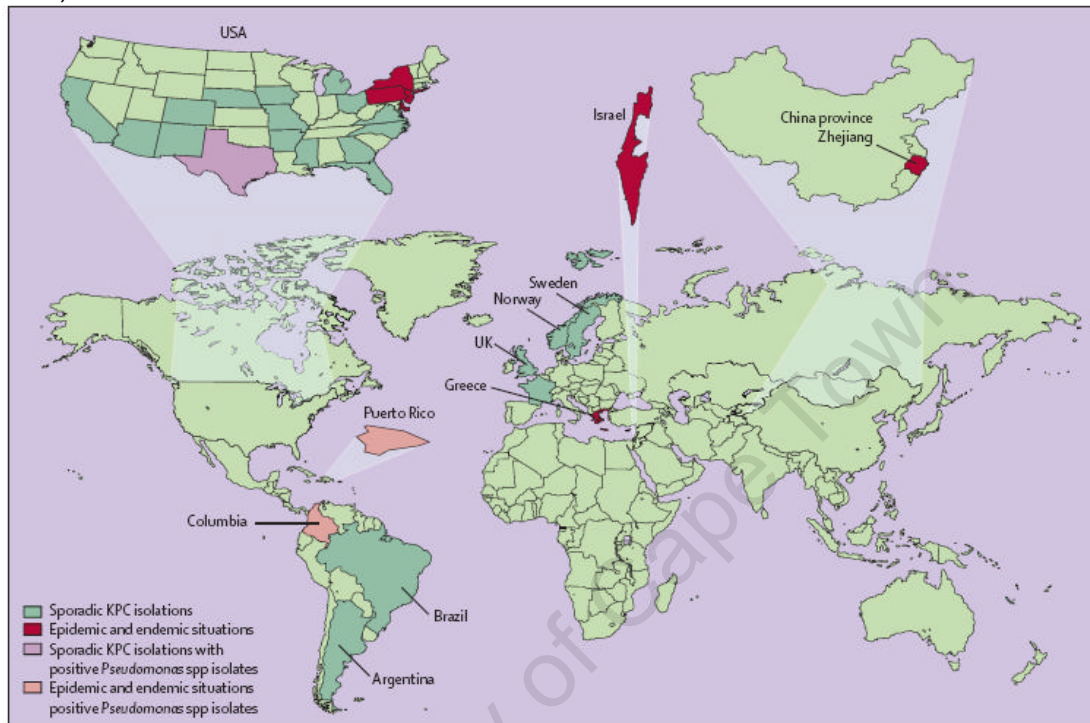
The Gram-negative bacteria, *K. pneumoniae*, is responsible for a variety of infections, including meningitis in patients that have undergone neurosurgery (Lu *et al.*, 1999), complicated skin and soft tissue infections of the extremities in patients with diabetes mellitus (Chang *et al.*, 2008), urinary, biliary and gastrointestinal tract infections, as well as wounds arising from trauma (Talbot *et al.*, 2006). *K. pneumoniae* infections are associated with high mortality rates if untreated (Lu *et al.*, 1999) as well as longer hospital stay prior to infection, treatment with newer antibiotics as well as hospitalization in an intensive care unit (Vatopoulos *et al.*, 1996). Furthermore, these organisms have increased their spectrum of antibiotic resistance and the problem is exacerbated by the lack of potential drugs with novel modes of action in the development pipeline (Talbot *et al.*, 2006).

In response to the development and use of successive generations of β -lactam antibiotics over the last 60 years, Gram-negative organisms are gaining a broader spectrum of resistance characteristics and are progressively becoming more difficult to treat with subsequent high mortality rates (Paterson *et al.*, 2003). The major concerns in the Enterobacteriaceae are the CTX-M extended-spectrum β -lactamases, plasmid-mediated AmpC β -lactamases and KPC carbapenemases (Livermore and Woodford, 2006). In members of the Gram-negative bacteria, the most important mechanism by which they display resistance to β -lactam antibiotics (penicillins) is the presence of plasmid-encoded β -lactamase enzymes. Further resistance to all β -lactam antibiotics is conferred by the extended-spectrum β -lactamase (ESBL) enzymes. Several studies have shown the prevalence of ESBL-producing clinical strains to be between 13 and 52% (Bell *et al.*, 2002; Marra *et al.*, 2006; Paterson *et al.*, 2003; Bratu *et al.*, 2005a). Cases have also been reported of single strains containing multiple different β -lactamases (Essack *et al.*, 2004; Giakouppi *et al.*, 2008; Moland *et al.*, 2007). It also appears as though the presence of these enzymes is becoming widespread in the family of Enterobacteriaceae (Hanson *et al.*, 2001).

Carbapenems have been used to treat ESBL-containing isolates of *K. pneumoniae* and resistance to the drug has been unusual in the past. However, there are increasing reports of resistance to carbapenems (Nordmann *et al.*, 2009; Mulvey and Simor, 2009; Bratu *et al.*, 2005a; Bratu *et al.*, 2005b) as is demonstrated in Figure 4, leaving colistin as the only available course of treatment (Mulvey and Simor, 2009). Carbapenem resistance in *Klebsiella* species and other members of Enterobacteriaceae is mediated by the KPC β -lactamases (Bratu *et al.*, 2005a). These strains are virtually resistant to all antibiotics and further compounding the problem is the fact that the microbiological detection of these strains is difficult and requires precise inoculum strengths (Bratu *et al.*, 2005a; Nordmann *et al.*, 2009). There have even been reports of a single ESBL-producing isolate of *K. pneumoniae*

acquiring resistance to ertapenem during the course of treatment by means of a porin loss (Elliott *et al.*, 2006).

Figure 4: The geographic distribution of carbapenemase-producing bacteria (Nordmann *et al.*, 2009)



Quinolone resistance in Gram-negative organisms is also a growing concern and appears to have arisen from multiple mechanisms including chromosomal mutations and plasmid-mediated resistance. A further concern is that quinolone resistance is typically associated with resistance to a wide range of other agents (Robicsek *et al.*, 2006; Strahelivits *et al.*, 2007). Increases in resistance to third-generation cephalosporins have also been reported (Lu *et al.*, 1999). Multi-drug resistant Gram-negative bacilli, defined as being resistant to more than two classes of antibiotics, are typically resistant to penicillins, cephalosporins, fluoroquinolones, trimethoprim-sulfamethoxazole and aminoglycosides (Mulvey and Simor, 2009).

1.1.3 *Staphylococcus aureus*

S. aureus is a serious human pathogen capable of causing a diverse variety of infections (Zetola *et al.*, 2005), an example of which is shown in Figure 5. These infections were originally mainly rampant in hospital settings, such as in surgical patients (Talbot *et al.*, 2006; Verhoef and Fluit, 2006) but are more frequently being identified in community-associated infections (Von K  ckritz-Blickwede *et al.*, 2008; Zetola *et al.*, 2005). Estimates suggest *S. aureus* involvement in between 11 to 38% of all cases of bacteraemia (Von K  ckritz-Blickwede *et al.*, 2008). A serious complication of infection with *S. aureus* is multiple organ failure and vascular damage as a result of sepsis and toxic shock syndrome (Von K  ckritz-Blickwede *et al.*, 2008). The first-line treatment of severe staphylococcal infections is vancomycin and second-line drugs include linezolid, daptomycin, clindamycine, tetracycline and co-trimoxazole (Zetola *et al.*, 2005).

Figure 5: Furuncle near the knee caused by *S. aureus* infection (Zetola *et al.*, 2005)



The emergence of *S. aureus* strains with resistance to initially methicillin and now vancomycin (Hiramatsu, 2001), the gold-standard therapy, as well as other newer drugs, has left a dire need for new anti-staphylococcal drugs, particularly those that are orally administered (Talbot *et al.*, 2006). There has been an increase in community-acquired MRSA infection, primarily skin furunculosis, with new virulence characteristics in relatively young, healthy people, associated with high morbidity and mortality (Zetola *et al.*, 2005). McDonald *et al.* (2003) found

that MRSA prevalence rates per 100 000 was 11.4 and 14.0 in North and South Ireland respectively in 1999. Resistance is even emerging against topical antibiotics, such as mupirocin and fucidic acid, used to treat superficial staphylococcal infections, such as in dermatitis and traumatic lesions (Critchley and Ochsner, 2008). Currently, no vaccination exists for the prevention of staphylococcal disease, although various veterinary and clinical trials have investigated the use of various live and attenuated *S. aureus* preparations (Hu *et al.*, 2009). Several new oxazolidinone derivatives are under investigation after the FDA approval of linezolid (Hilliard *et al.*, 2009; Barman *et al.*, 2009; Takhi *et al.*, 2008).

1.1.4 *Candida albicans*

The incidence of invasive fungal infections has increased substantially over the last twenty years. *Candida* infections have been identified as a common bloodstream pathogen with associated high mortality rates and increased hospital stays and treatment costs, particularly for the immunocompromised host. Furthermore, the incidence of new and emerging fungal pathogens, such as *Zygomycetes* and *Fusarium* species, which are difficult to treat, has increasingly been reported (Petrikos and Skiada, 2007; Weig and Brown, 2007). There are currently no vaccines available to combat invasive fungal infections (Thevissen *et al.*, 2007).

The publication of the genomes of several *Candida* species, although not leading directly to the development of an effective antifungal drug, has provided information on how the pathogen interacts with its host environment during the disease process. This information is envisaged to aid research into novel drug targets, such as genes necessary for virulence and viability, and diagnostic markers, as well as mapping the emergence and molecular basis of resistance (Weig and Brown, 2007; De Backer and Van Dijck, 2003). *C. albicans*, the species most frequently isolated from biological specimens (Weig and Brown,

2007), has displayed an ability to alter its phenotype and become resistant in the presence of a drug, but can revert back to its susceptible phenotype once the drug pressure has been removed, known as epigenetic resistance (White *et al.*, 1998). Various other cellular mechanisms of resistance are associated with fungi. Many of these organisms occur commensally in the host and become pathogenic when the host becomes immunocompromised. Some of these fungi are intrinsically resistant to antifungals, and in the presence of antifungal treatment, there can be replacement of the endogenous infection with a strain that has greater drug resistance. A similar pattern can occur between strains of the same organism (White *et al.*, 1998). Andes *et al.* (2006) also showed that *in vivo* dosing regimens involving the more frequent administration of drugs prevent the emergence of drug resistant *C. albicans*, whereas regimens resulting in sub-MIC (minimum inhibitory concentration) levels of drugs over prolonged periods tend to result in the emergence of drug resistant phenotypes.

C. albicans biofilm formation on biomaterials, such as intravenous and urinary catheters, contributes largely to hospital acquired infections as they are largely protected from the host immune system on the device surface (White *et al.*, 1998; Andes *et al.*, 2004). Andes *et al.* (2004) developed an *in vivo* *C. albicans* biofilm model and demonstrated a thick bilayered structure, with yeast cells embedded in an extracellular matrix close to the catheter surface, and yeast and hyphal forms close to the outer surface. These biofilms are also associated with hyper drug resistance.

In the past, treatment of *Candida* infections has been made difficult by the lack of suitable antifungal therapies (Rex *et al.*, 1995a). Polyenes are a class of antifungals including amphotericin B and nystatin that target ergosterol-containing membranes. Ergosterol is the predominant sterol found in fungal plasma membranes. These drugs have hydrophilic and hydrophobic sides, making them amphipathic, and are thought to disrupt the fungal membrane causing cell leakage. Amphotericin B deoxycholate (AmBD) was considered to

be the 'gold standard' for antifungal drug therapy for many years (White *et al.*, 1998; Petrikos and Skiada, 2007). It has, however, been associated with various toxicities and requires intravenous administration. Recently, new lipid preparations of this drug with decreased toxicity have been introduced (Petrikos and Skiada, 2007).

Included in the class of ergosterol biosynthesis inhibitors are the allylamines, thiocarbamates, azoles and morpholine. Fluconazole and itraconazole are first generation triazoles, but widespread-use of the former due to its good oral bioavailability and effective treatment of *Candida* infections led to the selection of fungal species with cross-resistance to other antifungals (Rex *et al.*, 1995b; Petrikos and Skiada, 2007). A newer extended spectrum azole is voriconazole, a product of fluconazole, used to treat invasive aspergillosis, oesophageal candidiasis, disseminated skin *Candida* infections, as well as infections caused by *Scedosporium apoispermum* and *Fusarium* species (Maschmeyer and Ruhnke, 2004; Petrikos and Skiada, 2007; Weig and Brown, 2007). Another second-line azole is the orally-administered posaconazole, a derivative of itraconazole, which gained FDA-approval in 2006 for treating invasive *Aspergillus* and *Candida* infections. The investigational azole, ravuconazole, was being evaluated in 2007 in phase II clinical trials, showing good *in vitro* activity against a wide range of fungi, including those with fluconazole-resistance (Petrikos and Skiada, 2007; Weig and Brown, 2007).

Echinocandins represent another class of antifungal, with a unique mode of action in that they inhibit (1,3)- β -D-glucan synthase, responsible for the production of a cell wall component in fungi. Drugs belonging to this class include caspofungin which gained FDA approval in 2001 for, amongst others, the treatment of invasive aspergillosis and oesophageal candidiasis and is as active as amphotericin B but better tolerated (Maschmeyer and Ruhnke, 2004; Petrikos and Skiada, 2007; Weig and Brown, 2007); micafungin, which was introduced in 2005 for the treatment of oesophageal candidiasis and as

prophylaxis for stem cell transplant patients; and anidulafungin, which was approved in 2006 for the treatment of oesophageal candidiasis, candidaemia, peritonitis and abdominal abscesses resulting from *Candida* species (Petrikkos and Skiada, 2007; Weig and Brown, 2007). These drugs are useful in the treatment of severe candidiasis due to their effectiveness against *Candida* species in biofilms (Weig and Brown, 2007). Another antifungal class, with an entirely different mechanism of action are the fluorinated pyrimidines, including 5-flucytosine, which inhibits fungal DNA and RNA synthesis, although it is often associated with haematological toxicity (White *et al.*, 1998; Rex *et al.*, 1995a).

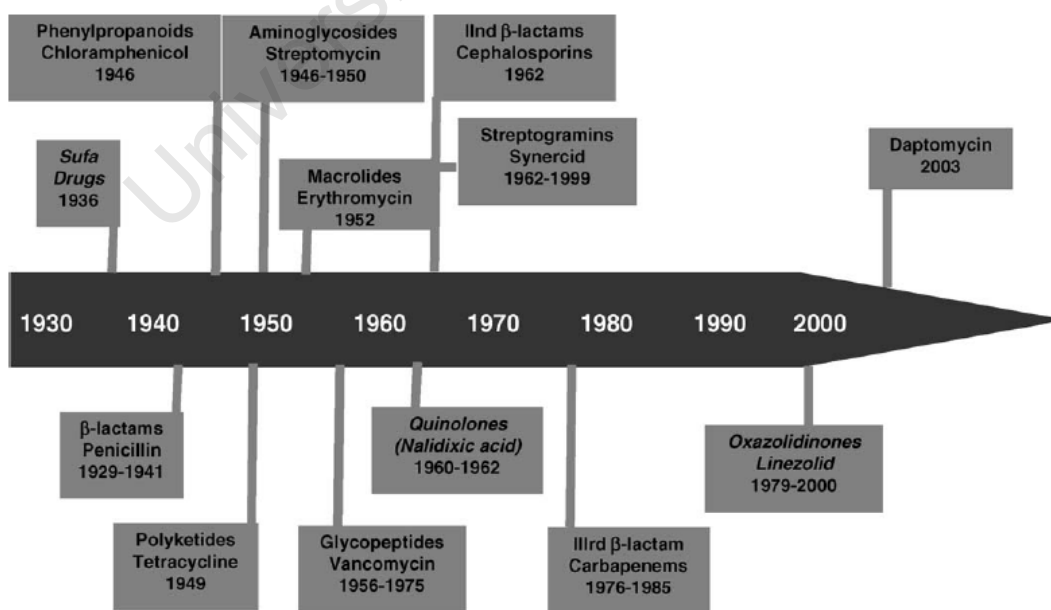
The introduction of new antifungal drugs has provided alternative, less toxic treatments to the previous gold standard, AmBD. Furthermore, the antifungal resources now consist of various drug classes with different modes of action, allowing for the possibility of combination therapy (Petrikkos and Skiada, 2007; Weig and Brown, 2007). Despite these advances, the current armourment of antifungal drugs are hampered by a limited spectrum of activity, are associated with rapid resistance development and many are fungistatic as opposed to fungicidal (Thevissen *et al.*, 2007). There is a continuous need for new antifungal agents, preferably with a unique mode of action to avoid cross-resistance with currently available drugs. Drug development should be focused on processes specifically involved in fungal cell wall biosynthesis (Weig and Brown, 2007). The fungal multi-drug efflux pumps could also be a good target for drug development as inhibiting their action could help the accumulation of drugs that would otherwise be rendered inactive. History has shown that antifungal drug discovery needs to be an ongoing process as fungi will continually develop resistance properties to available agents (White *et al.*, 1998).

1.2 Natural products and drug discovery

Natural products are typically secondary metabolites produced by living organisms as survival responses to their environment. It is estimated that about

a third to half of commercially available drugs are derived from natural products (Clark, 1996; Strohl, 2000). Several reviews have shown how natural products have contributed to the discovery of drugs such as lovastatin, cyclosporin A, paclitaxel, erythromycin, amphotericin, digoxin, penicillin, vincristine and vinblastine (Clark, 1996; Cordell, 2000; Strohl, 2000; Newman *et al.*, 2003). For the period from 1989 to 1995, Cragg *et al.* (1997) showed that over 60% of anticancer and anti-infective approved drugs and pre-New Drug Application agents were of natural product origin, while Newman *et al.* (2003) showed that from 1981 to 2002, an average of 62% of new anti-cancer chemical entities were non-synthetic. Several natural product-derived drugs were ranked amongst the top 35 selling ethical drugs between 2000 and 2002 internationally (40% in 2000, 24% in 2001 and 26% in 2002). Between 2000 and 2003, 15 new natural product-derived drugs were launched, 14 of which can be produced semi- or synthetically. In the same time period, another 15 compounds were in Phase III clinical studies or registration, of which ten are produced by semi-synthesis and four by total synthesis (Butler, 2004).

Figure 6: A timeline depicting the discovery of novel classes of antibiotics and introduction to the market place. Compounds listed in normal fonts are natural-product derived while those in italics are of synthetic origin (Singh and Barrett, 2006).



Sources of natural products include marine macro-organisms, terrestrial plants, lichens and microbes (Singh and Barrett, 2006). The latter have been shown to provide a valuable and largely untapped source of potential drugs, but difficulties in culturing these microbes have limited investigations into many ecosystems, as variations in growth conditions can lead to the production of substantially different metabolites from the same organism (Knight *et al.*, 2003; Peláez, 2006). Higher plants have to date not yielded any clinically relevant antibiotics (Singh and Barrett, 2006), although numerous authors have shown their potential in yielding compounds with antimicrobial properties (Cowan, 1999). As shown in Figure 6, all but three classes of antibiotics originate from natural products. The naturally-derived products typically have complex structures and many functional groups, a combination which often leads to their being very specific to the pathogen as opposed to the host (Singh and Barrett, 2006).

Drug discovery is generally based on three different principles, namely traditional, empirical and molecular. The traditional system is based on cultural knowledge of products used in traditional medicines, the empirical approach is based on knowledge of physiological processes and may involve further development of natural product-derived leads, while the molecular approach is based on knowledge of a molecular target for the therapeutic agent (Harvey, 1999). Natural products are an attractive source for the discovery of new drugs for several reasons. They are structurally diverse, many have drug-like properties and many are isolated as a family of homologues allowing for structure-activity studies. When one considers the percentage of natural biodiversity that has been investigated for potential medicinal properties, it would seem as though this field would remain attractive for the continued search of drug-like compounds (Harvey, 1999; Pieters and Vlietinck, 2005).

There is, however, declining interest in drug discovery from natural products by pharmaceutical companies for many reasons, including a move to high throughput screening of synthetic compound libraries, the development of

combinatorial chemistry, improvements in molecular and cellular biology leading to an increase in the number of molecular targets and a decreased interest in infectious disease therapies (Koehn and Carter, 2005; Butler, 2004; Patel and Gordon, 1996). With the genomes of many pathogenic organisms, such as *M. tuberculosis*, now completed, there is an expectation that with the use of molecular technology and combinatorial chemistry, new cellular targets for effective drugs will result in the next generation of novel drugs, as well as speeding up the development of vaccines and effective diagnostic tools (Barry *et al.*, 2000; Cole, 2002; Warner and Mizrahi, 2004). However, this trend may be changing as these strategies are not delivering the expected outcomes. Natural products are still a good source of leads due to their chemical diversity and biochemical specificity. Furthermore, they have gone through the process of evolutionary pressure which has enabled these compounds to interact with specific biological targets and proteins, as proven by the large number of natural product-derived drugs in use today (Koehn and Carter, 2005).

A disadvantage of drug discovery from natural products is the lengthy time and the more complicated drug development process (Balunas and Kinghorn, 2005; Koehn and Carter, 2005). However, improvements in the technologies associated with the isolation and identification of compounds, such as automation of fraction collectors attached to high pressure liquid chromatography (HPLC) instruments, ability of mass spectrometry (MS) technology to identify known compounds, new liquid chromatography (LC) columns enabling better separation and improved sensitivity of nuclear magnetic resonance (NMR) with smaller samples have the ability to streamline the lead discovery process (Harvey, 1999; Butler, 2004). The subsequent development and optimization of hyphenated techniques, such as LC-UV-MS (liquid chromatography-ultraviolet-mass spectrometry) and LC-NMR, has also allowed the fractionation of crude plant extracts prior to compound isolation to avoid isolating known constituents, as well as enabling partial or complete on-line compound identification within a crude extract matrix. These techniques can also be coupled to micro-

fractionation and immediate biological testing of the identified peaks using a method such as bio-autography, followed by the large-scale isolation of the active, unknown constituents (Wolfender *et al.*, 2005; Clarkson *et al.*, 2006). Furthermore, advances in molecular biology now aid the drug discovery process by enabling researchers to determine the mechanism of action of new compounds (Drews, 2000; Balunas and Kinghorn, 2005).

Several authors emphasize the need to determine suitable drug-like properties early on in the screening process (Koehn and Carter, 2005; Butler, 2004).

Drug discovery from natural products faces several challenges, including the cost of high throughput screening, the ability of early assays to determine drug-like properties, complications from testing complex natural product extracts in assays, delays in complicated structure elucidation and supply of large amounts of natural products to obtain enough pure compound for biological evaluation (Butler, 2004). Unfortunately, high throughput screening does not have the ability to predict the oral bioavailability and permeability of a compound, and compounds generated in this manner are typically more lipophilic and less soluble. Mechanisms by which the chemical and physical properties of a compound can lead to an immediate prediction of oral bioactivity early on during the drug discovery process would be enormously useful (Lipinski *et al.*, 2001).

Once a compound has been shown to have *in vitro* activity and no toxicity, it does not necessarily infer *in vivo* activity or safety as the compound may be metabolized into inactive metabolites or result in unexpected neurotoxicity. Despite the advances in the field of high-throughput screening and isolation procedures, available pharmacological methods are not able to accurately predict clinical efficacy and safety (Taylor *et al.*, 2001). Graz *et al.* (2007) argue that it could be more cost effective to perform clinical trials on human subjects involving crude extracts of traditional medicines that are currently in use as a means of focusing on meaningful clinical results. This would in turn give an immediate indication of the effectiveness or potential toxicity of the treatment. In the case of an observed benefit to the patients, the remedy could then be selected for

further, more sophisticated laboratory investigation. Some researchers have also provided scientific evidence that natural products in the form of extracts or mixtures of compounds ('natureceuticals') could be as effective as single compounds ('monoceuticals') (Núñez-Sellés *et al.*, 2007).

1.3 Traditional medicine in drug discovery

Natural products have been used for many centuries by humans as a source of medicine and have resulted in the development of many drugs used today (Newman *et al.*, 2000) or bioactive leads which have been developed into prospective drugs (Rates, 2001). Ethnopharmacology involves the research of traditional medicines that have been safely used for ages by cultural groups leading to the potential discovery of lead bioactive compounds with structurally diverse properties (Clark, 1996). This approach has been relatively successful as shown in a review by Fabricant and Farnsworth (2001) where 80% of the commercially available plant-derived drugs had uses the same as or similar to their ethnomedical origins.

Phytomedicines are still used by many people in the developing world due to lack of access to conventional western medicines. Plant medicines can be administered in many forms, including infusions, tinctures, powders and capsules (Rates, 2001). Not only is traditional medicine utilised as a primary means of treatment in developing countries, but it is widely recognised that many people in industrialised nations use traditional medicine in conjunction with western medicine (Bodeker, 2001). In South Africa, it is estimated that more than 80% of the population consult with the approximately 200 000 traditional healers who are now largely regulated by the government (Baleta, 1998; Kale, 1995). People consult with traditional healers for the treatment of various ailments, as well as for their personal well-being (Kale, 1995; Jäger, 2005; Cocks and Møller, 2002). Unfortunately these remedies are poorly controlled with very little safety data available (Rates, 2001) and many practitioners of Western medicine feel that

primary consultation with traditional healers might cause dangerous delays in seeking effective treatment for life-threatening illnesses (Smyth *et al.*, 1995).

Due to the rich natural biodiversity of South Africa, many investigations have been undertaken on the potential of local traditional medicines as bioactive leads in the drug development process (Van Vuuren, 2008). McGaw *et al.* (2008) have reviewed research performed on South African medicinal plants used to treat the symptoms associated with TB. One of the most famous South African traditional medicines, Umckaloabo[®], originating from *Pelargonium reniforme* and *Pelargonium sidoides*, was originally used by the Englishman, Charles Stevens, for the treatment of tuberculosis. This remedy gained widespread reputation in Europe in the early 1900's for its ability to heal tuberculosis sufferers (Bladt and Wagner, 2007). Urbanisation has led to a large trade in medicinal plants in South Africa, the end result being that many of these plants are now endangered species. Very few of these plants are known to be commercially cultivated, with the exception of *Warburgia salutaris* and *Siphonochilus aethiopicus* amongst others (Coetzee *et al.*, 1999). The use of many of these medicinal plants harvested from the wild is therefore not sustainable (Coetzee *et al.*, 1999). Currently, there is a lack of clinical evidence to support the use of these traditional medicines, but randomised trials might not be suited for testing the safety and efficacy of these treatments (Chaudhury, 2001).

1.4 Lichens as a source of antimicrobials

Lichens are formed from the symbiotic partnership of a fungus (mycobiont) and an algae and/or cyanobacteria (photobiont), capable of photosynthesis (Nash, 1996). Fossil evidence shows that lichen-like organisms have been around for millions of years (Yuan *et al.*, 2005) and occur across the globe (Galloway, 1996) in a variety of habitats, including marine environments (Kahng *et al.*, 2004), often existing in extreme conditions. Kranner *et al.* (2005) hypothesise that this symbiosis increases the overall reproductive success of the individual organisms

and enables them to survive desiccation and the accompanying increase in oxidative stress due to the unique antioxidant compounds produced in the lichenized state. Benko *et al.* (2002) have demonstrated the desiccation-tolerance of two *Cladonia* species which were able to recover their metabolic activity after four months of desiccation. Lichens are also very successful at utilizing water sources other than rain, such as fog and dew (Nash, 2006). Various lichen species have adapted structurally according to the environments in which they grow (Prinzing, 1999; Shirtcliffe *et al.*, 2006). For example, *Lecanora conizaeoides*, is super-hydrophobic, allowing rainwater to run off its surface easily and this, together with gas channels, allows this lichen to photosynthesize when other species are waterlogged (Shirtcliffe *et al.*, 2006).

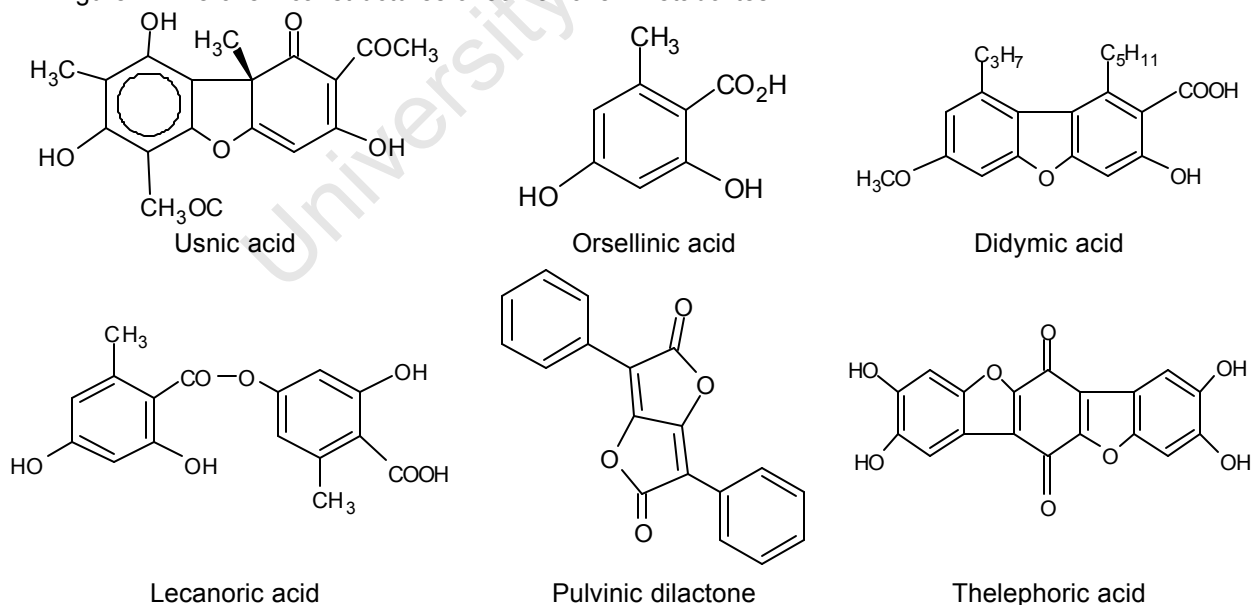
Lichens are broadly used for a wide range of purposes, including food to reindeer in Eurasia and caribou in North America during the winter months when plant material is not available. They are also used as a food-source by people in the Northern Hemisphere with *Umbilicaria esculenta* being sold commercially in Japan. Furthermore, lichens are widely used in traditional medicines globally, especially as laxatives (Dixon, 2005; Malhotra *et al.* 2008; Ingolfssdottir *et al.*, 1997; Podterob, 2008; Boustie and Grube, 2005). The lichen most widely used as an herbal remedy to treat ailments including tuberculosis, bronchitis and diarrhoea, is *Cetraria islandica* (Podterob, 2008). Very little published data on their use in traditional medicines in South Africa is available. Madomombe and Afolayan (2003) report that *Usnea barbata* is used in rural parts of the Eastern Cape Province to treat wounds in humans and mastitis in cattle. Furthermore, there have been reports of a community in the Richtersveld of the country utilizing various lichen species as herbal remedies (Prof. Timm Hoffman, University of Cape Town, personal communication). Lichens also provide raw materials for the perfume industry, in dyes and are a means for dating rock surfaces (Dixon, 2005) and monitoring environmental pollution (Baptista *et al.*, 2006; Monnet *et al.*, 2005; van Dobben *et al.*, 2001).

Lichen secondary metabolites are of fungal origin, however most of these compounds are unique to the lichenized state and are deposited on the walls of the fungal hyphae (Nash, 1996). Lichen metabolites can be aliphatic, cycloaliphatic, aromatic and terpenic compounds, all of which have displayed a plethora of biological activities (Huneck, 1999). Lichen metabolites are classified into four groups, depending on the biochemical pathway responsible for synthesis, namely, polyketide path, shikimic acid path, mevalonic acid path and the photosynthetic production of the photobiont (Huneck, 1999). These compounds are produced to afford the lichens protection from microbes, to increase the permeability of the cell walls of the phycobionts, to protect the organism from dangerous irradiation, to provide minerals from the substrate, as stress compounds in extreme conditions, to allow gaseous and water exchange (Huneck, 1999) and to deter predators (Gauslaa, 2005; Huneck, 1999; Boustie and Grube, 2005). Lichens have also been known to form depsides and depsidones (polyketide-derived aromatic compounds) through the esterification of aromatic carboxylic acid units (Kristmundsdóttir *et al.*, 2005).

There have been several literature reports on the *in vitro* bioactivity, primarily antimicrobial, antioxidant and antiviral, of extracts of various lichen species (Esimone and Adikwu, 1999; Gulluce *et al.*, 2006; Burkholder and Evans, 1945; Behera *et al.*, 2006a; Türk *et al.*, 2003; Madamombe and Afolayan, 2003; Paudel *et al.*, 2008; Perry *et al.*, 1999). Furthermore, several compounds with *in vitro* bioactive properties have been isolated (Campanella *et al.*, 2002; Choudhary *et al.*, 2005; De Carvalho *et al.* 2005; Kristmundsdóttir *et al.* 2005; Lauterwein *et al.*, 1995; Ingólfsdóttir *et al.*, 1997, Haroldsdóttir *et al.*, 2004; Müller, 2001; Kumar and Müller, 1999a; Kumar and Müller, 1999b; Perry *et al.*, 1999). The structures of several lichen metabolites are illustrated in Figure 7. The most well-known lichen-derived compound, the dibenzofuran derivative, usnic acid, has been shown to display a wide range of bioactivities, including antibacterial (Lauterwein *et al.*, 1995; Francolini *et al.*, 2004), including against drug-resistant strains of *E. faecalis* and *S. aureus* (Elo *et al.*, 2007), antimycobacterial (Ingólfsdóttir *et al.*,

1998), antiviral (Campanella *et al.*, 2002), antitrypanosomal (De Carvalho *et al.*, 2005), antiproliferative (Kumar and Müller, 1999a) and anticancer activity (Kristmundsdóttir *et al.*, 2005; Bézivin *et al.*, 2004). It is sold in Germany, Finland and Russia for the treatment of lupus, ringworm and athlete's foot (Dixon, 2005) and is widely used in various dietary supplements, including LipoKinetix (Syntrax, Cape Girardau, Missouri). However, the consumption of this specific capsule has been associated with severe hepatotoxicity (Favreau *et al.*, 2002). Even the crude extract of *Usnea* species are included in capsules which claim to 'promote a healthy urinary system' (www.gaiaherbs.com), although not being FDA-approved. It has also been shown that usnic acid can be produced in the laboratory by culturing the fungal component of usnic acid-containing lichens (Yamamoto *et al.*, 1985; Behera *et al.*, 2006b). Despite the fact that the fungal constituent can be cultured *in vitro*, it has been found that the growth of these fungi is slow and there is a variation in the levels and types of compounds produced when compared to that of the naturally-occurring lichen (Yamamoto *et al.*, 1993).

Figure 7: The chemical structures of some lichen metabolites



Over 800 compounds have been identified from lichens, but the pharmacological action and therapeutic relevance to medicine of most of these compounds is as

yet poorly studied (Kokubun *et al.*, 2007; Boustie and Grube, 2005). It is evident that South African lichens hold much promise as a relatively unstudied resource in the search for novel classes of antimicrobial drugs. Despite the fact that most of the secondary metabolites of lichens are of fungal origin and originate from fairly well-defined biochemical pathways dictated by a relatively small amount of genetic material, chemical variation within the same genus, and even species, has been reported in lichens, typically as a result of geographic and environmental variation (Fiscus, 1972; Hesbacher *et al.*, 1996; Culberson, 1967; Culberson *et al.*, 1973; Culberson, 1969).

1.5 Desiccation-tolerant plants as a source of antimicrobials

Almost all plant species have a phase of their life cycle that is either partially or completely tolerant of desiccation, such as seeds. However, there is a group of plants known as resurrection plants, making up less than 0.2% of total flora, which have the ability to cope with drought by being desiccation-tolerant and entering a quiescent state which can last for up to eleven years in some species (Scott, 2000; Benko *et al.*, 2002; Proctor and Tuba, 2002). Unlike other plants, resurrection plants have the ability to protect their vegetative tissues during drought stress. On addition of water, the plant immediately resumes growth and reproduction (Scott, 2000). These plants are often found in arid environments growing on rocky outcrops which can broaden the water catchment surface and allow any rainfall to accumulate in pools (Scott, 2000; Proctor and Tuba, 2002). Furthermore, these unique plants possess mechanisms that allow them to deal with various environmental stresses other than drought (Scott, 2000). The most notable metabolic change that occurs in the desiccated state is the accumulation of carbohydrates, particularly sucrose (Scott, 2000; Whittaker *et al.*, 2001; Pinheiro *et al.*, 2001; Illing *et al.*, 2005; Proctor and Tuba, 2002). Various authors have also reported mechanisms by which the plants protect themselves against oxidative damage during the desiccated state by means of antioxidants (Mowla *et al.*, 2002; Kranner *et al.*, 2002b; Illing *et al.*, 2005; Proctor and Tuba, 2002).

The most important property for a desiccation-tolerant plant to survive is the ability to promptly protect itself in response to rapidly changing environmental conditions (Scott, 2000). An early study of the tissue survival of South African desiccation-tolerant flowering plants by Gaff (1971) included the plants *Xerophyta retinervis* Baker (Family Velloziaceae) and *Myrothamnus flabellifolius* (Family Myrothamnaceae), the mature foliage of which were found to have no relative humidity. Proctor and Tuba (2002) supply a comprehensive list of genera containing desiccation-tolerant species which include *Selaginella* and *Cheilanthes* (Pteridophytes), as well as *Xerophyta* and *Myrothamnus* (Angiosperms), the four species investigated in this study.

The desiccation-tolerant plant, *M. flabellifolius*, has various uses in southern African traditional medicine, including infusions taken to treat colds and respiratory ailments, decoctions for kidney problems and backache, decoctions and powdered leaves applied to external abrasions and wounds and the inhalation of smoke to treat asthma (Hutchings *et al.*, 1996; Van Wyk *et al.*, 2002). Viljoen *et al.* (2002) found that the essential oil of *Myrothamnus flabellifolius* exhibited antibacterial and antifungal activity. The major components of the essential oil were pinocarvone and *trans*-pinocarveol. The authors speculate that the traditional use of this medicinal plant may arise from the presence of this potent essential oil. Other compounds isolated from this plant include camphor, eucalyptol and α -pinene (Van Wyk *et al.*, 2002), although none of these are associated with antimicrobial activity. Sherwin *et al.* (1998) examined the woody stem of *M. flabellifolius*, a characteristic that makes it unique from other desiccation-tolerant plants. They found that unusual knob-like structures of unknown chemical composition formed on the walls of the xylem vessels and that the mechanism applied for drought survival of this plant involves desiccation tolerance of the cellular constituents.

In southern Africa, the roots of *Xerophyta retinervis* have reportedly been smoked to treat asthma, while another species, *X. spekei*, is used as an anti-

inflammatory and to treat general aches and pains (Hutchings *et al.*, 1996; Van Wyk *et al.*, 2002). Furthermore, an unspecified species is reportedly used in Zulu traditional medicine, although further details are not supplied (Hutchings *et al.*, 1996). Flavonoids have been isolated from this genus, such as amentoflavone (Van Wyk *et al.*, 2002).

In southern Africa, *Selaginella cafferorum* is reportedly smoked with *Lycopodium* species to treat headaches. Other members of the family Selaginaceae are reportedly used to treat venereal diseases (Hutchings *et al.*, 1996). In India, *Selaginella* species are used for longevity, warding off infections, external ulcers and to treat urinary tract infections. One species, namely *S. involvens*, has been shown to exhibit immunomodulatory and antioxidant properties (Gayathri *et al.*, 2005). A flavonoid, 6-(2-hydroxy-5-acetylphenyl)-apigenin, was isolated from the medicinal plant *Selaginella tamariscina* in China (Liu *et al.*, 2009). Several *Cheilanthes* species (Family Adiantaceae) are used in medicinal remedies in southern Africa. *C. hirta* is used as an antihelminthic, to treat colds and sore throats, as well as a reported cure for cancer. *C. viridis* is a household remedy used by the Zulu people to treat sores and skin ailments, and is applied to burn wounds by other culture groups of South Africa (Hutchings *et al.*, 1996).

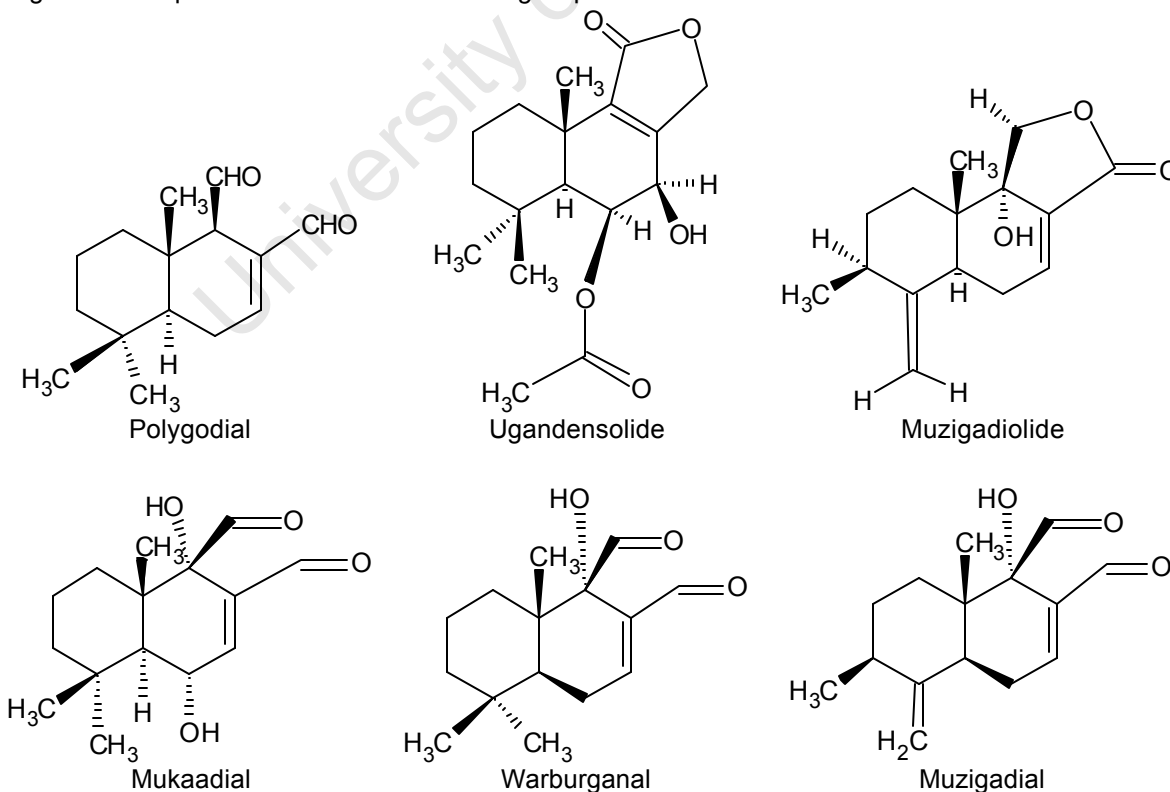
Multicellular organisms produce protective compounds as a means of controlling their environmental microflora or to protect themselves against infection by microbial pathogens. These pathogens may infect organisms belonging to different biological kingdoms and it stands to reason that defence components produced by members of one kingdom may be effective against microbial pathogens of another kingdom (Thevissen *et al.*, 2007). The ability of desiccation-tolerant plants to survive in a quiescent state for prolonged periods of time suggests the presence of compounds other than those involved in the desiccation-mechanism itself, which afford a certain amount of protection to the plant from herbivores and infective agents. Furthermore, when considering the traditional uses of the desiccation-tolerant plants reviewed, it becomes evident

that there could be an antimicrobial basis to all the remedies, which to date is largely unstudied.

1.6 The medicinal plant *Warburgia salutaris*

Warburgia species belong to the Family Canellaceae and are used throughout Africa as medicinal plants. *Warburgia salutaris* is widely used in southern Africa to treat various ailments. The Zulu people mix the powdered bark in water or alternatively smoke it to treat coughing. The cooked roots are also taken to treat coughs, while the bark is reportedly mixed with fat as an ointment for genital irritation/infection (Hutchings, 1996). Further uses in southern Africa include using primarily the bark for coughs, chest complaints, colds, venereal diseases, toothaches, backache, skin complaints, stomach ulcers, aphrodisiacs, constipation, influenza, fevers, pains, gastro-intestinal disorders, rheumatism and malaria (Hutchings *et al.*, 1996; Van Wyk *et al.*, 2002).

Figure 8: Compounds isolated from *Warburgia* species



The bio-activity of *Warburgia* species throughout Africa has been well-studied. Extracts from *W. stuhlmanii* have exhibited antimalarial activity (Muthaura *et al.*, 2007) while those of *W. salutaris* have shown 5-lipoxygenase, antioxidant and molluscidal activity (Frum and Viljoen, 2006; Muchuweti *et al.*, 2006; Clark and Appleton, 1997). The extracts of various parts of *W. ugandensis* showed cytotoxic and antileishmanial activity (Olila *et al.*, 2002; Ngure *et al.*, 2009). Numerous compounds have been isolated from the genus *Warburgia*, as shown in Figure 8. Many of these compounds are drimane sesquiterpenoids. Unsaturated aldehydes are widespread in nature as defence mechanisms for various organisms, including higher plants, liverworts, fungi, termites and molluscs. These compounds display a wide variety of bioactivities as summarised in Table 1, including antibacterial, antimycobacterial, antifungal and army worm antifeedant activity (Olila *et al.*, 2001a and b; Kubo and Taniguchi, 1988; Rabe and van Staden, 2000; Wube *et al.*, 2005; Clarkson *et al.*, 2007; Madikane *et al.*, 2007; Mashimbye, 1999; Kubo *et al.*, 1976; Forsby and Walum, 1996; Taniguchi *et al.*, 1988; Lunde and Kubo, 2000). Due to the popularity of *W. salutaris* bark in South African and African traditional medicine, the trees have become endangered. Drewes *et al.* (2001) have shown that some of the active sesquiterpenoid constituents are also found in the leaves of the plant, providing evidence for the substitution of bark for leaves in traditional remedies and the subsequent sustainable use of this plant in folk medicine.

Due to the fact that the medicinal plant, *Warburgia salutaris*, is so widely used and well-studied, it is envisaged that it could aid in the development of a method to study oral bioavailability of a group of natural product-derived compounds in a complex mixture to narrow the research focus onto those compounds with promising pharmacokinetic properties. This research has been made possible by the availability of *W. salutaris* material cultivated on a sustainable basis to supply the medicinal plant trade industry in southern Africa.

Table 1: Compounds with bioactivity isolated from various *Warburgia* species

Compound	Plant extract	Biological activity	Author
7a-hydroxy-8-drimen-11,12-olide	<i>W. ugandensis</i> bark DCM	MIC of 128µg/ml against <i>M. aurum</i> and <i>M. fortuitum</i>	Wube <i>et al.</i> , 2005
7β-hydroxy-4(13),8-coloratadien-11,12-olide	<i>W. ugandensis</i> bark DCM	MIC of 128µg/ml against <i>M. fortuitum</i>	Wube <i>et al.</i> , 2005
4(13),7-coloratadien-12,11-olide	<i>W. ugandensis</i> bark DCM	MIC of 128µg/ml against <i>M. aurum</i> , <i>M. fortuitum</i> and <i>M. smegmatis</i>	Wube <i>et al.</i> , 2005
11a-hydroxycinnamosmolide	<i>W. salutaris</i> bark DCM	Inhibits mycobacterial arylamine <i>N</i> -acetyltransferase	Clarkson <i>et al.</i> , 2007; Madikane <i>et al.</i> , 2007
11a-hydroxymuzigadiolide	<i>W. ugandensis</i> bark DCM		Wube <i>et al.</i> , 2005
3-hydroxymuzigadial	<i>W. salutaris</i> bark DCM	Component of antimycobacterial fraction	Clarkson <i>et al.</i> , 2007
3?, 9a,11a-trihydroxymuzigadiolide	<i>W. salutaris</i> bark DCM	Component of antimycobacterial fraction	Clarkson <i>et al.</i> , 2007
6a,9a,11a-trihydroxycinnamolide	<i>W. salutaris</i> bark DCM	Component of antimycobacterial fraction	Clarkson <i>et al.</i> , 2007
6a,9a-dihydroxy4(13),7-coloratadien-11,12-dial	<i>W. ugandensis</i> and <i>W. salutaris</i> bark DCM	Component of antimycobacterial fraction	Wube <i>et al.</i> , 2005; Clarkson <i>et al.</i> , 2007
6β,9a,11a-trihydroxycinnamolide	<i>W. salutaris</i> bark DCM	Component of antimycobacterial fraction	Clarkson <i>et al.</i> , 2007
Bemadienolide	<i>W. stuhlmanii</i> bark 60% methanol extract		Kubo <i>et al.</i> , 1976
Cinnamodial	<i>W. salutaris</i> bark DCM		Madikane <i>et al.</i> , 2007
Cinnamolide	<i>W. ugandensis</i> bark DCM; <i>W. stuhlmanii</i> bark 60% methanol extract		Wube <i>et al.</i> , 2005; Kubo <i>et al.</i> , 1976
Cinnamolide-3β-acetate	<i>W. ugandensis</i> bark DCM		Wube <i>et al.</i> , 2005
Isopolygodial	<i>W. salutaris</i> bark DCM		Mashimbye <i>et al.</i> , 1999
Linoleic acid	<i>W. ugandensis</i> bark DCM	MIC of 4µg/ml against <i>M. aurum</i> and <i>M. phlei</i> ; MIC of 8 and 16µg/ml against <i>M. fortuitum</i> and <i>M. smegmatis</i> respectively.	Wube <i>et al.</i> , 2005
Mukaadial	<i>W. ugandensis</i> and <i>W. salutaris</i> bark DCM	Component of antimycobacterial fraction	Clarkson <i>et al.</i> , 2007; Mashimbye <i>et al.</i> , 1999; Wube <i>et al.</i> , 2005
Muzigadial	<i>W. salutaris</i> bark ethyl acetate; <i>W. ugandensis</i> bark DCM and ethanol	MIC of 12.5µg/ml against <i>S. aureus</i> and <i>B. subtilis</i> ; MIC of 50µg/ml against <i>M. luteus</i> ; MIC of 100µg/ml against <i>E. coli</i> and <i>S. epidermis</i> ; inactive against <i>K. pneumoniae</i> ; MIC of 16 and 32µg/ml against <i>M. fortuitum</i> and <i>M. aurum</i> respectively; MIC of 64µg/ml against <i>M. phlei</i> and <i>M. smegmatis</i> . Anti-trypanosomal activity; Toxic in	Rabe and Van Staden, 2000; Wube <i>et al.</i> , 2005; Olila <i>et al.</i> , 2001

Muzigadiolide	<i>W. ugandensis</i> bark DCM	brine shrimp assay MIC of 64µg/ml against <i>M. phlei</i> ; MIC of 128µg/ml against <i>M. aurum</i> , <i>M. fortuitum</i> and <i>M. smegmatis</i> .	Wube <i>et al.</i> , 2005
Polygodial	<i>W. salutaris</i> bark DCM; <i>W. stuhlmanii</i> and <i>W. ugandensis</i> bark 60% methanol extract	African army worm antifeedant activity; Induces inositol phosphate mobilization in a concentration dependent manner; Potent fungicidal activity by damaging cell membranes or affection mitochondrial ATP synthase – MIC of 1.56µg/ml against <i>Candida utilis</i> and 0.78µg/ml to 3.13 against <i>Saccharomyces cerevisiae</i> .	Mashimbye <i>et al.</i> , 1999; Kubo <i>et al.</i> , 1976; Forsby and Walum, 1996; Taniguchi <i>et al.</i> , 1988; Lunde and Kubo, 2000
Salutarisolide	<i>W. salutaris</i> bark DCM		Mashimbye <i>et al.</i> , 1999
Ugandensidial	<i>W. ugandensis</i> and <i>W. salutaris</i> bark DCM; <i>W. stuhlmanii</i> and <i>W. ugandensis</i> bark 60% methanol extract	Component of antimycobacterial fraction; MIC of 128µg/ml against <i>M. fortuitum</i> ; African army worm antifeedant activity	Clarkson <i>et al.</i> , 2007; Wube <i>et al.</i> , 2005; Kubo <i>et al.</i> , 1976
Ugandensolide	<i>W. ugandensis</i> bark DCM		Wube <i>et al.</i> , 2005
Warburganal	<i>W. salutaris</i> bark DCM; <i>W. stuhlmanii</i> and <i>W. ugandensis</i> bark 60% methanol extract	African army worm antifeedant activity	Mashimbye <i>et al.</i> , 1999; Kubo <i>et al.</i> , 1976

Abbreviations: DCM – dichloromethane; MIC – minimum inhibitory concentration; ATP – adenosine triphosphate

1.7 Aims and objectives

A hit compound is defined as a nonreactive compound derived from high-throughput screening with *in vitro* activity of less than 20 μ M, while a lead compound is one that apart from its potency, shows selective activity and favourable pharmacokinetic properties (including distribution, metabolism, excretion, toxicity) for its eventual development into a small-molecule drug (Wunberg *et al.*, 2006). There is an increasing trend in the field of drug discovery to determine the physiochemical and pharmacological information of potential lead compounds earlier in the drug development process. One of the problems associated with novel compounds in preclinical drug development is the uncertain absorption of the compound across the gastro-intestinal tract (Gruppo *et al.*, 2006).

A further drawback associated with drug discovery from natural products is the length of time required to accumulate large enough quantities of material for identification, *in vitro* bioactivity testing and eventually *in vivo* efficacy and bioavailability studies. An objective of this project is to evaluate the feasibility of determining lead-like candidates earlier in the drug discovery process with the help of sensitive LC-MS/MS technology. Prospective 'hit' compounds within a fraction, as identified by *in vitro* bioactivity assaying, will be assessed for *in vivo* bioavailability in a small animal model, requiring as little as 10 μ l of blood per sampling time point. This will provide information on which compounds have the most favourable toxicity and oral bioavailability profiles, enabling the researcher to focus only on those compounds with good lead-like potential. Many compounds with good *in vitro* activity will be poorly bioavailable *in vivo*. These methods will therefore also eliminate the unnecessary efficacy testing in animal models of disease of compounds that are not good lead candidates.

The specific aims of this project are:

- To investigate the antimicrobial activity of ten South African lichens
- To investigate the antimicrobial activity of four South African desiccation-tolerant plants
- To investigate the antimicrobial activity of the cultivated South African medicinal plant, *Warburgia salutaris*
- To isolate and identify compounds responsible for observed activity
- To test the cytotoxicity of the active compounds
- To evaluate the pharmacokinetics of 'hit' compounds
- To develop a model for the pharmacokinetic evaluation of multiple compounds within a fraction with known *in vitro* antimicrobial activity and favourable cytotoxicity

Chapter 2

Lichens

2.1 Introduction

Very little work has been performed on the antimicrobial properties of South African lichens due to a lack of local experts capable of identifying the species and difficulty in accumulating sufficient quantities of active secondary metabolites for bioactivity studies. There has been a report on the antimicrobial extracts of local *Usnea barbata*, rurally used for the treatment of wounds in humans and mastitis in cattle (Madamombe and Afolayan, 2003). These natural products could represent a locally untapped reservoir of promising antimicrobial leads.

2.2 Results

Ten lichen specimens were collected from the Eastern and Western Cape provinces of South Africa. Of these, only eight were positively identified by means of genetic sequencing performed in Germany (Appendix Figures 90 to 99), as well as with the aid of electron microscope pictures, illustrated in Figure 9. In Figure A and B of these pictures, it is possible to see the flat thalli of the two *Xanthoparmelia* species, as well as the cup-like reproductive structures known as apothecia in Figure B. Figure D shows the finger-like isidia of the *Xanthoparmelia* species while Figure E depicts the stratified nature of lichen thalli. Figure F shows the radial branches of the *T. chrysophthalmum* thalli.

Figure 9: Electron microscopy pictures of (A) *Xanthoparmelia notata*, (B) *Xanthoparmelia semiviridis*, (C) unknown lichen from Eastern Cape (L14), (D) *Xanthoparmelia semiviridis* from Eastern Cape, (E) *Flavoparmelia soredicans* and (F) *Teloschistes chrysophthalmum*.

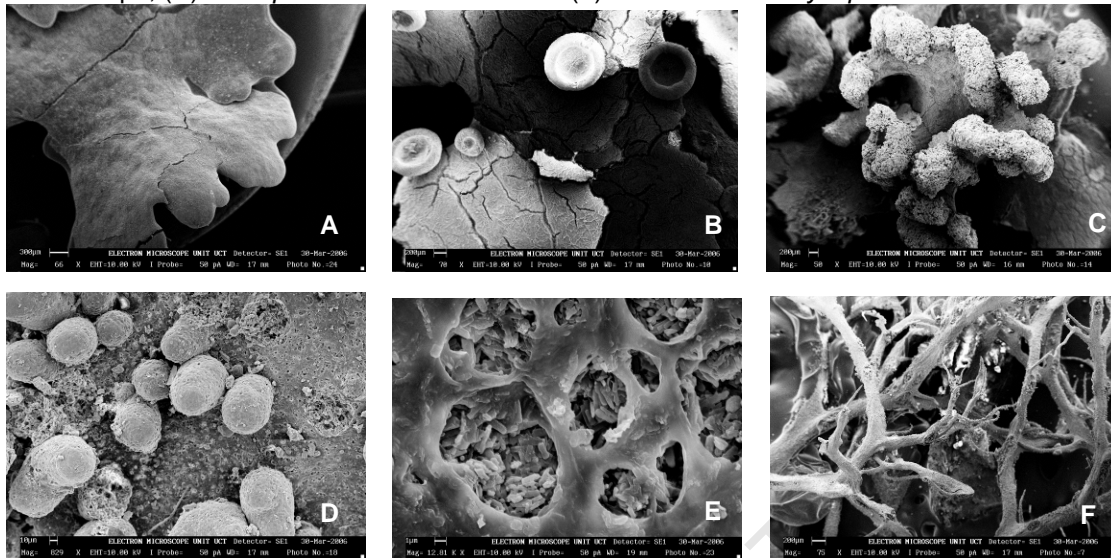


Table 2: The collection details of the ten investigated lichen species

Voucher specimen number	Lichen Name	Region	Location	Habitat	Substrate	GPS coordinates
1	<i>Xanthoria parietina</i>	Western Cape	Tulbagh	valley/river bank	tree	33°16'15"S 19°8' 43"E
8	<i>Xanthoparmelia notata</i>	Western Cape	Paarl Mountain Reserve	mountain	bare rock, granite	33°44'24"S 18°56'58" E
11	<i>Xanthoparmelia semiviridis</i>	Western Cape	Paarl Mountain Reserve	mountain	bare rock, granite	33°44'24"S 18°56'58" E
14	*Unkown1 (# <i>Parmotrema</i> sp.)	Eastern Cape	East London	coastal hilltop	house roof tiles	32°58'38"S 27°56' 26"E
15	<i>Xanthoparmelia semiviridis</i>	Eastern Cape	East London	coastal hilltop	house roof tiles	32°58'38"S 27°56'26"E
16	<i>Flavoparmelia soredicans</i>	Eastern Cape	East London	coastal hilltop	house roof tiles	32°58'38"S 27°56'26"E
17	<i>Teloschistes chrysophthalmum</i>	Eastern Cape	East London	coastal hilltop	house roof tiles	32°58'38"S 27°56'26"E
18	*Unknown 2	Western Cape	60km south of Swellendam	hilltop	stony soil	34°5'31"S 20°2'8" E
19	<i>Thamnolia subuliforme</i>	Western Cape	Swellendam	mountain slope	bare rock in water	33°59'33S 20°28' 51E
20	<i>Usnea rubrotincta</i>	Western Cape	Swellendam	mountain slope	bare rock in water	33°59'33S 20°28' 51E

*Genetic sequence does not match any known species.

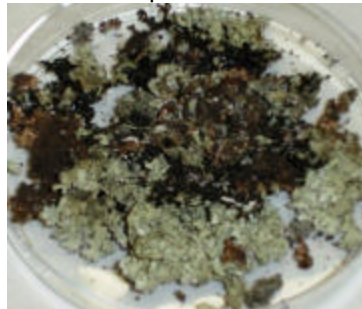
#Tentative visual identification made by Dr E. Timdal.

Abbreviations: GPS - global positioning system

Figure 10: Photographs of the investigated lichen species



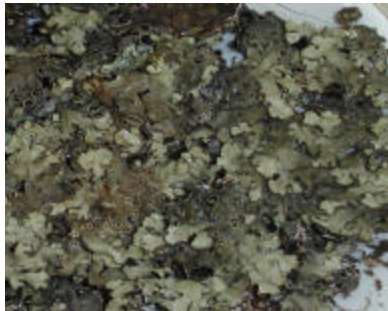
Xanthoria parietina



Xanthoparmelia notata



Teloschistes chrysophthalmum



Xanthoparmelia semiviridis
(Western Cape)



Unknown lichen L14



Unknown species L18



Usnea rubrotincta



Xanthoparmelia notata



Flavoparmelia soledicans



Xanthoparmelia semiviridis (Eastern Cape)



Thamnomia subuliforme

Six of the species originate from the Western Cape, while the remainder were collected in the Eastern Cape, as shown in Table 2. Seven of the lichens were found growing on exposed surfaces such as roof tiles and rock. Two of the

lichens were located in a running stream attached to the base rock, and one species was found growing on the bark of a tree. Photographs of the lichen specimens are illustrated in Figure 10.

2.2.1 Bioactivity testing of crude acetone extracts

Due to small sample quantities, acetone extracts were prepared from ten lichen species in an attempt to extract the greatest quantity of compounds available using one solvent, as recommended by Eloff (1998b). The extract yields are tabulated in the Appendix, Table 33. These acetone extracts were subsequently tested against *M. aurum* A+, *K. pneumoniae* ATCC 13883, *S. aureus* ATCC12600 and *C. albicans* ATCC 90028 using the broth micro-dilution method as described in Section 7.2. The results are displayed in Table 3.

For crude extracts exhibiting MIC's of 125µg/ml or less, IC₅₀ values were determined as specified under the criteria for active extracts in Chapter 7.2. The acetone extract of *Teloschistes chrysophthalmum* demonstrated the greatest activity against *S. aureus* with an IC₅₀ value of 1.1µg/ml, while none of the extracts showed activity at less than 1mg/ml against *K. pneumoniae*. One lichen species, the unknown foliose lichen species L18, showed activity at less than 500µg/ml against *C. albicans*. Five lichen species, namely *Xanthoparmelia notata*, *Xanthoparmelia semiviridis* (Eastern Cape), *Flavoparmelia soledicans*, *Thamnolia subuliforme* and *Usnea rubroincta* displayed activity against *M. aurum* at 125 to 250µg/ml. It is interesting to note the differences in activity between the two *X. semiviridis* lichen species collected from the Eastern and Western Cape Provinces of South Africa. The former displayed greater activity against *S. aureus* with an MIC ranging from 62.5-125µg/ml, while the latter had an MIC of 1000µg/ml.

Table 3: The *in vitro* antimicrobial activities of ten lichen acetone extracts in µg/ml. The results are expressed in terms of MIC's followed by IC₅₀ values, for extracts with activity of 125µg/ml or less.

	Lichen / Control drug	<i>S. aureus</i>	<i>K. pneumoniae</i>	<i>M. aurum</i>	<i>C. albicans</i>
L1	<i>Xanthoria parietina</i>	=2000	>2000	1000	2000
L8	<i>Xanthoparmelia notata</i>	125-250, 31.0±0.92	2000	250	1000
L11	<i>Xanthoparmelia semiviridis</i> (WC)	1000	4000	500	>500
L14	<i>Unkown1</i> (<i>Parmotrema</i> sp.)	250	1000	1000	1000
L15	<i>Xanthoparmelia semiviridis</i> (EC)	62.5-125, 46.1±8.06	2000	250	1000
L16	<i>Flavoparmelia soredicans</i>	125-250, 36.3±1.34	1000	250	1000
L17	<i>Teloschistes chrysophthalmum</i>	15.6-31.3, 1.1±0.73	>1600	400	1000
L18	<i>Unknown 2</i>	187.5-375	2000	500	250
L19	<i>Thamnolia subuliforme</i>	1000	>2000	188	>2000
L20	<i>Usnea rubrotincta</i>	62.5-125, 63.4±9.9	>2000	125, 56.8±5.9	>2000
	Dimethylsulfoxide	25, 10.6±1.6%	12.5, 6.9±0.3 %	12.5, 4.9±1.0 %	12.5, 8.6±1.8%
	Ciprofloxacin	0.313, 0.2±0.05	0.08, 0.042±0.002	n/a	n/a
	Nystatin	n/a	n/a	n/a	3.1, 1.5±0.4
	Isoniazid	n/a	n/a	0.08-0.16, 0.061±0.005	n/a

Abbreviations: MIC - minimum inhibitory concentration; n/a - not applicable; WC – Western Cape; EC – Eastern Cape

2.2.2 Bioactivity testing and profiling of usnic acid

The common lichen metabolite, usnic acid, was also evaluated for its antimicrobial activity, as shown in Table 4. This compound is known to be present in many lichen species and is often responsible for observed antimicrobial activity. Usnic acid ($C_{18}H_{16}O_7$, Mw = 344) is a granular yellow powder which fluoresces at 232 and 282nm (Roach *et al.*, 2006). This compound was also tested for antimalarial activity as described in Section 7.4, as no record of such testing could be found in the literature and the assay was available in the Division of Pharmacology, University of Cape Town.

Table 4: The antimicrobial activity of usnic acid and antimicrobial control drugs. The results are expressed in $\mu\text{g/ml}$ as an MIC, followed by the IC_{50} value, if appropriate, except for *P. falciparum*, where the result is expressed as an IC_{50} value.

Organism	Usnic acid	INH	Nys	Cip	CLQ
<i>M. aurum</i>	15.6, 6.9 \pm 0.9	0.078, 0.056 \pm 0.001	n/a	n/a	n/a
<i>S. aureus</i>	500	n/a	n/a	0.31-0.63, 0.25 \pm 0.069	n/a
<i>C. albicans</i>	>1000	n/a	3.13, 1.7 \pm 0.04	n/a	n/a
<i>K. pneumoniae</i>	>1000	n/a	n/a	0.08, 0.042 \pm 0.002	n/a
<i>P. falciparum</i>	15.1 \pm 3.4	n/a	n/a	n/a	0.015 \pm 0.002

Abbreviations: n/a - not applicable; MIC - minimum inhibitory concentration; INH - isoniazid; Nys - nystatin; Cip - ciprofloxacin; CLQ - chloroquine

Usnic acid proved to be completely inactive against *C. albicans* and *K. pneumoniae* at the highest concentration tested, namely 1mg/ml. It did, however, exhibit weak activity against *S. aureus* with an MIC value of 500 $\mu\text{g/ml}$. Similarly, usnic acid showed poor activity against *P. falciparum* with an IC_{50} value of 15.1 $\mu\text{g/ml}$, a thousand times less active than chloroquine, as shown in Table 4. This is the first report of the antimalarial activity of usnic acid. The most potent activity was observed against *M. aurum*, with an IC_{50} result of 6.9 $\mu\text{g/ml}$.

The extract exhibiting the most potent activity against *M. aurum* is that of *Usnea rubrotincta*, with an IC_{50} value of 56.8 μ g/ml. The secondary metabolite, usnic acid, is commonly found in *Usnea* species (Nash, 1996) and for this reason the extract was evaluated for the presence of usnic acid. An HPLC chromatogram of the acetone extract (Figure 12) was compared to that of pure usnic acid (Figure 11). The chromatogram in Figure 12 shows the presence of large quantities of usnic acid in the acetone extract of *U. rubrotincta*, to which the observed antimicrobial activity can be attributed. Due to the large wealth of knowledge already available on this lichen metabolite and its antimycobacterial activity, no further research was performed on this extract.

Figure 11: An HPLC chromatogram of usnic acid (Sigma) at 243.5nm with its PDA spectra inset.

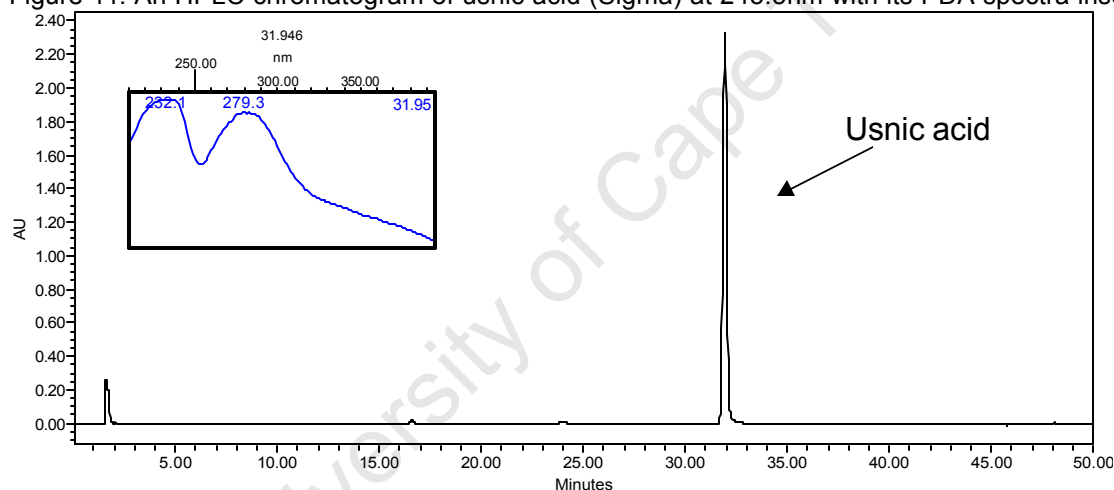
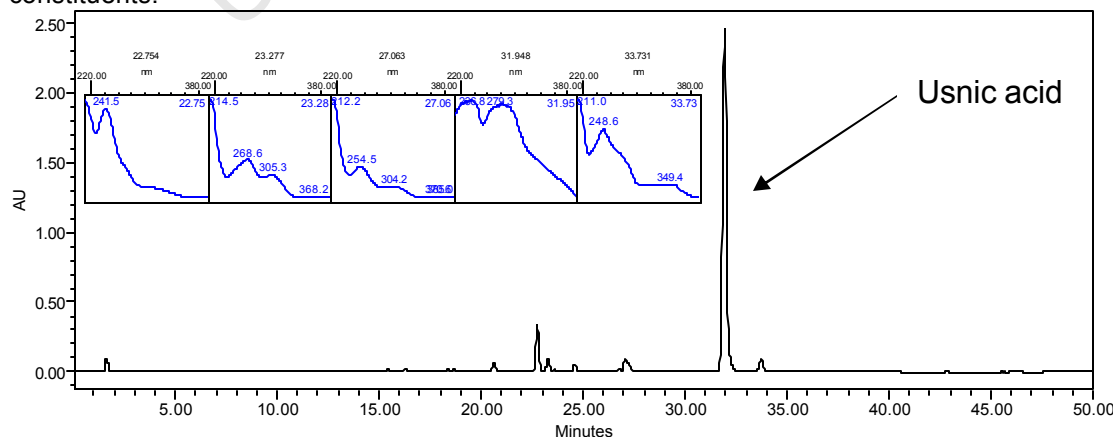


Figure 12: An HPLC chromatogram of the acetone extract of *Usnea rubrotincta* at 248.1nm showing the prominent peak of usnic acid and the inset PDA spectral absorbances of the constituents.



2.2.3 Antimicrobial activity of extracts of *Xanthoparmelia semiviridis* (Eastern Cape)

The acetone extract of *X. semiviridis* (L15) from the Eastern Cape exhibited activity against *S. aureus* (IC₅₀ value of 46.1µg/ml) and *M. aurum* (MIC of 250µg/ml) as shown in Table 3. Due to the large quantity of lichen material collected from the roof tiles of a house, sequential extracts were prepared of this lichen, the yields of which are depicted in the Appendix, Table 34. During the extraction process, precipitates formed in several of the samples. These were collected and tested separately, together with the crude extracts, against *M. aurum* A+, *C. albicans* ATCC 90028, *S. aureus* ATCC 12600 and *K. pneumoniae* ATCC 13883, and the results are shown in Table 5.

Table 5: The activity of *Xanthoparmelia semiviridis* (Eastern Cape) extracts and precipitates against four organisms. The results are described as MIC's in µg/ml followed by IC₅₀ values, if applicable.

Extract	<i>M. aurum</i>	<i>C. albicans</i>	<i>S. aureus</i>	<i>K. pneumoniae</i>
Petroleum ether	125, 84.4±14.5	>2000	250-500	>2000
Dichloromethane	250	2000	2000	>2000
Dichloromethane precipitate	250	>2000	125, 93.0±6.65	>2000
Ethyl acetate	250-500	2000	500-1000	=2000
Ethyl acetate precipitate	1000-2000	2000	=2000	=2000
Methanol	250-500	1000	1000-2000	>2000
Methanol precipitate	500-1000	2000	=2000	>2000
Water	>2000	2000	>2000	>2000
Cip, Nys, INH	0.08-0.16 ± 0.057	1.6 ± 0.11	0.625 ± 0.007	0.042 ± 0.002

In Table 5 it is evident that only two extracts display activity at 125µg/ml or less, namely the petroleum ether extract with an MIC of 125µg/ml against *M. aurum* and the dichloromethane precipitate with an MIC of 125µg/ml against *S. aureus*. From the HPLC profiles of the petroleum ether (PE) extract and dichloromethane (DCM) precipitate displayed in Figures 13 and 14 respectively, together with the yellow colour of both samples, it became apparent that the extracts contained

usnic acid. The DCM precipitate consisted almost entirely of this common lichen metabolite (86.4%). The observed bioactivity corresponds to the reported activity of pure usnic acid described in Table 4. Due to the wealth of literature reports available on the bioactivities of usnic acid, no further work was carried out on these samples.

Figure 13: An HPLC chromatogram of the petroleum ether extract of *Xanthoparmelia semiviridis* from the Eastern Cape at 233.1nm with the individual compound absorbance displayed in the insert.

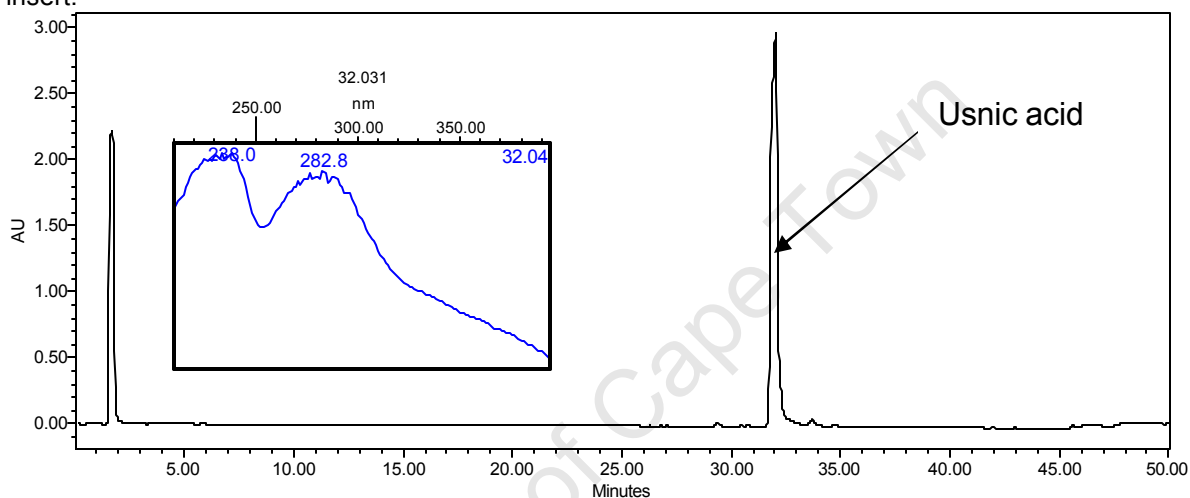
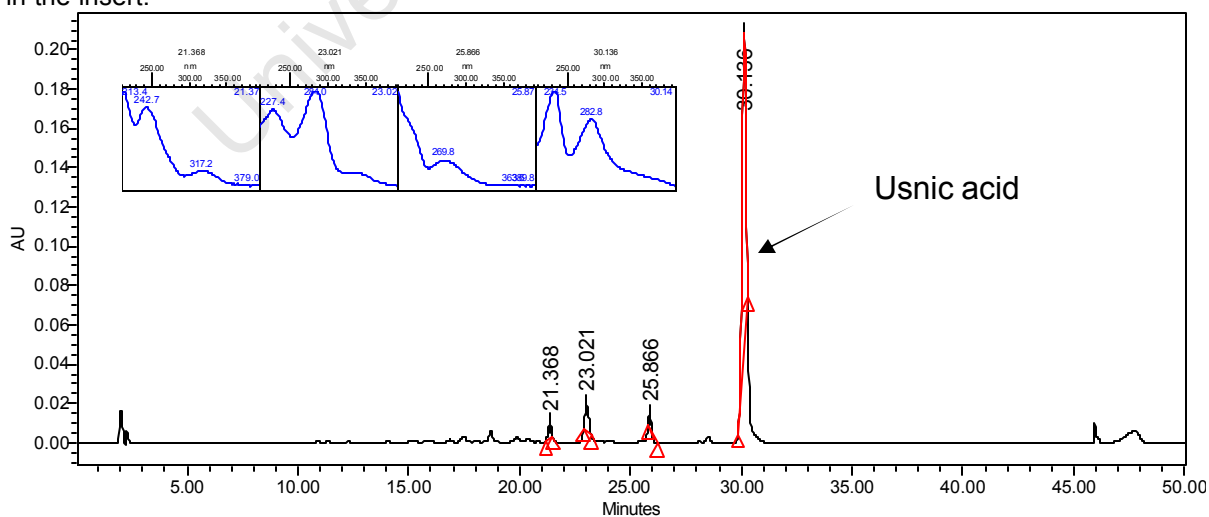


Figure 14: An HPLC chromatogram of the dichloromethane precipitate of *Xanthoparmelia semiviridis* from the Eastern Cape at 254nm with the individual compound absorbances displayed in the insert.



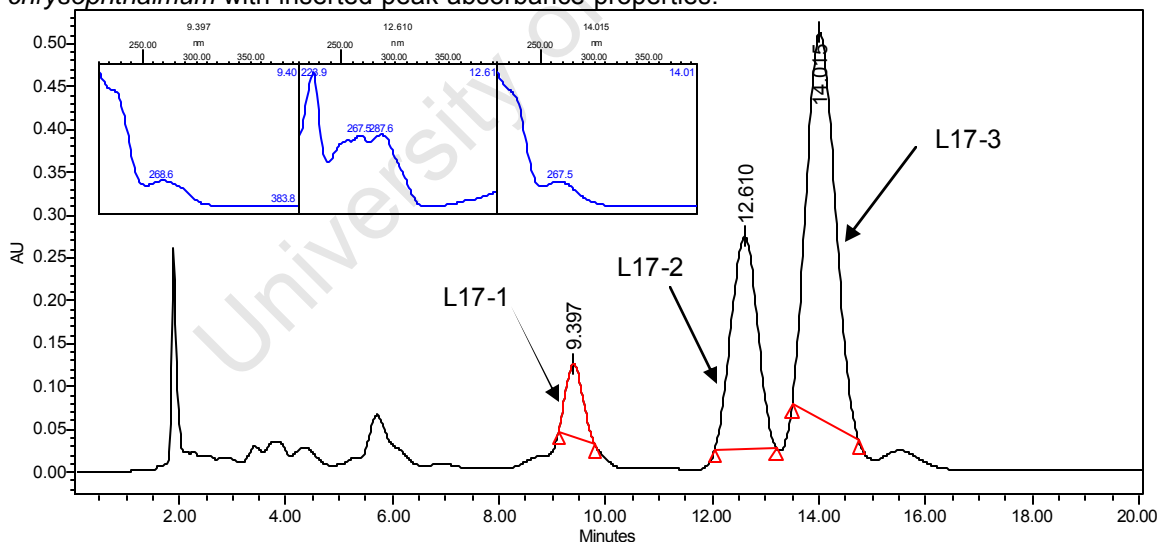
2.2.4 Isolation of compounds from *Teloschistes chrysophthalmum*

The potent anti-Staphylococcal activity of the acetone extract of *T. chrysophthalmum*, as depicted in Table 2, prompted an investigation into its active metabolites.

2.2.4.1 Bioactivity testing of fractions and compounds from *Teloschistes chrysophthalmum*

A liquid-liquid separation of the acetone extract of *T. chrysophthalmum* yielded an acetonitrile (ACN) and a PE fraction as described in Section 7.7.6.1. The ACN fraction was further fractionated into its individual constituents by means of reversed-phase HPLC, as illustrated in Figure 15. Three peaks were collected, eluting at 11.0, 14.6 and 16.7 minutes. Peak 1 (L17-1) had a prominent absorbance at 269.8nm, peak 2 (L17-2) at 223.9nm and peak 3 (L17-3) at 267.5. Peak 2 had a distinctive orange colour.

Figure 15: A chromatogram of the ACN fraction of the acetone extract of *Teloschistes chrysophthalmum* with inserted peak absorbance properties.



These three compounds, L17-1 to L17-3, together with the ACN and PE fractions, were tested for activity against drug sensitive (Figure 16) and methicillin-resistant (MRSA) (Figure 17) *S. aureus*, as well as for cytotoxicity to CHO cells (Figure 18), the results of which are presented in Table 6. The

selectivity indices (SI) for each compound, defined as the quotient of the cytotoxicity and the activity, have also been calculated.

From the data in Table 6, it is evident that the ACN and PE fractions of the acetone extract of *Teloschistes chrysophthalmum* had very similar activity against drug-sensitive *S. aureus*, although the ACN fraction displayed greater activity against MRSA. Subsequent isolation and testing of the three primary constituents of the ACN fraction indicated that compounds L17-1 and L17-3 have moderate MIC values of 31.3 and 15.6 µg/ml respectively, but good IC₅₀ values of 1.1 and 0.7 µg/ml respectively against the drug-sensitive reference strain of *S. aureus* (Figure 16). Both compounds exhibit weaker activity against the reference strain of MRSA, with IC₅₀ values of 11.1 and 11.4 µg/ml respectively (Figure 17). Furthermore, this activity has been shown to be bactericidal against both the drug-sensitive and –resistant strains of *S. aureus*. These compounds exhibit almost no *in vitro* cytotoxicity (IC₅₀'s of 81 and >100 µg/ml respectively; Figure 18) in comparison to the emetine drug control, which displays an IC₅₀ of 25 ng/ml. L17-3 in particular has very low cytotoxicity, with no negative effect being observed at the highest tested concentration, namely 100 µg/ml, and an SI value of greater than or equal to 142.9, while L17-1 displayed an SI value of 73.6. A value of ten or greater would indicate a compound worth investigating as a promising lead-candidate, depending on its drug-like properties.

Table 6: The activity of fractions and pure compounds originating from the lichen *Teloschistes chrysophthalmum* against drug-sensitive and – resistant reference strains of *Staphylococcus aureus*, as well as the toxicity of the two active compounds against CHO cells. Results are described as MIC's and IC₅₀'s in µg/ml.

Fractions/ compounds	CHO cells	Drug-sensitive <i>Staphylococcus aureus</i>				Methicillin-resistant <i>Staphylococcus aureus</i>			
		MIC	IC ₅₀	MBC	SI	MIC	IC ₅₀	MBC	SI
ACN fraction	n/a	19.5-39.1	1.3±0.76	n/a	n/a	31.25	13.7±2.3	n/a	n/a
PE fraction	n/a	39.1	3.1±2.6	n/a	n/a	62.5- 125	32.6±3.1	n/a	n/a
L17-1	81.0±17.8	31.3	1.1±0.8	31.3	73.6	31.3	11.1±4.8	31.3	7.3
L17-2	n/a	>250	n/a	n/a	n/a	>250	n/a	n/a	n/a
L17-3	>100	15.6	0.7±0.2	15.6 – 31.3	>142.9	31.3- 62.5	11.4±3.2	62.5	>8.8
Ciprofloxacin	n/a	0.3	0.236± 0.01	0.3	n/a	0.6	0.225± 0.004	0.6	n/a
Emetine	0.025± 0.003	n/a	n/a	n/a	n/a	n/a	n/a	n/a	n/a

Abbreviations: SI - selectivity index (IC₅₀ cytotoxicity/IC₅₀ antimicrobial activity), CHO - Chinese hamster ovarian cells, DMSO - dimethylsulfoxide, ACN - acetonitrile, PE - petroleum ether, MIC - minimum inhibitory concentration, MBC – minimum bactericidal concentration, n/a – not applicable

Figure 16: The dose response curves of (A) the acetone extract, (B) the ACN fraction, (C) the PE fraction, (D) L17-1 and (E) L17-3 from *Teloschistes chrysophthalmum* against drug sensitive *S. aureus* ATCC 12600. Figure F represents the effect of ciprofloxacin. Each data point represents the average of at least four replicates from two separate experiments and the results are expressed as the percentage organism viability across the log concentration range in $\mu\text{g/ml}$.

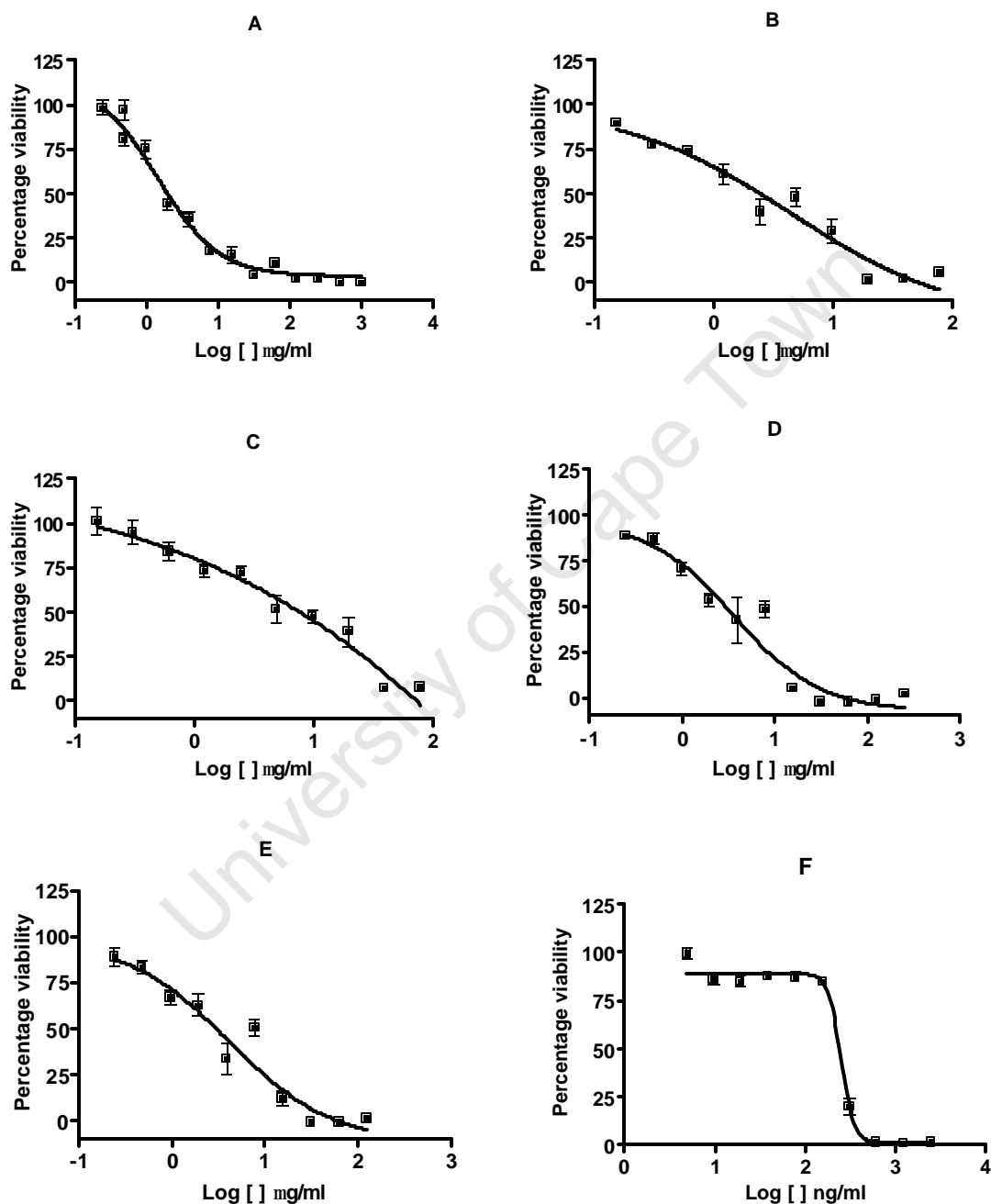


Figure 17: The dose response curves of (A) the ACN fraction, (B) the PE fraction, (C) L17-1 and (D) L17-3 from *Teloschistes chrysophthalmum* against methicillin-resistant *S. aureus* ATCC 43300. Figure E represents the effect of ciprofloxacin. Each data point represents the average of at least four replicates from two separate experiments and the results are expressed as the percentage organism viability across the log concentration range in $\mu\text{g/ml}$.

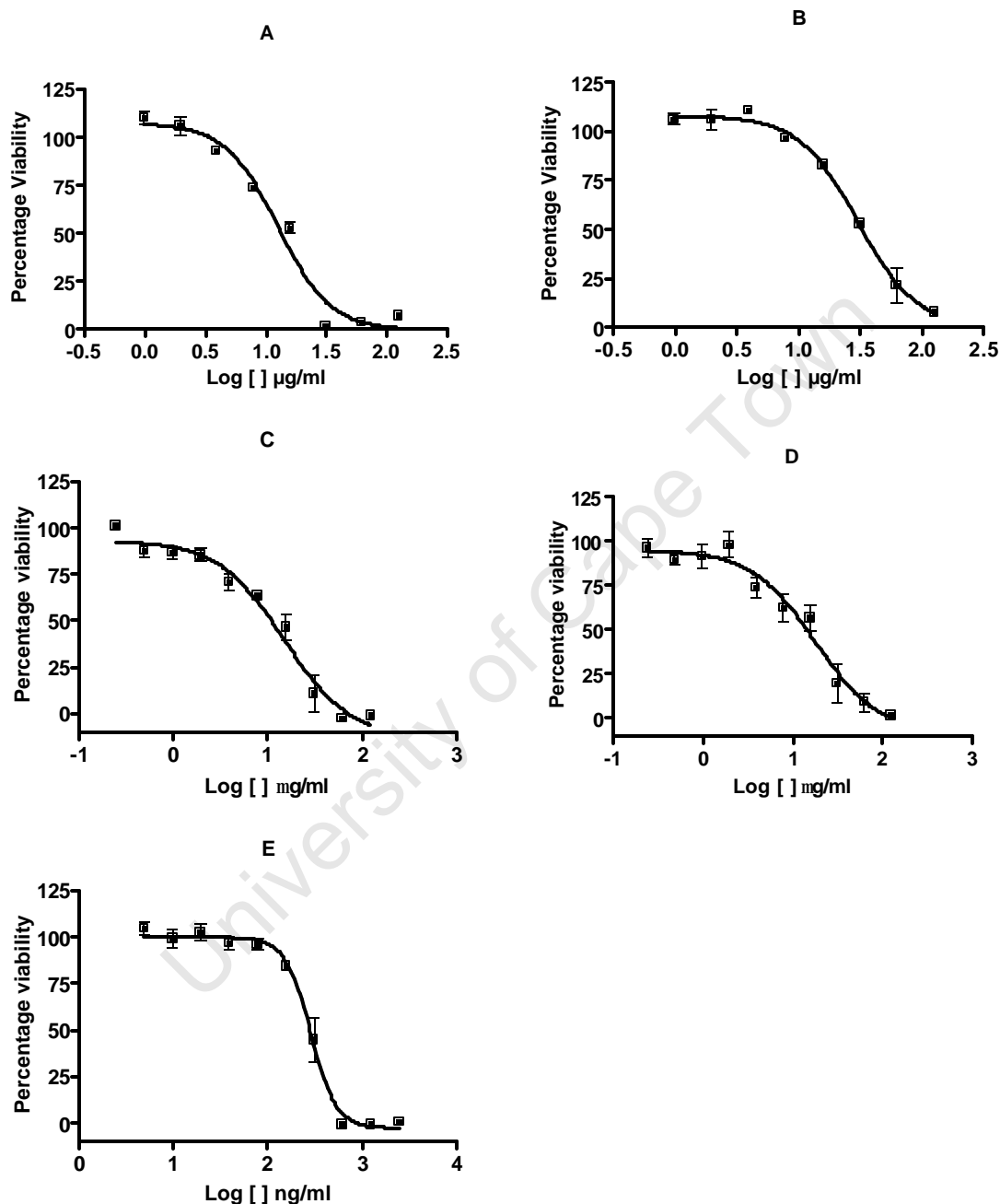
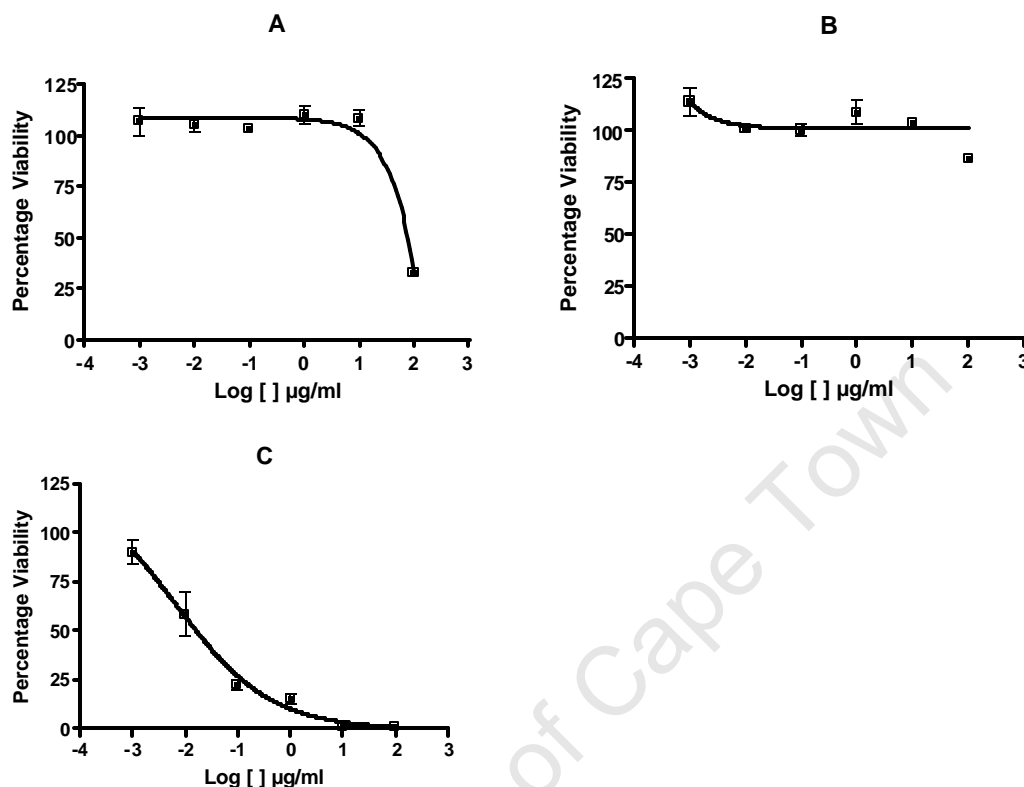


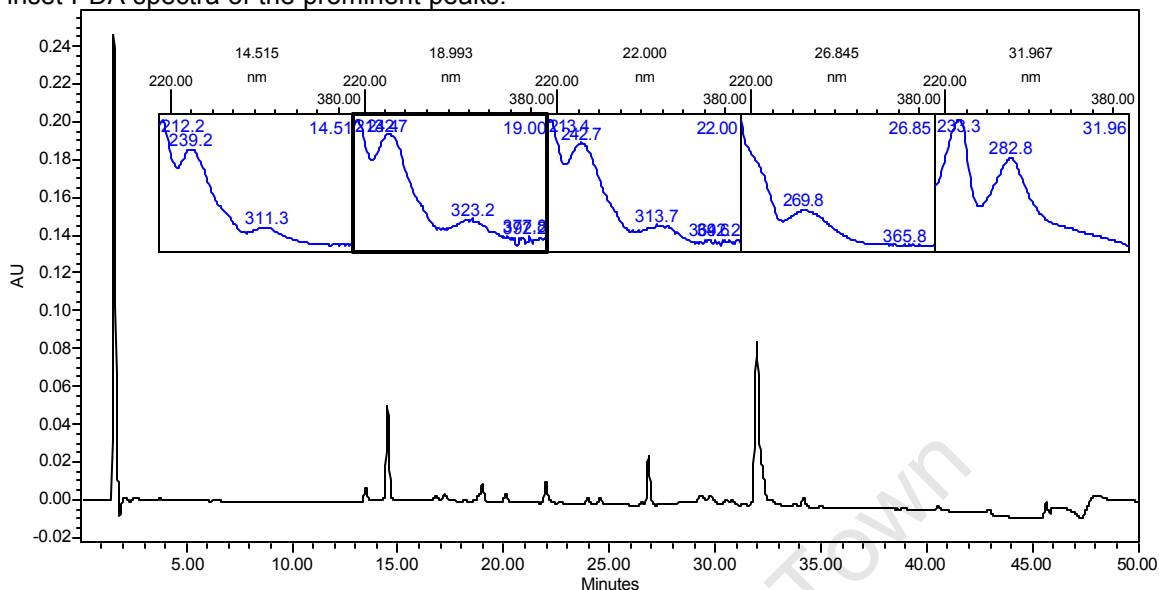
Figure 18: The dose-response curves depicting the effect of L17-1 (A) and L17-3 (B) from *Teloschistes chrysophthalmum* and the drug control, emetine (C) on CHO cells. Each data point represents the average of at least four replicates from two separate experiments and the results are expressed as the percentage organism viability across the log concentration range in $\mu\text{g/ml}$.



2.2.4.2 Comparison of the constituents of the PE and ACN fractions of *Teloschistes chrysophthalmum* to those of the acetone extract of the growth substrate

A comparison of the fractions originating from the acetone extract of *T. chrysophthalmum* and the roof tile substrate on which the lichen was found growing was performed to ensure that the active constituents did not originate from the substrate, but were in fact lichen metabolites. The HPLC chromatogram of the acetone extract of the roof tiles is depicted in Figure 19, while those of the ACN and PE fractions of the acetone extract of the lichen are shown in Figures 20 and 21 respectively.

Figure 19: An HPLC chromatogram of the acetone extract of the roof tiles at 242.3nm with the inset PDA spectra of the prominent peaks.



The chromatogram above of the acetone extract of the roof tile substrate on which the lichen was found growing, shows three prominent peaks at 14.5, 26.8 and 31.9 minutes. These three peaks have prominent absorbances at 239.2 and 311.3, 269.8 and 365.8, and 233.3 and 282.8nm respectively.

Figure 20: An HPLC chromatogram of the acetonitrile fraction of the acetone extract of *Teloschistes chrysophthalmum* at 242.3nm with the inset PDA spectra of the prominent peaks.

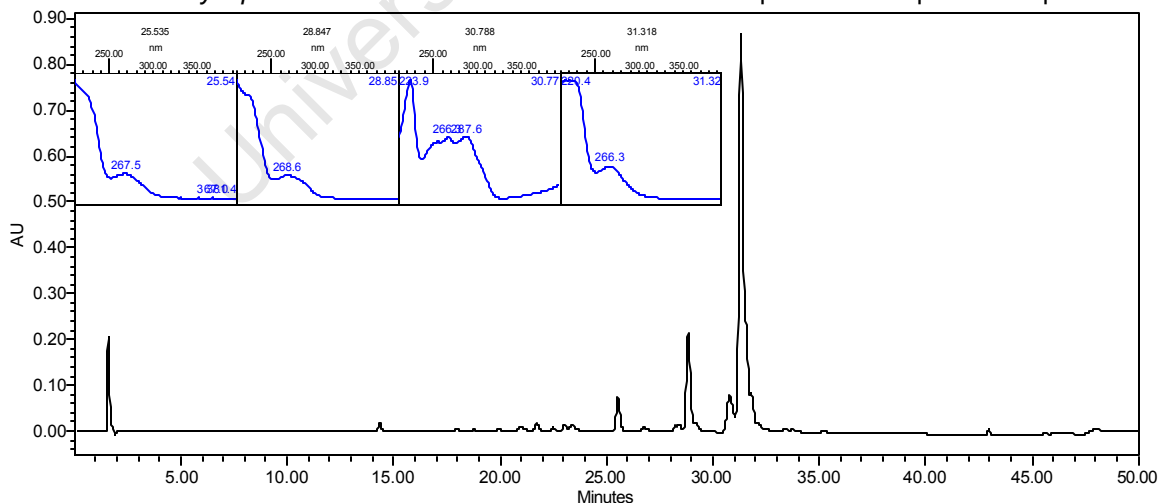
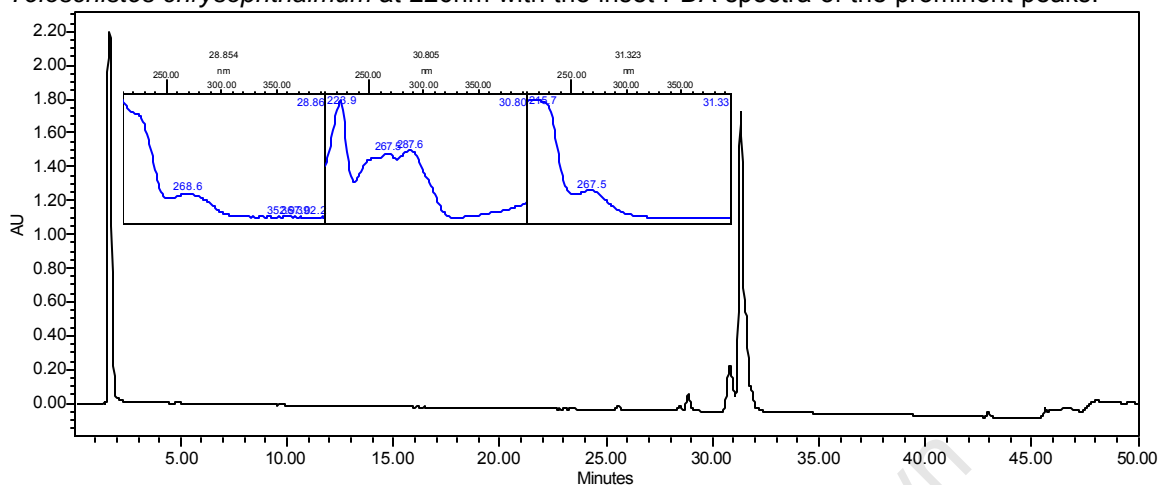


Figure 21: An HPLC chromatogram of the petroleum ether fraction of the acetone extract of *Teloschistes chrysophthalmum* at 226nm with the inset PDA spectra of the prominent peaks.



The chromatograms of the ACN and PE fractions of the acetone extract of *T. chrysophthalmum* (Figure 20 and 21 respectively) indicate that these two fractions contain the same primary peaks eluting at 28.8, 30.8 and 31.3 minutes. Furthermore, these peaks appear to have the same absorbance spectra as indicated by the PDA spectral inserts in the chromatograms. It is clear, however, that these fractions do not share any similar constituents with the acetone extract of the roof tiles, indicating that the isolated active compounds are of lichen origin.

2.2.4.3 Identification of active compounds from *Teloschistes chrysophthalmum*

The active constituents of the acetone extract of the lichen, *T. chrysophthalmum*, were subjected to NMR analysis on 600 MHz and 900 MHz instruments as described in Section 7.7.6.3, as well as tandem mass spectrometry (LC-MS/MS) and high-resolution mass spectrometry (HR-MS) as described in 7.7.6.4 in an effort to identify their molecular structures. The ^1H and ^{13}C spectra of L17-1 are illustrated in Figures 22 and 23 respectively.

Figure 22: The ^1H NMR Spectrum of L17-1 isolated from *Teloschistes chrysophthalmum*.

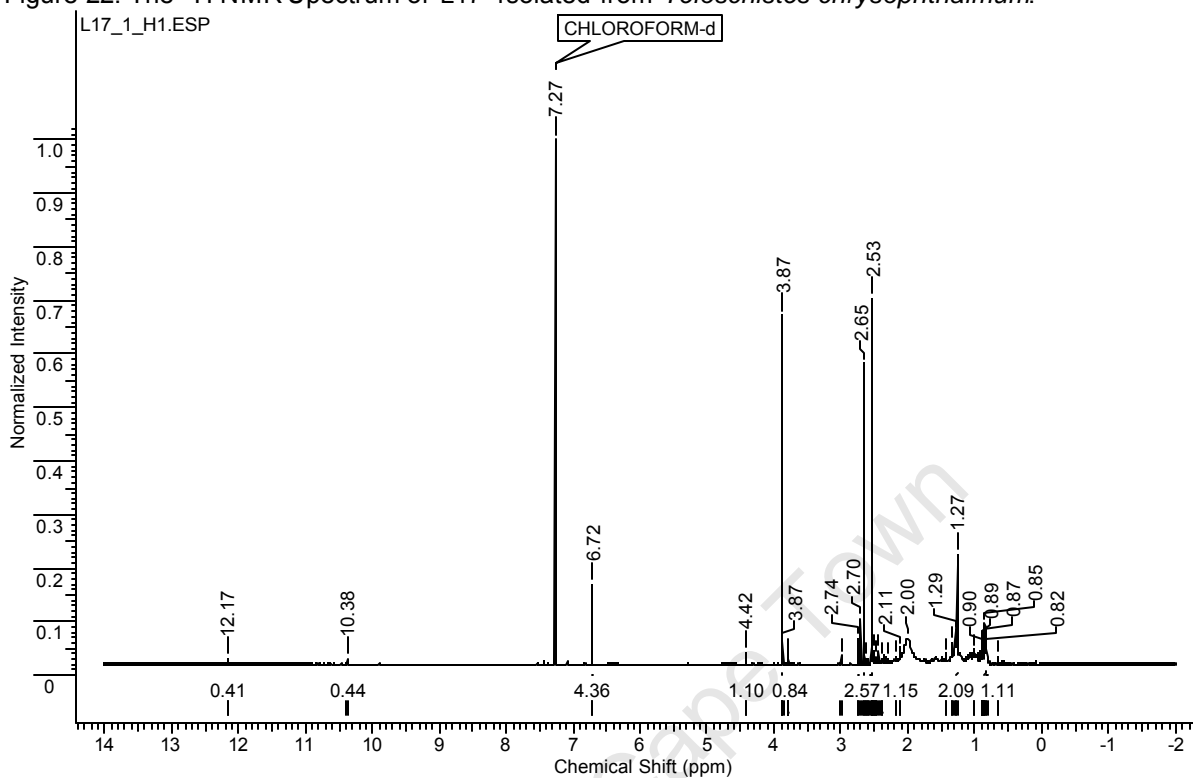
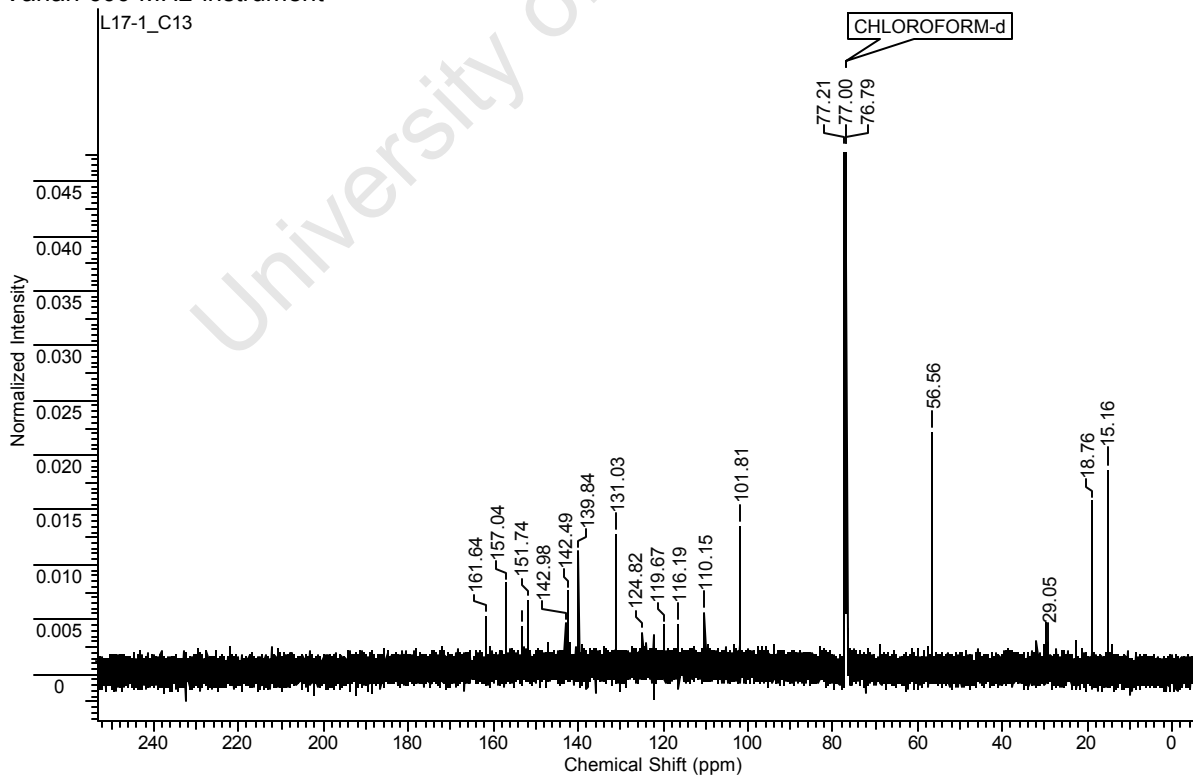


Figure 23: The ^{13}C spectrum of L17-1 isolated from *Teloschistes chrysophthalmum* obtained on a Varian 600 MHz instrument



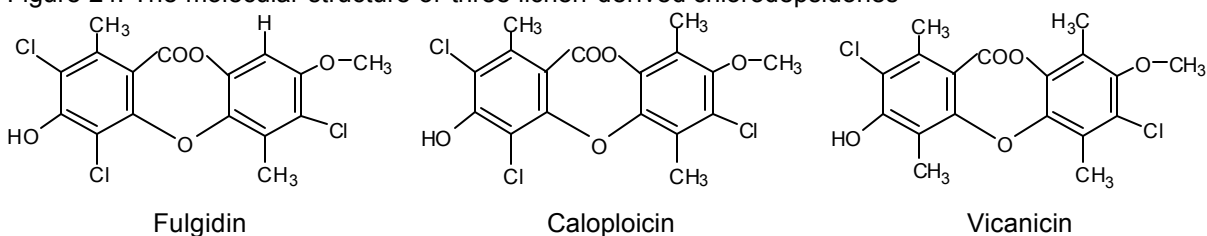
From the ^1H spectrum of L17-1 illustrated in Figure 22 and the two-dimensional spectra shown in the Appendix, Figures 61 to 65, the presence of a single aromatic proton is detected at a chemical shift of 6.72 bonded to the carbon resonating at 101.8 and within two to three bonds of the carbon resonating at a chemical shift of 153.1 (Table 7). This suggests that the aromatic ring/s is/are fully substituted with the exception of a single protonated carbon.

Table 7: The NMR chemical shift values and two-dimensional correlations for L17-1

^1H (d)	^{13}C (GHSQC) (d)	GHMBC (d)	DEPT
2.53	18.8	139.8, 119.7, 116.2	CH_3
2.65	15.2	143.0, 131.0, 119.7	CH_3
3.87	56.6	153.1	CH_3
6.72	101.8	153.1, 143.0, 142.5, 119.7	CH

Furthermore, the strong resonance on the ^1H spectrum at a chemical shift of 3.87 is associated with a carbon with a chemical shift of 56.6 within two to three bonds of the carbon with a resonance typical of that associated with a methoxy group ($\text{d}=153.1$). From the DEPT spectrum, it is evident that there are a further two methyl groups at 18.8 and 15.2 with the associated protons resonating at a chemical shift of 2.53 and 2.65 respectively. Both of these methyl groups are within two to three bonds of the carbon resonating at 119.7, as is the aromatic proton at $\text{d} = 6.72$. The ^{13}C spectrum suggests the potential presence of two carbonyl groups resonating at a chemical shift of 161.64 and 157.04. However, without X-ray crystallographic information, it is not possible at this stage to determine the exact location of the substituents on the molecular structure.

Figure 24: The molecular structure of three lichen-derived chlorodepsidones



The aromatic ring of L17-1 shares the same NMR characteristics as those reported by Mahandru and Gilbert (1979) for the aromatic ring of the depsidone, fulgidin, illustrated in Figure 24. Briefly, the aromatic rings contains two methyl groups (1H d 2.50 and 2.56), an aromatic methoxy group (1H d 3.97), two chlorine atoms and an aromatic proton (1H d 6.57). As illustrated by the mass spectrum in Figure 25, L17-1 has an accurate mass of 386.9383 with molecular ions of 386.9, 388.9, 390.9 and 392.9 at a ratio of 21.3:21.3:7.3:1 in the negative ion mode. Similarly, fulgidin has molecular ions at 388, 390, 392 and 394 at a ratio of 27:27:9:1, typical of a compound containing three chlorine atoms (molecular formula $C_{16}H_{11}Cl_3O_3$). However, the mass differences suggest the absence of one proton on L17-1, potentially with regards to the hydroxyl group, as no hydroxy-associated proton resonances are apparent for L17-1.

Figure 25: The high-resolution mass spectrum and predicted elemental composition of compound L17-1

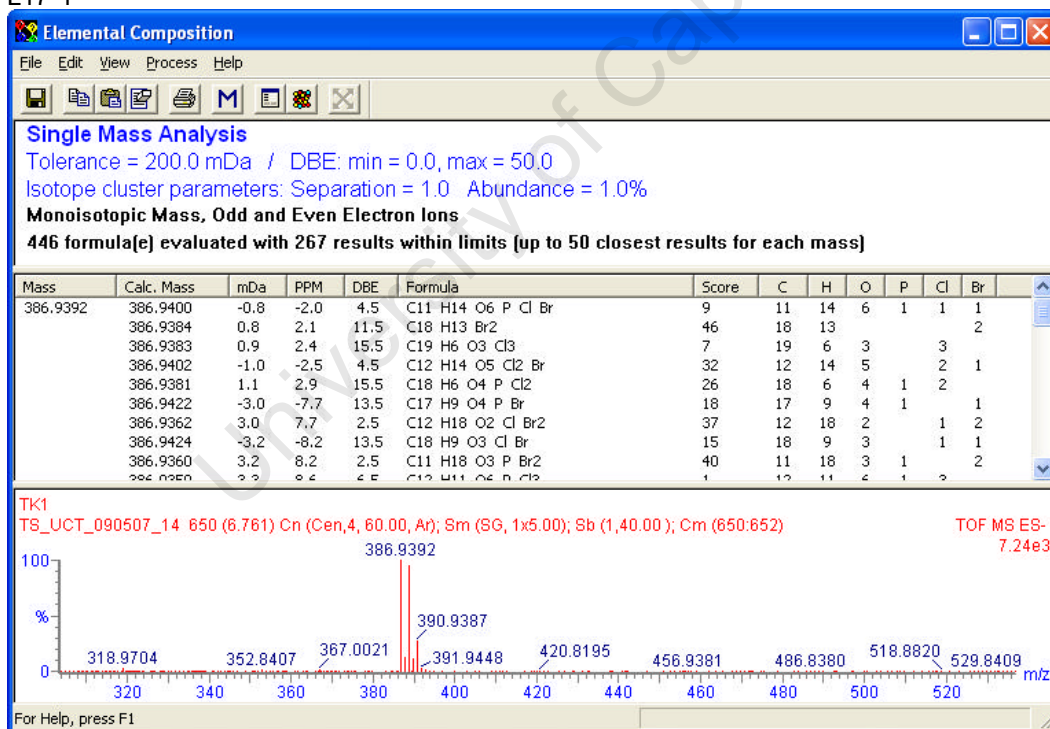
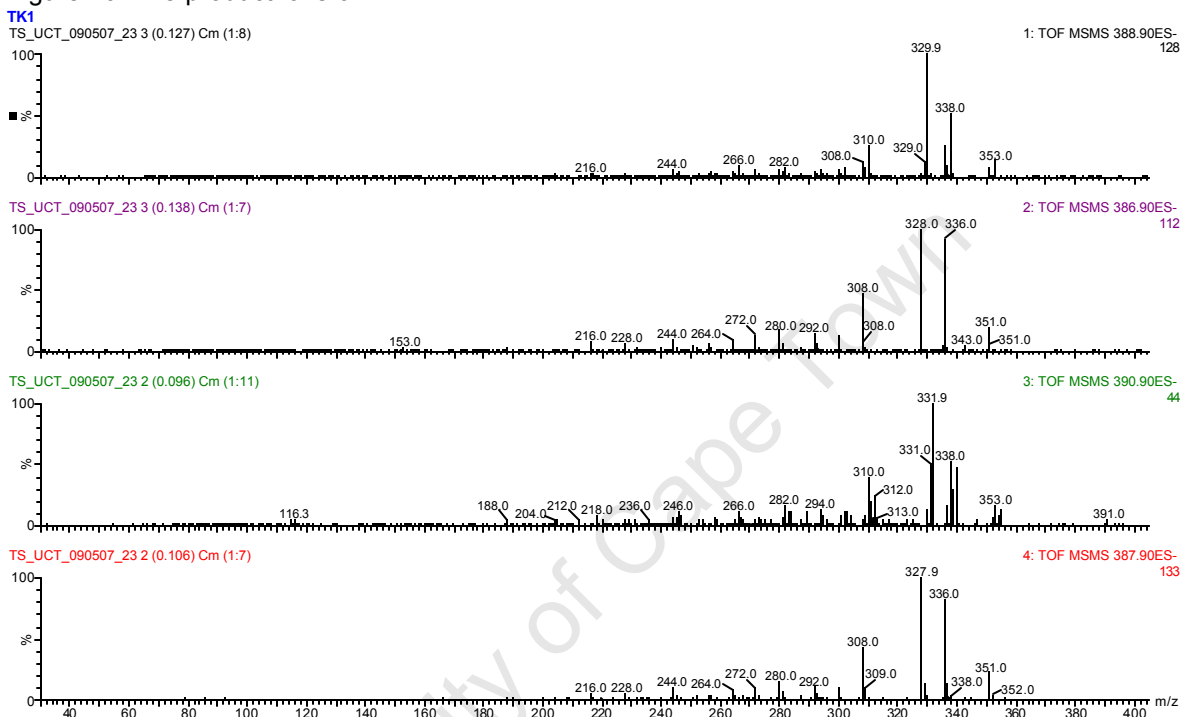


Figure 25 resulting from HR-MS, suggests a likely molecular formula of L17-1 to be $C_{19}H_6O_3Cl_3$. The most promising predicted elemental composition suggested the presence of bromine atoms. However, the arrangement of ions on the mass

spectrum suggests the presence of chlorine isotopes, with the characteristic variation of two mass units. The most abundant product ions were shown to have masses of 328 and 308, as shown in Figure 26. Initial losses of three masses of 15 suggest the loss of methyl groups (353 ? 338 ? 308).

Figure 26: The product ions of L17-1



The ^1H and ^{13}C spectra obtained for L17-3 are depicted in Figures 27 and 28 respectively, while the 900 MHz and two-dimensional NMR spectral data are illustrated in the Appendix Figures 66 to 79. L17-3 appears to be closely related to L17-1, with the exception of the absence of a proton on the aromatic ring, which appears to be fully substituted, as well as an extra methyl group. As shown in Table 8, the strong resonance at 3.79 on the ^1H spectrum could indicate either the presence of chlorine atoms or the protons of a methoxy group bonded to a carbon with a chemical shift value of 60.4.

The methoxy group is attached to the carbon on the aromatic ring with a chemical shift value of 152.4. The proton resonances at 2.32 and 2.44 which are bonded to the carbon possessing a chemical shift of 10.5 suggest a methyl

group, the protons of which are separated from the aromatic carbon at d152.4 by two to three bonds. The DEPT spectrum indicates the presence of a further two methyl groups (^{13}C d15.1 and 18.9). As with L17-1, the ^{13}C spectrum suggests the presence of two carbonyl groups (d161 and 156). As with L17-1, it is not possible to determine the exact location of the substituents without X-ray crystallographic information.

Table 8: The NMR chemical shift values and two-dimensional correlations for L17-3

^1H (d)	^{13}C (GHSQC) (d)	GHMBC(d)	COSY(d)	DEPT
2.32	10.5	122.6, 141.4, 152.4, 10.5	2.52, 2.62	CH_3
2.44	10.5	114.4, 153.6, 161.5, 18.9		CH_3
2.52	18.9	125.8, 127.7, 146.1, 10.5	2.32	CH_3
2.54	18.9	116.3, 119.8, 139.8, 15.1		CH_3
2.62	15.1	125.8, 127.7, 146, 18.9	2.32	OCH_3
3.79	60.4	152.4		CH_3

Figure 27: The ^1H NMR spectrum of L17-3 isolated from *Teloschistes chrysophthalmum* obtained on a Varian 600 MHz instrument

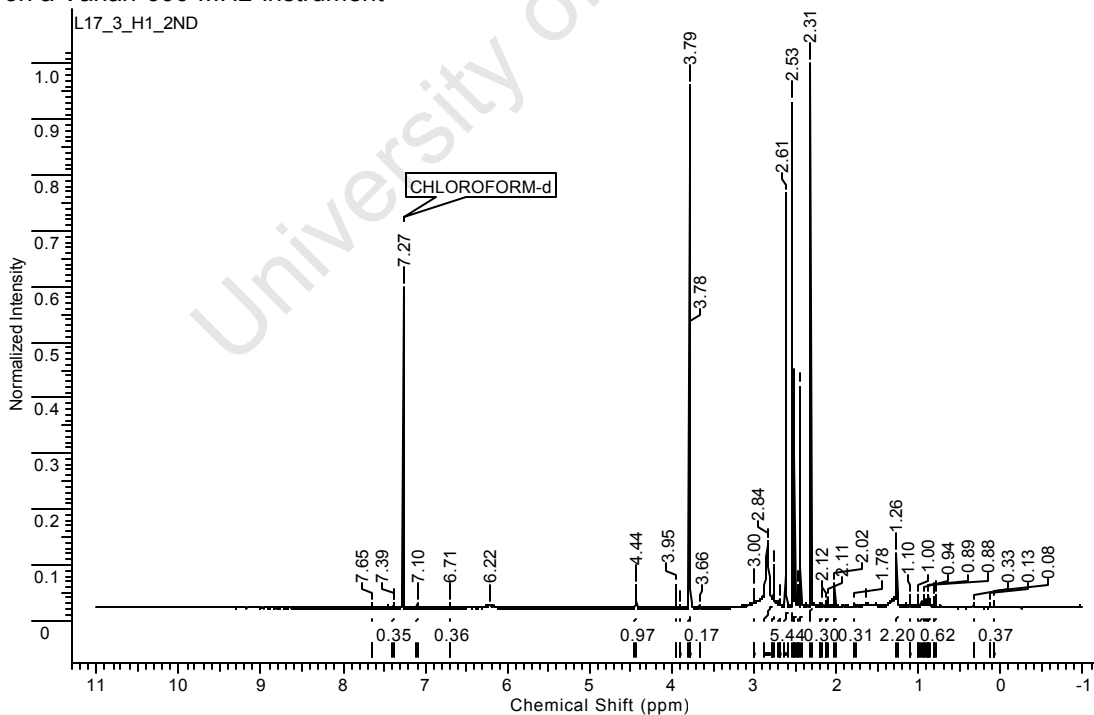


Figure 28: The ^{13}C NMR spectrum of L17-3 isolated from *Teloschistes chrysophthalmum* obtained on a Varian 600 MHz instrument

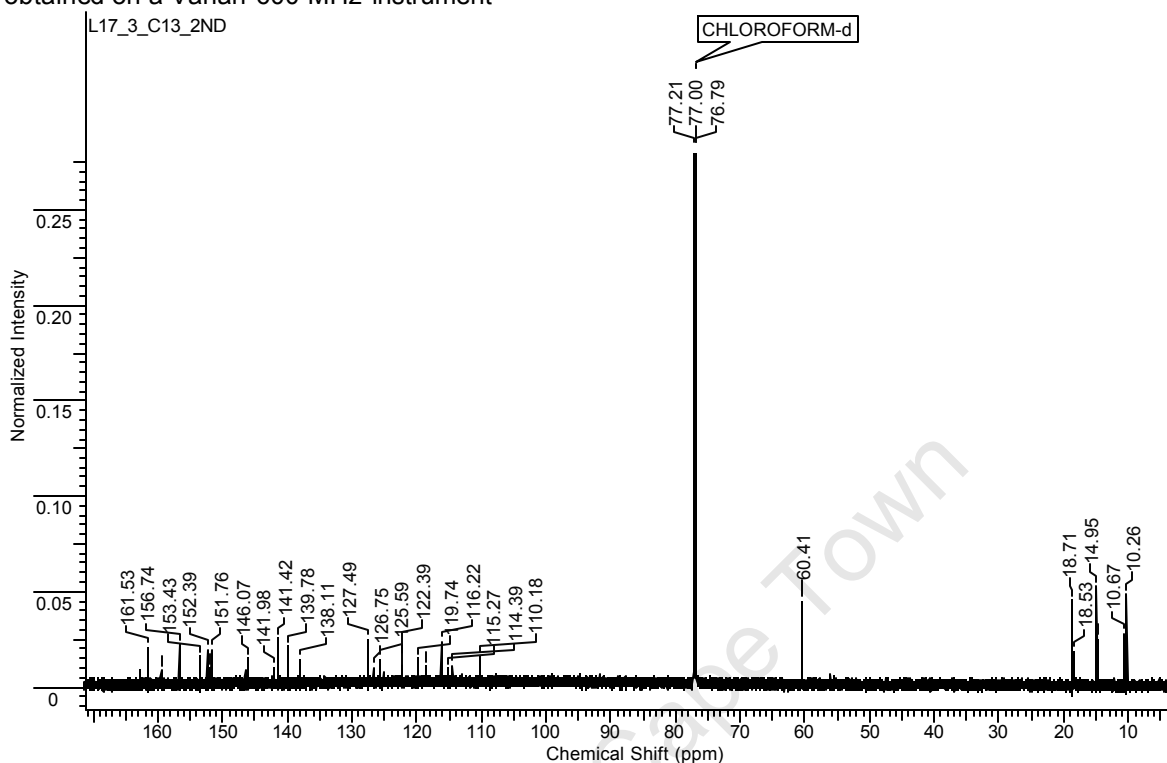


Figure 29: The high-resolution mass spectrum and predicted elemental composition of L17-3

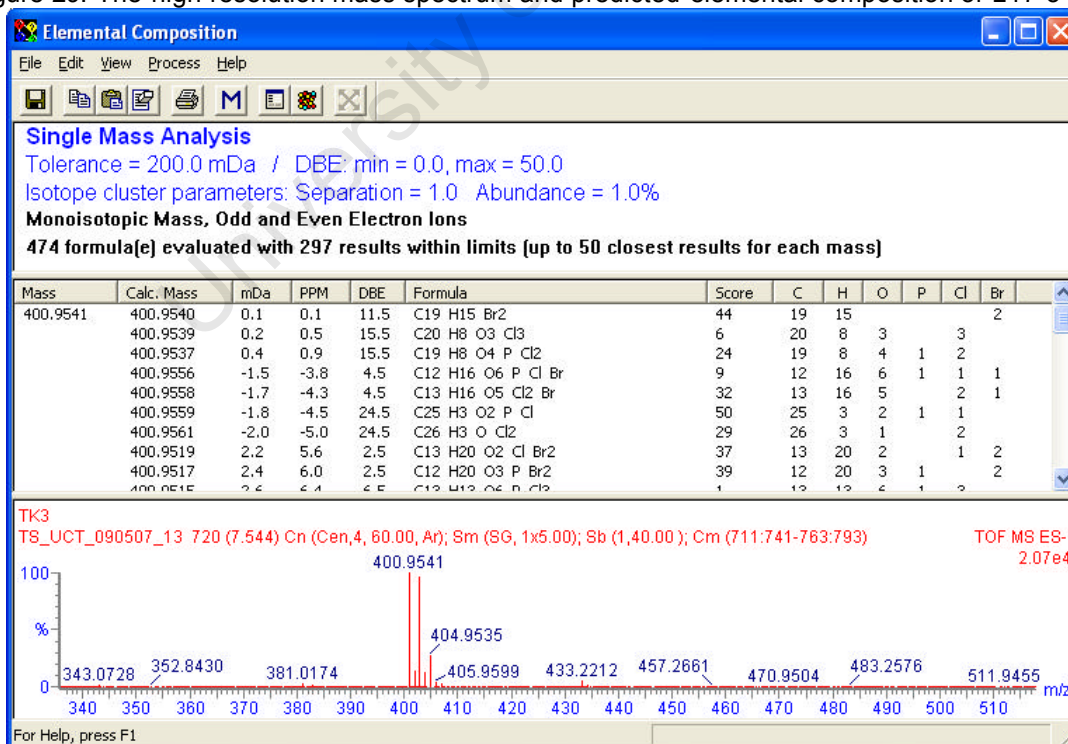
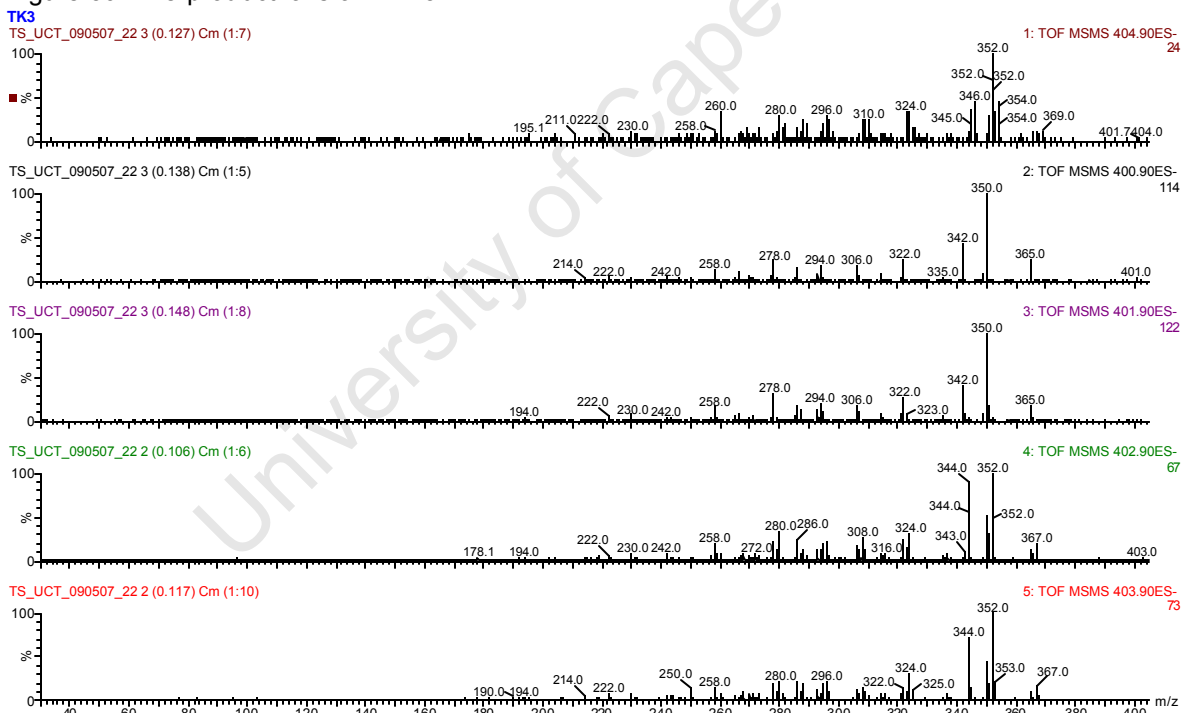


Figure 29 illustrates the high resolution mass spectrum of L17-3, the accurate mass of which was determined to be 400.9541. Molecular ions at 400.95, 402.95, 404.95 and 405.95 at a ratio of 12.8:12.8:4:1 once again indicates the presence of chlorine atoms with the characteristic two mass unit variation. A likely elemental composition of this compound is predicted to be $C_{20}H_8O_3Cl_3$, as is shown in Figure 29. The most prominent product ions of L17-3 have masses of 350.0, 342.0, 322 and 278.0, as depicted in Figure 30. The loss of a chlorine atom explains the loss of 35 mass units from 400 ? 365, while a loss of 15 could account for the loss of a methyl group from a mass of 365 ? 350. The further loss of a 12 mass units can be attributed to the loss of a carbon atom to a mass of 342.

Figure 30: The product ions of L17-3



2.3 Discussion

Very little work has been performed on the pharmacological usefulness of lichens to medicine, most likely due to the difficulties in identification of species, slow growth rate, problematic axenic culture, as well as collection of large enough quantities for biological evaluation and isolation of compounds (Boustie and Grube, 2005). Eloff (1998b) showed that extraction of plant material with acetone yields the highest number of compounds, subsequently resulting in the best antimicrobial activity when compared to other extraction solvents such as ethanol, methanol and water. Due to the small quantities of lichen material collected, as well as previous literature reports on extract preparation from lichens (Madamombe and Afolayan, 2003), acetone was therefore used as the primary extractant. In an attempt to produce research of a high quality, every effort was taken to work according to internationally acceptable recommendations, as proposed by Cos *et al.* (2006).

The acetone extract of *Teloschistes chrysophthalmum* displayed the greatest activity against any of the micro-organisms tested exhibiting an MIC of 15.6 to 31.3 µg/ml (IC₅₀ of 1.1 µg/ml) against *S. aureus*. Antimicrobial activity has previously been reported from a *Teloschistes* species in New Zealand (Perry *et al.*, 1999). In general, none of the lichen extracts displayed good activity against *C. albicans* and *K. pneumoniae*. Paudel *et al.* (2008) similarly reported activity of extracts of Antarctic lichens against Gram-positive organisms, but no activity against Gram-negative bacteria or fungi was observed. The fact that none of the crude lichen extracts exhibited activity against *K. pneumoniae* is not surprising, as Gram-negative bacteria are known to be intrinsically more resistant to antimicrobial agents as a result of their relatively impermeable cell wall, as well as efficient efflux systems which actively pump the drug out of the cell (Berlanga *et al.*, 2004; Verhoef and Fluit, 2006). In a similar study involving plant extracts, Rabe and Van Staden (1997) found that almost all of the observed activity from their 21 plant extracts was against Gram-positive organisms, while none of the extracts exhibited activity against *K. pneumoniae*.

Other than *T. chrysophthalmum*, only two other extracts showed promising activity, namely that of *X. semiviridis* of the Eastern Cape against *S. aureus* and *U. rubroincta* against *S. aureus* and *M. aurum*. The differences in the activities of the two *X. semiviridis* species collected from two different provinces of South Africa shows the impact of habitat on the compounds produced by the lichens and subsequently affecting activity, as has been described in the literature by various authors (Fiscus, 1972; Hesbacher *et al.*, 1996; Culberson, 1967; Culberson *et al.*, 1973; Culberson, 1969).

Bio-autography is a useful tool in pin-pointing active compounds within a mixture (Cos *et al.*, 2006; Nostro *et al.*, 2000). However, this method was unsuccessful in the evaluation of lichen extracts due to the requirement of high levels of either formic acid or trifluoroacetic acid in the mobile phase to facilitate adequate separation. Despite various attempts to remove residual acid from the plates, remaining traces were enough to inhibit organism growth, as mentioned in the literature (Cos *et al.*, 2006). Therefore, for the purposes of identifying those compounds responsible for the observed activity in the crude fractions, HPLC was used as the primary means of isolation.

The common lichen metabolite, usnic acid, has previously been shown to display potent activity against mycobacteria (Ingólfssdóttir *et al.*, 1998) and moderate to good activity against bacteria (Lauterwein *et al.*, 1995, Francolini *et al.*, 2004), including activity of the salt thereof against drug-resistant bacterial pathogens (Elo *et al.*, 2007), but its activity against the malaria-causing organism, *Plasmodium falciparum*, albeit moderate, has not been reported previously. By means of HPLC analysis, the presence of usnic acid was found in the lichen *U. rubroincta*, and its moderate activity against *M. aurum* and *S. aureus* was attributed to the presence of this compound. Extracts of a related species, *U. barbata*, from the Eastern Cape Province of South Africa, has also displayed a wide range of antimicrobial activity, particularly against Gram-positive organisms.

Although the active principle was not isolated, it seems plausible that usnic acid was responsible for the observed activity (Madamombe and Afolayan, 2003). Similarly, usnic acid was also found in the petroleum ether and dichloromethane precipitate of *X. semiviridis* from the Eastern Cape, explaining their activities against the same two organisms. Lauterwien *et al.* (1995) showed that usnic acid exhibited an MIC of 2µg/ml against clinical isolates of *S. aureus*. In this study utilizing a reference strain of *S. aureus*, the compound exhibited an MIC of 500µg/ml. The results of broth micro-dilution testing showed that usnic acid had an MIC of 15.6µg/ml against *M. aurum*, similar to the findings of Ingólfssdóttir *et al.* (1998) who found that it inhibited the growth of *M. aurum* at a concentration of 32µg/ml. Further work on these two lichens was therefore not continued.

The acetone extract of the most active lichen, namely *T. chrysophthalmum*, was fractionated using ACN and PE to further prepare the sample for reversed-phase HPLC, as acetone has the ability to extract very non-polar, fatty substances which could damage a C₁₈ column. Three compounds were subsequently isolated from the ACN fraction. L17-1 and L17-3 displayed moderate MIC values, but potent IC₅₀ values of 1.1 and 0.7µg/ml respectively against drug-sensitive *S. aureus*, while L17-2 was inactive at the highest concentration tested, namely 250µg/ml. As suggested by Cos *et al.*, (2006), a hit against the drug sensitive strain of *S. aureus* was followed up with testing against a reference strain of MRSA. These compounds showed less activity against MRSA, with IC₅₀ values of 11.1 and 11.4µg/ml for compounds L17-1 and L17-3 respectively. L17-1 and L17-3 displayed cytotoxicity at 81 and greater than 100µg/ml respectively, resulting in very promising selectivity indices of 73.6 and >100 respectively against drug-sensitive *S. aureus*. An SI value of greater than ten indicates a promising compound with good *in vitro* activity and low cytotoxicity which should be further evaluated in the drug-development process (Orme, 2001).

Furthermore, to ensure that the anti-Staphylococcal compounds isolated were in fact lichen-metabolites and not compounds originating from the growth substrate,

HPLC analysis was performed on extracts of the lichen and the substrate. From these chromatograms, it is apparent that the isolated compounds are lichen metabolites. These results also showed that the PE fraction of the acetone extract of *T. chrysophthalmum* also contains a high concentration of L17-3 isolated from the ACN fraction.

Despite obtaining NMR spectral data from 600 MHz and 900 MHz NMR instruments, as well as high-resolution mass spectrometry data, it has not been possible to completely decipher the structures of L17-1 and L17-3 isolated from *T. chrysophthalmum*. Furthermore, attempts to grow crystals for X-ray crystallographic purposes have been unsuccessful over a period of eight months. Time constraints have forced the continuation of this project in the absence of structural information. It is recognized that identification of lichen metabolites can be challenging, and that crystallization is often required to confirm structural characteristics (Boustie and Grube, 2005). However, the aromatic ring of L17-1 shares the same characteristics as those reported by Mahandru and Gilbert (1979) for the aromatic ring of the depsidone, fulgidin, containing two methyl groups, an aromatic methoxy group, two chlorine atoms and an aromatic proton. L17-1 further displays resonances associated with two carbonyl groups. L17-3 has similar characteristics for the aromatic ring, differing from L17-1 only with regards to the absence of an aromatic proton, suggesting a fully substituted aromatic ring. Other depsidones with similar structures include fulgoicin, caloploicin and vicanicin, the latter of which have fully substituted aromatic rings, but whose masses do not correspond to that of L17-3. Furthermore, these compounds possess an aromatic hydroxyl group which does not appear to be present in L17-3.

Over 800 compounds have been identified from lichens, but most of these compounds have not been well studied for pharmacological activity (Kokubun *et al.* 2007). Kokubun *et al.* (2007) evaluated the activities of several lichen-derived compounds against MRSA and multidrug-resistant *S. aureus* strains. The

authors found that depsidones containing long alkyl chains on both aromatic rings were active against the panel of bacterial strains tested in ranges comparable to those of clinical antibacterial drugs, results suggesting a novel mechanism of action. These depsidones exhibited activity against the various strains of *S. aureus* with MIC's ranging from 16 to 128µg/ml, values similar to those displayed by L17-1 and L17-3. Despite the structures of L17-1 and L17-3 being unclear at this stage, the possibility exists that they may in fact be depsidones, based on the similarities of the A-ring spectral data. However, the compounds isolated in this project definitely contain chlorine atoms, a feature not present in the compounds tested by Kokubun *et al.* (2007). Depsidones, aromatic rings linked with ester bonds, have previously been shown to display antiviral, anti-inflammatory and photoprotective properties (Müller, 2001). Abdou *et al.* (2010) evaluated four depsidones (no chlorine atoms), botryorhodines A to D, isolated from an endophytic fungus, for biological activity. The authors found that two of the four compounds displayed moderate to weak cytotoxicity (96.97 and 36.41µg/ml) while the other two compounds displayed no cytotoxicity. Furthermore, two of the compounds displayed mild antibacterial activity (data not shown), while the other two compounds also displayed moderate activity against pathogenic fungi.

The genres of the family Teloschistaceae have much morphological and ecological heterogeneity, often distinguished by the yellow/orange colour due to the presence of anthraquinones (Gaya *et al.*, 2008). Several compounds have been isolated from the genus, *Teloschistes*, including fatty acids (Reis *et al.*, 2005) and polysaccharides (Reis *et al.*, 2002). The former authors found that the degree of saturation of these compounds changed with each season and that the fatty acid composition of the lichen and its individual symbionts did not correspond. The anthraquinones parietin, teloschistin, emodin and 7-chloroemodin have been isolated from *T. exilis* and *Caloplaca erhythrantha* (Rosso *et al.*, 2003). Furthermore, the authors successfully isolated parietin and 7-chloroemodin from the respective cultured mycobionts. In the current project,

attempts were made to culture the fungal component of the lichen species, as described by Crittendon *et al.* (1995) and Kranner *et al.* (2002a) (data not shown). Repeated wide-spread contamination of the culture plates and the distinct possibility of the produced metabolites being lichen-specific, both of which have been previously reported, led to the halting of culture efforts (Boustie and Grube, 2005; Crittendon *et al.*, 1995 and Kranner *et al.*, 2002a).

In comparison to literature reports of promising antibiotic lead compounds, the two lichen-derived compounds with anti-Staphylococcal activity isolated in this study have moderate activity. Three novel promising 1 β -methylcarbanpenems exhibited activity against drug-sensitive *S. aureus* with MIC's of 0.016 to 0.031 μ g/ml and against MRSA with MIC's of 24 μ g/ml (Ueda and Sunagawa, 2003). A promising drug candidate, the 3-(heteroarylthio)cepham RWJ333441, displayed *in vitro* activity against methicillin susceptible and resistant strains of *S. aureus* at 0.25 μ g/ml and 2 μ g/ml respectively (Glinka *et al.*, 2003). Similarly a synthetic compound arising from high-throughput screening of a compound library showed *in vitro* activity against drug-sensitive and -resistant strains of *S. aureus* with MIC's of 1 μ g/ml. Another 1 β -methyl carbapenem with broad-spectrum Gram-positive activity, SM-17466, had an *in vitro* MIC₉₀ of 0.006 μ g/ml against *S. aureus* and 3.13 μ g/ml against MRSA. In comparison, vancomycin has MIC₉₀'s of 1.56 μ g/ml against methicillin sensitive and resistant *S. aureus*. Furthermore, this activity against MRSA was shown to be bactericidal (Sumita *et al.*, 1995). Despite L17-1 and L17-3 having moderate MIC values in comparison to literature reports of promising anti-Staphylococcal drug candidates, both compounds appear to have growth inhibitory effects at much lower concentrations, with subsequently low IC₅₀ values of 0.7 and 1.1 μ g/ml. This activity, together with the apparent lack of cytotoxicity, counts in the favour of these two compounds, particularly L17-3, which showed no toxicity at the highest concentration tested, namely 100 μ g/ml.

Chapter 3

Desiccation-tolerant plants

3.1 Introduction

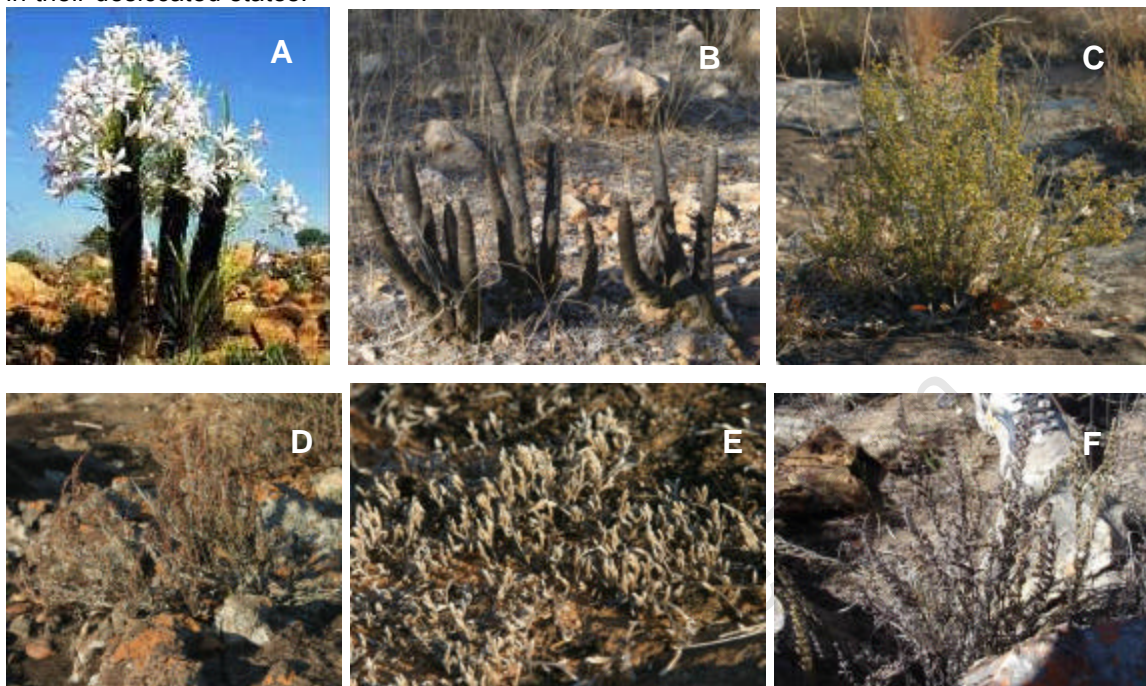
Higher plants with the ability to survive drought conditions represent a potentially interesting source of uniquely bioactive compounds. Desiccation-tolerant plants have the ability to enter a quiescent state during prolonged dry periods and then spring back to life in the presence of water by channeling essential compounds into storage organelles. Other than the compounds involved in the desiccation mechanisms, it is possible that these plants produce defensive metabolites to protect them from herbivores or environmental microbial pathogens. Furthermore, many of these plants have a history of use in traditional medicines. This project aimed to evaluate several desiccation-tolerant plants occurring in southern Africa for antimicrobial activity.

3.2 Results: Desiccation-tolerant plants

3.2.1 Antimicrobial activities of crude extracts

As described in Section 7.8.2, sequential extracts were prepared from the plant material of four desiccation-tolerant plants, namely *Myrothamnus flabellifolius* (whole plant), *Xerophyta retinervis* (stem, husks and leaves), *Cheilanthes contract* (whole plant) and *Selaginella dreggier* (whole plant). The extract yields are illustrated in Table 35 of the Appendix. Figure 31 illustrates the four studied desiccation-tolerant plants. The extracts were tested for activity against *Staphylococcus aureus*, *Klebsiella pneumoniae*, *Candida albicans* and *Mycobacterium aurum* using the broth microdilution method as described in Section 7.2. The results are exhibited in Table 9 as MIC's. IC₅₀ values were calculated for extracts with activity at less than or equal to 125µg/ml.

Figure 31: Pictures of *Xerophyta retinervis* in flower (A) (R. Botha) and (B) desiccated state at collection (P.C. Zietsman); *Myrothamnus flabellifolius* in wet (C) and desiccated (D) states (P.C. Zietsman); *Selaginella dregei* (E) (P.C. Zietsman) and *Cheilanthes contracta* (F) (T. Kellermann) in their desiccated states.



The antimicrobial controls were within an acceptable range for these assays and the highest concentration of DMSO, namely 2.5%, had no negative effect on organism growth when compared to the drug-free growth control. For all of the assays, the organism-free wells remained free of growth indicating growth medium sterility. Samples with an MIC of less than or equal to 125µg/ml were considered to be active. None of the extracts exhibited activity against *S. aureus* or *K. pneumoniae* at the highest concentration tested, namely 2mg/ml. Of the 30 extracts tested, only the methanol extract of the stems of *X. retinervis* and the methanol extract of *M. flabellifolius* exhibited any activity. The former was active against *C. albicans* with an MIC of 62.5µg/ml and against *M. aurum* with an MIC of 125µg/ml. The methanol extract of the leaves and husks of *X. retinervis* did not exhibit the same activity, indicating the presence of compounds with antimicrobial activity unique to the stem, or alternatively present at large enough quantities in the stem to display appreciable activity.

Table 9: The antimicrobial activity of four South African desiccation-tolerant plants. Results are expressed as MIC's followed by IC₅₀ values, where applicable, in µg/ml.

Plant	Extract	<i>S. aureus</i>	<i>K. pneumoniae</i>	<i>C. albicans</i>	<i>M. aurum</i>
<i>Myrothamnus flabellifolius</i>	PE	>2000	>2000	>2000	>2000
	DCM	>2000	>2000	2000	2000
	EA	>2000	>2000	2000	2000
	MeOH	>2000	1000	<7.8 to >2000*	>2000
	water	>2000	>2000	>2000	>2000
<i>Xerophyta retinervis</i> stems	PE	>2000	>2000	>2000	1000
	DCM	>2000	>2000	>2000	1000-2000
	EA	2000	>2000	>2000	2000
	MeOH	1000	>2000	62.5, 30.8 ± 0.5	125, 34.7 ± 4.6
	water	contamination	>2000	>2000	>2000
<i>Xerophyta retinervis</i> leaves	PE	>2000	>2000	>2000	2000
	DCM	1000-2000	>2000	2000	2000
	EA	2000	>2000	2000	>2000
	MeOH	>2000	>2000	>2000	>2000
	water	2000	2000	>2000	>2000
<i>Xerophyta retinervis</i> husks	PE	>2000	>2000	>2000	>2000
	DCM	>2000	>2000	>2000	>2000
	EA	2000	>2000	2000	>2000
	MeOH	1000	2000	1000	1000
	water	contamination	>2000	>2000	>2000
<i>Selaginella dregei</i>	PE	>2000	>2000	>2000	1000-2000
	DCM	>2000	>2000	2000	>2000
	EA	>2000	>2000	2000	>2000
	MeOH	>2000	>2000	>2000	>2000
	water	>2000	>2000	>2000	>2000
<i>Cheilanthes contracta</i>	PE	>2000	>2000	>2000	>2000
	DCM	>2000	>2000	>2000	>2000
	Ac	>2000	>2000	2000	>2000
	MeOH	>2000	>2000	250	>2000
	water	>2000	>2000	2000	>2000
Antimicrobial controls	Cip, Nys, INH	0.625, 0.247 ± 0.103	0.078, 0.042 ± 0.002	0.78-1.6, 0.9 ± 0.02	0.078, 0.0337±0.0003

*variable activity which could not be replicated despite testing on eight separate occasions

Abbreviations: MIC - minimum inhibitory concentration, PE - petroleum ether, DCM - dichloromethane, EA - ethyl acetate, Ac - acetone, MeOH - methanol, contam - contamination, Cip - ciprofloxacin, Nys - nystatin, INH - isoniazid

The methanol extract of the whole plant of *M. flabellifolius* showed variable activity against *C. albicans*, initially as extremely potent activity (less than the lowest concentration tested, namely 7.8µg/ml) which became weaker with subsequent testing, eventually showing no activity at all. The sample was freshly prepared on each day of testing from the solvent-free, but oily, crude extract to counteract the possibility of sample degradation, to no avail.

3.2.2 *Myrothamnus flabellifolius* fractions

Due to the large quantity of *M. flabellifolius* available and the interesting, but variable, activity observed in the methanol extract, an exhaustive investigation of its possible pharmacological properties was undertaken, as illustrated by the flow-diagram in Figure 32. As indicated in Chapter 7, IC₅₀ values were only calculated for fractions with MIC's of 62.5µg/ml or less.

The DCM extract of *M. flabellifolius* did not show activity in the broth microdilution methods employed (Table 9). Despite these findings, this extract was further fractionated by means of liquid-liquid fractionation with ACN and PE to evaluate the possible existence of low levels of active compounds in a less complex mixture. Bio-autography was used for the detection of possible actives in the fractions. The ACN fraction of the DCM extract exhibited inhibition against *S. aureus* over a zone from the origin to an R_f value of 0.75 and against *M. aurum* A+ over a zone from R_f 0.4 to 0.69, as shown in Figure 33a. The PE fraction exhibited no activity against *S. aureus*, but two clear zones of inhibition at R_f 0.36 and 0.4, as well as a more faint zone at R_f 0.28, were observed against *M. aurum* as shown in Figure 33b. TLC bands 1-3 from the PE fraction with activity against *M. aurum* were isolated as described in Section 7.8.4 and tested against *M. aurum*, *S. aureus* and *K. pneumoniae* in the broth microdilution assay. The PE extract was also further investigated using bio-autography against *M. aurum* and no zones of activity were observed.

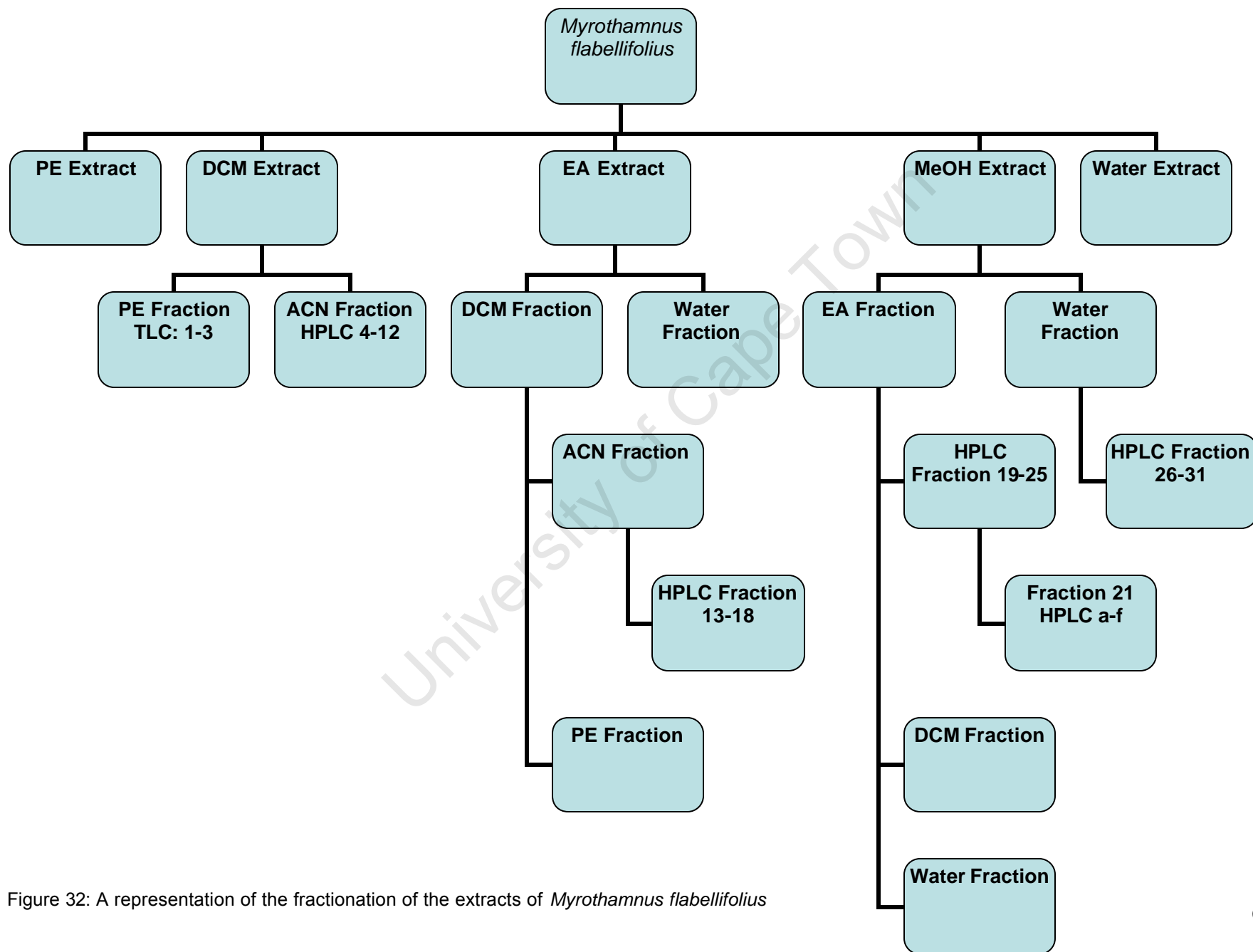
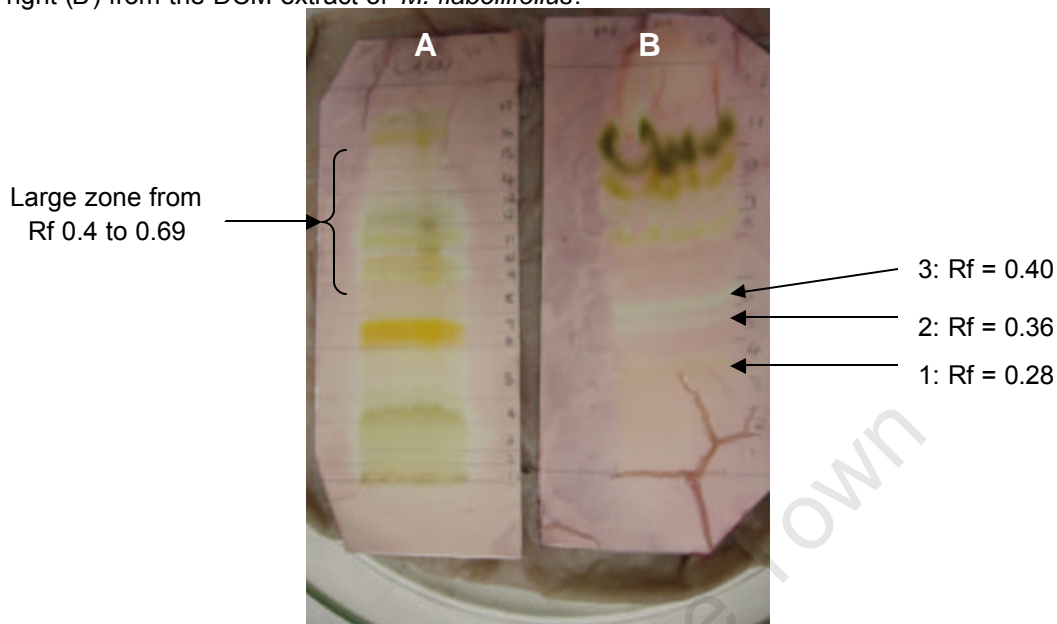


Figure 32: A representation of the fractionation of the extracts of *Myrothamnus flabellifolius*

Figure 33: An example of bio-autographic plates containing *M. aurum* A+ exhibiting a large zone of inhibition in the ACN fraction on the left (A) and three zones of inhibition in the PE fraction on the right (B) from the DCM extract of *M. flabellifolius*.



The three active bands from the PE fraction of the DCM extract were subsequently isolated from a reference TLC plate and tested in the broth micro-dilution method. Despite showing activity against *M. aurum* in the bioautography assay, none of the three TLC bands had MIC's of less than 1000µg/ml against this organism (Table 10).

The ACN fraction of the DCM extract which showed a broad zone of activity against *S. aureus* and *M. aurum* using bio-autography was subsequently further purified into its constituents by means of HPLC to generate nine fractions (4-12). The small quantity of these fractions available was used to test for activity against *S. aureus*, *C. albicans*, *M. aurum* and *K. pneumoniae* and the results are exhibited in Table 10. None of the fractions displayed potent activity against any of the organisms. Fractions 4 to 11 exhibited MIC's of 250µg/ml and fraction 12 had an MIC of 250-500µg/ml against *M. aurum*, while fractions 9 to 12 displayed MIC's of 250 to 500µg/ml against *S. aureus*.

Table 10: The bioactivity of fractions originating from the dichloromethane and ethyl acetate extracts of *Myrothamnus flabellifolius*. The results are described as MIC's followed by IC₅₀ values, if applicable, in µg/ml.

Extract	Fraction	Source	<i>S. aureus</i>	<i>K. pneumoniae</i>	<i>C. albicans</i>	<i>M. aurum</i>
DCM	PE	L-L	>2000	>2000	>2000	>2000
	1	TLC	125-250	125-250	n/t	>1000
	2	TLC	125-250	125-250	n/t	>1000
	3	TLC	250-500	125	n/t	>1000
	ACN	L-L	1000-2000	>2000	2000	1000
	4	HPLC	>1000	>1000	>1000	250
	5	HPLC	>1000	>1000	>1000	250
	6	HPLC	=1000	>1000	>1000	250
	7	HPLC	1000	>1000	>1000	250
	8	HPLC	500-1000	>1000	1000	250
	9	HPLC	250-500	>1000	>1000	250
	10	HPLC	250-500	>1000	>1000	250
	11	HPLC	250-500	>1000	>1000	250
	12	HPLC	250-500	>1000	>1000	250-500
EA	Water	L-L	=2000	2000	=2000	2000
	DCM	L-L	>2000	>2000	2000	125-250
	PE	L-L	>2000	>2000	=2000	2000
	ACN	L-L	500-1000	=2000	250	250
	13	HPLC	>1000	>1000	>1000	>125
	14	HPLC	>1000	>1000	>1000	>125
	15	HPLC	>1000	>1000	1000	>500
	16	HPLC	>1000	>1000	500	>500
	17	HPLC	1000	>1000	=1000	>500
	18	HPLC	500-1000	>1000	>125	>500
Cip			0.39-0.63, 0.265 ± 0.11	0.08, 0.042 ± 0.002	n/a	n/a
INH			n/a	n/a	n/a	0.08-0.16, 0.06 ± 0.007
Nys			n/a	n/a	3.1, 1.7 ± 0.04	n/a

Abbreviations: MIC- minimum inhibitory concentration, TLC- thin layer chromatography, HPLC- high performance liquid chromatography, DCM - dichloromethane, ACN - acetonitrile, EA - ethyl acetate, L-L - liquid-liquid extraction, Cip - ciprofloxacin, INH - isoniazid, Nys - nystatin; n/t - not tested

The ethyl acetate extract of *M. flabellifolius* was subjected to liquid-liquid extraction with DCM and water. When evaluated against *S. aureus*, the DCM fraction exhibited a zone of inhibition over an R_f range of 0.13 to 0.44. Further liquid-liquid extraction of the DCM fraction with ACN and PE was performed to prepare the sample for HPLC fractionation. The ACN fraction was further purified by means of HPLC into six fractions (13-18), as described in Section 7.8.4. The small quantities of these fractions obtained were tested for activity

against *S. aureus*, *K. pneumoniae*, *M. aurum* and *C. albicans* and the results are shown in Table 10. None of these fractions displayed activity against any of the organisms tested.

The initial potent activity exhibited by the methanol extract of *M. flabellifolius* against *C. albicans* in the broth micro-dilution method (Table 9) prompted a thorough fractionation and investigation into the bioactive constituents. A liquid-liquid extraction of the extract yielded an ethyl acetate and a water fraction. The ethyl acetate fraction was further fractionated by means of HPLC, as described in Section 7.8.4, into seven fractions (19-25). These seven HPLC fractions were tested against a range of organisms at three concentrations (0.5, 1 and 2 mg/ml) and the results are displayed in Table 11 below. Similarly, the water fraction was also further fractionated into six fractions (26-31) and these samples were tested only against *C. albicans* due to small sample quantities and potent activity displayed against this organism of the precursor water fraction. However, none of these samples displayed activity at less than 500µg/ml (data not shown).

Table 11: The MIC's (µg/ml) of the seven fractions resulting from the semi-preparative HPLC separation of the ethyl acetate fraction of the methanol extract of *Myrothamnus flabellifolius*. The precursor fractions arising from the liquid-liquid extraction of the methanol extract with ethyl acetate and water are also recorded here.

Fraction	<i>M. aurum</i>	<i>S. aureus</i>	<i>K. pneumoniae</i>	<i>C. albicans</i>
Water	>2000	>2000	>2000	<7.8 - >2000*
EA	1000	2000	2000	<7.8 - >2000*
19	> 2000	> 2000	2000	= 2000
20	> 2000	1000	1000	2000
21	> 2000	<500	1000	>2000
22	> 2000	1000	1000	>2000
23	> 2000	2000	2000	= 2000
24	> 2000	> 2000	2000	= 2000
25	> 2000	2000	>2000	>2000

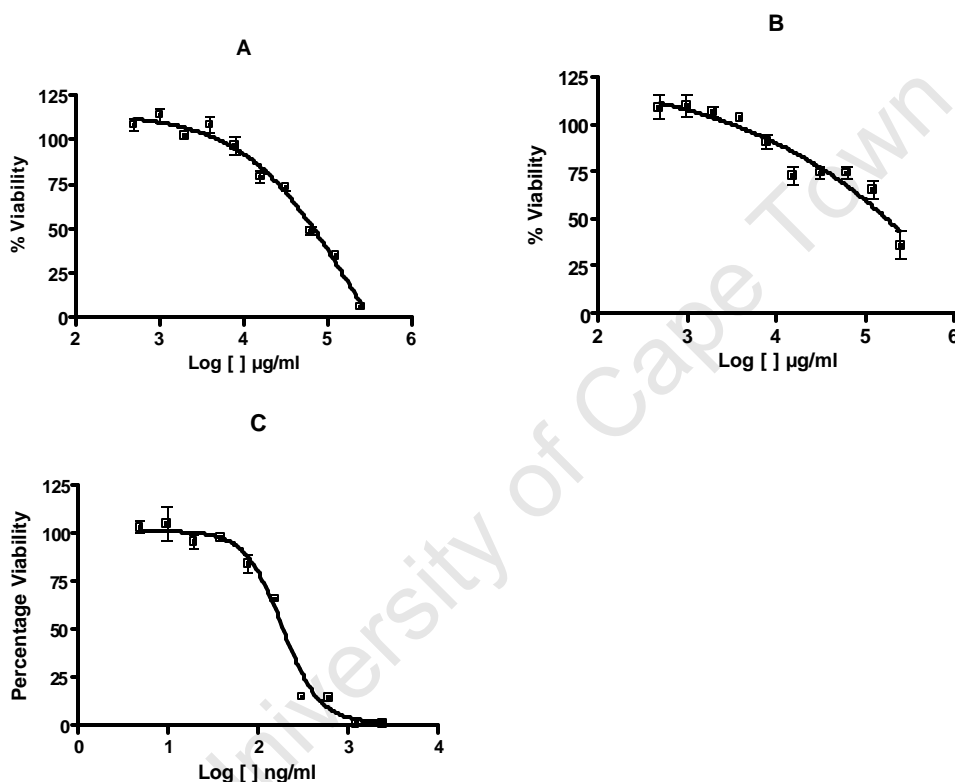
*activity dissipates with repeated testing

Abbreviations: EA - ethyl acetate

None of the HPLC fractions originating from the EA fraction of the methanol extract of *M. flabellifolius* exhibited activity against *M. aurum* A+ at the highest concentration tested, namely 2mg/ml. Fraction 21 was the only sample to exhibit activity, with an MIC of less than 0.5mg/ml against *S. aureus*. Despite the initial

excellent activity of the crude methanol extract, as well as the EA and water fractions thereof, against *C. albicans* (original MIC of less than 7.8µg/ml), none of the HPLC fractions exhibited inhibition at less than 2mg/ml against this organism. Interestingly, fractions 20 to 22 exhibited some activity, albeit poor, against *K. pneumoniae* with MIC's of 1mg/ml.

Figure 34: The dose response curves of (A) compound 21c (pure) and (B) fraction 21d from the third HPLC fraction of the methanol extract of *M. flabellifolius* against *S. aureus* ATCC 12600. Figure (C) illustrates the effect of ciprofloxacin on *S. aureus*.



Based on the results described in Table 11, further HPLC purification of fraction 21 arising from the ethyl acetate fraction of the methanol extract of *M. flabellifolius* was performed. This fractionation step, as described in Chapter 7.8.4, yielded six partially or completely pure compounds (21a-f). These fractions/compounds were tested against *S. aureus* ATCC 12600 at serially diluted concentrations ranging from 0.5 to 250µg/ml. Fractions/compounds a, b, e and f did not exhibit activity at the highest concentration tested, while compound c displayed an MIC of 250µg/ml and an IC₅₀ value of 67.8µg/ml as

illustrated by the dose response curve in Figure 34A. Fraction d showed slight inhibition of bacterial growth (IC_{50} 175 μ g/ml) (Figure 34B).

It appears from this set of data that despite the initial potent antifungal activity exhibited by the methanol extract of *M. flabellifolius* and its subsequent liquid-liquid fractions, activity deteriorates with subsequent testing, as well as with further chromatographic purification. Due to the variable nature of this activity, as well as time constraints, further work on *M. flabellifolius* was discontinued.

3.3 Discussion

Of the 30 crude extracts prepared from four species of desiccation-tolerant plants, only two samples exhibited activity at less than or equal to 125 μ g/ml, namely the methanol extract of the stems of *X. retinervis* and the methanol extract of *M. flabellifolius*. Two other parts of *X. retinervis*, namely the husks and leaves, were also sequentially extracted and did not exhibit the same activity as seen in the methanol extract of the stems. It can therefore be concluded that the compounds responsible for activity are either unique to the stems or are present in the husks and leaves in much smaller quantities. The acetone and methanol extracts of *X. retinervis* have previously been shown to exhibit moderate activity (greater than or equal to 250 μ g/ml) against a range of Gram-positive and – negative bacteria, as well as *C. albicans* (Seaman, 2005). Compounds with anti-malarial activity have been isolated from *X. retinervis* and the related *X. villosa* (Wiesner, 2007). Further work on *X. retinervis* in this project was discontinued due to the availability of more potent antibacterial compounds isolated from the lichen *T. chrysophthalmum*, as described in Chapter 2.

The activity of the methanol extract of *M. flabellifolius* against *C. albicans* was variable. Initial experiments showed the activity to be very low (less than 7.8 μ g/ml), but these results could not be confirmed with the activity becoming weaker with subsequent testing, despite freshly prepared samples being used for

each experiment. Further fractionation of the extracts also led to a loss of antifungal activity. Despite the intensive fractionation of all but the petroleum ether extracts, none of the fractions exhibited activity at less than 125µg/ml. It is possible that the initial potent activity exhibited by the methanol extract of *M. flabellifolius* could have resulted from the co-extraction of the active essential oil, which has been shown to exhibit antifungal activity (Viljoen *et al.*, 2002). This particular extract had a very oily texture, despite the solvent being removed under nitrogen. Essential oils contain many volatile components which could be prone to evaporation over time if not stored under conditions suitable for such a substance. The possibility also exists that the instability of the active ingredient led to its degradation (Taylor *et al.*, 2001) and subsequent loss of activity. Even in the unlikely event that the active constituent of this plant was isolated, its potential instability would make it an unsuitable drug-like compound. For this reason, further work on this plant was discontinued.

Kelmanson *et al.* (2000) found that the methanol extracts of *Cheilanthes viridis* leaves and stems from South Africa exhibited antimicrobial activity against Gram-positive and -negative bacteria using the disc diffusion method. The methanol extract of the leaves was shown to have MIC's of 4mg/ml against *S. aureus*, *P. aeruginosa* and *Micrococcus luteus*, and an MIC of 8mg/ml against *Bacillus subtilis* in the broth micro-dilution method. However, the results of this project found that a related species, namely *C. contracta*, with similar desiccation tolerance, did not exhibit any activity against the bacteria tested. It should be noted, however, that the extracts in this project were tested at a maximum concentration of 2mg/ml as higher concentrations of crude extracts affect visualisation of results due to colour interference. Furthermore, extracts were only considered to be active and worth pursuing if activity of 125µg/ml or less was observed, as recommended by various authors (Cos *et al.*, 2006; Newton *et al.*, 2002; Rios and Recio, 2005), while some even recommend a lower cut-off point (McGaw *et al.*, 2008).

The results of the antimicrobial testing of these South African desiccation-tolerant plants are somewhat surprising, as most of these species, or related species, are used in the medicinal treatment of microbial-associated diseases (Hutchings *et al.*, 1996; Van Wyk *et al.*, 2002). It is possible that these plants are in fact not used to kill or inhibit the growth of disease-causing organisms, but rather to alleviate the symptoms of the disease (Newton *et al.*, 2002), or alternatively to boost the host immune system (Cos *et al.*, 2006). Furthermore, it has been suggested that higher plants in fact only produce antimicrobial substances when counteracting a pathogenic infection, as the manufacture of such substances requires an enormous amount of energy (Lewis and Ausubel, 2006).

University of Cape Town

Chapter 4

Warburgia salutaris

4.1 Introduction

Trees belonging to the *Warburgia* genus are widely used across the African continent as potent traditional medicines (Muthaura *et al.*, 2007; Olila *et al.*, 2001). In Southern Africa, the bark of *W. salutaris* is used to treat a wide variety of ailments, including coughs, colds and miscellaneous chest complaints (Hutchings *et al.*, 1996; Van Wyk *et al.*, 2002). Plant parts of commercially cultivated *W. salutaris* were made available for this project with the intention of investigating the pharmacological efficacy of this plant. As described in Section 7.9.2, sequential extracts were prepared from the bark, leaves, stems and twigs which were subsequently tested for *in vitro* antimicrobial activity. The most active extracts and resulting fractions or compounds were then also tested for cytotoxicity with the intention of evaluating a fraction with *in vitro* activity, consisting of identified compounds, in an animal model to determine which compounds have the most promising pharmacological profile.

4.2 Results: *Warburgia salutaris*

4.2.1 Bioactivity of crude extracts

DCM, ethyl acetate and methanol extracts of various plant parts of *W. salutaris* were prepared, as described in Section 7.9.2 and the extract yields are tabulated in the Appendix, Table 36. The crude extracts of the leaves, bark, stem and twigs of *Warburgia salutaris* were tested against *S. aureus*, *K. pneumoniae*, *C. albicans* and *M. aurum* as described in Chapter 7.2. The results are displayed in Table 12. Four extracts had activity at 125µg/ml or less, namely the DCM extracts of the bark, stems and twigs, as well as the ACN fraction originating from

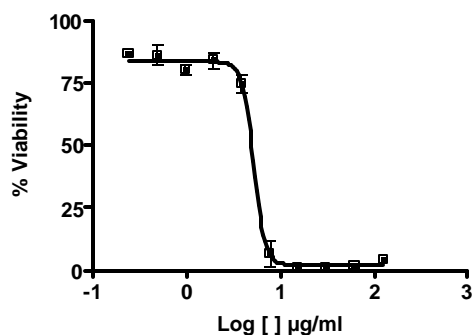
the DCM extract of the leaves. These extracts were all active against *C. albicans*, with the DCM extract of the bark having the lowest MIC of 7.8 to 15.6µg/ml, and an IC₅₀ value of 4.24µg/ml, as illustrated in Figure 35. The DCM extract of the bark also exhibited activity against *S. aureus* and *M. aurum* (MIC's of 62.5 and 125µg/ml respectively).

Table 12: The activity of *Warburgia salutaris* extracts against *Staphylococcus aureus*, *Klebsiella pneumoniae*, *Candida albicans* and *Mycobacterium aurum*. The results are described as MIC's followed by the IC₅₀ value, if applicable, in µg/ml.

Plant Part	Extract	<i>Staphylococcus aureus</i>	<i>Klebsiella pneumoniae</i>	<i>Candida albicans</i>	<i>Mycobacterium aurum</i>
Leaves	PE	>2000	>2000	>2000	>2000
	DCM	1000-2000	2000	250	1000
	EA	2000	>2000	>2000	2000
	MeOH	>2000	>2000	>2000	>2000
	ACN	250	2000	31, 20.64±2.85	250
Bark	DCM	62.5, 19.4±2.2	>2000	7.8– 15.6, 4.2±0.4	125, 60.9±6.4
	EA	>2000	>2000	250-500	2000
	MeOH	2000	>2000	>2000	2000
Stems	DCM	250-500	2000	31, 17.4±0.3	250
	EA	>2000	>2000	>2000	2000
	MeOH	>2000	>2000	>2000	>2000
Twigs	DCM	250	>2000	31, 17.6±0.5	500
	EA	>2000	>2000	>2000	2000
	MeOH	>2000	>2000	>2000	>2000
Controls	Cip	0.3-0.6, 0.18±0.001	0.078, 0.042±0.002	n/a	n/a
	Nys	n/a	n/a	1.6, 0.96±0.25	n/a
	INH	n/a	n/a	n/a	0.078, 0.062±0.014

Abbreviations: PE - petroleum ether; DCM - dichloromethane; EA - ethyl acetate; MeOH - methanol; ACN - acetonitrile; Cip - ciprofloxacin; Nys- nystatin; INH - isoniazid

Figure 35: The dose response curve of the dichloromethane extract of *Warburgia salutaris* bark against *Candida albicans* ATCC 90028. This data represents nine replicates performed over three separate experiments.



A comparison of the chromatographic profiles of the DCM extracts of the leaves (ACN fraction), bark, stems and twigs indicate that the same predominant compounds appear in all of these plant parts eluting at approximately 17.5, 18.3, 21.2 and 22.6 minutes. These HPLC profiles are shown in Figures 36 to 39 respectively, generated as described in Section 7.9.3.

Figure 36: A chromatogram of the acetonitrile fraction of the dichloromethane extract of the leaves of *Warburgia salutaris* at 210nm.

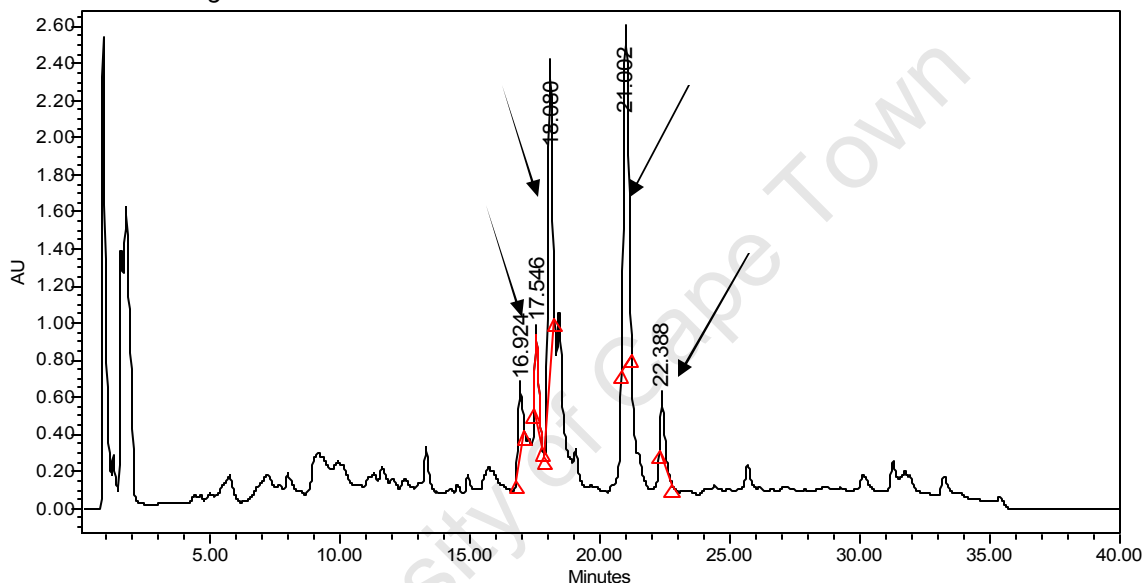


Figure 37: A chromatogram of the dichloromethane extract of the bark of *Warburgia salutaris* at 210nm.

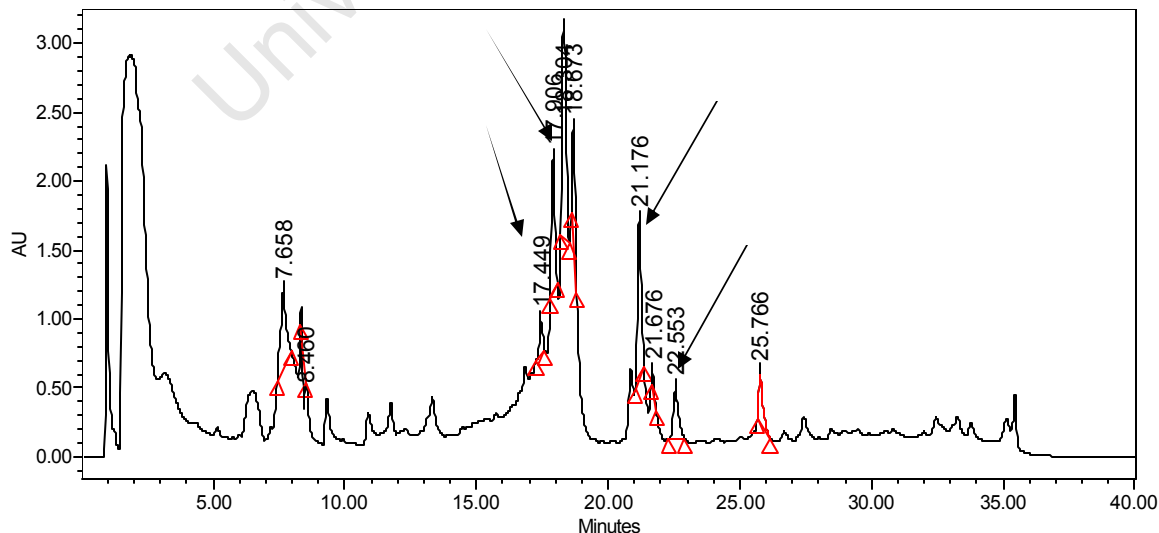


Figure 38: A chromatogram of the dichloromethane extract of the stems of *Warburgia salutaris* at 210nm.

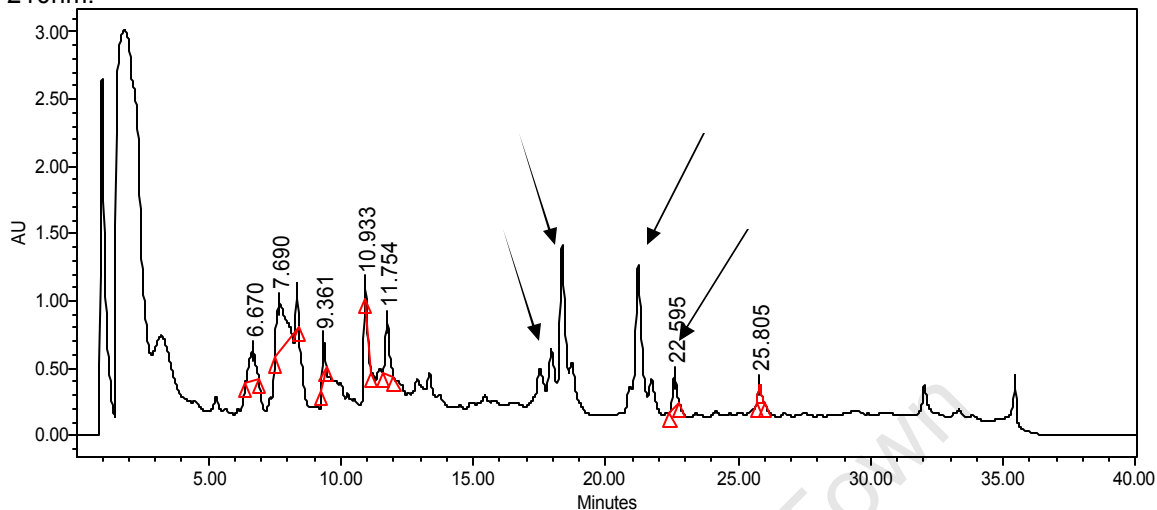
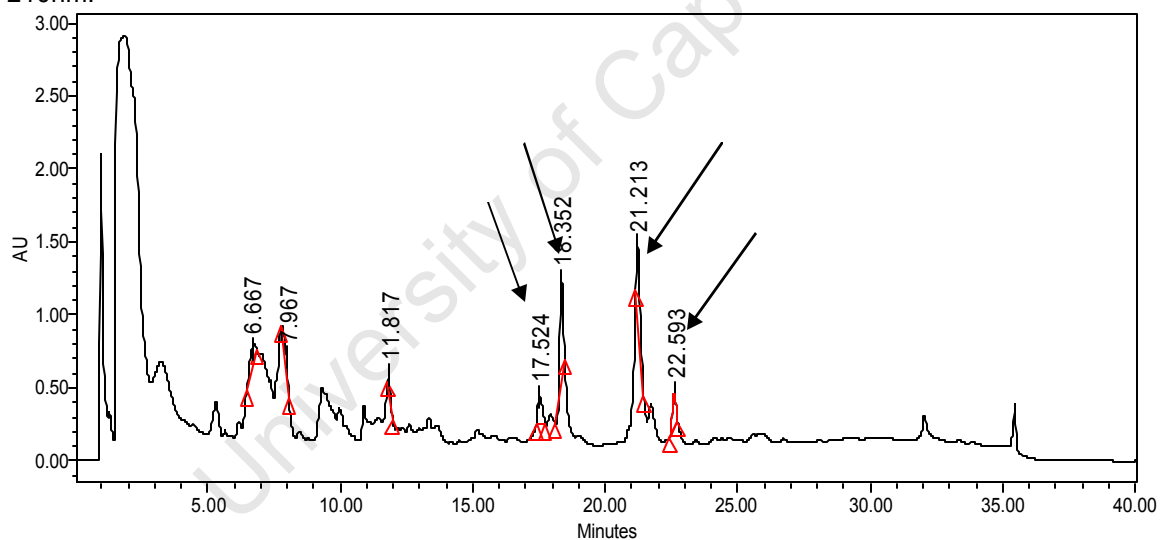


Figure 39: A chromatogram of the dichloromethane extract of the twigs of *Warburgia salutaris* at 210nm.



The most active extracts, namely the DCM extracts of the leaves (ACN fraction), bark, stems and twigs were further evaluated for cytotoxicity against CHO cells, the methodology of which is described in Section 7.5. The results are reported in Table 13.

Table 13: The cytotoxicity of the four most active crude extracts from *Warburgia salutaris*. The results are displayed as IC₅₀ values in µg/ml and the selectivity indices (cytotoxicity/activity against *C. albicans*) are shown.

Plant part	Extract	IC ₅₀ value	SI value
Leaves	ACN fraction from DCM	3.791±0.296	0.18
Bark	DCM	3.829±2.929	0.90
Stems	DCM	5.218±3.511	0.30
Twigs	DCM	6.209±1.031	0.36
Control	Emitine	0.085±0.004	n/a

Abbreviations: SI - selectivity index; ACN - acetonitrile; DCM - dichloromethane

From Table 13, it is evident that the extracts which exhibited the most potent antimicrobial activity are also extremely toxic to CHO cells as indicated by the IC₅₀ values of less than 10µg/ml. Furthermore, the selectivity indices were calculated for the activity against *C. albicans* (the most potent antimicrobial activity observed) and the values are very low for all of the tested extracts. For a pure compound to be considered a promising hit it should have a value of 10 or greater, indicating low cytotoxicity coupled with good antimicrobial activity (Orme, 2001). In the instance of crude extracts which may consist of many different compounds, it is possible that only one or a few of the compounds are responsible for the potent cytotoxicity. For this reason, it was decided to continue with the fractionation of the extract which exhibited the most potent broad-spectrum antimicrobial activity together with the best SI value, namely the DCM extract of the bark of *W. salutaris*. This is also the plant part most frequently utilized in traditional medicine applications (Van Wyk *et al.*, 2002; Hutchings *et al.*, 1996).

4.2.2 Antimicrobial activity of the bark dichloromethane fractions

The DCM extract of the bark of *W. salutaris*, which displayed the most potent activity against *C. albicans*, was further fractionated by means of liquid-liquid fractionation into a petroleum ether fraction (WSBD1), an insoluble layer (WSBD2); the green 'oily' (WSBD4) ACN fraction and a white ACN component

(WSBD3). These four fractions were tested for activity against *C. albicans* and *M. aurum* and the results are exhibited in Table 14.

Table 14: The effect of the fractions of the dichloromethane extract of the bark of *Warburgia salutaris* on *Candida albicans* and *Mycobacterium aurum*. The results are expressed as MIC's followed by IC₅₀ values where applicable, in µg/ml.

Fraction	<i>Candida albicans</i> ATCC 90028	<i>Mycobacterium aurum</i> A+
WSBD1	31.3, 16.4±0.4	>250
WSBD2	31.3 – 62.5, 17.9±1.1	>250
WSBD3	7.8, 4.3±0.2	125, 53.6±8.0
WSBD4	7.8, 4.0±0.5	62.5, 47.8±12.7
Nystatin	0.8, 0.6±0.4	n/a
Isoniazid	n/a	0.08 – 0.16, 0.066±0.004

HPLC chromatograms of these four fractions, generated as described in Section 7.9.4 and displayed in Figures 59 and 60 of the Appendix, indicated similarities between WSBD1 and WSBD2, reflected by similar bioactivities. Fractions WSBD3 and WSBD4 had MIC's of 7.8µg/ml against *C. albicans* and also displayed similar bioactivity (MIC of 125 and 62.5µg/ml respectively) against *M. aurum*. Furthermore, these two fractions also showed similar chromatographic profiles, as shown in Figures 40 and 41. They were subsequently collected together and referred to as the acetonitrile fraction of the DCM extract of *W. salutaris* (WSBDA).

Figure 40: The HPLC chromatogram of fraction WSBD3 from the acetonitrile fraction of the dichloromethane extract of the bark of *Warburgia salutaris* at 244nm.

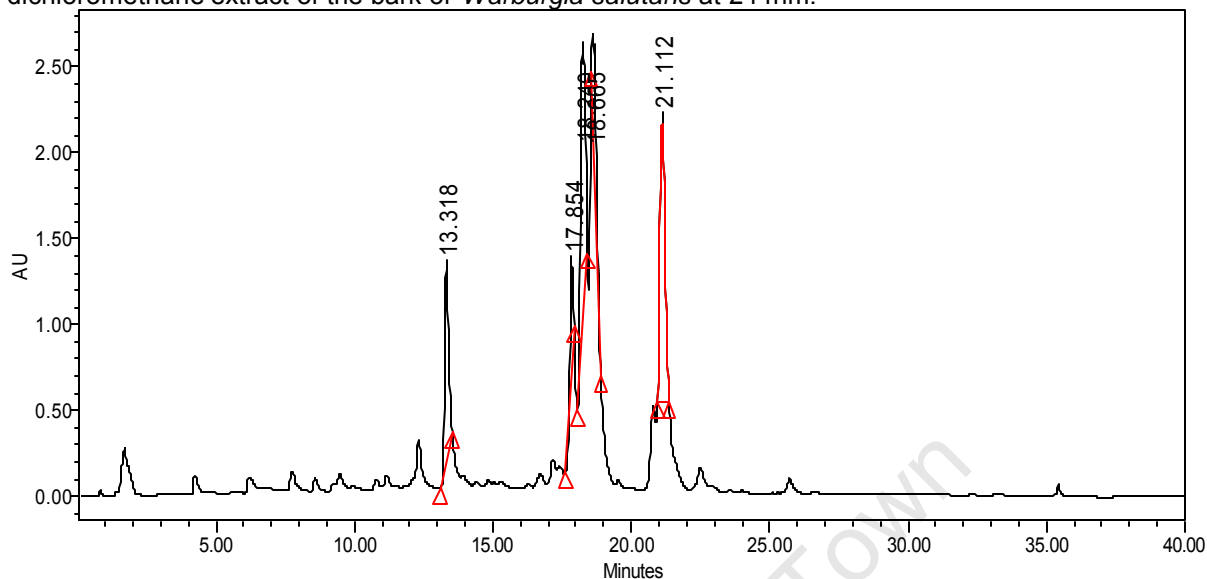
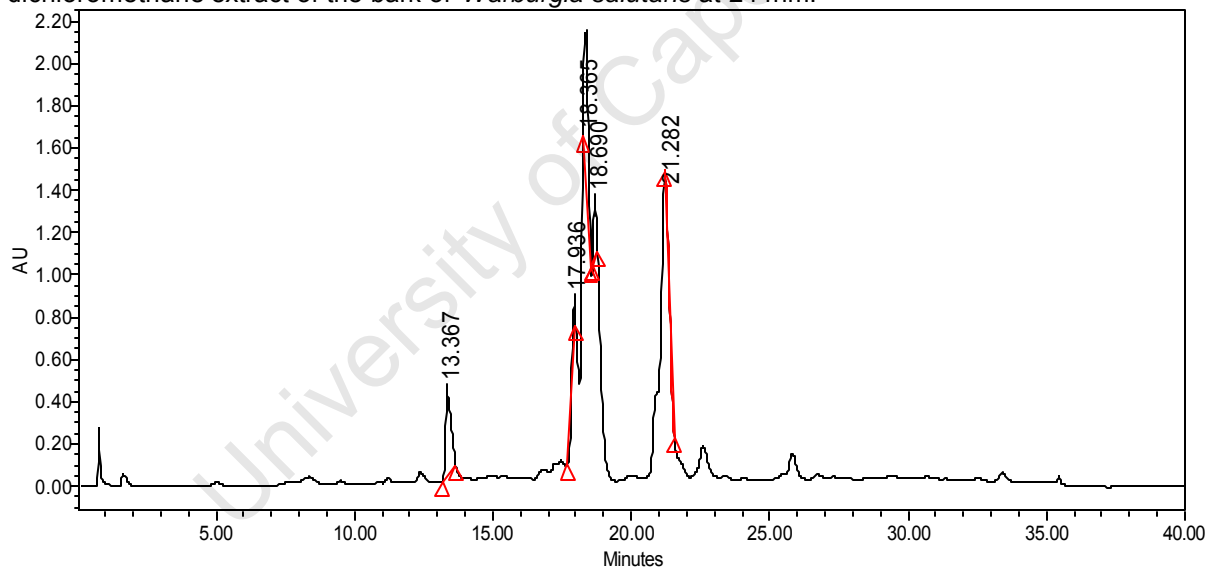


Figure 41: The HPLC chromatogram of fraction WSBD4 from the acetonitrile fraction of the dichloromethane extract of the bark of *Warburgia salutaris* at 244nm.



Eight HPLC fractions were subsequently collected from WSBD4, as described in Chapter 7.9.4 and exhibited in Figure 57. These fractions were tested against *C. albicans* and *M. aurum*, as well as for cytotoxicity against CHO cells, as shown in Table 15. Fractions three and five were accidentally combined and therefore tested together.

Table 15: The effect of eight HPLC fractions isolated from WSBDA, the acetonitrile fraction of the dichloromethane extract of the bark of *Warburgia salutaris*, on *Candida albicans* and *Mycobacterium aurum*. The results are expressed in terms of MIC's and IC₅₀'s, where applicable, in µg/ml. The cytotoxicity results against CHO cells are recorded as IC₅₀ values in µg/ml.

	<i>C. albicans</i> ATCC90028		<i>M. aurum</i> A+		<i>CHO</i>
Fraction	MIC	IC₅₀	MIC	IC₅₀	IC₅₀
1	>250	n/a	>250	n/a	>100
2	=250	n/a	>250	n/a	15.3±11.49
3+5	125	33.0±6.1	250	n/a	8.5±3.24
4	31.3 - 62.5	19.2±0.2	62.5	28.0±7.1	1.4±0.77
6	7.8 – 15.6	5.8±0.9	125	27.5±6.3	2.6±0.15
7	7.8	4.7±0.3	125 - 250	n/a	21.7±4.78
8	62.5 - 125	32.9±15.6	62.5 - 125	41.4±11.3	1.4±0.60
Nystatin	1.6	1.2±0.3	n/a	n/a	n/a
Isoniazid	n/a	n/a	0.078	0.0698±0.0008	n/a
Emitine	n/a	n/a	n/a	n/a	0.08±0.006

Table 15 shows that fractions six and seven exhibit the greatest antifungal activity with IC₅₀ values of 5.8 and 4.7µg/ml, respectively, while fractions four and six show the strongest antimycobacterial activity with IC₅₀ values of 28.0 and 27.5µg/ml respectively. However, fractions 4 and 8 display the greatest cytotoxicity with IC₅₀ values of 1.44 and 1.43µg/ml respectively. Due to the fact that fraction six was available in the largest quantities and appeared to have the most complex chromatographic profile, it was further purified into its seven primary constituents, as described in Section 7.9.4. These seven fractions/compounds were subsequently tested for activity against *C. albicans* and *M. aurum*, as well as for cytotoxicity against CHO cells (Table 16).

From Table 16, it is evident that as with the DCM extract of the bark of *W. salutaris*, the subsequent pure/semi-pure compounds arising from the ACN fraction of this extract responsible for bioactivity are also extremely cytotoxic. Compounds 4, 5 and 6, subsequently identified as the well-known drimane sesquiterpenoids muzigadial, warburganal and ugandensidial, exhibited the most potent activity against both *C. albicans* and *M. aurum*, but other than compound/fraction 1, were also the most toxic.

Table 16: The bioactivity of seven HPLC fractions and pure compounds isolated from fraction six of the acetonitrile fraction of *Warburgia salutaris* bark dichloromethane extract. The antimicrobial results are described as MIC's, followed by IC₅₀ values, if applicable, in µg/ml. The cytotoxicity results are described as IC₅₀ values in µg/ml.

Fraction/ compound	<i>C. albicans</i>	<i>M. aurum</i>	Cytotoxicity	SI for <i>C. albicans</i>
H6-1	125	125	0.5±0.06	n/a
H6-2a	=250	>250	50.3±3.8	n/a
H6-2b	250	>250	55.6±7.95	n/a
H6-3	125	>250	32.5±6.1	n/a
H6-4 (muzigadial)	3.9-7.8, 2.1±0.04	125	4.3±2.3	2.1
H6-5 (warburganal)	7.8-16.6, 4.5±0.08	125	1.7±1.3	0.4
H6-6 (ugandensidial)	31.3-62.5, 25.2±11.41	125	1.2±1.6	0.05
Nystatin	1.6, 0.78±0.06	n/a	n/a	n/a
Isoniazid	n/a	0.156, 0.124±0.008	n/a	n/a
Emetine	n/a	n/a	0.045±0.03	n/a

The other two fractions arising from the HPLC separation of the ACN fraction of the DCM extract of *W. salutaris* bark exhibiting potent antimycobacterial and antifungal activity, namely fractions 4 and 7 (Table 15), were also subjected to HPLC fractionation and those pure/semi-pure compounds were further tested against *C. albicans* and *M. aurum* (Table 17).

Of the 12 pure/semi-pure compounds arising from HPLC fractions 4 and 7 of the ACN fraction of the DCM extract of the bark of *W. salutaris*, the most promising activity was from H7-4, which exhibited an IC₅₀ of 15.3µg/ml against *C. albicans*. The only fraction for which sufficient quantities remained for cytotoxicity testing was H7-1 with an IC₅₀ of 2.05µg/ml. The observed moderate to poor activity of these 12 pure/semi-pure compounds prevented further collection and subsequent structural identification.

Table 17: The activity of the fractions/compounds isolated from the HPLC fractions 4 and 7 of the acetonitrile fraction of the dichloromethane extract of *Warburgia salutaris* bark against *Candida albicans* and *Mycobacterium aurum*. Each result is displayed as an MIC value, followed by the IC₅₀ value where applicable, in µg/ml.

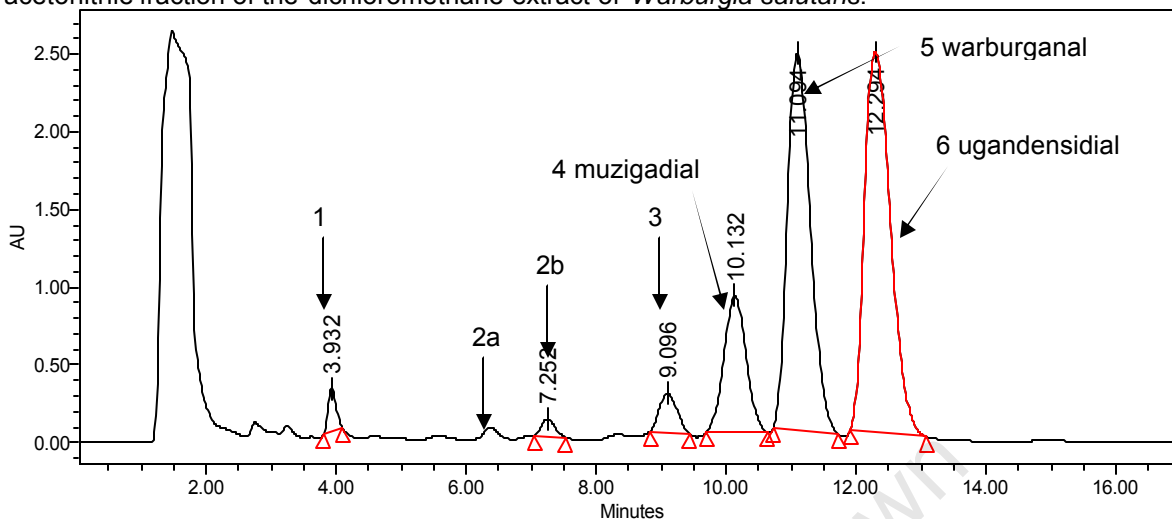
Fraction/compound	<i>C. albicans</i>	<i>M. aurum</i>
H4-1	>250	125
H4-2	125-250	125-250
H4-3	>250	>250
H4-4	>250	>250
H4-5	62.5, 38.9±0.56	=250
H4-6	62.5-125, 45.0±17.15	125-250
H7-1	31.3-62.5, 13.2±6.66	125-250
H7-2	125	250
H7-3	15.6-31.3, 19.1±1.86	>250
H7-4	31.3, 15.3±4.17	>250
H7-5	>250	>250
H7-6	=250	>250
Nystatin	1.6, 0.78±0.11	n/a
Isoniazid	n/a	0.15, 0.068±0.002

Due to the cytotoxic nature of the most active compounds and fractions isolated in this study, the use of an active fraction of *Warburgia salutaris* for the development of an *in vivo* method to fast-track pharmacokinetic profiling of lead-like compounds was not continued.

4.2.3 Identification of compounds isolated from *W. salutaris*

The structures of the three most active compounds isolated from fraction six arising from the HPLC separation of the ACN fraction of the DCM extract of the bark of *W. salutaris*, namely compounds 4, 5 and 6 shown in Figure 42 were subsequently elucidated.

Figure 42: A chromatogram at 229nm of fraction six originating from the HPLC separation of the acetonitrile fraction of the dichloromethane extract of *Warburgia salutaris*.



The spectroscopic methods used for structure elucidation are described in Section 7.9.5. The compounds were identified as the drimane sesquiterpenoids muzigadial (4), warburganal (5) and ugandensidial (6). The ^{13}C and ^1H NMR spectra are displayed in the Appendix, Figures 80 to 85, while the assigned resonances are displayed in Tables 18 and 19. The chemical structures are depicted in Figure 43.

Figure 43: The chemical structures of muzigadial (4), warburganal (5) and ugandensidial (6) isolated from the bark of *Warburgia salutaris*.

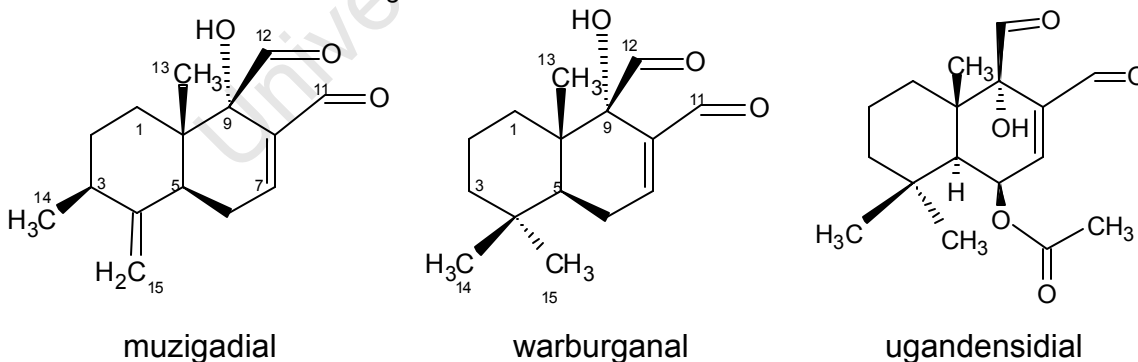


Table 18: The resonances of the ^{13}C NMR spectra of muzigadial, warburganal and ugandensidial isolated from the bark of *Warburgia salutaris*.

	Muzigadial (d)	Warburganal (d)	Ugandensidial (d)
C1	31.95	31.36	32.02 or 32.79
C2	31.09	17.95	17.88
C3	38.43	41.50	44.21
C4	151.85	33.25	34.21
C5	40.47	41.93	45.16
C6	27.84	26.16	66.26
C7	136.07	157.72	148.86
C8		140.53	141.14
C9	77.86	77.90	
C10	43.23	41.67	41.85
C11	201.43	202.4	201.32
C12	192.89	192.86	193.24
C13	15.32	33.25	32.02 or 32.79
C14	18.64	22.31	24.96
C15	106.31	17.29	20.15
			CH ₃ CO 21.67
			CH ₃ C=O 170.27

All three of these drimane sesquiterpenoids have the characteristic aldehydes resonances at positions 11 and 12 (d = 201 to 202 and 192 to 193 respectively). The carbon spectrum of ugandensidial corresponds well with that described by Clarkson *et al.* (2007), the most prominent feature being the resonances of the carbons corresponding with the acetoxy group (21.67 and 120.27). The three compounds all have methyl groups at position 13, and warburganal and ugandensidial each have a further two methyl groups at position 4. In this same position on muzigadial, a double bonded methine group occurs, and a further methyl resonance (d = 18.64) is located at position 3 on the aromatic ring.

Table 19: The resonances of the ^1H NMR spectra of muzigadial, warburganal and ugandensidial isolated from the bark of *Warburgia salutaris*.

	Muzigadial (d)	Warburganal (d)	Ugandensidial (d)
H-1			a: 1.77 (d, J=12, 5.5Hz) β: 0.98 (m)
H-2	2.00 (2H, m)		a: 1.52 (dm, J=12, 6Hz) β: 1.59 (qt, J=12, 4.5Hz)
H-3	4.39 (1H, m, J=6Hz)		a: 1.27 (tm, J=18, 9Hz) β: 1.39 (dm, J= 12Hz)
H-5	2.63 (1H, m)	1.89 (1H, dd, J=6, 6Hz)	2.04 (1H, d, J=6Hz)
H-6		a: 2.58 (1H, dt; J=18, 6Hz) β: 2.34 (1H, ddd, J=12, 6Hz)	5.89 (1H, t, J=6Hz)
H-7	7.23 (m)	7.25 (m)	7.00 (1H, d, J=4.8Hz)
H-11	9.65 (1H, s)	9.72 (1H, s)	9.76 (1H, s)
H-12	9.44 (1H, s)	9.41 (s)	9.48(1H, s)
H-13	0.87 (3H, s)	0.94 (3H, s)	1.02 (s)
H-14	1.08 (1H, d, J=6Hz)	0.99 (3H, s)	1.16 (s)
H-15	4.93 and 4.76 (2x1H, 2xbr)	1.09 (3H, s)	1.33 (s)
9-OH		4.08 (1H, s)	4.10 (1H, brs)
CH ₃ CO			2.14 (s)

For muzigadial and warburganal, the multiplicity of the proton resonating at approximately 7.23 to 7.26 was obscured due the solvent peak, chloroform. The proton spectrum for all three compounds showed the presence of two aldehyde groups (d = 9.7, H-11; 9.4, H-12) and an olefinic hydrogen doublet or multiplet at d = 7.0 (H-7). Ugandensidial shows a resonance for a methine group (d = 5.89, H-6) associated with an acetoxy group (d = 2.14). Warburganal and ugandensidial each have three methyl singlets (H-13, H-14, and H-15). Muzigadial is characterized by the methine group at H-15 (d4.93 and 4.76). This compound has a molecular formula of $\text{C}_{15}\text{H}_{20}\text{O}_3$ and a reported molecular mass of 248.1412. The molecular formula for ugandensidial is $\text{C}_{17}\text{H}_{24}\text{O}_5$ and the compound has a reported mass of 308.1624, while warburganal has a m/z of 250.1569 (M^+) and a molecular formula of $\text{C}_{15}\text{H}_{22}\text{O}_3$.

4.3 Discussion

Testing of the extracts of various plant parts of *W. salutaris* revealed that the dichloromethane extracts of the woody material, namely the bark, stems and twigs, displayed potent activity against yeast and moderate activity against Gram-positive bacteria and mycobacteria. Poor activity of crude plant extracts against Gram-negative bacteria as observed in this project has previously been reported (Rabe and Van Staden, 1997).

This study adds to the wealth of knowledge available on the potent antimicrobial activity of the bark of this genus. The methanol and water extracts of the bark of *W. salutaris* have been reported to exhibit activity against Gram-positive bacteria in the disc-diffusion assay, while the methanol extract also showed some activity against *E. coli* (Rabe and Van Staden, 1997). When evaluating the methanol extract in a broth micro-dilution assay, the authors observed an MIC of 0.5mg/ml against *S. aureus* and *B. subtilis*, and an MIC of 2mg/ml against *Staphylococcus epidermis*. In the current project, the methanol extract of the bark of *W. salutaris* exhibited an MIC of 2mg/ml against *S. aureus*. This observed difference in activity to that reported by Rabe and Van Staden could be due to many factors, including environmental influences. However, it is most likely that in the current project the active components were extracted earlier in the sequential extraction process, while these authors only prepared methanol and aqueous extracts of the plant material. Extracts of the stem bark of a related species, *W. ugandensis*, have previously been shown to have antibacterial and antifungal activity, with the component responsible for the antifungal activity being muzigadial (Olila *et al.*, 2001).

Extracts of the bark of this genus have also displayed antimalarial activity against chloroquine sensitive and resistant strains of *Plasmodium falciparum*, while exhibiting very low comparative cytotoxicity ($IC_{50} = 233\mu\text{g/ml}$) (Muthaura *et al.*,

2007), as well as antileishmanial activity (Ngure *et al.*, 2009). Despite not showing good antimicrobial activity in this study, extracts of the leaves of *W. salutaris* have previously been shown to exhibit *in vitro* anti-inflammatory and antioxidant activity, suggesting a basis for their use in treating topical skin diseases in Southern Africa (Frum and Viljoen, 2006; Muchuweti *et al.*, 2006). An aqueous extract of the leaves has also been shown to have good molluscidal activity (Clark and Appleton, 1997).

The extracts with good *in vitro* antimicrobial activity were evaluated for *in vitro* cytotoxicity against CHO cells. The results indicated that all of the extracts were more cytotoxic than they were active. *In vitro* cytotoxicity from crude extracts of the genus *Warburgia* has previously been reported (Olila *et al.*, 2002). However, there have also been reports of weak cytotoxicity from extracts of the stem bark of this genus. Ngure *et al.* (2009) found that the hexane extract *W. ugandensis* displayed less toxicity to VERO cells than the control drug, pentostam, but the dichloromethane and ethyl acetate extracts were more toxic. However, the authors report that none of the extracts were toxic at less than 31.25µg/ml and the hexane and DCM extracts had cytotoxicity comparable to that of amphotericin B (Ngure *et al.*, 2009). Similarly, Muthaura *et al.* (2007) reported the cytotoxicity of the methanol extract of the bark against VERO cells as being 233µg/ml (IC₅₀). In this project, the dichloromethane extracts of the bark, stem and twigs all exhibited potent cytotoxicity of less than 10µg/ml. It is possible that the difference in cytotoxicity compared to the two latter literature reports is due to the use of the CHO cell line for *in vitro* cytotoxicity testing as opposed to VERO cells.

Despite the observed cytotoxicity, further fractionation of the very active dichloromethane extract was continued due to the possibility that only a small portion of the compounds are responsible for the toxic effects. A liquid-liquid extraction of the crude plant material was prepared using acetonitrile and petroleum ether. The two components of the acetonitrile fraction showed good

activity against *C. albicans* (IC₅₀'s of 4.3 and 4.0 µg/ml) and moderate activity against *M. aurum*. The similar chromatographic profile allowed for these fractions to be combined and separated by means of HPLC into eight further fractions. Fractions 6 and 7 displayed the most potent activity against *C. albicans* with IC₅₀'s of 5.75 and 4.7 µg/ml respectively, while fractions 4 and 6 displayed moderate activity against *M. aurum* (IC₅₀'s of 28.0 and 27.5 µg/ml respectively). *In vitro* cytotoxicity testing against CHO cells revealed that fractions 4, 6 and 7 had IC₅₀'s of 1.44, 2.6 and 21.7 µg/ml respectively. These three fractions were still further purified to obtain 6, 7 and 6 pure or partially pure compounds respectively. These 19 pure/semi-pure compounds were tested against *M. aurum* and *C. albicans*.

The compound with the most promising antifungal activity was H6-4 with an IC₅₀ of 2.07 against *C. albicans*. This compound also displayed cytotoxicity with an IC₅₀ 4.3 µg/ml, resulting in an SI value of 2.1. H6-4 was identified as the drimane sesquiterpenoid muzigadial, which has previously been identified as the primary compound responsible for antifungal activity in *W. ugandensis* (Olila *et al.*, 2001). The proton spectrum for muzigadial is in agreement with that published by Kioy *et al.* (1990) and Ying *et al.* (1995). Muzigadial has also been shown to display potent antibacterial activity (Rabe and Van Staden, 2000). H6-5 also had good antifungal activity with an IC₅₀ value of 4.45 µg/ml against *C. albicans*, and cytotoxicity at 1.7 µg/ml, leading to an SI value of 0.4. Spectroscopic methods led to it being identified as warburganal, another well-known drimane sesquiterpenoid with antimicrobial activity frequently isolated from the family Canellaceae (Taniguchi *et al.*, 1984). The NMR spectra of warburganal are in agreement with those published by Kioy *et al.* (1990), Mashimbye *et al.* (1999) and Hollinshead *et al.* (1983). The most abundant compound in fraction 6 was identified as the structurally related ugandensidial, with moderate antifungal (IC₅₀ of 25.2 µg/ml) activity and potent cytotoxicity (IC₅₀ of 1.16 µg/ml). The structure for ugandensidial is in agreement with that proposed by Clarkson *et al.* (2007) and Kioy *et al.* (1990). This compound has been shown to be present in an

antimycobacterial fraction arising from an extract of *W. salutaris* bark (Clarkson *et al.*, 2007). However, this research has shown that ugandensidial only exhibits moderate activity against mycobacteria (MIC of 125µg/ml). Three further pure/semi-pure compounds showed moderate antifungal activity, namely H7-1 (IC₅₀ of 13.2µg/ml), H7-3 (IC₅₀ of 19.1µg/ml) and H7-4 (IC₅₀ of 15.3µg/ml). However, the isolated pure/semi-pure compounds of fractions 4 and 7 exhibited decreased activity against *C. albicans* and *M. aurum* in comparison to the original fractions, suggesting that the compounds may work together synergistically to obtain the observed bioactivity. None of the 19 compounds displayed activity against *M. aurum* at less than 125µg/ml.

Two comprehensive reviews by Jansen and De Groot (1991 and 2004) summarise the occurrence and biological activity of drimane sesquiterpenoids based on literature reports up to 2003. These bioactivities include antibacterial, antifungal, antifeedant, plant-growth regulatory, cytotoxic, phytotoxic, piscicidal and molluscicidal effects. Drimane sesquiterpenoids are relatively rare in nature (Jansen and De Groot, 2004), but occur frequently within the family Canellaceae (Bastos *et al.*, 1999) and have been isolated from fungi, molluscs and marine sponges (Jansen and De Groot 1991 and 2004). Several methods have been proposed for the synthesis of these bioactive compounds, including enzymatic, cationic polyolefin cyclization, from decalones, radical cyclizations and by cycloaddition reactions (Jansen and De Groot, 2004). Hollinshead *et al.* (1983) have shown that it is possible to synthesise drimane sesquiterpenoids by means of diels-alder reactions. Furthermore, research has shown that sesquiterpenoid dialdehydes may function as vanilloid receptors, and therefore may represent leads for the development of vanilloid drugs (Szallasi *et al.*, 1998; Sterner and Szallasi, 1999).

Taniguchi *et al.* (1984) have shown that muzigadial and warburganal have similar antimicrobial activity, while polygodial has greater activity, suggesting that the hydroxyl group at C-9 is not necessary for activity. Furthermore, they suggest

that the 9 β -aldehyde group confers antimicrobial activity and that the activity of the *Warburgia* sesquiterpene dialdehydes can potentially be attributed to their very specific reactivity with sulfhydryl groups at the enal moiety. Wube *et al.* (2005) noted that the polarity of these compounds appears to influence antimycobacterial activity, where greater lipophilicity elicits better *in vitro* activity. Kubo and Taniguchi (1988) isolated three drimane sesquiterpenoids, namely polygodial, muzigadial and warburganal, from *W. ugandensis* and *W. stuhlmanii*. They demonstrated that the structurally most simple of these compounds, polygodial, was more active than the commercial antifungal, amphotericin B, which is also highly toxic to humans. Furthermore, the authors demonstrated that polygodial used in conjunction with actinomycin D against *Saccharomyces cerevisiae*, remarkably improved the activity of this drug. This same drug is relatively inactive against *Candida utilis*. However, when used in combination with polygodial, the activity was significantly improved. The primary target of polygodial action was shown to be the plasma membrane and the authors hypothesize that this compound could be used to facilitate the movement of drugs into cells by punching holes in the membrane, which could furthermore allow for the use of safer, lower doses of conventional drugs.

An aim of this project was to develop a method in which the pharmacokinetic profile of an active fraction of a well-known medicinal plant, namely *W. salutaris*, could be evaluated. Current pre-clinical drug development focuses on testing the bioavailability of a single active compound at a time. However, in medicinal plants the activity does not necessarily arise as a result of a single active, but instead due to multiple active components. The ability to test an active fraction containing many compounds could speed up the drug development process significantly. However, the medicinal plant chosen for this evaluation showed severe toxicity in all of the active extracts and fractions tested, making it unsuitable for *in vivo* testing, despite widespread use in medicinal preparations.

Chapter 5

***In vivo* bioavailability of lichen-derived compounds**

5.1 Introduction

Two compounds with promising *in vitro* activity against *S. aureus* and low cytotoxicity were isolated from the lichen *Teloschistes chrysophthalmum*, as described in the Chapter 2. The next step in the drug development process is to determine whether or not these hit compounds have good lead-like properties. Some of the properties that need to be investigated are *in vivo* toxicity and bioavailability to determine whether or not the compounds would theoretically be capable of clearing an *S. aureus* infection *in vivo* (Koehn and Carter, 2005; Butler, 2004; Lipinski *et al.*, 2001; Wunberg *et al.*, 2006).

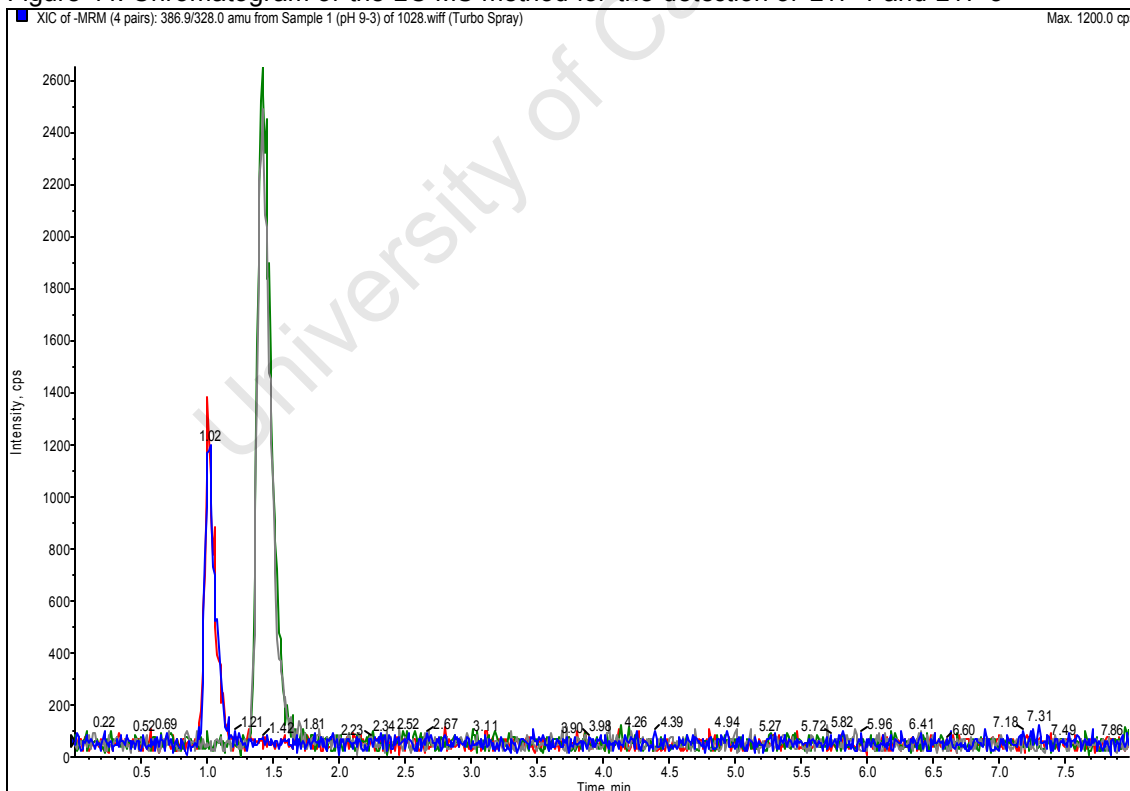
Traditionally, researchers would immediately test promising compounds for efficacy in an *in vivo* model of disease. However, the majority of compounds with promising *in vitro* activity are either toxic or poorly absorbed. It therefore makes sense to first determine bioavailability of the test compound in a small animal model. The advantage of performing these experiments earlier on in the drug development process is that within a relatively short period of time, one can determine whether or not the compound is bioavailable or is toxic to the test animals. Furthermore, from an ethical perspective, in most cases it will negate the need to inflict unnecessary trauma on test animals as would be the case in a disease model. Previous work done at the Division of Pharmacology has shown that it is possible to do bioavailability studies on small numbers of mice by using 10µl of blood per sampling point with the use of LC-MS/MS technology. It is therefore not necessary to sacrifice an animal at every sampling point and valuable data can be obtained in a short period of time.

5.2 Results

5.2.1 Assay development

Firstly, a sensitive LC-MS/MS method for the detection of both compounds in small volumes of mouse blood was developed, as described in Section 8.3. Briefly, it was found that both compounds ionised well in the negative ion mode and the API 2000 mass spectrometer was optimized for maximum detection ability, the parameters of which are tabulated in Section 8.3.1, Tables 31 and 32. A chromatographic method was then developed for the optimal separation of the two compounds in a single run, as shown in Figure 46 below. Briefly, a gradient was run at a flow rate of 300 μ l/min from 32 to 77% ACN with 2.5mM ammonium bicarbonate in 2.9 minutes, followed by an equilibration step in 32% ACN up to 8 minutes.

Figure 44: Chromatogram of the LC-MS method for the detection of L17-1 and L17-3

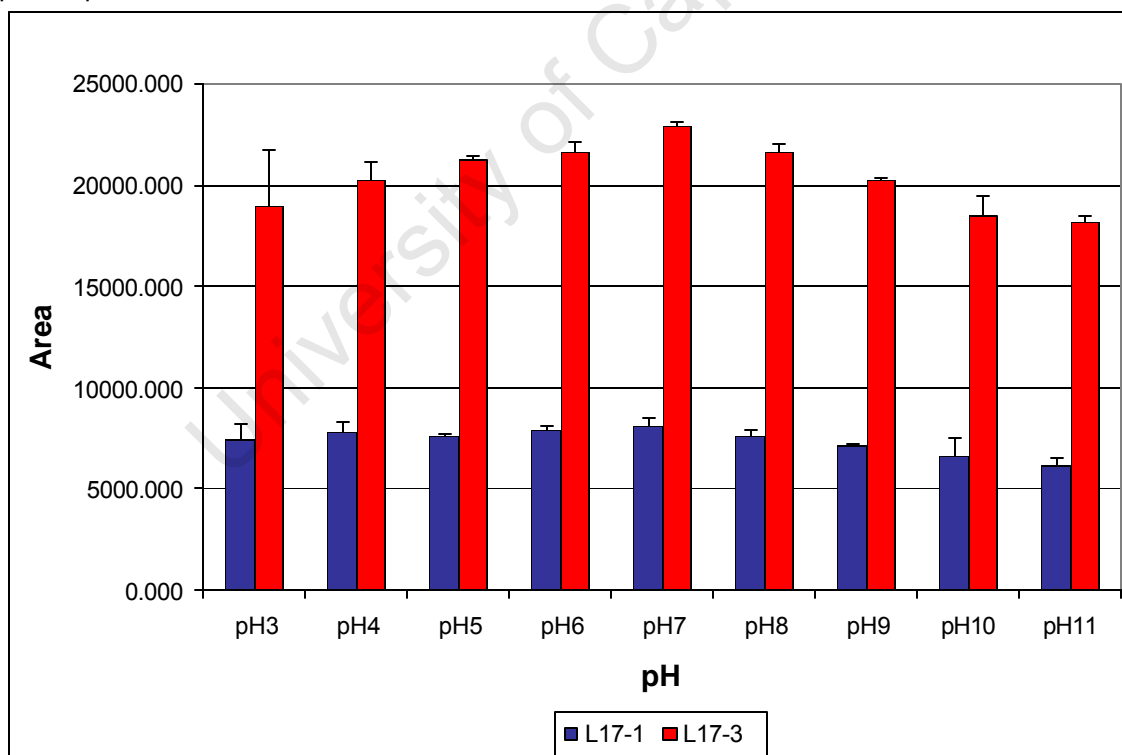


Red and blue: L17-1 (386 ? 328; 386 ? 350)
Green and grey: L17-3 (400 ? 349; 400 ? 364)

L17-1 eluted at approximately 1.0 minute, while L17-3 eluted at 1.5 minutes. These methods were then also applied to an API 4000 LC/MS-MS for greater sensitivity in the negative ion mode.

After development of a suitable method for the detection of L17-1 and L17-3 on the LC-MS/MS, a liquid-liquid extraction method for the optimal extraction of both compounds from 10µl of mouse whole blood was investigated. Ethyl acetate was chosen as an extraction solvent and a wide pH range of buffers examined as described in Section 8.3.3, to determine the pH at which the highest concentration of compounds would be extracted. The results are depicted in Figure 45 below, each bar of the graph representing an average of three replicates per pH.

Figure 45: The relative quantities of L17-1 and L17-3 extracted from mouse whole blood using pH3 to pH11 Universal buffer.



The compounds were well extracted across the entire pH range with pH7 buffer resulting in the extraction of the highest quantities of L17-1 and L17-3 from mouse whole blood. However, pH9 was chosen for the extraction method as it would theoretically result in the extraction of fewer neutral components of the blood matrix which could in turn result in ion suppression. Furthermore, for both compounds, pH9 resulted in less variation amongst the three replicates than pH7, as indicated by the standard deviations.

Further optimization of the extraction method was not performed due to limited sample quantities and the fact that the current method as described in Figure 58 of Section 8.3.3 utilizing ethyl acetate and pH9 buffer resulted in adequate retrieval of both compounds (approximately 100%) from mouse whole blood.

The assay method was also evaluated for sensitivity. The lowest level of quantification (LLOQ) for L17-3 was determined to be 781ng/ml on an API 2000 LC-MS/MS, as shown in Table 20. The same method applied to an API 4000 mass spectrometer reached an LLOQ of 24.4ng/ml (Table 21), a 32-fold increase in sensitivity. Figure 46 shows the peak obtained for L17-3 at 24.4ng/ml on an API 4000 with a good signal to background ratio. Similarly, the LLOQ for L17-1 on an API 4000 mass spectrometer was also 24.4ng/ml.

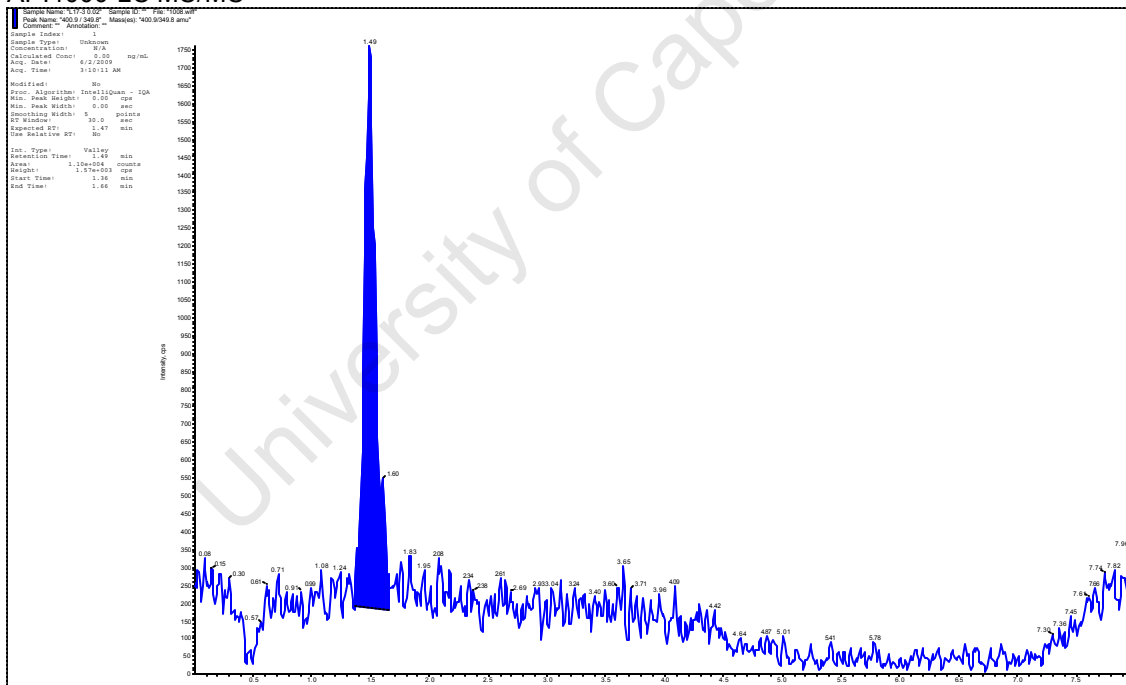
Table 20: A representative table to illustrate the lowest level of quantification for L17-3 as being 781ng/ml on an API 2000 mass spectrometer.

Analyte Concentration (ug/mL)	Calculated Concentration (ug/mL)	Accuracy (%)
25	25.53	102.13
12.5	11.73	93.87
6.25	6.65	106.45
3.125	3.18	101.65
1.563	1.55	99.17
0.781	0.76	97.14
0.391	No peak	n/a

Table 21: A representative table to illustrate the lowest level of quantification for L17-3 as being 24ng/ml on an API 4000 mass spectrometer.

Analyte concentration (µg/ml)	Calculated concentration (µg/ml)	Accuracy (%)
25	25.87	103.49
12.5	N/A	N/A
6.25	5.66	90.54
3.13	2.73	87.17
1.56	1.47	93.99
0.781	0.94	120.49
0.391	0.45	114.74
0.195	0.19	97.61
0.0977	0.089	91.25
0.0488	0.048	99.25
0.0244	0.025	101.56
0.0122	No peak	n/a

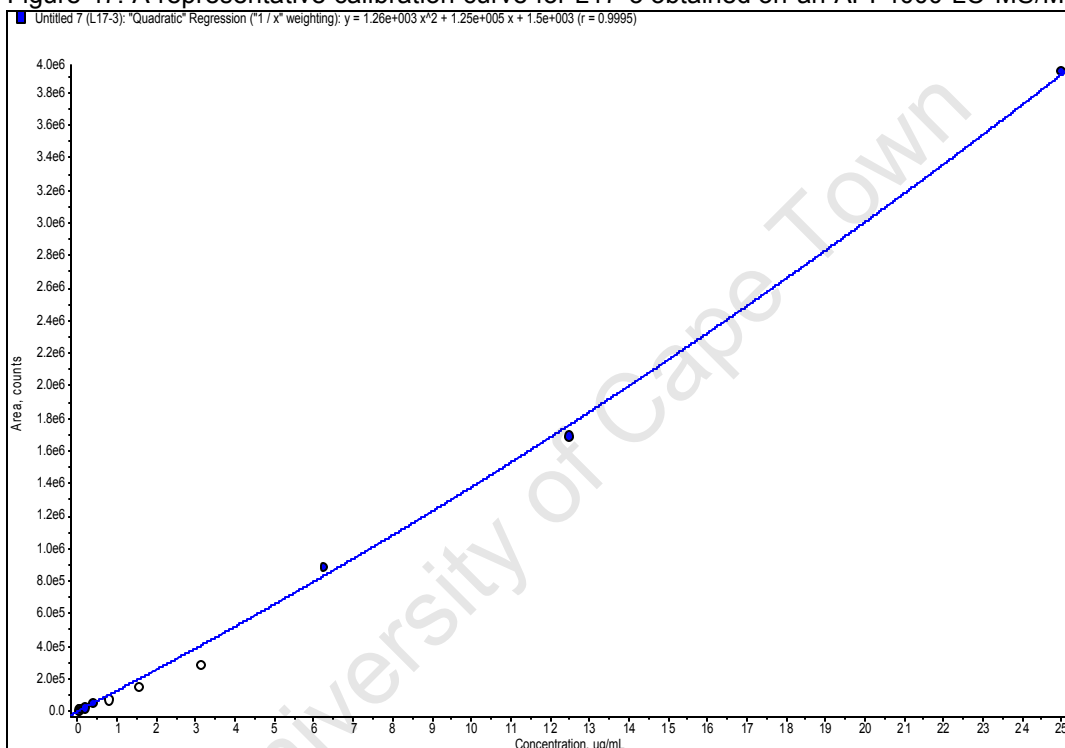
Figure 46: A chromatogram depicting the lowest level of quantification of L17-3, 24.4ng/ml, on an API4000 LC-MS/MS



To obtain greater sensitivity for the detection of L17-1 and L17-3 from 10µl mouse whole blood samples, an API 4000 LC-MS/MS was therefore utilized for the analysis of samples from *in vivo* experiments. Calibration standards were prepared in mouse whole blood for both compounds from 12ng/ml to 25µg/ml.

These standards were included in every batch of samples analysed to establish the integrity of the data. A representative curve for the calibration standards of L17-3 is illustrated in Figure 47 below. Three of the data points for this particular batch of samples were considered to be outliers and were excluded from the data set, resulting in the curve being generated from 9/12 (75%) of the calibration standards, a percentage considered to be acceptable.

Figure 47: A representative calibration curve for L17-3 obtained on an API 4000 LC-MS/MS.



5.2.2 Initial bioavailability study of L17-1 and L17-3

An initial *in vivo* experiment was performed to obtain information on the length of time for which compounds L17-1 and L17-3 remained at detectable levels in the blood. The two compounds in combination were administered orally and subcutaneously to three mice per group at a concentration of 10mg/kg each in DMSO:water 1:9 (v/v). A volume of 10µl of whole blood was collected from each mouse at one, three, five and seven hours after dosing. The samples were extracted as described in Section 8.3.3 and analysed as described in 8.3.1 and

8.3.2. The subsequent pharmacokinetic parameters for each compound and administration route are shown in Tables 22 to 25 and the average levels of L17-1 and L17-3 over the seven hour test period are shown in Figures 48 and 49. The graphs pertaining to the levels of L17-1 and L17-3 in each of the three mice are found in the Appendix (Figures 86 to 89).

Table 22: The pharmacokinetic parameters of L17-1 after oral administration at 10mg/kg to three mice in combination with L17-3.

Parameters	Mouse 1	Mouse 2	Mouse 3	Average
T_{max} (hours)	1.000	1.000	1.000	1.000 ± 0.000
C_{max} (µg/ml)	4.546	3.344	3.988	3.959 ± 0.602
t_{1/2z} (hours)	1.3444	3.0577	1.16	1.854 ± 1.046
AUC_{0-tlast} (µg.h/ml)	13.292	11.815	10.241	11.783 ± 1.526
AUC_{0-8 obs} (µg.h/ml)	13.806	15.9396	10.4803	13.409 ± 2.751

The acceptable RSQ values for the data set resulting from the oral dosing of three mice with L17-1 at 10mg/kg (average of 0.952 ± 0.044), allow for the determination of the average elimination half life of this compound, which is 1.85 hours. Similarly, the elimination half-life after subcutaneous administration is 1.94 hours, as shown in Table 23 below (RSQ values of 0.985 ± 0.006). A comparison of the AUC values for the two administration routes shows that subcutaneous dosing results in a greater area under the curve, with resultant greater bioavailability.

Table 23: The pharmacokinetic parameters of L17-1 after subcutaneous administration at 10mg/kg to three mice in combination with L17-3.

Parameters	Mouse 1	Mouse 2	Mouse 3	Average
T_{max} (hours)	1.000	3.000	1.000	1.667 ± 1.155
C_{max} (µg/ml)	4.553	3.624	3.961	4.046 ± 0.470
t_{1/2z} (hours)	1.3934	2.9217	1.492	1.936 ± 0.855
AUC_{0-tlast} (µg.h/ml)	15.9895	17.7945	11.3385	15.041 ± 3.331
AUC_{0-8 obs} (µg.h/ml)	16.9183	23.7083	11.9261	17.518 ± 5.914

From Figure 48 it is evident that levels of L17-1 steadily decrease from one to seven hours in the bloodstream after both oral and subcutaneous dosing. The

highest level measured (3.96 and 4.05 $\mu\text{g/ml}$ for the oral and subcutaneous groups respectively) was at one hour after dosing for all three mice in the oral group and two of the three mice in the subcutaneous group. After seven hours, mice dosed orally had average levels of 0.45 $\mu\text{g/ml}$ and those dosed subcutaneously had levels of 0.71 $\mu\text{g/ml}$. Over the entire test period with the exception of the one hour time point, those mice that received subcutaneous doses appeared to have higher levels of L17-1 in the bloodstream, as can be verified by the greater AUC values for this administration route.

Figure 48: Levels of L17-1 in mouse whole blood after the administration of 10mg/kg by oral and subcutaneous dosing. Each data point represents the average of levels in three mice with standard deviations.

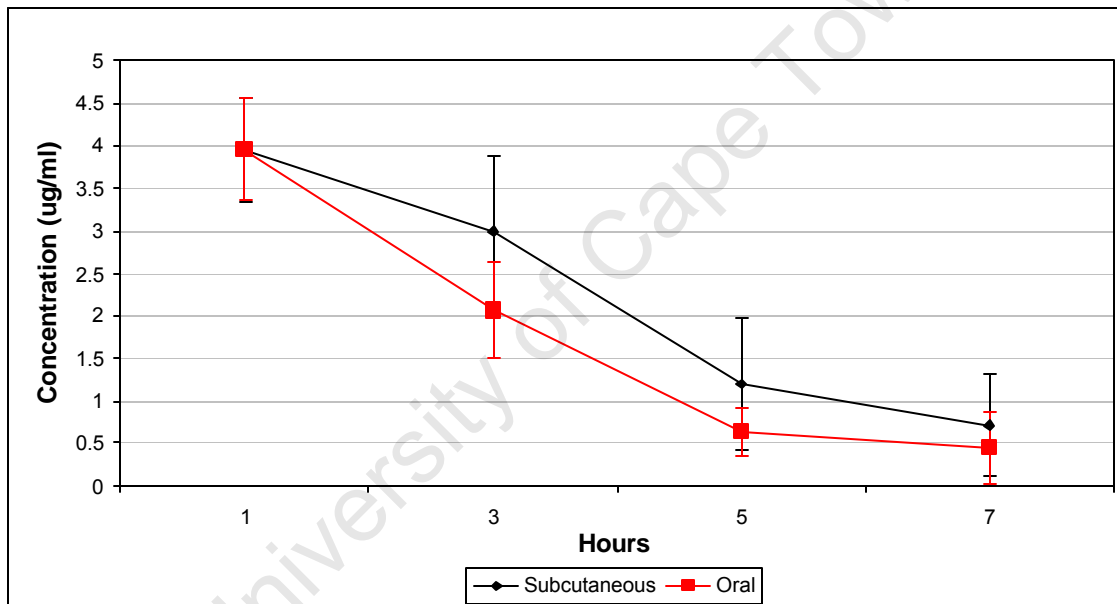


Figure 49 indicates that high levels of L17-3 remained in the bloodstream after seven hours after both oral and subcutaneous dosing. This prevented the calculation of an elimination rate constant, as there was no evidence of an elimination phase in the profile and therefore also affected the ability to determine most of the pharmacokinetic parameters, as witnessed by the RSQ values of less than 0.9.

Table 24: The pharmacokinetic parameters of L17-3 after oral administration at 10mg/kg to three mice in combination with L17-1.

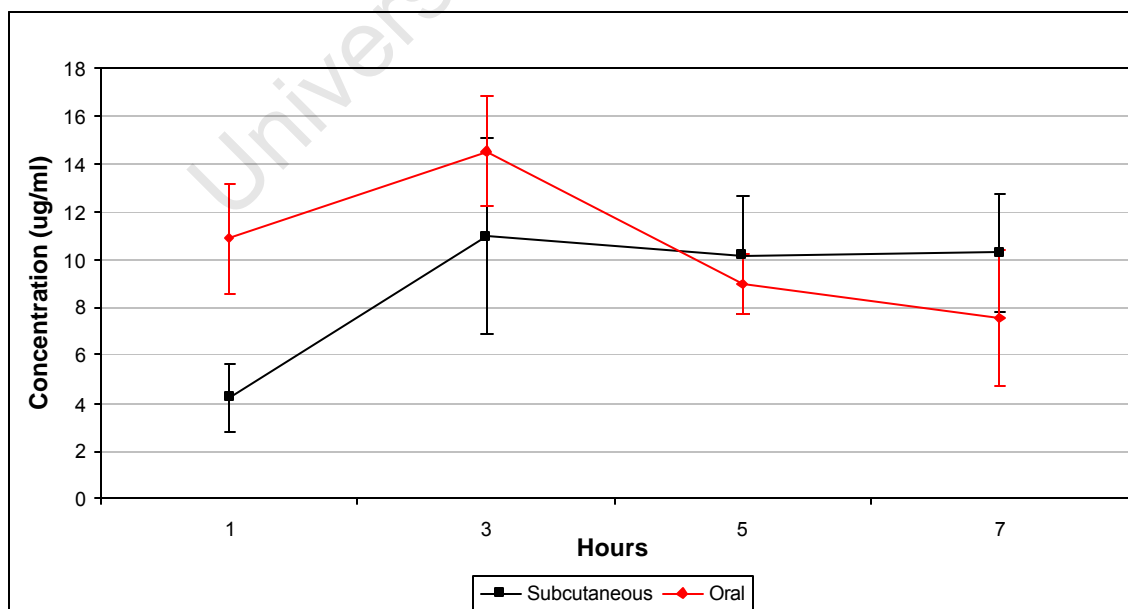
Parameters	Mouse 1	Mouse 2	Mouse 3	Average
T_{\max} (hours)	3.000	3.000	3.000	3.000 \pm 0.000
C_{\max} ($\mu\text{g/ml}$)	17.153	13.486	12.897	14.512 \pm 2.3061
$t_{1/2z}$ (hours)	3.066	n/a	2.9359	n/a

In Table 24 above, the only subject for which an accurate half-life after oral dosing of L17-3 could be calculated (2.94 hours) as witnessed by the RSQ value of 0.9773, is subject 3. Similarly, only subject 1 could be used to determine the half-life after subcutaneous dosing (Table 25 below) and this was shown to be 6.4 hours (RSQ value of 0.9996).

Table 25: The pharmacokinetic parameters of L17-3 after subcutaneous administration at 10mg/kg to three mice in combination with L17-1.

Parameters	Mouse 1	Mouse 2	Mouse 3	Average
T_{\max} (hours)	3.000	7.000	3.000	4.333 \pm 2.3094
C_{\max} ($\mu\text{g/ml}$)	15.653	12.825	9.275	12.5843 \pm 3.1958
$t_{1/2z}$ (hours)	6.4165	n/a	n/a	n/a

Figure 49: Levels of L17-3 in mouse whole blood after the administration of 10mg/kg by oral and subcutaneous administration. Each data point represents the average of levels in three mice with standard deviations.



The levels of L17-3 at one hour after oral administration are more than double (average of 10.9 µg/ml versus 4.2 µg/ml) those receiving the subcutaneous dose. The C_{\max} concentrations of L17-3 were 14.5 µg/ml after oral dosing, and 12.6 µg/ml after subcutaneous administration were reached at three and 4.3 hours respectively.

From this initial *in vivo* experiment in which both compounds were co-administered to mice via oral and subcutaneous routes, it is evident that the sampling time needed to be extended beyond seven hours. Furthermore, L17-3 reaches much higher levels in the bloodstream than L17-1, suggesting that it is more bioavailable.

5.2.3 Bioavailability study of L17-3 in mice

Based on the initial *in vivo* experiment described in section 5.2.2 using oral and subcutaneous dosing of L17-1 and L17-3 in combination, further *in vivo* work focused on the bioavailability of L17-3 only. Furthermore, the experiment was lengthened up to 96 hours to allow for more sampling time points. The dosage of L17-3 per mouse was also halved due to the high levels observed in mouse whole blood in the initial experiment. An extra group of six mice to be dosed intravenously were also included in the subsequent study to allow for the actual oral and subcutaneous bioavailability determination. The experimental details are described in Section 8.5.

5.2.3.1 Oral

Oral dosing of L17-3 at 5mg/kg and sampling over a period of 96 hours resulted in a C_{\max} value 2.8 ± 0.7 µg/ml at a T_{\max} time of 3.4 hours as shown in Table 26. At 24 hours, all but one of the mice showed levels of L17-3 below the LLOQ of 24.4ng/ml (Appendix, Table 37). The half life ($t_{1/2z}$) of the compound in the animals is on average 2.98 hours. None of the mice displayed any signs of toxicity after dosing. The data for each mouse was also found to be within acceptable limits, as indicated by the RSQ values (average of 0.983 ± 0.0068).

Figure 50: Blood levels of L17-3 in 5 individual mice after oral administration of 5mg/kg

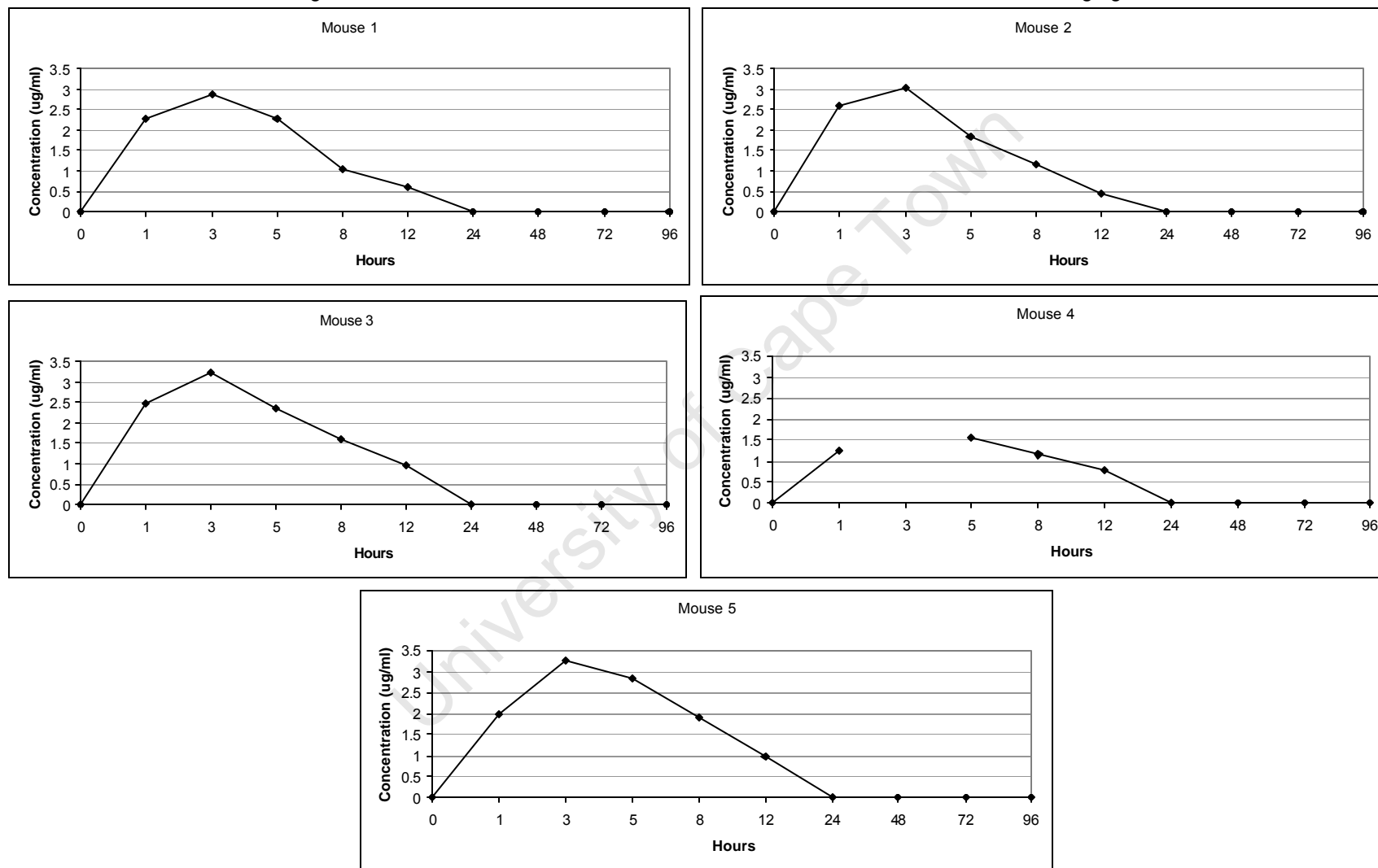


Table 26: The pharmacokinetic parameters as obtained by WinNonlin analysis for the oral dosing of five mice with L17-3 at 5mg/kg.

PK parameters	Mouse 1	Mouse 2	Mouse 3	Mouse 4	Mouse 5	Average
$t_{1/2z}$ (hours)	3.9092	3.4011	2.6540	2.7303	2.2132	2.9816 ± 0.6703
T_{max} (hours)	3.0000	3.0000	3.0000	5.0000	3.0000	3.4000 ± 0.8944
C_{max} (µg/ml)	2.8500	3.0200	3.2200	1.5700	3.2600	2.7840 ± 0.6983
$AUC_{0-tlast}$ (µg.h/ml)	19.8100	19.4810	29.6778	19.2116	31.2666	23.8894 ± 6.0392
AUC_{all} (µg.h/ml)	23.5600	22.2290	30.0234	19.5008	31.4478	25.3522 ± 5.1522
$AUC_{0-8\text{ obs}}$ (µg.h/ml)	23.3349	21.7283	29.7881	19.3065	31.3148	25.0945 ± 5.2118
RSQ	0.9760	0.9925	0.9837	0.9771	0.9863	0.9831 ± 0.0068

Abbreviations: AUC - area under the concentration curve

Figure 50 shows the graphs of each individual mouse after oral dosing with L17-3, while the actual levels in each mouse over the experimental period are tabulated in the Appendix, Table 37. The sample taken at three hours from mouse 4 was excluded from the analysis of the data due to experimental error. The observed levels in each mouse appear to follow the same trend over the 96 hour experiment.

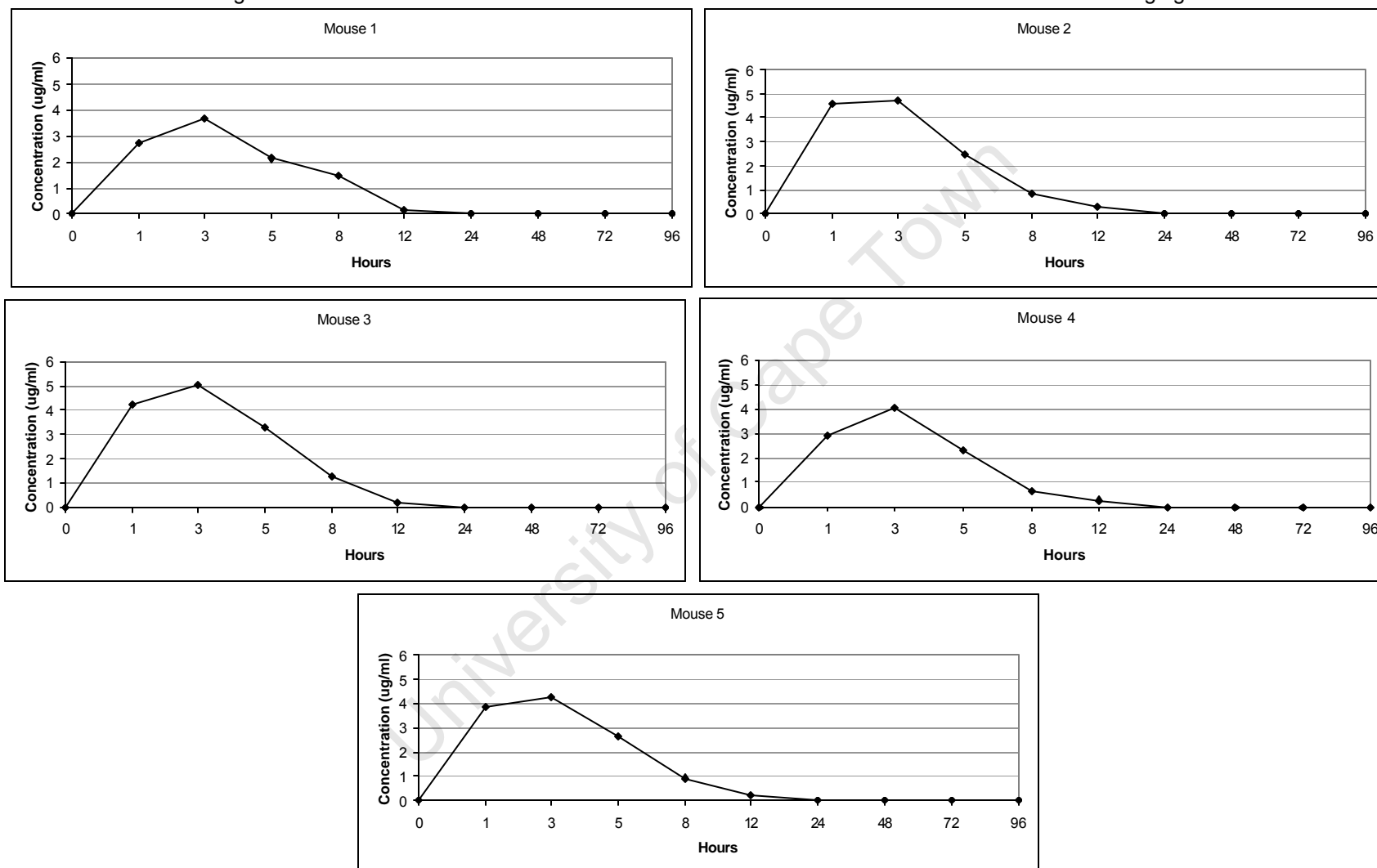
5.2.3.2 Subcutaneous

The half-life of L17-3 after subcutaneous administration is 2.04 hours with a T_{max} value at 3 hours and a C_{max} concentration of 4.35µg/ml (Table 27). The parameters for each mouse are within acceptable limits as shown by the RSQ values (average of 0.9765 ± 0.03). At 24 hours, all the mice showed levels of L17-3 below the level of quantification (Appendix, Table 38). The dose of compound administered did not appear to have any negative effects on the mice.

Table 27: The pharmacokinetic parameters as obtained by WinNonlin analysis for the subcutaneous dosing of five mice with L17-3 at 5mg/kg.

PK parameters	Mouse 1	Mouse 2	Mouse 3	Mouse 4	Mouse 5	Average
$t_{1/2z}$ (hours)	2.1646	2.1807	1.5943	2.2682	1.9695	2.0355 ± 0.2697
T_{max} (hours)	3.0000	3.0000	3.0000	3.0000	3.0000	3.0000 ± 0.0000
C_{max} (µg/ml)	3.6520	4.6950	5.0170	4.0740	4.3030	4.3482 ± 0.5314
$AUC_{0-tlast}$ (µg.h/ml)	22.1580	25.8260	29.2210	21.0960	24.6340	24.5870 ± 3.2054
AUC_{all} (µg.h/ml)	23.2680	27.4760	30.1930	22.8000	25.9720	25.9418 ± 3.0597
$AUC_{0-8\text{ obs}}$ (µg.h/ml)	22.7357	26.6912	29.5936	22.0253	25.2676	25.2627 ± 3.0685

Figure 51: Blood levels of L17-3 in the 5 individual mice after subcutaneous administration of 5mg/kg



As observed in Figure 51, the levels of L17-3 in the individual mice appear to follow the same trends, with all obtaining maximum concentrations in the bloodstream of between 3.65 to 5.02µg/ml at 3 hours after dosing.

5.2.3.3 Intravenous

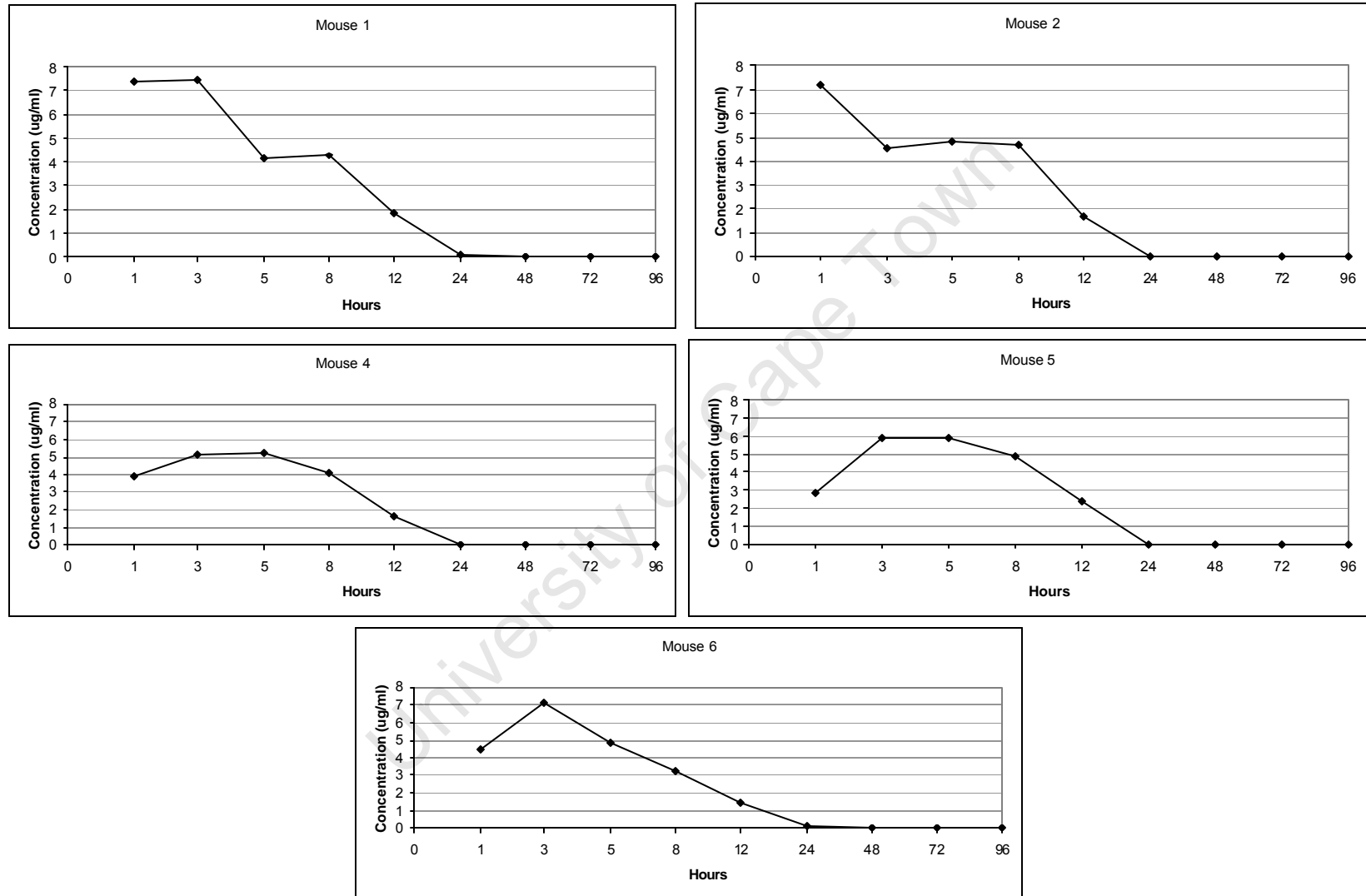
Six mice were dosed intravenously with 5mg/kg of L17-3. However, one mouse (subject 3) died immediately. A heart puncture was performed and it was found that the mouse had 34.05µg/ml of compound in its blood, more than 4.5 times the amount seen in the other mice one hour after dosing. This was most likely as a result of initial leakage and re-administration of the compound during the dosing procedure. These data was therefore omitted from the analysis. However, at this dosage, the mice remained inert for one hour after dosing. Within three hours the mice appeared to have recovered and remained healthy for the duration of the experiment. In Table 28 it is evident that the elimination half-life of L17-3 after intravenous administration is 3.28 hours. It is not possible to calculate the C_{max} concentration, as the compound should be at its highest levels immediately after being injected directly into the bloodstream. At 24 hours, three of the remaining five mice had levels of L17-3 below the LLOQ of 24.4ng/ml and by 48 hours the compound had been eliminated completely from the bloodstream (Appendix, Table 39).

Table 28: The pharmacokinetic parameters as obtained by WinNonlin analysis for the intravenous dosing of five mice with L17-3 at 5mg/kg.

PK parameters	Mouse 1	Mouse 2	Mouse 4	Mouse 5	Mouse 6	Average
t_{1/2z} (hours)	2.8737	6.1400	2.0737	1.9997	3.3293	3.2833 ± 1.6913
AUC_{0-tlast} (µg.h/ml)	66.3680	51.4700	56.9660	67.0995	56.2420	59.6291 ± 6.8256
AUC_{all} (µg.h/ml)	67.4840	61.4480	57.2300	67.3755	57.6220	62.2319 ± 5.0231
AUC_{0-8 obs} (µg.h/ml)	66.7536	66.2010	57.0318	67.1659	56.7944	62.7893 ± 5.3758

Figure 52 shows the levels of L17-3 in each of five mice after intravenous administration at 5mg/kg. Various differences are noted in the five animals. For mice 2, 4 and 5 the levels of L17-3 remain constant between 3 and 5 hours and

Figure 52: Blood levels of L17-3 in the 5 individual mice after intravenous administration of 5mg/kg



for mice 1 and 2 the levels stay relatively unchanged between 5 and 8 hours. After 8 hours the concentration of compound in the bloodstream of all the mice decreases steadily until it is eliminated from the system between 24 and 48 hours (Appendix, Table 39). The RSQ value for mouse 2 is very low at 0.804 and it is possible that omitting this data could confer greater uniformity to the data set as a whole.

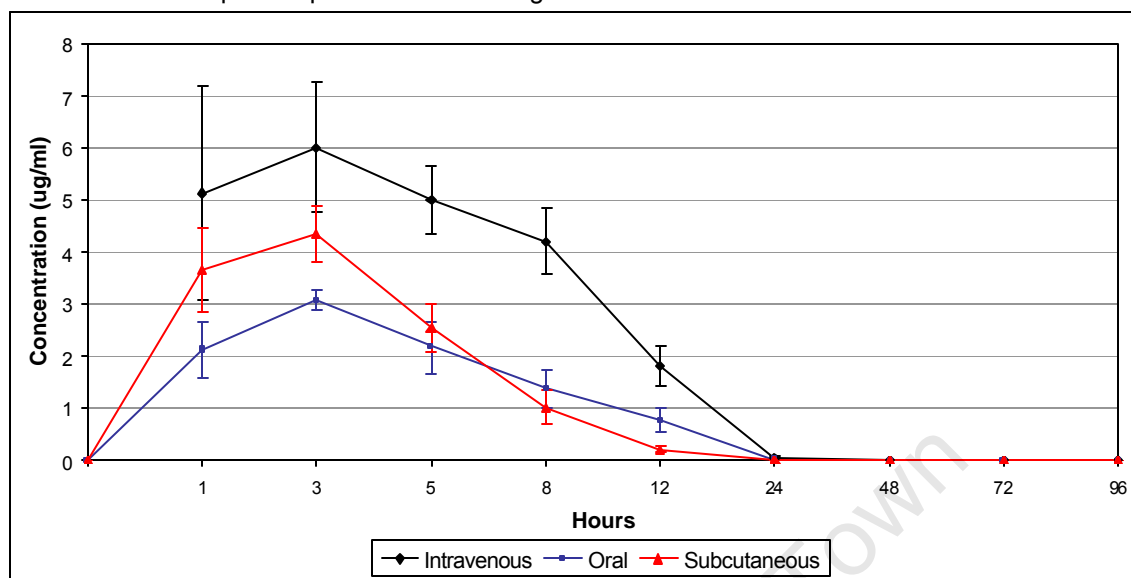
The pharmacokinetic parameters of L17-3 after intravenous, oral and subcutaneous administration are summarised in Table 29 while the levels of L17-3 after the various administration routes over 96 hours are shown in Figure 53. The highest C_{max} concentration is obtained by subcutaneous administration (4.35µg/ml) followed by oral (2.78µg/ml). The time at which the highest levels of compound in the blood are observed is at 3.4 hours for oral and at 3 hours after subcutaneous dosing. The half-life of L17-3 in the bloodstream is greatest for IV dosing, followed by oral and then subcutaneous administration. After subcutaneous dosing, the compound levels decrease most rapidly with an average of 0.23µg/ml being detected at 12 hours in comparison to 0.78 and 1.80µg/ml for the oral and IV groups respectively (Appendix). At 24 hours, only the IV group of mice had on average levels of L17-3 above the LLOQ (0.05µg/ml).

Table 29: The average pharmacokinetic parameters of L17-3 after intravenous, oral and subcutaneous dosing at 5mg/kg.

PK parameters	Intravenous	Oral	Subcutaneous
T_{max} (hours)	n/a	3.4000 ± 0.8944	3.0000 ± 0.0000
C_{max} (µg/ml)	n/a	2.7840 ± 0.6983	4.3482 ± 0.5314
$t_{1/2z}$ (hours)	3.2833 ± 1.6913	2.9816 ± 0.6703	2.0355 ± 0.2697
AUC _{0-tlast}	59.6291 ± 6.8256	23.8894 ± 6.0392	24.5870 ± 3.2054
AUC _{all}	62.2319 ± 5.0231	25.3522 ± 5.1522	25.9418 ± 3.0597
AUC _{0-8obs}	62.7893 ± 5.3758	25.0945 ± 5.2118	25.2627 ± 3.0685

Abbreviations: n/a – not applicable

Figure 53: The levels of L17-3 after oral, subcutaneous and intravenous dosing at 5mg/kg over 96 hours. Each data point represents the average of 5 mice with standard deviations.



By comparing the respective oral and subcutaneous AUC values to the AUC value after intravenous dosing, it is possible to determine the overall oral and subcutaneous bioavailability of the compound.

$$F_{\text{(bioavailability)}} = (\text{AUC}_{\text{all oral}} / \text{AUC}_{\text{all IV}}) \times 100 = (25.3522/62.2319) \times 100$$

$$= 40.74\%$$

$$F_{\text{(bioavailability)}} = (\text{AUC}_{\text{all sub}} / \text{AUC}_{\text{all IV}}) \times 100 = (25.9418/62.2319) \times 100$$

$$= 41.69\%$$

From the equation above it is evident that the bioavailability of L17-3 after oral and subcutaneous dosing is 40.7 and 41.7% respectively. Furthermore, Figure 53 above indicates that higher compound concentrations are achieved in mouse blood after subcutaneous administration, although the levels drop more quickly after subcutaneous than oral dosing.

5.3 Discussion

The purpose of this work was to determine whether compounds exhibiting good *in vitro* activity exhibited good lead-like properties (no toxicity and good bioavailability) *in vivo*. One of the major problems in drug-development is that many compounds showing efficacy *in vitro*, have poor bioavailability and/or exhibit toxicity in pre-clinical small animal studies, partly due to enzymes involved in drug metabolism (Guengerich, 2006). Several researchers have suggested microdosing in humans as a means of predicting drug pharmacokinetics to aid in the early selection of drug candidates. This method involves dosing humans with trace subpharmacological amounts of drug, thereby reducing the need for the intensive safety approval associated with a study utilizing the full drug dosage (Lappin *et al.*, 2006). A drawback of natural product research is the length of time required to generate the large quantities of pure compound required for *in vivo* efficacy and bioavailability experiments. Previous work performed in the Division of Pharmacology at the University of Cape Town has shown that it is possible to study the pharmacokinetics of test compounds in very small quantities (10µl) of blood (Wiesner, 2008). This permits the use of smaller numbers of experimental animals as it is not necessary to sacrifice an animal at each sampling point and multiple data sets can subsequently be obtained from a single subject. Furthermore, it reduces the amount of pure test compound required for the detection of low levels in the blood for bioavailability research.

The method developed for the detection of two compounds derived from the lichen *T. chrysophthalmum*, namely L17-1 and L17-3, proved to be capable of detecting small quantities of compound from 10µl of mouse whole blood. The method was developed on an Applied Biosystems API 2000 mass spectrometer which allowed for an LLOQ of 781ng/ml for both compounds in the negative ion mode. When this method was directly applied to the more sensitive Applied Biosystems API 4000 LC-MS/MS, it allowed for a greatly improved level of quantification, namely 24.4ng/ml. It is possible that the method could still be optimized further on this instrument to allow for even greater sensitivity. The

extraction method based on ethyl acetate and pH9 universal buffer was effective at retrieving the compounds from the blood matrix. Despite the fact that pH7 buffer resulted in slightly better retrieval of the compounds, a more alkaline buffer (pH9) was used as it resulted in less variability amongst the replicates and would theoretically reduce the extraction of neutral blood components. These matrix components could result in ion suppression or enhancement of the analyte which could in turn affect the quantitation of the drug in a biological fluid (Van Eeckhaut *et al.*, 2009). To further refine this method, the matrix effects would need to be investigated more thoroughly. In the case of greater sample quantities, this method could be even further optimized by investigating other extraction solvents in a cost-effective liquid-liquid system, such as hexane or dichloromethane.

A cursory *in vivo* experiment was set up to determine the ideal sampling time for the bioavailability study of the two compounds of interest. Furthermore, this experiment served to determine whether or not one can investigate the bioavailability of a mixture of known compounds in a single mouse. The advantage of such an approach would be the use of fewer animals to obtain data on more than one compound. This has been made possible by using small (10µl) blood samples at each collection point, avoiding the sacrificing of a single mouse per time point. This experiment could also prove to be relevant in the study of natural products, which rarely occur as single compounds. The isolation and accumulation of large enough quantities of a single compound from a complex mixture to perform *in vivo* work is time-consuming and often impossible due to limited material, such as in the case of lichens. Performing bioavailability studies on a mixture of known compounds could greatly decrease the amount of material and time required to accumulate pure compounds while focusing research efforts on those few compounds that are bioavailable and therefore have drug-like potential.

The results of the initial *in vivo* study involving two groups of three mice each, one group dosed orally with 10mg/kg of each compound in combination, the

other group dosed subcutaneously with the same amount of compound, showed that at this dosage, the compounds had no toxic effects on the mice. Furthermore, it became evident that the compounds were still detectable in the bloodstream at 7 hours after dosing. Each 20g mouse received 200µg of each compound, and after one hour, L17-1 was measured at approximately 4µg/ml for both administration routes. Thereafter, the levels decreased until the last sampling point, namely 7 hours. The subcutaneously administered L17-1 was available at higher levels at 3, 5 and 7 hours than that arising from oral dosing. In comparison, L17-3 administered orally was available at an average of 10.9µg/ml at one hour, increasing to 14.5µg/ml at 3 hours. Thereafter the levels decreased steadily, reaching a concentration of 7.5µg/ml at 7 hours. Although the subcutaneously administered L17-3 did not reach the same levels as that administered orally, it also reached T_{max} at 3 hours, as for the oral dose. However, the levels of L17-3 then remained fairly constant until 7 hours (approximately 10µg/ml).

This initial experiment clearly showed that L17-3 is more bioavailable than L17-1, reaching the highest concentration of 14.5µg/ml after oral dosing in comparison to 4.0µg/ml for L17-1 – more than a three-fold difference. Furthermore, while the levels of L17-1 steadily decrease from 1 to 7 hours, L17-3 concentrations increase until three hours, after which they decrease to seven hours for the oral dose and remain constant for the subcutaneous dose. It is possible that the co-administration of two closely-related compounds could have an effect on the bioavailability of each compound in the bloodstream.

Based on the initial *in vivo* experiment, a subsequent investigation was undertaken to determine the bioavailability of the most promising compound, namely L17-3. In this experiment, two groups of five mice and one group of six mice were dosed at 5mg/kg by means of oral, subcutaneous and intravenous administration respectively. Samples were taken from one to 96 hours after dosing. Half the dosage was used compared to the initial *in vivo* experiment due

to small sample quantities and good bioavailability. As for the initial experiment, none of the animals were negatively affected by the oral and subcutaneous doses. However, the mice receiving the IV dose remained inert for one hour after dosing, but recovered and remained healthy for the remainder of the experiment. One animal in this group died, probably as a result of overdosing, with levels of 34µg/ml being detected from a heart puncture performed one hour after dosing. Although unfortunate, this information could be useful as it provides an end-point of toxicity, information which is necessary in the development and approval of a potential drug candidate (Guengerich, 2006). In this case, it is apparent that toxicity occurred as a result of over-dosing as opposed to the compound's mechanism of action, bioactivation or immunological reactions (Guengerich, 2006). Typically, IV doses are administered at a concentration of ten-fold less than the oral dose, and realistically, one would expect to see some adverse effects at such a high dose.

For the oral administration route, T_{max} was reached at 3.4 hours, whereas the subcutaneous dose resulted in T_{max} at three hours. It is interesting to note that for the IV dose which is injected directly into the bloodstream, the levels of L17-3 peak at 3.4 hours, suggesting potential tissue absorption. Future work should include sampling points between zero and one hour to investigate the bioavailability of the compound immediately after dosing. It is possible that the one mouse that died immediately after IV dosing, despite the near certainty that the animal was overdosed, could in fact give a more accurate reflection of compound levels in the blood shortly after dosing, suggesting that the compound is in fact available at higher levels before one hour as opposed to after one hour. Many compounds are subjected to enterohepatic recycling *in vivo*, which could also explain the perceived delayed peak concentration after IV administration. Briefly, this phenomenon occurs as a result of biliary excretion and reabsorption of the solute into the intestine, leading to the appearance of multiple peaks and an apparent longer half-life. Some well-known drugs that are subjected to a

certain degree of enterohepatic cycling include morphine, cardiac glycosides, rifampicin and ampicillin (Roberts *et al.*, 2002).

The highest C_{\max} concentration was achieved by subcutaneous and then oral administration. The fact that subcutaneous dosing results in greater levels of compound in the mice than oral administration is in contrast to the results of the initial *in vivo* experiment performed which showed higher levels of L17-3 after oral dosing. This can be explained by the fact that in the initial *in vivo* experiment, it was noticed that there was a small amount of 'leakage' from the puncture wound after subcutaneous administration. Therefore, less compound would have been administered by subcutaneous dosing in comparison to oral dosing. In the subsequent experiment, care was taken to administer the same dosages by all administration routes. For both the oral and subcutaneous doses, levels of L17-3 were below the LLOQ by 24 hours, whereas the levels were completely eliminated after 48 hours for the IV dose. All three curves representing the compound levels over the experiment duration followed roughly the same trend. A comparison of the areas under the curves showed that the oral and subcutaneous bioavailabilities were very similar at 40.7 and 41.7% respectively.

When considering the *in vitro* and *in vivo* data together, it is evident that L17-1, with *in vitro* activity against *S. aureus* of 31.3 µg/ml (MIC) and an IC_{50} of 1.1 µg/ml, is also more cytotoxic *in vitro* and was more poorly bioavailable with a C_{\max} of approximately 4 µg/ml after oral and subcutaneous administration at 10mg/kg. For L17-3, after dosing mice orally at 10mg/kg, a C_{\max} of 14.5 µg/ml is achieved, a level just below the *in vitro* MIC of 15.6 µg/ml (IC_{50} of 0.7 µg/ml) and MBC of 15.6 to 31.3 µg/ml against *S. aureus*. At this dosage, the mice displayed no signs of toxicity, and it is conceivable that a higher dosage, for instance 20mg/kg, would also be well tolerated as the two test compounds were administered together at a total concentration of 20mg/kg in the initial experiment with no signs of toxicity. Intravenous administration of L17-3 would result in higher blood levels of the

compound, but at a dose of 5mg/kg, which only results in an average C_{max} of 6.6µg/ml, the mice appeared to be adversely affected shortly after dosing, although they did make a full recovery. Furthermore, subcutaneous administration of L17-3 in the second experiment resulted in a higher C_{max} than for oral administration, with similar lack of toxicity. It is possible that subcutaneous administration of 10mg/kg or 20mg/kg may in fact yield a blood concentration of L17-3 capable of neutralising a systemic *S. aureus* infection. The concentration of L17-3 required to kill 50% of *S. aureus in vitro* is 0.7µg/ml and this compound exerts bactericidal activity at 15.6 to 31.3µg/ml. In practice, one may find that prolonged or repeated exposure to a sublethal dose of L17-3 may in fact be sufficient to eliminate a systemic *S. aureus* infection. There is evidence to suggest that the instant killing of bacterial cells in an infection is not always desirable, for instance in central nervous system infections. Sudden lysis of the bacterial cell wall (for example by vancomycin) results in the release of cellular components which trigger cytokine production and potentially lethal inflammation (Finberg *et al.*, 2004).

How do these results measure up to published reports of established or promising antibiotics? During efficacy studies in animal models of disease, which could not be performed in this project, a 50% effective dose (ED_{50}) is determined. For instance, the ED_{50} of the widely-used antibiotic, ciprofloxacin, has been shown to be 10mg/kg in an *in vivo* model of *S. aureus* sepsis (Freiberg *et al.*, 2006). A promising drug candidate, the 3-(heteroarylthio)cepham RWJ333441, displayed an ED_{50} of 0.39mg/kg in a mouse model of sepsis. (Glinka *et al.*, 2003). This same compound showed *in vitro* activity against methicillin susceptible and resistant strains of *S. aureus* at 0.25µg/ml and 2µg/ml respectively. There are also reports of compounds which have potent *in vitro* efficacy, but require a relatively high *in vivo* dose to clear disease from an animal model. For instance, Freiberg *et al.* (2006) evaluated pseudopeptide antibiotic derivatives with an *in vitro* MIC of 0.1µg/ml against *S. aureus* in an *in vivo* model

of *S. aureus* sepsis and found that the most active derivative had a 100% effective dose of 25mg/kg.

A study involving a natural product-derived compound, AC98-6446, found that the compound had an ED₅₀ of 0.08mg/kg of body weight after IV administration in a murine acute lethal *S. aureus* infection model. The ED₅₀ for MRSA was 0.27mg/kg. After a 20mg/kg IV dose, the C_{max} in mice was 316µg/ml with an AUC of 164µg/h/ml and a half-life of 3.3 hours (Weiss *et al.*, 2004). In comparison, the most promising compound in this project, namely the lichen-derived L17-3, had a similar half-life after IV and oral administration, but the mice showed adverse effects after IV administration at a quarter of the dose.

Similarly a synthetic compound arising from high-throughput screening of a compound library showed *in vitro* activity against drug sensitive and resistant strains of *S. aureus* with MIC's of 1µg/ml, significantly better *in vitro* activity than L17-3. Furthermore, this compound showed oral efficacy (ED₅₀) at 19.5mg/kg against MRSA in a mouse model of systemic infection. When administered subcutaneously, this compound displayed an ED₅₀ of 12.5mg/ml and was non-toxic up to 200mg/kg (Miller *et al.*, 2008). When administered at an oral dose of 20.3mg/kg, this compound had a half-life of 0.9 hours and a C_{max} of 15.7µg/ml (AUC of 27.6µg h/ml). In the current project, L17-3 had a longer half-life than this compound and at half the oral dose, the observed C_{max} was not much lower at 12.6µg/ml.

Recently, several groups have undertaken work on promising oxazolidinone derivatives. Takhi *et al.* (2008) investigated oxazolidinone derivatives *in vitro* and after oral administration in a mouse model of systemic *S. aureus* infection. The most active derivative had an ED₅₀ of 18.9 mg/kg/day in comparison to the approved oxazolidinone drug linezolid which had an ED₅₀ of 5.3mg/kg/day. Furthermore, this compound displayed a C_{max} of 0.68µg/ml and a half-life of 2.17 hours (AUC 2.25 µg h/ml) while linezolid had a C_{max} of 6.3µg/ml, a half-life of

1.37 hours (AUC 10.98 $\mu\text{g h/ml}$). Two further oxazolidinones under investigation showed *in vitro* MIC's of 0.25 and 1 $\mu\text{g/ml}$ against *S. aureus* and MIC's of 0.5 and 2 $\mu\text{g/ml}$ against MRSA. These two compounds exhibited *in vivo* ED₅₀'s of 6.25 and 9.92 mg/kg for a once –daily dose and 4.96 and 5.56 mg/kg for a twice daily dose in a model of systemic MRSA infection. The two compounds furthermore had oral bioavailabilities of 48% and 73% with half-lives of 13.5 and 3.2 hours (Barman *et al.*, 2009). Hilliard *et al.* (2009) also investigated the *in vivo* efficacy of another promising oxazolidinone, RWJ-416457, in murine models of systemic and skin *S. aureus* infections. This compound had an ED₅₀ ranging from 1.5 to 5 mg/kg of body weight per day for systemic staphylococcal infection. After an oral dose of 10 mg/kg, a C_{max} of 3.5 $\mu\text{g/ml}$ was achieved at two hours, with an AUC₂₄ of 13 and a half-life of 3.4 hours.

An example of a promising drug candidate with favourable pharmacokinetic properties is MK-826, a 1 β -methyl carbapenem with broad-spectrum antibiotic activity (Gill *et al.*, 1998). After a single 10 mg/kg dose in mice, this compound displayed a long half-life (3.2 hours) compared to ceftriazone (2.3 hours) and also had a higher peak concentration in serum (62.8 $\mu\text{g/ml}$) as well as a larger area under the curve (150.8 $\mu\text{g hr/ml}$). Furthermore, MK-826 levels decrease slowly with levels of 3.6 $\mu\text{g/ml}$ being detected at 6 hours after treatment. For murine systemic *S. aureus* infection, the ED₅₀ of MK-826 was 1.58 mg/kg of body weight (MIC of 0.125 $\mu\text{g/ml}$). In comparison, L17-3 has a similar half-life, but much lower C_{max} and AUC. Interestingly, after the same dose of L17-3, higher levels (10.3 and 7.5 $\mu\text{g/ml}$) are detected at seven hours.

Similarly, another 1 β -methyl carbapenem with broad-spectrum Gram-positive activity, SM-17466, had an *in vitro* MIC₉₀ of 0.006 $\mu\text{g/ml}$ against *S. aureus* (ED₅₀ of 0.021 mg/kg) and 3.13 $\mu\text{g/ml}$ against MRSA (ED₅₀ of 8.0 mg/kg). In comparison, vancomycin has MIC₉₀'s of 1.56 $\mu\text{g/ml}$ against methicillin sensitive (ED₅₀ of 1.8 mg/kg) and resistant (ED₅₀ of 9.5 mg/kg) *S. aureus*. Furthermore, this activity against MRSA was shown to be bactericidal. After a subcutaneous dose of

25mg/kg, this compound achieved a C_{max} of 53.9µg/ml at 15 minutes in comparison to 32.9µg/ml at the same sampling point for vancomycin. SM-17466 displayed a half-life of 17.9 minutes (vancomycin has a half-life of 21.8minutes) and an AUC of 19112µg·min/ml (Sumita *et al.*, 1995). As can be seen from the C_{max} parameters of these drugs, a shortfall of the current study is the lack of sampling points prior to one hour after dosing. It is possible that the highest drug levels are in fact observed prior to the first sampling point.

Topical antibiotics are very useful in the treatment of skin infections as they provide high local concentrations of drug which in turn reduces the chance of resistance development and avoids systemic toxicity (Critchley and Ochsner, 2008). One such drug-candidate is REP8839, a fluorovinylthiophene-containing diaryldiamine, which inhibits bacterial methionyl rRNA synthetase. It has MIC's of 0.5µg/ml against methicillin-sensitive and -resistant *S. aureus* and less than or equal to 0.008 to 0.5µg/ml against mupirocin-resistant *S. aureus*. In comparison, mupirocin has MIC's of 0.12 and 16µg/ml against methicillin-sensitive and -resistant *S. aureus*. Although there are no standardised models for the evaluation of topical antibiotics, this drug (2% w/v) has been shown to effectively clear *S. aureus* infection in porcine skin wounds (Critchley and Ochsner, 2008).

So, in the absence of efficacy studies, certain pharmacokinetic-pharmacodynamic (PK-PD) parameters can aid in the prediction of antimicrobial efficacy. Three such indicators are firstly, the amount of time for which the drug levels remain above the *in vitro* MIC ($T > MIC$), secondly the ratio of the maximum drug concentration to the MIC ($C_{max}:MIC$) and thirdly, the ratio of the area under the curve at 24 hours to the MIC ($AUC_{0-24}:MIC$). Some antibiotics display concentration-dependent activity, such as streptomycin, while others display time-dependent activity, such as penicillin. An investigation into a promising drug candidate for the treatment of *S. aureus* bacteraemia, oritavancin, showed that in subjects achieving an $fT > MIC$ value of $\geq 22\%$ of the dosing interval, 93% responded well in comparison to 76% that responded favourably when a lesser

exposure was achieved. These predictive parameters can also facilitate the understanding of drug exposure levels necessary to avoid the development of drug resistant bacterial populations (Ambrose *et al.*, 2007).

The two lichen-derived compounds identified in this study have been tested for *in vivo* bioavailability, but not for *in vivo* efficacy in a disease model, which was not possible due to lack of such a model and limited sample quantities. When taking these PK-PD parameters into consideration, it is evident that neither L17-1 nor L17-3 reach *in vivo* concentrations above the *in vitro* MIC's, irrespective of administration route at the highest dosage investigated. L17-3, however, reaches levels marginally short of the MIC after oral administration at 10mg/kg. The possibility exists that between the time of administration and one hour, the compound levels do reach higher levels in the bloodstream than those detected at one hour. Furthermore, it is possible that the oral and subcutaneous dose of L17-3 could be increased substantially above 10mg/kg without showing signs of toxicity. The IV administration resulted in the highest blood levels of L17-3, but at this exceptionally high dosage of 5mg/kg, the mice appeared to be briefly adversely affected. The most promising compound, L17-3, exhibited a C_{max} :MIC ratio of 1:1.08 after oral administration of 10mg/kg. After IV dosing at 5mg/kg, the most favourable AUC:MIC ratio was obtained, namely 1:0.54. Therefore, in the instance of L17-1, the PK-PD predictive parameters suggest that this compound does not have favourable lead-like properties. However, in comparison to literature reports of promising anti-staphylococcal antibiotics in development, L17-3 does have good pharmacokinetic properties, displaying an elimination half life of 3 to 3.4 hours and achieving a C_{max} concentration after a non-toxic dose just short of the *in vitro* MIC, with the distinct possibility of increasing the dosage without toxicity being observed. Furthermore, it is relatively slowly removed from the bloodstream and is still detectable at high levels eight hours after dosing.

Limited sample quantities and the slow growth rate of *T. chrysophthalmum* have unfortunately made efficacy studies in mice impossible at this time, but it is envisaged that such work will be performed when more material becomes available. A method similar to that utilized by Ueda and Sunagawa (2003) should be evaluated, looking at septicaemia and subcutaneous abscesses in murine models of *S. aureus* infection. A complimentary method that would not require an animal model of disease, is one suggested by Gruppo *et al.* (2006), who developed an *in vivo* assay to measure compound bioavailability after oral administration to mice. Briefly, they tested the serially diluted serum in a broth micro-dilution fashion against the bacterium of choice. This assay therefore measures the antimicrobial activity of the free, unbound drug or active metabolites thereof. Furthermore, synthetic analogues and metabolites of L17-3 would be investigated for *in vitro* bioactivity and *in vivo* pharmacokinetics for the purpose of understanding the mechanism of action and improving on the current *in vitro* antibiotic activity. Biotransformation reactions, such as those performed in microsomes *in vitro*, could be performed to generate active metabolites, which could in turn become lead candidates for new drugs in their own right (Fura, 2006). .

Chapter 6

Conclusion

The objective of this project was to contribute to the field of drug discovery from South African natural products, as well as to introduce potentially useful approaches to distinguishing a promising lead-like compound from a simple 'hit' arising from *in vitro* testing. Due to the lack of research performed on South African lichens, as well as the unique and often extreme local environments in which lichens are found, an investigation was conducted into the antimicrobial activities of ten lichen species growing in various parts of the country. South Africa is deemed a semi-arid country, often being exposed to periods of drought. Subsequently, several true desiccation-tolerant plant species are found with the unique ability to enter a dormant state during dry periods, only to flourish with the arrival of rain. The hypothesis was made that other than those compounds that aid in the process of desiccation-tolerance, these plants could make unique defensive compounds as a means of protection against microbial infections and grazing by herbivores, particularly when in a perceived vulnerable state of quiescence. Furthermore, there have been reports of the use of both lichens and several desiccation-tolerant species in traditional medicines. Another well-used traditional remedy throughout Africa, is the pepper-bark tree, *Warburgia salutaris*. Commercially cultivated plant material of this species was made available for this project with the intention of performing an intensive investigation into the antimicrobial activity, with the aim of researching the *in vivo* bioavailability of individual compounds within a relatively complex fraction.

None of the lichen extracts showed marked activity against Gram-negative bacteria or yeast. Only one extract, that of *Usnea rubrotincta*, displayed activity against *Mycobacterium aurum*, later attributed to the presences of large quantities of usnic acid, previously shown to exhibit antimycobacterial activity. The anti-Staphylococcal activity of this lichen, together with that of

Xanthoparmelia semiviridis, was also attributed to the presence usnic acid. Despite being well-researched, this common lichen metabolite has never been tested for antimalarial activity, and was subsequently found to have moderate activity against the causative organism, *Plasmodium falciparum* (IC₅₀ of 15.1 µg/ml). Several extracts exhibited good activity against the Gram-positive *Staphylococcus aureus*, the most potent being the acetone extract of *Teloschistes chrysophthalmum*, with an MIC of 15.6 to 31.3 µg/ml. Further fractionation of this extract led to the isolation of three compounds, two of which exhibited potent anti-Staphylococcal activity with IC₅₀'s of 1.1 (L17-1) and 0.7 µg/ml (L17-3) against a drug-sensitive reference strain. When tested against methicillin-resistant *S. aureus*, these compounds displayed less activity, with IC₅₀'s of 11.1 (L17-1) and 11.4 µg/ml (L17-3). Due to the good *in vitro* antimicrobial activity, these compounds were also evaluated for *in vitro* cytotoxicity. Both exhibited favourable toxicity, with L17-1 having an IC₅₀ of 81 µg/ml and L17-3 not showing toxicity at the highest concentration tested, namely 100 µg/ml. The resultant selectivity indices for L17-1 and L17-3 against drug sensitive *S. aureus* are therefore 73.6 and greater than 142.9 respectively, with a value of greater than ten indicating a promising 'hit' compound. Various attempts to elucidate the complete structures of these two compounds were unsuccessful.

Four desiccation-tolerant plants were investigated for antimicrobial activity, namely *Xerophyta retinervis*, *Myrothamnus flabellifolius*, *Cheilanthes contracta* and *Selaginella dregei*. Of the 30 sequential extracts generated, only two displayed any activity, surprising considering the reported use of these plants or related species in traditional medicines. The methanol extract of *X. retinervis* exhibited activity against *C. albicans* and *M. aurum* with MIC's of 62.5 and 125 µg/ml. The most potent activity observed was from the methanol extract of *M. flabellifolius* against *C. albicans*, exhibiting an initial MIC of less than 7.8 µg/ml. However, this activity slowly dissipated with repeated tested, eventually showing no activity at the highest concentration tested. Subsequent liquid-liquid

fractionation of this extract yielded similar results, initially as active, eventually becoming inactive with repeated testing as a means to confirm activity. In an attempt to isolate the compound/s responsible for this potent, but variable activity, exhaustive fractionation of the sequential extracts was performed, using liquid-liquid fractionation, TLC and HPLC. The most active stable compound eventually isolated was that originating from the methanol extract, exhibiting an IC_{50} of 67.8 $\mu\text{g/ml}$. It is evident that this was not the original compound responsible for the potent activity of the extract. The variable nature of this activity could be attributed to the presence of volatile components that either degrade or evaporate over time, as is possible with an essential oil, such as has reportedly been isolated from the plant in question, displaying potent antifungal activity. Due to the moderate and/or variable nature of activity from extracts of the desiccation-tolerant plants, as well as the potent lichen-derived compounds isolated, further work in this field was not continued.

Sequential extracts prepared from the bark, stems, leaves and twigs of the medicinal tree, *W. salutaris*, revealed that the DCM extracts of the bark, stems and twigs exhibited potent antifungal and moderate antimycobacterial activity, with the DCM extract of the bark displaying the most potent IC_{50} of 4.24 $\mu\text{g/ml}$. HPLC chromatograms revealed that the DCM extracts of these three plant parts all appeared to contain the same predominant compounds. The bark extract was further fractionated, leading to the isolation of 19 pure/semi-pure compounds. Three of the compounds exhibiting potent antifungal activity were identified as muzigadial, warburganal and ugandensidial, with IC_{50} 's against *C. albicans* of 2.07, 4.45 and 25.2 $\mu\text{g/ml}$ respectively. However, these compounds also displayed potent toxicity against CHO cells with IC_{50} values of 4.3, 1.7 and 1.2 $\mu\text{g/ml}$ respectively. The fraction from which these compounds was isolated exhibited an IC_{50} of 5.8 $\mu\text{g/ml}$ against *C. albicans*, but displayed toxicity against CHO cells at 2.6 $\mu\text{g/ml}$, therefore rendering it more toxic than active. Despite the promising antifungal activity, the cytotoxicity of the individual compounds, as well as the original fraction, made this fraction unsuitable for *in vivo* testing as a

means of determining which hit-compound displayed the best oral bioavailability, thereby making it the most promising lead-candidate. Fraction 7 arising from the ACN fraction of the bark of the DCM extract of *W. salutaris*, was the only fraction to display good activity against *C. albicans* (IC₅₀ of 4.7 µg/ml) and relatively weak cytotoxicity, with an IC₅₀ value of 21.7 µg/ml. However, upon isolation of the individual compounds, a subsequent loss of activity was noted, with the most active compound (H7-1) displaying an IC₅₀ of 13.16 µg/ml against *C. albicans*. This resultant moderate activity suggests compounds acting together synergistically to confer activity against *C. albicans*, or perhaps the loss of the most active component, possibly due to degradation. Once again, in comparison to the active and non-toxic hit compounds and fractions isolated from the lichen, *T. chrysophthalmum*, further work on the well-known medicinal plant, *W. salutaris*, as a vehicle to study oral bioavailability of a complex mixture, was abandoned.

To date, no clinically-relevant antibiotics have been discovered in higher plants, a trend confirmed in this study. Furthermore, none of the plant material tested exhibited any activity against Gram-negative bacteria, most likely due to the organisms' cell wall which is known to act as a virtually impenetrable permeability barrier. It has been suggested that higher plants only produce antimicrobial substances when threatened with a microbial invasion (Lewis and Ausubel, 2006), a possible explanation for the lack of *in vitro* activity. However, the more evolutionary primitive lichens yielded a greater number of hits, particularly against Gram-positive bacteria and mycobacteria, most likely produced by the fungal component of the symbiosis. This research confirms previous reports of the enormous potential that lichens have in the drug discovery process. Many antibiotics currently on the market originate from fungi, such as penicillin and streptomycin. It is widely recognized that as a result of the symbiosis of fungi and algae and/or cyanobacteria, a range of compounds often distinct from those produced by the individual constituents are produced, despite lichens having fairly well-defined biochemical pathways (Culberson, 1967; Culberson *et al.*,

1973; Culberson, 1969). Furthermore, the promising bioavailability of the lichen-derived L17-3 suggests that, in comparison to compounds from higher plants with substituents easily recognized by mammalian enzymes *in vivo* making them prone to being metabolized, lichens may in fact produce antibiotic substances with more favourable drug-like properties. This work therefore indicates that the unique compounds produced by lichens represent a largely untapped source of pharmacologically interesting antimicrobial substances.

The most promising hit compounds discovered in this study, were L17-1 and L17-3 derived from the lichen, *T. chrysophthalmum*, with potent *in vitro* anti-Staphylococcal activity and low cytotoxicity. As a means of determining which compound exhibited the most promising *in vivo* bioavailability, an initial experiment was designed in which the two compounds were administered in combination at 10mg/kg each to mice and the pharmacokinetic parameters evaluated from four sampling time points to a maximum of seven hours. This was made possible by collecting only 10µl samples from each experimental animal at each time point, negating the need to sacrifice an animal for each sampling point. With the use of sensitive LC-MS/MS technology, these initial results showed that L17-3 was available at greater quantities after oral and subcutaneous administration to mice than L17-1, reaching a C_{max} concentration of 14.5µg/ml at 3 hours after oral dosing. Furthermore, the mice displayed no signs of toxicity on administration of the two compounds in combination at 10mg/kg each.

Based on these initial results, L17-3 was selected for further pharmacokinetic evaluation. Three groups of mice were further dosed orally, subcutaneously and intravenously with 5mg/kg of compound and evaluated up to 96 hours, collecting 10µl of blood from each animal per sampling time point. The mice appeared to be briefly adversely affected after IV dosing at this concentration, but were not affected by oral and subcutaneous administration. As to be expected, the IV dosing resulted in a greater AUC (62 µg.h/ml) compared to subcutaneous and

oral, which exhibited similar values of 25.9 and 25.4. The subcutaneous group achieved a C_{\max} of 4.4 $\mu\text{g/ml}$ at 3 hours and the oral group a C_{\max} of 2.8 $\mu\text{g/ml}$ at 3.4 hours. L17-3 exhibited a relatively good half life of 3 and 3.3 hours after oral and IV dosing respectively. The absolute bioavailability after subcutaneous and oral administration was 41.7 and 40.7% respectively.

The lack of sampling time points directly after dosing up to one hour is a weakness of this experiment. However, with the data in hand, it is evident that L17-3 reaches a C_{\max} level after oral dosing at 10mg/kg only slightly lower than the *in vitro* MIC of 15.6 $\mu\text{g/ml}$. It is conceivable that increasing the oral or subcutaneous dosing to above 10mg/kg will achieve bloodstream levels of above the *in vitro* MIC, making it theoretically possible to clear a *Staphylococcus aureus* infection *in vivo*. When one considers that the *in vitro* IC_{50} of this compound is 0.7 $\mu\text{g/ml}$, it is possible that prolonged or repeated exposure of sub-lethal doses of antibiotic to gradually clear the infection could in fact be beneficial in the treatment of a systemic bacterial infection.

An obstacle to natural product-based drug discovery is the length of time required to isolate large enough quantities of compound to enable *in vivo* efficacy and bioavailability work. From a methodology perspective, this project has shown the utility of bioavailability testing of relatively small quantities of compounds or fractions considered to be hits from *in vitro* high throughput screening before performing efficacy work in animal models of disease. Furthermore, it provides a more ethical alternative to immediately testing efficacy in an animal model of disease, as many compounds with *in vitro* activity will not be bioavailable and by association, good lead-like compounds. Based on the pharmacokinetic information gained, L17-3 was shown to be a better lead-candidate than L17-1 early on in the drug discovery process, displaying bioavailability at higher concentrations in the blood as well as a longer half-life. This information has enabled the research to focus on the more bioavailable compound. Based on the information at hand, it is possible that L17-3 will be capable of clearing a

systemic *S. aureus* infection in an animal model of disease. However, future work will involve determining the bioavailability of L17-3 immediately after dosing as well as obtaining the chemical structures of these two compounds. In the event of promising data as a result of this work, efficacy studies will be considered to assess the ability of this lead-candidate to clear either a systemic or localised Staphylococcal infection.

University of Cape Town

Chapter 7

Materials and methods

7.1 Chemicals and reagents

Analytical grade petroleum ether, dichloromethane, ethyl acetate, methanol and acetone used for extract preparation were obtained from KIMIX (Cape Town, South Africa) or Merck (Darmstadt, Germany) and distilled using a Buchi rotary evaporator. HPLC grade LiChrosolv[®] methanol, water and acetonitrile were obtained from Merck (Darmstadt, Germany). Test samples were typically dissolved in dimethyl sulphoxide (DMSO) (uniLAB) and organism stocks were stored in glycerol uniVAR, both from Saarchem (Wadeville, South Africa). Formic acid (99%) was sourced from Merck (Darmstadt, Germany) while trifluoroacetic acid was obtained from Riedel-de Haën (Sigma-Aldrich, St Louis, USA).

7.2 Broth micro-dilution assay

Each plant extract was evaluated against a panel of drug-sensitive test organisms comprising of a Gram-positive bacterium, a Gram-negative bacterium, a mycobacterium and a fungus, as recommended by Cos *et al.* (2006). The basic broth micro-dilution assay (Eloff, 1998a) was adapted for each organism, as described in sections 7.2.1 (mycobacteria), 7.2.2 (bacteria) and 7.2.3 (yeast) below. The results are expressed in terms of a minimum inhibitory concentration (MIC) defined as the lowest concentration at which no visible organism growth is present. An MIC was determined for a minimum of four replicates, performed in two separate experiments. An IC₅₀ value was further determined for active samples, defined as the value at which 50% of organism growth is inhibited. An average IC₅₀ value was determined from a minimum of four replicates performed in two separate experiments. These IC₅₀ values were determined for extracts with an MIC of 125µg/ml or less, for partially purified fractions with an MIC of

62.5µg/ml or less, and for pure compounds with an MIC of 31.25µg/ml or less. For samples with strong colour interference, an IC₅₀ value could not be calculated and this information is stated in the results. For active pure compounds, the minimum bactericidal or fungicidal activity (MBC or MFC), termed as the lowest concentration at which bacterial or fungal death occurs (Finberg et al, 2004), was determined.

7.2.1 Antimycobacterial assay

The method described by Chung *et al.* (1995) and Eldeen and van Staden (2007) was used to determine the susceptibility of *Mycobacterium aurum* A+ to the test samples, with a few minor modifications. The organism was stored at -70°C in 20% glycerol and 500µl of this suspension was used to inoculate a Lowenstein-Jensen (LJ) slant, which was incubated at 37°C for one week, or until sufficient growth was obtained. For the broth micro-dilution assay, a sterile loop was used to inoculate from the LJ into 5ml of Middlebrook 7H9 (Difco™, Becton Dickinson, Sparks, MD, USA) containing 10% OADC (oleic acid, albumin, dextrose, catalase; Becton Dickinson) and this inoculum was incubated overnight at 37°C. For the assay, 7H9 Middlebrook medium was prepared at double the strength (1.88g in 160ml Millipore water) and autoclaved with 0.8ml glycerol at 121°C for 15 minutes. Once cooled, 40ml of OADC was added to the solution to yield a concentration of 20%. This solution will be referred as 2x7H9. A volume of 100µl of sterile distilled water was added to all the wells of a 96-well flat bottomed plate. The test sample, prepared in a maximum of 10% DMSO at the desired concentration, isoniazid (Sigma-Aldrich, St Louis, USA) and solvent control were added at a volume of 100µl to the wells of column three. A serial doubling dilution was then performed by removing 100µl from column three and resuspending it in the wells of column four, before transferring the same volume to column five. This dilution series was affected from columns three to twelve. The remaining 100µl was discarded. The *M. aurum* A+ inoculum was prepared by adding 1ml of an overnight culture into 20ml of double strength 7H9 with 20% OADC, yielding an approximate inoculum strength of 0.5 MacFarland standard

(approximately 1×10^5 CFU/ml). Each well was inoculated with 100µl of this suspension, excepting for the wells of column one, which received the same volume of organism-free medium. In instances where sample quantities were low, the assay volumes specified above were halved to 50µl, with reproducible and accurate results. The plates were sealed in plastic packets and incubated at 37°C for 72 hours.

After incubation, 40µl of 0.4mg/ml of *p*-iodonitrotetrazolium salt (INT, Fluka, Sigma-Aldrich, Steinheim, Austria) was added to each well of the microtitre plate and the plate was incubated for six hours. The plate was visualized for the red colour produced in the presence of metabolizing organisms. The MIC is termed as the lowest concentration of extract with no visible growth (red). The value at which 50% of organism growth is inhibited, or IC₅₀, was determined for samples with no colour interference. The wells of the 96-well plate were resuspended and read at 600nm on a Midas Microplate Reader (Turner BioSystems, California, USA). The cell viability was calculated for wells in a 96-well plate using the formula:

$$\% \text{ Cell Viability} = \frac{\text{absorbance at 600nm test well (cells + drug)}}{\text{absorbance at 600nm cell control well (cells + no drug)}} \times 100$$

GraphPad Prism Version 4.00 software was used to construct dose response curves using non-linear dose response curve fitting analyses from the percentage viability data (Microsoft Excel) of cells. The concentration of the compound at which 50% of the cell growth was inhibited (IC₅₀ values) was determined from the dose response curves generated by GraphPad Prism. Each data point represents the average of at least four wells of a microtitre plate from two experiments.

7.2.2 Antibacterial assay

The method as described by Eloff (1998a) was utilized for testing of the Gram-positive *Staphylococcus aureus* ATCC 12600 and the Gram-negative *Klebsiella pneumoniae* ATCC 13883. A sterile loop was used to inoculate a tryptone soya agar (TSA, Oxoid, Basingstoke, England) plate from a 20% glycerol stock originally stored at -70°C. The plate was incubated overnight at 37°C. A single colony was picked from the plate and used to inoculate 5ml of sterile tryptone soya broth (TSB, Oxoid). This inoculum was incubated overnight at 37°C. The Middlebrook medium specified for the antimycobacterial broth micro-dilution assay was substituted with TSB, prepared as per manufacturer's instructions. The assay inoculum was prepared by resuspending 100µl of the overnight culture in 20ml of TSB to yield an inoculum of approximately 10⁵ CFU/ml. The 96-well plates were incubated at 37°C overnight, after which INT was added, as above. The plates were incubated for three hours at 37°C and an MIC and/or IC₅₀ value determined. This method was also shown to be robust when decreasing the assay volumes by half, as with the antimycobacterial assay.

To determine if an active compound exhibited bactericidal or bacteristatic effects, 50µl of each well of the 96-well plate in which growth was not observed was plated out onto TSA quarter plates, as recommended by Cos *et al.* (2006), which were subsequently incubated overnight at 37°C. The minimum bactericidal concentration (MBC), defined as the minimum concentration at which less than 1% of growth is observed in comparison to the untreated control, was determined.

7.2.3 Antifungal assay

The NCCLS M27-A2 reference method for broth dilution antifungal susceptibility testing of yeasts (Clinical and Laboratory Standards Institute) was utilized, with the following changes. A sterile loop was used to inoculate Soubaroud-dextrose agar (SDA, Oxoid) from a 20% glycerol stock containing *Candida albicans* ATCC 90028 originally stored at -70°C. This inoculum was incubated at 35°C overnight

in sterile RPMI medium (Highveld Biologicals, Lyndhurst, South Africa) at pH 7.0, prepared as per manufacturer's instructions. For the assay, 1ml of the overnight culture was used to inoculate 20ml of sterile double strength RPMI at pH7.0 to yield an inoculum strength of between 10^3 and 10^4 CFU/ml (Cos *et al.*, 2006). The 96-well plate was prepared as described in section 6.2.1 and 100 μ l of inoculum added to each well. The plate was incubated at 35°C for 48 hours, after which INT was added, followed by a further six hour incubation at 35°C. MIC and IC₅₀ values were determined as described previously. As with the antimycobacterial broth micro-dilution assay, the method also proved to be accurate when reducing volumes by half, as has similarly been shown by Rex *et al.* (1995a).

7.3 Bio-autography

Bio-autography is primarily used as a means of pin-pointing active constituents of a complex sample, such as a crude extract (Nostro *et al.*, 2000; Cos *et al.*, 2006). In this project, bio-autography was performed with *M. aurum* A+, *S. aureus* ATCC 12600, *K. pneumoniae* ATCC 13883, and *C. albicans* ATCC 90028. In this investigation the use of direct bio-autography in the search for activity against *C. albicans* has been accomplished successfully, despite a previous report that suggested this method not possible, alternatively making use of agar-overlay bioautography (Hostettmann and Marston, 1994). The inocula for each respective organism was prepared as described in sections 7.2.1, 7.2.2 and 7.2.3 and applied by means of sterile cotton wool to a TLC plate dried of all mobile phase. The TLC plate was placed on wet, sterile paper towel in a large Petri dish and sealed in a plastic packet to avoid dehydration. The plate was incubated for 24 (37°C), 48 (35°C) or 72 (37°C) hours for the bacteria, fungi and mycobacterium, respectively, after which it was sprayed with a solution of 0.4mg/ml INT and allowed to develop for four to six hours at the appropriate temperature. Active compounds were indicated by zones of inhibition against a background of red as a result of the tetrazolium salt. Active bands were scraped

from an organism-free reference plate, dissolved in the original extractant, and evaluated by means of HPLC.

7.4 Antimalarial assay

Testing against the malaria parasite, *Plasmodium falciparum*, was performed by Mrs Sumaya Salie under the supervision of Dr Carmen Lategan in the Division of Clinical Pharmacology, University of Cape Town. The parasites were routinely cultured as described by Trager and Jensen (1976). The *in vitro* parasite lactate dehydrogenase assay (pLDH) was performed according to the procedures described by Makler *et al.* (1993). The control drug, chloroquine (Sigma-Aldrich), and the test samples were prepared at 2mg/ml in DMSO:water 1:9 (v/v). For the 96-well assay, a parasite stock solution of 2% hematocrit and 2% parasitaemia is prepared. The wells of row one contain the assay 'blanks' consisting of 100µl of 2% hematocrit and 100µl of complete medium (CM) (10% heat inactivated foetal calf serum, Highveld Biologicals, Lyndhurst, South Africa + 45% Dulbecos modified Eagles Medium, Gibco, Auckland, New Zealand + 45% F-12 HAM, Sigma-Aldrich). For the positive control in row two, 100µl of 2% parasitaemia and 100µl of CM is added to each well. The test samples are added to the wells of row three in duplicate and 100µl of CM is added to rows four to twelve. Serial doubling dilutions are then prepared from rows three to twelve, after which 100µl of 2% parasitaemia is added to all the wells of rows three to twelve. The final volume in each well is therefore 200µl. The plate is then placed in a gassing chamber, gassed for two minutes and incubated at 37°C for 48 hours.

After incubation, the contents of each well are resuspended. A volume of 100µl of Malstat (Sigma-Aldrich) is added to each well of a separate microtitre plate, followed by 15µl of the cell suspension. Thereafter, 25µl of nitro blue tetrazolium salt (NBT) (Sigma-Aldrich) is added. Air bubbles are removed and the plate is kept in a dark cupboard while developing, after which the absorbance is measured on a Midas microplate reader at 600nm.

7.5 Cytotoxicity assay

Toxicity testing against Chinese hamster ovarian (CHO) cells was performed by Mrs Sumaya Salie under the supervision of Dr Carmen Lategan in the Division of Clinical Pharmacology, University of Cape Town. The cells were routinely maintained as adherent monolayers in 75cm³ culture flasks in CM. The cells were incubated in a 5% carbon dioxide (CO₂)-air humidified atmosphere at 37°C. The culture medium was changed every two to three days and the cells sub-cultured once confluent, which involved digestion of the cellular matrix with a 1% trypsin solution.

A volume of 100µl of a 10⁵/ml cell concentration was added to each well, except those in row H (blank) in a 96 well plate. The plates were incubated at 37°C for 24 hours in a humidified atmosphere containing 5% CO₂ after which the medium was carefully aspirated from the adherent cells and replaced with 100µl of the control and test compound dilutions. An initial stock of 2mg/ml emitine (Sigma-Aldrich), the positive control was prepared in Millipore water. Six ten-fold dilutions of the positive control and test samples were prepared in CM on the day of experimentation. Test samples were originally prepared at 2mg/ml in DMSO/sterile distilled water 1:9 (v/v) and have a final test concentration range of 1ng/ml to 100µg/ml. Each concentration was at least tested in duplicate. 100µl of CM was then added to all wells containing cells and test samples, and 200µl of CM was added to row H (blank) and column 2 (culture control). The plate was incubated at 37°C for 48 hours.

The MTT (3-[4,5-Dimethylthiazol-2-yl]-2,5-diphenyltetrazolium bromide) (Sigma-Aldrich) assay described by Mosmann (1983) was used to determine the effect of the test samples on mammalian cell survival and proliferation. This colorimetric assay is based on the ability of cells to metabolize the yellow water soluble tetrazolium salt into a water-insoluble purple formazan product, thereby measuring cell survival. The intensity of the formazan product is proportional to

the metabolic activity and number of cells in the wells and was measured using a Midas microplate reader.

After incubation, 25µl of sterile MTT (Sigma-Aldrich) (5mg/ml in PBS, Oxoid) was added to each well and the plate re-incubated for 4 hours at 37°C. The plates were centrifuged for 10 minutes at 2050rpm and the supernatant aspirated from the wells without disturbing the formazan crystals. 100µl of DMSO was added to each well and the plate was gently shaken for 5 minutes on a microplate shaker to dissolve the crystals. The microplate reader was set at a wavelength of 540nm and the plate blanked on the wells in row H after which the absorbance of the formazan was measured. The cell viability was calculated in each well using the formula:

$$\% \text{ Cell Viability} = \frac{\text{absorbance at 540nm test well (cells + drug)}}{\text{absorbance at 540nm cell control well (cells + no drug)}} \times 100$$

GraphPad Prism V.4.00 software was used to construct dose response curves using non-linear dose response curve fitting analyses from the percentage viability data (Microsoft Excel) of cells. The concentration of the compound at which 50% of the cell growth was inhibited (IC₅₀ values) was determined from the dose response curves generated by GraphPad Prism. Each data point represents the average of at least four wells of a microtitre plate from two experiments.

7.6 High performance liquid chromatography

All the methods used for the analysis and collection of extracts, fractions and compounds in this project were generated using a Waters 1525 Binary HPLC pump connected to a Waters 996 photodiode array detector controlled by Millenium³² version 4.00 software. The sample was introduced by means of a Midas (Spark Holland) auto-sampler. The column temperature was kept constant at 30°C. Solvents were first fed through a Supelco degasser before being introduced into the binary pumps and fractions/compounds were collected

by means of a Waters Fractions Collector III programmed according to elution time.

7.7 Lichen materials and methods

7.7.1 Collection of lichen material

Lichen material was collected in Paarl, Swellendam and Tulbagh regions of the Western Cape of South Africa, predominantly within the Fynbos biome. Further collections were also performed in the Eastern Cape Province of South Africa in the city of East London. The collection details are specified in Table 2 and the lichen pictures are illustrated in Figure 10 in Chapter 2 'Lichens'. Voucher specimens were prepared and are housed in the Lichen Collection of the Bolus Herbarium at the University of Cape Town, Cape Town, South Africa.

7.7.2 Lichen identification

Lichens were genetically identified by Dr Tassilo Feuerer of the University of Hamburg (Germany), with the assistance of electron micrographs which were provided by Miranda Waldon at the Electron Microscopy Department of the University of Cape Town. The electron micrograph images were obtained using a LEO S440 electron microscope with an electron high tension (EHT) probe of 10kV and a working distance of 10 to 15 mm, as illustrated in Figure 9.

Despite having the genetic sequences of the lichens available, a lichen from the Eastern Cape and another from the Western Cape are unknown, although the former was tentatively identified as a *Parmotrema* species on visual inspection by Dr E. Timdal (Natural History Museum, University of Oslo, Norway). Seven of the ten collected lichen species are foliose lichens, while three, namely *T. chrysophthalmum*, *U. rubrotincta* and *T. subuliforme*, are classified as fruiticose lichens (Büdel and Scheidigger, 1996).

7.7.3 Extract preparation

The lichen material was rinsed with water to remove sand and debris. The samples were then left to air dry before being finely ground with an electric grinder. The ground material was then exhaustively extracted with acetone, as recommended in the literature (Eloff, 1998), on a Labcon laboratory shaker at room temperature. Furthermore, for samples of which sufficient quantities were available, sequential extractions were prepared with solvents of increasing polarity (petroleum ether, dichloromethane, ethyl acetate, methanol and water). The extracts were dried under reduced pressure with a Buchi rotary evaporator and under nitrogen gas. Water was removed from the extracts by means of a freeze-dryer. The extracts were quantified, and stored at -20°C until required. Together with the lichen samples, a finely ground sample of the roof tiles on which the lichens from the Eastern Cape were found growing was also extracted with acetone and concentrated to dryness as described above.

7.7.4 HPLC profiles of lichen extracts and precipitates

Each extract or precipitate thereof was prepared at a concentration of 20mg/ml in 100% DMSO. The common lichen metabolite, usnic acid (Sigma-Aldrich) was prepared at 1mg/ml in ACN/DMSO 1:1 (v/v). For the comparison of the acetone extract of the roof tiles and the ACN and PE fractions of the *T. chrysophthalmum* acetone extract, the samples were prepared at 2.5mg/ml in ACN/DMSO 1:1 (v/v). The samples were thoroughly vortexed to dissolve and then centrifuged to pellet insoluble extract. Between 10 to 30µl of the supernatant was injected onto a Supelco Discovery reversed-phase C18 analytical column (4.6 x 150mm, 5µ particle size) coupled to a Waters HPLC run by Millenium Version 4.00 software. The mobile phase was run over 40 minutes from 10% ACN/ 90% 0.1% TFA in water to 100% ACN.

7.7.5 Bioactivity testing

Lichen extracts were tested for activity against *S. aureus* ATCC 12600, *K. pneumoniae* ATCC 13883, *C. albicans* ATCC 90028 and *M. aurum* A+ as described in Sections 7.2.1 to 7.2.3. The active compounds were furthermore tested for cytotoxicity against CHO cells as described in the section 7.5. Fractions and compounds isolated from *T. chrysophthalmum* were also tested against the reference strain of methicillin-resistant *S. aureus* ATCC 43300 as described in Section 7.2.2 for the broth micro-dilution assay for drug-sensitive *S. aureus*.

Crude extracts were prepared at 80mg/ml in 100% DMSO. A ten-fold dilution was then prepared in sterile distilled water to 8mg/ml. The samples were tested in duplicate against each organism from 3.9 to 2000µg/ml and activity was confirmed in a further experiment containing two replicates of each sample. The highest concentration of DMSO in the assay was therefore 2.5%. The ACN and PE fractions of *T. chrysophthalmum* had to be further diluted in sterile distilled water and were tested from 0.2 to 2500µg/ml. The pure compounds from the same species were prepared at 10mg/ml in 100% DMSO and diluted ten-fold in sterile distilled water to 1mg/ml. These compounds were tested against two strains of *S. aureus* from 0.5 to 250µg/ml. Viable counts performed indicated that for testing against *S. aureus* ATCC 12600 an inoculum of 2.30×10^5 cuf's was added to each well, while 2.25×10^5 cuf's was added to each well for MRSA ATCC 43300.

7.7.6 Isolation of compounds from *Teloschistes chrysophthalmum*

7.7.6.1 Fractionation of the acetone extract

The acetone extract of *T. chrysophthalmum* was subjected to liquid-liquid extraction with ACN and PE. Briefly, 114mg of extract was alternatively dissolved in 50ml of ACN and 50ml of PE, which was combined and added to a separation funnel. The mixture was shaken vigorously and left to settle into two

distinct layers. The two layers were collected and dried under reduced pressure and under nitrogen gas.

7.7.6.2 HPLC collections

The ACN fraction of *T. chrysophthalmum* acetone extract was prepared at 30mg/ml in DMSO/ACN 2:1 (v/v). The sample was then centrifuged at 5000rpm for five minutes and the supernatant removed from the pellet. A volume of 30µl of this sample was injected onto a Supelco Discovery reversed-phase C₁₈ analytical column in an isocratic solvent system consisting of 58% ACN / 42% 0.1% TFA in water over 20 minutes at a flow rate of 1ml/min. By means of auto-sampling, repeated injections allowed the collection of three HPLC peaks eluting at 10.9, 14.6 and 16.7 minutes with the use of a fraction collector. The solvent was removed from the three samples under reduced pressure and the water with the help of a freeze-dryer. The dried samples were frozen at -20°C until required.

7.7.6.3 Nuclear Magnetic Resonance

NMR spectral analysis was performed at the University of Stellenbosch, South Africa, on a Varian ^{Unity}Inova 600 NMR spectrometer with a ¹H frequency of 600 MHz and ¹³C frequency of 150 MHz. Two dimensional spectral data (GHSQC, GHMBC, GCOSY and DEPT) were also obtained. The samples were analysed in deuterated chloroform with TMS as internal standard. Due to the inability to resolve the structures of L17-1 and L17-3 from these one and two dimensional data, approximately 100µg of L17-3 was analysed by Dr Mary Grace of North Carolina State University (USA) on a Bruker 950MHz instrument to obtain ¹H, GHSQC, GHMBC and GCOSY spectra.

7.7.6.4 Mass spectrometry

Compounds L17-1 and L17-3 were prepared at a concentration of 10µg/ml in ACN/ 10mM ammonium acetate 1:1 (v/v) and infused from a 4.6 diameter Hamilton syringe in an external syringe pump at a flow rate of 10µl/min onto an API 2000 LC/MS/MS system (Applied Biosystems, MDS Sciex). The compound masses were thereafter confirmed by high resolution LCMS performed at the University of Stellenbosch on a Waters API Q-TOF Ultima instrument at a flow rate of 300µl/min and an injection volume of 5µl of a 1µg/ml concentration of each compound. (ESI source; capillary voltage 3.5kV; cone voltage 35; RFI 40; source 100°C; desolvation temperature 350°C; desolvation gas 350L/h; cone gas 50L/h). The most likely elemental composition was also determined by means of single mass analysis.

7.7.6.5 Compound identification

Despite having both 600 MHz and 900 MHz NMR spectral data, together with LC-MS/MS and HR-MS data, the structures of L17-1 and L17-3 could not be resolved. Various futile attempts were also made to grow crystals for each compound at the Department of Chemistry, University of Cape Town (Cape Town, South Africa) with the aim of obtaining X-ray crystallography information.

7.7.7 *Fractionation of Xanthoparmelia semiviridis (Eastern Cape)*

7.7.7.1 Preparation of extracts

Due to large sample quantities, sequential extractions were performed on *X. semiviridis*. During the drying process, precipitates were noticed in the DCM, ethyl acetate and methanol extracts. The drying process was halted and the sample centrifuged to pellet the precipitate. The supernatant was then dried and stored separately. The extracts and precipitates were all tested individually for a range of antimicrobial activity, as described in Sections 7.2.1 to 7.2.3.

7.7.7.2 HPLC evaluation of the active extracts

The petroleum ether extract and precipitate of the dichloromethane extract were evaluated by means of HPLC for the presence of usnic acid as described in Section 7.7.4.

7.8 Materials and methods for desiccation-tolerant plants

7.8.1 Plant collection

Myrothamnus flabellifolius and *Selaginella dregei* (Family Selaginellaceae) were collected in the Mpumulanga province of South Africa by P.C. Zietsman (collector number 4354) in winter (July) in the vicinity of Belvedere near the Blyde River Canyon and voucher specimens NMB22617 and 22618 respectively were deposited in the herbarium of the National Museum in Bloemfontein, South Africa. *Xerophyta retinervis* was also collected by P.C. Zietsman in winter (July) on a farm near Hoedspruit, Mpumulanga, South Africa (GPS coordinates 24° 20' 6.9 "E; 30°51' 4.9 "S) and a voucher specimen NMB 22616 lodged with the same herbarium. *Cheilanthes contracta* was collected in Autumn (April) near Swellendam in the Western Cape growing on a rocky outcrop (GPS coordinates 30°5' 3 "S; 20° 2' 8 "E). This species was identified by Dr J.P. Roux of the Compton Herbarium at Kirstenbosch National Botanical Gardens (Cape Town, South Africa) and is represented by voucher bar code 40283 lodged at the Bolus herbarium of the University of Cape Town (Cape Town, South Africa). Pictures of these plants are shown in Figure 31.

7.8.2 Extract preparation

The plant material was allowed to air dry before being finely ground with an electric laboratory grinder. For all the plants except *X. retinervis*, the whole plant was used to prepare the extracts. The husks, leaves and stem of *X. retinervis*

were extracted separately. The plants were exhaustively extracted with distilled petroleum ether, dichloromethane, ethyl acetate or acetone, methanol and finally water, on a Labcon laboratory shaker at room temperature. An extra extraction was performed with distilled acetone for all the individual plant parts of *X. retinervis* as the yields of the first extraction process remained very low, possibly due to the fibrous nature of the plant material, even after grinding. The samples were dried under reduced pressure using a Buchi Rotary Evaporator and nitrogen. Water was removed by freezing at -20°C and freeze-drying on a DuraDry MP freeze dryer. Samples were quantified and stored at -20°C until required.

7.8.3 Bioactivity testing

7.8.3.1 Microtitre-plate assays

Extracts and fractions were prepared at 80mg/ml in 100% DMSO and dissolved by vortexing and sonicating. A ten-fold dilution was prepared in sterile distilled water to 8mg/ml and the samples were tested against *S. aureus* ATCC 12600, *K. pneumoniae* ATCC 13883, *C. albicans* ATCC90028 and *M. aurum* A+ as described in Sections 7.2.1 to 7.2.3. The samples were tested in duplicate from 3.9 to 2000µg/ml and activity confirmed by duplicate testing in a separate experiment. Fractions/compounds 21a to 21f arising from the ethyl acetate fraction of the methanol extract of *M. flabellifolius* were tested against *S. aureus* ATCC 1600 using the broth micro-dilution method. These samples were prepared at a concentration of 1mg/ml in ACN/water 1:9 (v/v), resulting in a test concentration range of 0.5 to 250µg/ml. Each sample was tested in duplicate in two separate experiments. The ethyl acetate and water fractions of the methanol extract of *X. retinervis* stems were prepared at 4mg/ml in DMSO/sterile distilled water 1:1 (v/v) for bioactivity testing against *C. albicans* and *M. aurum*.

7.8.3.2 Bio-autography

Bio-autography, as described in Section 7.3, was used to test the bioactivity of several extracts and fractions. Each extract was prepared in the original extractant. The mobile phases used to effectively separate each extract/fraction on a TLC plate are described in Table 30 below.

Table 30: The TLC conditions applied and the bioactivity tested for using the bioautography method.

Plant	Extract	Fraction	Mobile Phase
<i>M. flabellifolius</i>	PE, 2.5mg	n/a	toluene: ethyl acetate (8:2)
<i>M. flabellifolius</i>	DCM	PE, 1.2mg	toluene: ethyl acetate (4:1)
<i>M. flabellifolius</i>	DCM	ACN, 1.2mg	toluene: ethyl acetate (3:2)
<i>M. flabellifolius</i>	EA	DCM, 0.4mg	toluene: ethyl acetate:methanol (1:1:0.1)

Abbreviations: PE - petroleum ether; EA - Ethyl acetate; DCM - dichloromethane

7.8.4 Fractionation and isolation of compounds from *M. flabellifolius*

7.8.4.1 Dichloromethane extract

Fractions responsible for activity were identified from the DCM extract by means of bio-autography and these active bands were scraped from the reference TLC plates and dissolved in 1ml DCM with sonication for 5 minutes. The samples were centrifuged for 2 minutes at 10800rpm and the supernatant removed. The DCM was removed from each sample under nitrogen and the sample was dissolved in 50µl DMSO.

A mass of 2g of DCM extract was further fractionated by means of liquid-liquid separation using PE and ACN. Each fraction was concentrated to dryness under reduced pressure. The ACN fraction amounted to roughly 32% of the original dry extract. The ACN fraction was then prepared at a concentration of 150mg/ml in ACN/DMSO 1:1 (v/v) and centrifuged at 10000rpm for 5 minutes. A volume of 50µl of the supernatant was injected onto a semi-preparative Supelco Discovery reversed-phase C₁₈ column (250 x 10mm; 5µ particle size). The mobile phase

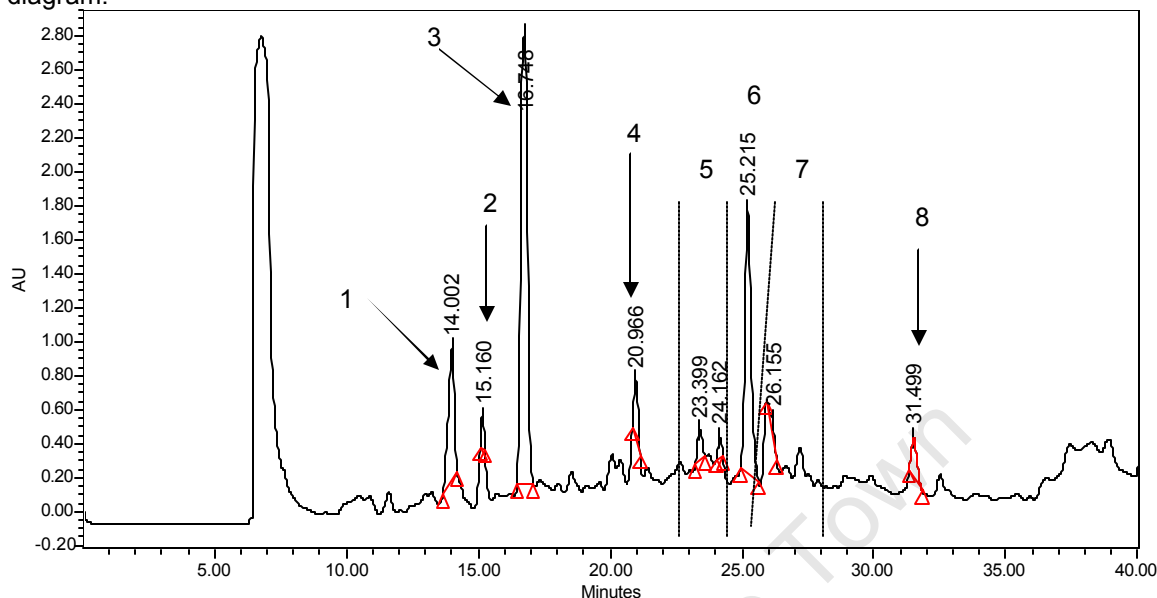
was run at 2ml/min over a gradient from 50% ACN in water to 100% ACN over 30 minutes, after which the column was washed with 100% ACN for 3 minutes and allowed to equilibrate in 50% ACN for 5 minutes. Nine fractions were collected and dried of ACN under reduced pressure and of the aqueous phase by freeze-drying.

7.8.4.2 Ethyl acetate extract

Liquid-liquid extraction was performed on the ethyl acetate extract of *M. flabellifolius* using ethyl acetate and water, where after the ethyl acetate fraction was further fractionated using DCM and water. The active zone (R_f of 0.13 to 0.44) of the DCM fraction, as determined by bioautography, was scraped off of the reference plate and dissolved in 200 μ l ethyl acetate with sonication. This mixture was centrifuged at 10800rpm for 2 minutes and the supernatant was removed from the silica and dried under nitrogen. The sample was dissolved in DMSO and 50 μ l was injected onto an analytical reversed-phase C_{18} column (4.6 x 150mm, 5 μ particle size; Supelco, Discovery). A gradient of 20% to 100% ACN in water was run over 40 minutes to obtain an initial profile.

The above-mentioned TLC method was repeated on a larger scale. The active TLC zone was scraped off and dissolved in ethyl acetate with sonication for 30 minutes and centrifuged at 700rpm for 3 minutes to pellet the silica. The supernatant was concentrated under reduced pressure and the remainder of the ethyl acetate removed under nitrogen. Of a total mass of 144mg of DCM fraction applied to TLC plates, the final mass of the active band was 27.57mg (19.2% yield). This sample was prepared at a concentration of 20mg/ml in 50% DMSO/ACN. The sample was further fractionated by means of HPLC using a reversed-phase semi-preparative C_{18} column (250 x 10mm, 5 μ particle size; Supelco Discovery). An injection volume of 50 μ l was run at a flow rate of 2ml/min at a gradient of 30 to 70% ACN in water over 30 minutes. Eight fractions were collected, as shown in Figure 54.

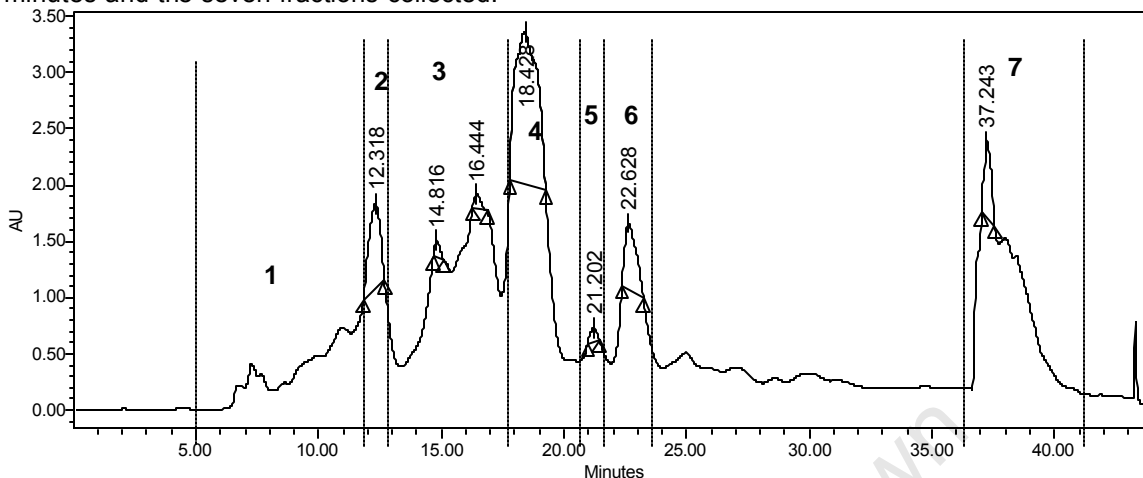
Figure 54: The HPLC profile at 210nm of the active TLC band originating from the DCM fraction of the ethyl acetate extract of *M. flabellifolius*. Eight fractions were collected, as indicated on the diagram.



7.8.4.3 Methanol extract

The methanol extract was further fractionated by means of liquid-liquid extraction with ethyl acetate and water. The ethyl acetate fraction was again concentrated to dryness under reduced pressure, while the water fraction was frozen at -20°C and dried on a freeze-dryer. The ethyl acetate fraction was prepared to a concentration of 200mg/ml in 100% DMSO. The sample dissolved completely. A volume of 40 μl of this sample was injected onto a Supelco Discovery® semi-preparative reversed phase C_{18} column (25 cm x 10mm) with a 5 μm particle size. A gradient ranging from 18% acetonitrile in water to 30% acetonitrile over 30 minutes yielded the best separation of peaks at a flow rate of 2ml/min. This was followed by an increase to 100% ACN in three minutes, a three minute wash with 100% ACN, a decrease to 18% ACN in three minutes and equilibration at this concentration for five minutes. A Waters fraction collector was programmed to collect fractions as shown in Figure 55. The ACN was removed from the fractions by evaporation under reduced pressure, followed by freeze-drying of the aqueous phase to produce the dried sample.

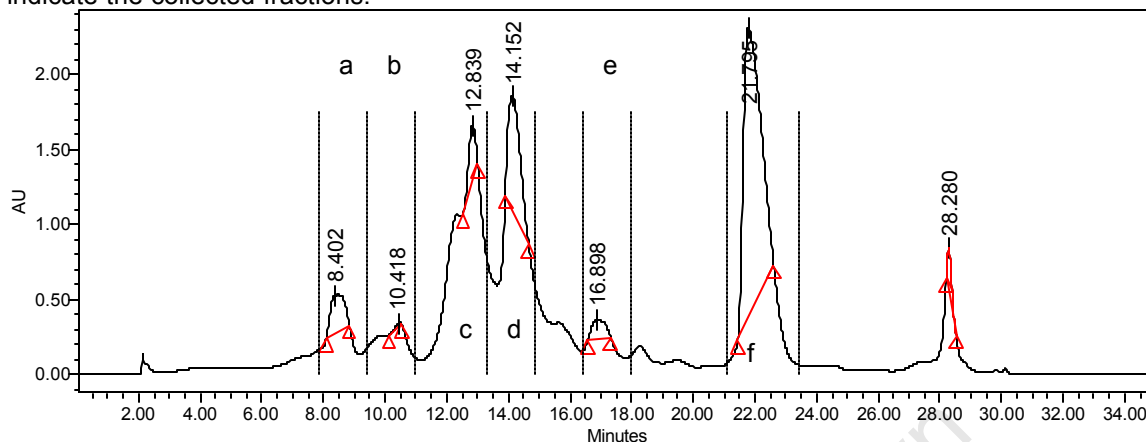
Figure 55: The HPLC chromatogram at 254nm of the ethyl acetate fraction of the methanol extract of *Myrothamnus flabellifolius* run at 2ml/min over a gradient of 18 to 30% ACN in 30 minutes and the seven fractions collected.



The purity of the fractions was determined using a Supelco Discovery analytical C₁₈ column (150 x 4.6mm) with a 5µm particle size. The mobile phase consisted of ACN and 0.1% TFA in water at a flow rate of 1ml/min. A volume of 25µl of a 5mg/ml (DMSO/ACN 1:1, v/v) concentration of each fraction was injected onto the system and run from 10% ACN to 50% ACN over 30 minutes.

Fraction 21 resulting from the HPLC separation of the ethyl acetate fraction of the MeOH extract was prepared at a concentration of 50mg/ml in 100% DMSO. An injection volume of 20µl was added to an analytical C16 amide column (4.6 x 150mm; particle size) and run over a gradient of 15% to 22% acetonitrile in water containing 0.1% TFA over 25 minutes. This was followed by a three minute wash with 50% ACN after which the column was equilibrated for five minutes. Six fractions were collected, as indicated in Figure 56.

Figure 56: The HPLC profile of the subsequent collections from fraction 21 (semi-preparative HPLC) of the ethyl acetate fraction of the methanol extract of *M. flabellifolius*. The dotted lines indicate the collected fractions.



7.9 Materials and methods: *Warburgia salutaris*

7.9.1 Plant material

Plant material was provided by Mr Rodger Stewart of New Guelderland Sugar Estates (NGSE; KwaZulu-Natal, South Africa) where *W. salutaris* is farmed commercially to supply the traditional medicines trade.

7.9.2 Extract preparation

The dried plant material was finely ground with a laboratory grinder and subjected to sequential exhaustive extraction with dichloromethane, ethyl acetate and methanol on a Labcon laboratory shaker at room temperature. The dichloromethane extract of the leaves was further fractionated with petroleum ether and acetonitrile. Extracts were dried on a Buchi rotary evaporator and under nitrogen.

7.9.3 HPLC profiling of crude extracts of *W. salutaris*

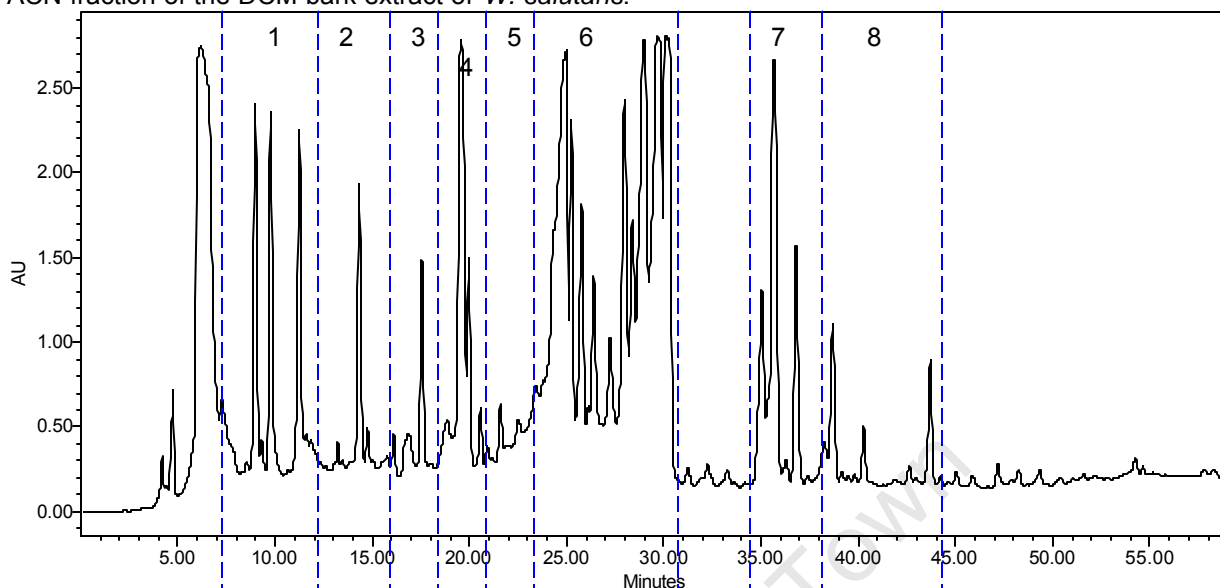
Crude extract profiles were obtained by preparing the extracts at 30mg/ml in 100% DMSO, centrifuging at 10 000rpm for 5 minutes, and injecting 30µl of the supernatant onto an Agilent reversed-phase XDB C₁₈ analytical column (4.6 x

150 mm; 5 μ particle size). A gradient of 10 to 100% ACN with water was run over 30 minutes, followed by a three minute wash at 100% ACN and an equilibration at 10% ACN for a total run time of 40 minutes at a flow rate of 1ml/min.

7.9.4 Fractionation of dichloromethane bark extract

W. salutaris DCM bark extract was further fractionated using liquid-liquid separation with petroleum ether and acetonitrile. The petroleum ether fraction (WSBD1); insoluble layer (WSBD2); ACN fraction separated into green 'oily' (WSBD4) and white component (WSBD3). The chromatographic analysis of the fractions arising from the liquid-liquid separation of the DCM bark extract with ACN and PE (WSBD1-4) was performed under the same conditions described for the extracts, but the samples were prepared at 25mg/ml in 100% DMSO. Similar chromatographic profiles subsequently led to the combination of fractions WSBD3 and 4 to form WSBD4. This fraction was separated on a Supelco Discovery reversed-phase C₁₈ semi-preparative column using a gradient of 25 to 100% ACN with water over 40 minutes at a flow rate of 2ml/min. The column was washed at 100% ACN for three minutes and equilibrated for 14 minutes for a total run time of 60 minutes. Eight fractions were collected, as shown in Figure 57. The sample was prepared at 30mg/ml in ACN/ DMSO 2:3 (v/v) and centrifuged at 10 000 rpm for 5 minutes injecting 50 μ l of the supernatant per run.

Figure 57: A chromatogram at 210nm depicting the eight collected fractions originating from the ACN fraction of the DCM bark extract of *W. salutaris*.



Fraction six was subsequently further fractionated using an Agilent Eclipse XDB C₁₈ reversed-phase column (4.6 x 150mm; 5 μ particle size). The sample was prepared at 20mg/ml in 100% DMSO, centrifuged at 10 000rpm for 5 minutes, and 30 μ l of the supernatant injected at a time. An isocratic method at ACN / 0.1% formic acid 45:55 (v/v) in water for 17 minutes at a flow rate of 1ml/min yielded seven well separated peaks which were subsequently collected.

7.9.5 Compound identification

NMR spectral analysis was performed at the University of Stellenbosch, South Africa, on a Varian ^{Unity}Inova 600 NMR spectrometer with a ¹H frequency of 600 MHz and ¹³C frequency of 150 MHz. Only three of the seven compound structures could be resolved based on comparison with spectral data in published reports.

Chapter 8

In vivo materials and methods

8.1 Ethics approval

Ethics approval was obtained from the Animal Research Ethics Committee in the Faculty of Health Sciences at the University of Cape Town (HSFAEC 009/024) prior to commencement of *in vivo* experiments. All work was based on guidelines for the ethical use of animals in research (Austin *et al.*, 2004).

8.2 Test animals

Six to seven week old male C57/BL6 mice obtained from the University of Cape Town Medical School Animal Unit were used in this study. Males were utilized as the intravenous administration was performed via the dorsal penis veins. Animals were caged in groups of five in filter top cages (30cm x 15cm x 15cm) with a constant supply of food and water. Animals were monitored twice daily and at every time point on the days of experimentation. At the completion of the study, animals were killed with 4% halothane and the carcasses were bagged, frozen and incinerated.

8.3 Assay development for detection of compounds in whole blood

8.3.1 Mass spectrometer optimisation

Compounds L17-1 and L17-3 were each prepared at 10mg/ml in 1:1 (v/v) ACN and 0.1% formic acid in water as well as at 10mg/ml in 1:1 (v/v) ACN and 10mM ammonium acetate (Sigma-Aldrich) in water for scans in the positive and negative ESI modes respectively on an API 2000 mass spectrometer (Applied Biosystems, MDS Sciex) to search for the molecular ion of interest. The compounds were infused into the mass spectrometer at a flow rate of 10µl/min from an external syringe pump (Harvard Apparatus II Plus). An API 4000 mass

spectrometer (Applied Biosystems, MDS Sciex) was also tuned to detect the molecular ions of L17-1 and L17-3 by preparing the compounds at 100ng/ml in 1:1 (v/v) ACN and 2.5mM ammonium bicarbonate (Sigma-Aldrich), infusing these solutions into the mass spectrometer at 10µl/min from an external syringe pump (Harvard Apparatus II Plus).

The molecular ions of interest were best observed in the negative ion mode for both compounds and these were selected and further fragmented to form product ions, the most abundant of which were used to set the MS in the MRM (multi reaction monitoring mode). The mass spectrometer was set to detect L17-1 (386.9 ? 328.0) and L17-3 (400.9 ? 349.7) in the MRM mode on an API 2000 mass spectrometer in a single method. The instrument settings are summarised in Tables 31 and 32 below. This method was developed on an API 2000 mass spectrometer and also applied to an API 4000 mass spectrometer for the purpose of greater sensitivity in the negative ion mode.

Table 31: ESI settings for compounds L17-1 and L17-3 on an API 2000 LC-MS/MS

Curtain gas (CUR) (arbitrary value)	20
Collision gas (CAD) (arbitrary value)	5
Ionspray voltage (IS) (volts)	-4200
Temperature (TEM) (°C)	450
Ion source gas 1 (GS1) (arbitrary value)	50
Ion source gas 2 (GS2) (arbitrary value)	60
Resolution	unit

Table 32: MS/MS settings for compounds L17-1 and L17-3 on an API 2000 LC-MS/MS

Setting	L17-1		L17-3	
Q1 Mass	386.9	386.9	400.9	400.9
Q3 Mass	328.0	350.6	349.7	364.6
Dwell time (msec)	150	150	150	150
Declustering potential (volts)	-41	-41	-26	-26
Focusing potential (volts)	-350	-350	-240	-240
Entrance potential (volts)	-3.5	-3.5	-5	-5
Collision cell entrance potential (volts)	-18	-18	-20	-20
Collision energy (volts)	-24	-22	-26	-22
Collision cell exit potential (volts)	-54	-58	-56	-58

Two product ions (Q3 mass) were selected for each compound, one as a qualifier to ensure the detected peaks on LC-MS are not matrix-derived, and the other as a quantifier, used to determine the drug concentration.

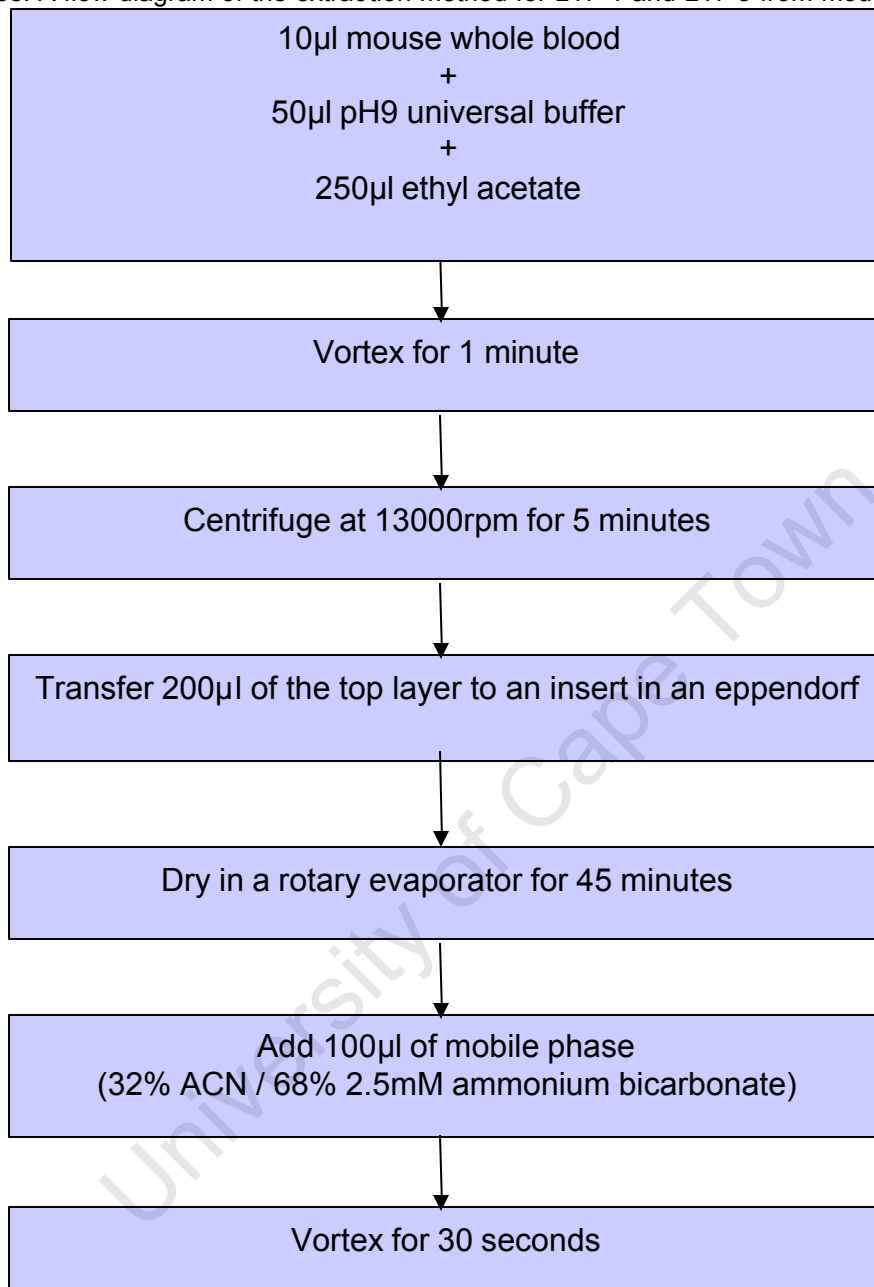
8.3.2 Chromatography development

Liquid chromatography for the optimal separation of L17-1 and L17-3 in the same sample was achieved using a Phenomenex NX column (5µm particle size, 2mm x 5cm) and a flow rate of 300µl/min. The mobile phase consisted of ACN and 2.5mM ammonium bicarbonate run over a gradient of 32 to 77% ACN in 2.9 minutes followed by an equilibration step of 32% ACN until 8 minutes. L17-1 and L17-3 eluted at approximately 1.02 and 1.5 minutes respectively. The temperature of the column compartment was maintained at 20°C and the autosampler temperature at 5°C.

8.3.3 Extraction

A liquid-liquid extraction procedure was developed for the retrieval of the lichen-derived compounds from blood. Firstly, a range of pH buffers was evaluated for the optimal extraction of compounds L17-1 and L17-3 from mouse whole blood. Mouse whole blood was spiked with 25µg/ml of L17-1 and L17-3 from a 5mg/ml stock of each compound prepared in 100% DMSO. Briefly, 50µl of Britton-Robinson Universal buffer (pH 3 to 11) was added to 10µl of mouse whole blood,

Figure 58: A flow diagram of the extraction method for L17-1 and L17-3 from mouse whole blood



together with 250µl of ethyl acetate. Each pH was tested in triplicate and samples were kept on ice at all times. The samples were vortexed for 1 minute and centrifuged at 13000 rpm for five minutes. A volume of 200µl of the top solvent layer was then transferred into an insert and dried under vacuum in a rotary evaporator for approximately 45 minutes, after which the samples were resuspended in 100µl of mobile phase (32% ACN/68% 2.3mM ammonium

bicarbonate). The samples were vortexed for 30 seconds and 5µl of each sample injected onto an API 2000 LCMS (Applied Biosystems). Based on the results of this experiment (section 5.2.1), pH 9 buffer was used for the extraction method. The complete method is illustrated in Figure 58.

8.3.4 Preparation of calibration standards

Stock solutions of 250µg/ml of L17-1 and L17-3 were prepared in DMSO/ water 5:95, v/v. Calibration standards were prepared from these stocks by performing half dilutions in mouse whole blood. Each concentration was prepared in triplicate ranging from 12ng/ml to 25µg/ml for L17-1 and 1.53ng/ml to 25µg/ml for L17-3. These samples were extracted using pH9 Universal buffer as described in section 8.3.3 together with unspiked whole mouse blood, which was finally resuspended in mobile phase spiked with 6.25µg/ml of L17-3. A volume of 20µl of each sample was analysed on an API 2000 LCMS under the conditions described in sections 8.3.1 and 8.3.2 to allow for quantification of results for the initial *in vivo* experiment described in section 8.4 below. Furthermore, a volume of 5µl of each sample was analysed on an API 4000 LCMS under the same conditions described in sections 8.3.1 and 8.3.2 to generate a calibration curve on this instrument for the quantification L17-1 and L17-3 in the initial *in vivo* experiment as well as for L17-3 in the bioavailability study described in section 8.5. Calibration standards were included in each batch of test samples analysed.

8.4 Initial bioavailability study of lichen compounds administered together in mice

An initial *in vivo* experiment was performed by administering compounds L17-1 and L17-3 combined in a single dose by means of two administration routes, namely orally and subcutaneously. This experiment was performed on three animals in each group to provide an indication as to the level of absorption of both compounds and the optimal sampling time range.

8.4.1 Oral dose

Each of the two compounds was prepared at 20mg/ml in 100% DMSO and then further diluted to 2mg/ml in sterile distilled water. Equal volumes were combined to prepare a mixture containing 1mg/ml of each compound. A volume of 200µl of this solution was administered by gastric gavage to three healthy mice to yield a dose of approximately 10mg/kg (average mice mass of 20g). The mice were closely observed for potential toxicity. Samples were collected at one, three, five and seven hours by making a nick in the end of the tail and collecting 10µl of blood which was immediately added to 50µl of pH7 buffer in an eppendorf on ice. The samples were vortexed and frozen at -20°C until extraction. The extraction procedure as described in section 8.3.3 was performed with one exception in that pH7 buffer was utilized instead of pH9. A volume of 20µl of each sample was analysed on an API 2000 LC-MS/MS.

8.4.2 Subcutaneous dose

The two compounds were prepared as described above for the oral dosage and a volume of 200µl of the mixture was administered to each of three healthy mice subcutaneously. Once again, the mice were closely observed for any signs of toxicity. Samples were collected at three, five and seven hours as described above for the oral dose and extracted and analysed as described in section 8.4.1.

8.5 Bioavailability study of L17-3 in mice

From the results of the initial *in vivo* study in which L17-1 and L17-3 were co-administered, it appeared that L17-3 was more bioavailable than L17-1 and therefore the former was used for continued *in vivo* investigation. Furthermore, the high levels of L17-3 observed in the bloodstream over a relatively long period of time, lead to a lower concentration being administered in further experiments.

8.5.1 Oral dose

L17-3 was prepared at 5mg/ml in 100% DMSO after which a ten-fold dilution was prepared in sterile distilled water to a concentration of 500µg/ml in 10% DMSO.

A volume of 200µl of this solution was administered by gastric gavage to five healthy mice. Mice were closely observed for any signs of toxicity and were weighed on each day of testing. A nick was made on the end of the tail vein at each time point and 10µl of blood collected and added to 50µl of pH9 Universal buffer. Samples were taken before administration of the compound and after 1, 3, 5, 8, 12, 24, 48, 72 and 96 hours. The samples were frozen at -20°C until extraction as described in section 8.3.3 and analysis on an API 4000 mass spectrometer as described in sections 8.3.1 and 8.3.2.

8.5.2 Subcutaneous dose

L17-3 was prepared to 500µg/ml in 10% DMSO as described above and 200µl of this solution was administered subcutaneously to five healthy mice. The mice were closely monitored for signs of toxicity and were weighed on each day of testing. The blood samples were collected, stored, processed and analysed as described in the same manner as for the oral dosage.

8.5.3 Intravenous dose

The same stock of L17-3 as for the oral and subcutaneous doses was used for the intravenous administration. Seven mice were used for this group to allow for any potential problems with the dosing procedure. The animals were anaesthetized with a mixture of ketamine (120mg/kg) and xylazine (16mg/kg) after which 200µl of the test compound was injected under a microscope into the dorsal penis vein. The mice were closely monitored for any signs of toxicity and were weighed on each day of the experiment. The blood samples were collected, stored, processed and analysed as for the oral and subcutaneous doses.

8.5.4 Data analysis

WinNonlin® noncompartmental analysis (Version 5.2 Build 200701231637) was used to analyse the data set by Mrs Jennifer Norman of the Division of Pharmacology.

References

1. Abdou R., Scherlach K., Dahse H-M., Sattler I. and Hertweck C. (2010) Botryorhodines A-D, antifungal and cytotoxic depsidones from *Botryosphaeria rhodina*, and endophyte of the medicinal plant *Bidens pilosa*. *Phytochemistry* 71: 110-116
2. Ambrose P.G., Bhavani S.M., Rubino C.M., Louie A., Gumbo T., Forrest A. and Drusano G.L. (2007) Pharmacokinetics-pharmacodynamics of antimicrobial therapy: it's not just for mice anymore. *Clinical Infectious Diseases* 44: 79-86
3. Andersson D. I. (2003) Persistence of antibiotic resistant bacteria. *Current Opinion in Microbiology* 6: 452-456
4. Andes D., Lepak A., Nett J., Lincoln L. and Marchillo K. (2006) *In vivo* fluconazole pharmacodynamics and resistance development in a previously susceptible *Candida albicans* population examined by microbiologic and transcriptional profiling. *Antimicrobial Agents and Chemotherapy* 50(7): 2384 - 2394
5. Andes D., Nett J., Oschel P., Albrecht R., Marchillo K. and Pitula A. (2004) Development and characterization of an *in vivo* central venous catheter *Candida albicans* biofilm model. *Infection and Immunity* 72(10): 6023 – 6031
6. Andries K., Verhasselt P., Guillemont J., Göhlmann H.W.H., Neefs J-M., Winkler H., Van Gestel J., Timmerman P., Zhu M., Lee E., Williams P., De Chaffoy D., Huitric E., Hoffner S., Cambau E., Truffot-Pernot C., Lounis N. and Jarlier V. (2005) A diarylquinoline drug active on the ATP synthase of *Mycobacterium tuberculosis*. *Science* 307: 223-227
7. Austin J.C., du Toit D., Fraser N., Lloyd P., Mansfield D., Macleod A., Odendaal J.S.J. and Seier J. (2004) Guidelines on Ethics for Medical Research: Animals in Research and Training. *South African Medical Research Council ISBN 1-919809-53-8*

8. Baleta A. (1998) South Africa to bring traditional healers into mainstream medicine. *The Lancet* 352: 554
9. Ballell L., Field R.A., Duncan K. and Young R.J. (2005) New small-molecule synthetic antimycobacterials. *Antimicrobial Agents and Chemotherapy* 49(6): 2153-2163
10. Balunas M.J. and Kinghorn A.D. (2005) Drug discovery from medicinal plants. *Life Sciences* 78: 431-441
11. Baptista M.S., Vasconcelos M.T., Cabral J.P., Freitas M.C. and Pacheco A.M.G. (2006) The ability of biological and organic synthetic materials to accumulate atmospheric particulates containing copper, lead, nickel and strontium. *Journal of Environmental Monitoring* 8: 147-152
12. Barman T.K., Pandya M., Mathur T., Bhadauriya T., Rao M., Khan S., Singhal S., Bhateja P., Sood R., Malhotra S., Das B., Paliwal J., Bhatnagar P.K. and Upayhyay D.J. (2009) Novel biaryl oxazolidinones: *in vitro* and *in vivo* activities with pharmacokinetics in an animal model. *International Journal of Antimicrobial Agents* 33: 280-284
13. Barry III C.E., Slayden R.A., Sampson A.E. and Lee R.E. (2000) Use of genomics and combinatorial chemistry in the development of new antimycobacterial drugs. *Biochemical Pharmacology* 59: 221-231
14. Bastos J.K., Kaplan M.A.C. and Gottlieb O.R. (1999) Drimane-type sesquiterpenoids as chemosystematic markers of Canellaceae. *Journal of the Brazilian Chemistry Society* 10(2): 136-139
15. Behera B.C., Verma N., Sonone A. and Makhija U. (2006a) Determination of antioxidative potential of lichen *Usnea ghattensis* *in vitro*. *LWT* 39: 80-85
16. Behera B.C., Verma N., Sonone A. and Makhija U. (2006b) Experimental studies on the growth of usnic acid production in "lichen" *Usnea ghattensis* *in vitro*. *Microbiological Research* 161: 232-237
17. Bell J.M., Turnidge J.D., Gales A.C., Pfaller M.A., Jones R.N., the SENTRY APAC Study Group (2002) Prevalence of extended spectrum β -lactamase (ESBL)-producing clinical isolates in the Asia-Pacific region and

- South Africa: regional results from SENTRY Antimicrobial Surveillance Program (1998-99). *Diagnostic Microbiology and Infectious Disease* 42: 193-198
18. Benko Z., Juhász A., Pócs T. and Tuba Z. (2002) Desiccation survival times in different desiccation-tolerant plants. *Acta Biologica Szegeadiensis* 46(3-4): 231-233
 19. Berlanga M., Montero M.T., Hernández-Borrell J. and Viñas M. (2004) Influence of the cell wall on ciprofloxacin susceptibility in selected wild-type Gram-negative and Gram-positive bacteria. *International Journal of Antimicrobial Agents* 23: 627-630
 20. Bézivin C., Tomasi S., Rouaud I., Delcros J-G and Boustie J. (2004) Cytotoxic activity of compounds from the lichen *Cladonia convoluta*. *Planta Medica* 70: 874-877
 21. Bladt S. and Wagner H. (2007) From the Zulu medicine to the European phytomedicine Umckaloabo®. *Phytomedicine* 14: SVI 2-4
 22. Bodeker G. (2001) Lessons on integration from the developing world's experience. *British Medical Journal* 322: 164-167
 23. Boustie J. and Grube M. (2005) Lichens – a promising source of bioactive secondary metabolites. *Plant Genetic Resources* 3(2): 273-287
 24. Bradley J.S., Guidos R., Baragona S. and Bartlett J.G. (2007) Anti-infective research and development – problems, challenges, and solutions. *Lancet Infectious Diseases* 7: 68-78
 25. Bratu S., Landman D., Haag R., Recco R., Eramo A., Alam M. and Quale J. (2005a) Rapid spread of carbapenem-resistant *Klebsiella pneumoniae* in New York City. *Archives of Internal Medicine* 165: 1430-1435
 26. Bratu S., Mooty M., Nichani S., Landman D., Gullans C., Pettinato B., Karumudi U., Tolaney P and Quale J. (2005b) Emergence of KPC-possessing *Klebsiella pneumoniae* in Brooklyn, New York: epidemiology and recommendations for detection. *Antimicrobial Agents and Chemotherapy* 49(7): 3018-3020

27. Burkholder P.R. and Evans A.W. (1945) Further studies on the antibiotic activity of lichens. *Bulletin of the Torrey Botanical Club* 72(2): 157-164
28. Butler M.S. (2004) The role of natural product chemistry in drug discovery. *Journal of Natural Products* 67: 2141-2153
29. Campanella L., Delfini M., Ercole P., Iacoangeli A. and Risuleo G. (2002) Molecular characterization and action of usnic acid: a drug that inhibits proliferation of mouse polyomavirus *in vitro* and whose main target is RNA transcription. *Biochimie* 84: 329-334
30. Chang C-M., Lee H-C., Lee N-Y., Lee I-W., Wu C-J., Chen P-L., Lee C-C., Ko N-Y and Ko W-C. (2008) Community-acquired *Klebsiella pneumoniae* complicated skin and soft-tissue infections of extremities: emphasis on cirrhotic patients and gas formation. *Infection* 36: 328-334
31. Chatterjee D. (1997) The mycobacterial cell wall: structure, biosynthesis and sites of drug action. *Current Opinion in Chemical Biology* 1: 579-588
32. Chaudhury R.R. (2001) Commentary: Challenges in using traditional systems of medicine. *British Medical Journal* 322: 167
33. Chaulet P. (1998) Rifapentine: A viewpoint. *Drugs* 56(4): 617
34. Choudhary M.I., Azizuddin, Jalil S., Atta-ur-Rahman (2005) Bioactive phenolic compounds from a medicinal lichen, *Usnea longissima*. *Phytochemistry* article in press
35. Chung G.A.C., Aktar Z., Jackson S. and Duncan K. (1995) High-throughput screen for detecting antimycobacterial agents. *Antimicrobial Agents and Chemotherapy* 39(10): 2235-2238
36. Clark A.M. (1996) Natural products as a resource for new drugs. *Pharmaceutical Research* 13(8): 1133 - 1141
37. Clark T.E. and Appleton C.C. (1997) The molluscicidal activity of *Apodytes dimidiata* E. Meyer ex Arn (Icacinaceae), *Gardenia thunbergia* L.f. (Rubiaceae) and *Warburgia salutaris* (Bertol. F.) Chiov. (Cannellaceae), three South African plants. *Journal of Ethnopharmacology* 56: 15-30
38. Clarkson C., Madikane E.V., Honoré Hansen S., Smith P.J. and Jaroszweski J.W. (2007) HPLC-SPE-NMR characterization of

- sesquiterpenoids in an antimycobacterial fraction of *Warburgia salutaris*. *Planta Medica* 73: 578-584
39. Clarkson C., Stærk D., Hansen S.H., Smith P.J. and Jaroszweski J.W. (2006) Discovery new natural products directly from crude extracts by HPLC-SPE-NMR: chinane diterpenes in *Harpagophytum procumbens*. *Journal of Natural Products* 69(4): 527-530
 40. Clinical and Laboratory Standards Institute, formerly NCCLS. M27-A2. Reference Method for Broth Dilution Antifungal Susceptibility Testing of Yeasts; Approved Standard-Second Edition. Volume 22 Number 15. ISBN 1-56238-469-4
 41. Cocks M. and Møller V. (2002) Use of indigeneous and indigenised medicines to enhance personal well-being: a South African case study. *Social Science and Medicine* 54: 387-397
 42. Coetzee C., Jeffthas E. and Reinten E. (1999) Indigenous plant genetic resources of South Africa. *Perspectives On New Crops and New Uses*. 160-163 J. Janick (ed), ASHS Press, Alexandria, VA.
 43. Cole S.T. (2002) Comparitive mycobacterial genomics as a tool for drug target and antigen discovery. *European Respiratory Journal* 20 (Supplement 36):78s-86s
 44. Cole S.T., Brosch R., Parkhill J., Garneir T., Churcher C., Harris D., Gordon S.V., Eiglmeier K., Gas S., Barry III C.E., Tekaia F., Badcock K., Basham D., Brown D., Chillingworth T., Connor R., Davies., Devlin K., Feltwell T., Gentles S., Hamlin N., Holroyd S., Hornsby T., Jagels K., Krogh A., McLean J., Moule S., Murphy L., Oliver K., Osborne J., Quall M.A., Rajandream M.-A., Rogers J., Rutter S., Seeger K., Skelton J., Squares R., Squares S., Sulston J.E., Taylor K., Whitehead S. and Barrell B.G. (1998) Deciphering the biology of *Mycobacterium tuberculosis* from the complete genome sequence. *Nature* 393: 537-544
 45. Cordell G.A. (2000) Biodiversity and drug discovery – a symbiotic relationship. *Phytochemistry* 55: 463-480

46. Cos P., Vlietinck A.J., Vanden Berghe D. and Maes L. (2006) Anti-infective potential of natural products: how to develop a stronger *in vitro* 'proof-of-concept'. *Journal of Ethnopharmacology* 106: 290-302
47. Courvalin P. and Davies J. (2003) Antimicrobials: time to act! *Current Opinion in Microbiology* 6: 425-426
48. Cowan M.M. (1999) Plant products as antimicrobial agents. *Clinical Microbiology Reviews* 12(4): 564-582
49. Cragg G.M., Newman D.J. and Snader K.M. (1997) Natural products in drug discovery and development. *Journal of Natural Products* 60: 52-60
50. Critchley I.A. and Ochsner U.A. (2008) Recent advances in the preclinical evaluation of the topical antibacterial agent REP8839. *Current Opinion in Chemical Biology* 409-417
51. Crittenden P.D., David J.C., Hawksworth D.L. and Campbell F.S. (1995) Attempted isolation and success in the culturing of a broad spectrum of lichen-forming and lichenicolous fungi. *New Phytologist* 130(2): 267-297
52. Culberson C.F. (1970) Supplement to the 'Chemical and botanical guide to lichen products'. *The Bryologist* 73(2): 177-377
53. Culberson C.F. and Hale Jr. M.E. (1973) Chemical and morphological evolution in *Parmelia* Sect. *hypotrachyna*: product of ancient hybridization? *Brittonia* 25(2): 162-173
54. Culberson W.L. (1967) Analysis of chemical and morphological variation in the *Ramalina siliquosa* species complex. *Brittonia* 19(4): 333-352
55. Culberson W.L. (1969) The use of chemistry in the systematics of the lichens. *Taxon* 18(2): 152-166
56. Daffé M. and Etienne G. (1999) The capsule of *Mycobacterium tuberculosis* and its implication for pathogenicity. *Tubercle and Lung Disease* 79(3): 153-169
57. De Backer M.D. and Van Dijck P. (2003) Progress in functional genomics approaches to antifungal drug target discovery. *Trends in Microbiology* 11(10):470-478

58. De Carvalho E.A.B., Andrade P.P., Silva N.H., Pereira E.C. and Figueiredo R.C.B.Q. (2005) Effect of usnic acid from the lichen *Cladonia substellata* on *Trypanosoma cruzi* in vitro: an ultrastructural study. *Micron* 36: 155-161
59. DiMasi J.A., Hansen R.W. and Grabowski H.G. (2003) The price of innovation: new estimates of drug development costs. *Journal of Health Economics* 22: 151-185
60. Dixon B. (2005) Liking lichens. *The Lancet* 5: 534
61. Drewes S.E., Crouch N.R., Mashimbye M.J., de Leeuw B.M. and Horn M.M. (2001) A phytochemical basis for the potential use of *Warburgia salutaris* (pepper –bark tree) leaves in the place of bark. *South African Journal of Science* 97 : 383-386
62. Drews J. (2000) Drug discovery: A historical perspective. *Science* 287: 1960-1964
63. Duncan K. (2003) Progress in TB drug development and what is still needed. *Tuberculosis* 83: 201-207
64. Ehrhardt A.F. and Russo R. (2001) Clinical resistance encountered in the Respiratory Surveillance Program (RESP) study: a review of the implications for the treatment of community-acquired respiratory tract infections. *American Journal of Medicine* 111(9A): 30S-35S
65. Elliott A.M., Luo N., Tembo G., Halwiindi B., Steenbergen G., Machiels L., Pobe J., Nunn P., Hayes R.J. and McAdam K.P.W.J. (1990) Impact of HIV on tuberculosis in Zambia: a cross sectional study. *British Medical Journal* 301: 412-415
66. Elliott E., Brink A.J., Van Greune J., Els Z., Woodford N., Turton J., Warner M. and Livermore D.M. (2006) In vivo development of ertapenem resistance in a patient with pneumonia caused by *Klebsiella pneumoniae* with an extended spectrum β -lactamase. *Clinical Infectious Diseases* 42: e95-98
67. Elo H., Matikainen J. and Pelttari E. (2007) Potent activity of the lichen antibiotic (+)-usnic acid against clinical isolates of vancomycin-resistant

- enterococci and methicillin-resistant *Staphylococcus aureus*.
Naturwissenschaften 94: 465-468
68. Eloff J.N. (1998a) A sensitive and quick microplate method to determine the minimal inhibitory concentration of plant extracts for bacteria. *Planta Medica* 64: 711-713
 69. Eloff J.N. (1998b) Which extractant should be used for the screening and isolation of antimicrobial components from plants? *Journal of Ethnopharmacology* 60: 1-8
 70. Esimone C.O. and Adikwu M.U. (1999) Antimicrobial activity and cytotoxicity of *Ramalina farinacea*. *Fitoterapia* 70: 428-431
 71. Essack S.Y., Hall L.M.C. and Livermore D.M. (2004) *Klebsiella pneumoniae* isolate from South Africa with multiple TEM, SHV and AmpC β -lactamases. *International Journal of Antimicrobial Agents* 23: 398-400
 72. Fabricant D.S. and Farnsworth N.R. (2001) The value of plants used in traditional medicine for drug discovery. *Environmental Health Perspectives* 109 (supplement 1): 69 – 75
 73. Fauci A.S. (2001) Infectious diseases: considerations for the 21st century. *Clinical Infectious Diseases* 32: 675-685
 74. Favreau J.T., Ryu M.L., Braunstein G., Orshansky G., Park S.S., Coody G.L., Love L.A. and Fong T-L. (2002) Severe hepatotoxicity associated with the dietary supplement LipoKinetix. *Annals of Internal Medicine* 136:590-595
 75. Fendrick A.M., Saint S., Brook I., Jacobs M.R., Pelton S. and Sethi S. (2001) Diagnosis and treatment of upper respiratory tract infections in the primary care setting. *Clinical Therapeutics* 23(10): 1683-1706
 76. Fennell C.W., Lindsey K.L., McGaw L.J., Sparg S.G., Stafford G.I., Elgorahsi E.E., Grace O.M. and Van Staden J. (2004) Assessing African medicinal plants for efficacy and safety: pharmacological screening and toxicology. *Journal of Ethnopharmacology* 94: 205-217
 77. File Jr T.M. (1999) Overview of resistance in the 1990's. *Chest* 115: 3S-8S

78. Finberg R.W., Moellering R.C., Tally F.P., Craig W.A., Pankey G.A., Dellinger E.P., West M.A., Joshi M., Linden P.K., Rolston K.V., Rotschafer J.C. and Rybak M.J. (2004) The importance of bactericidal drugs: future directions in infectious disease. *Clinical Infectious Diseases* 39: 1314-1320
79. Fiscus S.A. (1972) A survey of the chemistry of the *Usnea florida* group in North America. *The Bryologist* 75(3): 299-304
80. Forsby A. and Walum E. (1996) Polygodial induces inositol phosphate turnover in human neuroblastoma SH-SY5Y cells. *Neuroscience Letters* 217: 50-54
81. Francolini I., Norris P., Piozzi A., Donelli G. and Stoodley P. (2004) Usnic acid, a natural antimicrobial agent able to inhibit bacterial biofilm formation on polymer surfaces. *Antimicrobial Agents and Chemotherapy* 48(11): 4360-4365
82. Freiberg C., Pohlmann J., Nell P.G., Endermann R., Schuhmacher J., Newton B., Ottendeder M., Lampe T., Häbich D. and Ziegelbauer K. (2006) Novel bacterial acetyl coenzyme A carboxylase inhibitors with antibiotic efficacy *in vivo*. *Antimicrobial Agents and Chemotherapy* 50(8): 2707-2712
83. Frum Y. and Viljoen A.M. (2006) *In vitro* 5-lipoxygenase and anti-oxidant activities of South African medicinal plants commonly used topically for skin diseases. *Skin Pharmacology and Physiology* 19: 329-335
84. Fu L.M. and Fu-Liu C.S. (2002) Is *Mycobacterium tuberculosis* a closer relative to Gram-positive or Gram-negative bacterial pathogens? *Tuberculosis* 82(2/3): 85-90
85. Fujii K., Saito H., Tomioka H., Mae T. and Hosoe K. (1995) Mechanism of action of antimycobacterial activity of the new benzoxazinorifamycin KRM-1648. *Antimicrobial Agents and Chemotherapy* 39(7): 1489-1492
86. Fura A. (2006) Role of pharmacologically active metabolites in drug discovery and development. *Drug Discovery Today* 11(3/4): 133-142

87. Gaff D.F. (1971) Desiccation-tolerant flowering plants in Southern Africa. *Science* 174: 1033-1034
88. Galloway D.J. (2006) Chapter 11: Lichen biogeography. In Lichen Biology edited by Nash III T.J. Cambridge University Press, 1996
89. Gauslaa Y. (2005) Lichen palatability depends on investments in herbivore defence. *Oecologia* 143: 94-105
90. Gaya E., Navarro-Rosinés P., Llimona X., Hladun N. and Lutzoni F. (2008) Phylogenetic reassessment of the Teloschistaceae (lichen-forming Ascomycota, Lecanoromycetes). *Mycological Research* 112: 528-546
91. Gayathri V., Asha V.V. and Subramoniam A. (2005) Preliminary studies on the immunomodulatory and antioxidant properties of *Selaginella* species. *Indian Journal of Pharmacology* 37(6): 381-385
92. Giakkoupi P., Vourli S., Vatopoulos A.C., Kanellopoulou M., Papafrangas E. and Raitsiu B. (2008) A multiresistant *Klebsiella pneumoniae* clinical isolate carrying CTX-M-15 and VIM-1 β -lactamases, harboured by different plasmids. *International Journal of Antimicrobial Agents* 33: 183-192
93. Gill C.J., Jackson J.J., Gerckens L.S., Pelak B.A., Thompson R.K., Sundelof J.G., Kropp H. and Rosen H. (1998) *In vivo* activity and pharmacokinetic evaluation of a novel long-acting carbapenem antibiotic, MK-826 (L-749,345). *Antimicrobial Agents and Chemotherapy* 42(8): 1996-2001
94. Glinka T., Huie K., Cho A., Ludwikow M., Blais J., Griffith D., Hecker S. and Dudley M. (2003) Relationships between structure, antibacterial activity, serum stability, pharmacokinetics and efficacy in 3-(heteroarylthio)cephems. Discovery of RWJ-333441 (MC-04,546). *Bioorganic and Medicinal Chemistry* 11: 591-600
95. Goulding C.W., Apostol M., Anderson D.H., Gill H.S., Smith C.V., Kuo M.R., Yang J.K., Waldo G.S., Suh S.W., Chauhan R., Kale A., Bachhawat N., Mande S.C., Johnston J.M., Lott J.S., Baker E.N., Arcus V.L., Leys D., McLean K.J., Munro A.W., Berendzen J., Sharma V., Park M.S.,

- Eisenberg D., Sacchettini J., Alber T., Rupp B., Jacobs Jr. W. and Terwilliger T.C. (2002) The TB Structural Genomics Consortium: providing a structural foundation for drug discovery. *Current Drug Targets – Infectious Disorders* 2: 121-141
96. Graz B., Elisabetsky E. and Falquet J. (2007) Beyond the myth of expensive clinical study: assessment of traditional medicines. *Journal of Ethnopharmacology* 113: 382 – 386
97. Gruppo V., Johnson C.M., Marietta K.S., Scherman H., Zink E.E., Crick D.C., Adams L.B., Orme I.M. and Lenaerts A.J. (2006) Rapid microbiologic and pharmacologic evaluation of experimental compounds against *Mycobacterium tuberculosis*. *Antimicrobial Agents and Chemotherapy* 50(4): 1245-1250
98. Guardiola-Diaz H.M., Foster L-A., Mushrush D. and Vaz A.D.N. (2001) Azole-antifungal binding to a novel cytochrome P450 from *Mycobacterium tuberculosis*: implications for treatment of tuberculosis. *Biochemical Pharmacology* 61: 1463-1470
99. Guengerich F.P. (2006) Cytochrome P450s and other enzymes in drug metabolism and toxicity. *The AAPS Journal* 8(1): E101-E111
100. Gulluce M., Aslan A., Somkmen M., Sahin F., Adiguzel A., Agar G. and Sokmen A. (2006) Screening the antioxidant and antimicrobial properties of the lichens *Parmelia saxatilis*, *Platismatia glauca*, *Ramalina pollinaria*, *Ramalina polymorpha* and *Umbilicaria nylanderiana*. *Phytomedicine* 13: 515-521
101. Hampton T. (2005) TB drug research picks up the pace. *Journal of the American Medical Association* 293(22): 2705-2707
102. Hanson N.D., Smith Moland E. and Pitout J.D.D. (2001) Enzymatic characterization of TEM-63, a TEM-type extended spectrum β -lactamase expressed in three different genera of Enterobacteriaceae from South Africa. *Diagnostic Microbiology and Infectious Disease* 40: 199-201
103. Haraldsdóttir S., Guólaugsóttir E., Ingólfssdóttir K. and Ögmundstóttir H.M. (2004) Anti-proliferative effects of lichen-derived lipoxygenase inhibitors

- on twelve human cancer cell lines of different tissue origin *in vitro*. *Planta Medica* 70: 1098-1100
104. Harvey A.L. (1999) Medicines from nature: are natural products still relevant to drug discovery? *Trends in Pharmacological Sciences* 20: 196 – 198
 105. Hesbacher S., Fröberg L., Baur A., Baur B. and Proksch P. (1996) Chemical variation within and between individuals of the lichenized ascomycete *Tephromela atra*. *Biochemical Systematics and Ecology* 24(7/8): 603-609
 106. Hilliard J.J., Fernandez J., Melton J., Macielag M.J., Goldschmidt R., Bush K. and Abbanat D. (2009) *In vivo* activity of the pyrrolopyrazolyl-substituted oxazolidinone RWJ-416457. *Antimicrobial Agents and Chemotherapy* 53(5): 2028-2033
 107. Hiramatsu K. (2001) Vancomycin-resistant *Staphylococcus aureus*: a new model of antibiotic resistance. *Lancet Infectious Diseases* 1: 147-155
 108. Hollinshead D.M., Howell S.C., Ley S.V., Mahon M. and Ratcliffe N.M. (1983) The Diels-Alder route to drimane related sesquiterpenes; synthesis of cinnamolide, polygodial, isodrimeninol, drimenin and warburganal. *Journal of the Chemical Society Perkin Transactions* 1579-1589
 109. Hu D-L, Narita K., Hyodo M., Hayakawa Y., Nakane A. and Karaolis D.K.R. (2009) c-di-GMP as a vaccine adjuvant enhances protection against systemic methicillin-resistant *Staphylococcus aureus* (MRSA) infection. *Vaccine* 27(35): 4867-4873
 110. Huneck S. (1999) The significance of lichens and their metabolites. *Naturwissenschaften* 86: 559-570
 111. Hutchings A., Scott A.H., Lewis G. and Cunningham A. (1996) Zulu Medicinal Plants: An Inventory. University of Natal Press, Pietermaritzburg, South Africa.
 112. Illing N., Denby K.J., Collett H., Shen A. and Farrant J.M. (2005) The signature of seeds in resurrection plants: a molecular and physiological

- comparison of desiccation tolerance in seeds and vegetative tissues. *Integrative and Comparative Biology* 45: 771-787
113. Ingólfssdóttir K., Chung G.A.C., Skúlason V.G., Gissurarson S.R. and Vilhelmsdóttir M. (1998) Antimycobacterial activity of lichen metabolites *in vitro*. *European Journal of Pharmaceutical Sciences* 6: 141-144
 114. Ingólfssdóttir K., Hjalmarsdóttir M.A., Sigurdsson A., Gudjonsdóttir G.A., Brynjólfssdóttir A. and Steingrímsson O. (1997) *In vitro* susceptibility of *Helicobacter pylori* to protolicheterinic acid from the lichen *Cetraria islandica*. *Antimicrobial Agents and Chemotherapy* 41(1): 215-217
 115. Iseman M.D. (2002) Tuberculosis therapy: past, present and future. *European Respiratory Journal* 20: Supplement 36:87s-94s
 116. Jäger A.K. (2005) Is traditional medicine better off 25 years later? *Journal of Ethnopharmacology* 100: 3-4
 117. Jansen B.J.M. and De Groot A. (1991) The occurrence and biological activity of drimane sesquiterpenoids. *Natural Product Reports* 8: 309-318
 118. Jansen B.J.M. and De Groot A. (2004) Occurrence, biological activity and synthesis of drimane sesquiterpenoids. *Natural Product Reports* 21: 449-477
 119. Jarlier V. and Nikaido H. (1994) Mycobacterial cell wall: structure and role in natural resistance to antibiotics. *FEMS Microbiology Letters* 123: 11-18
 120. Jia L., Tomaszewski J.E., Hanrahan C., Coward L., Noker P., Gorman G., Nikonenko B. and Protopopova M. (2005) Pharmacodynamics and pharmacokinetics of SQ109, a new diamine-based antitubercular drug. *British Journal of Pharmacology* 144: 80-87
 121. Kahng H.-Y., Yoon B.-J., Kim S.-H., Shin D.-J., Hur J.-S., Kim H.-W., Kang E.-S., Oh K.-H. and Koh Y.-J. (2004) Introduction of saxicolous lichens distributed in coastal rocks of U-do islet in Jeju, Korea. *The Journal of Microbiology* 42(4): 292-298
 122. Kale R. (1995) South Africa's health: traditional healers in South Africa: a parallel health care system. *British Medical Journal* 310: 1182-1185

123. Kelmanson J.E., Jäger A.K. and Van Staden J. (2000) Zulu medicinal plants with antibacterial activity. *Journal of Ethnopharmacology* 69: 241-246
124. Kioy D., Gray A.I. and Waterman P.G. (1990) A comparative study of the stem-bark drimane sesquiterpenes and leaf volatile oils of *Warburgia ugandensis* and *W. stuhlmannii*. *Phytochemistry* 29(11): 3535-3538
125. Knight V., Sanglier J.-J., DTullio D., Braccili S., Bonner P., Waters J., Hughes D. and Zhang L. (2003) Diversifying microbial natural products for drug discovery. *Applied Microbiology and Biotechnology* 62: 446-458
126. Koehn F.E. and Carter G.T. (2005) The evolving role of natural products in drug discovery. *Nature Reviews* 4: 206-220
127. Kokubun T., Shiu W.K.P. and Gibbons S. (2007) Inhibitory activities of lichen-derived compounds against methicillin- and multidrug-resistant *Staphylococcus aureus*. *Planta Medica* 73(2): 176-179
128. Kranner I., Beckett R.P. and Varma A.K. (2002) Protocols in Lichenology: Culturing, Biochemistry, Ecophysiology and Use in Biomonitoring. Springer-Verlag Berlin Heidelberg New York. ISBN 3540411399
129. Kranner I., Beckett R.P., Wornik S., Zorn M. and Pfeifhofer H.W. (2002) Revival of a resurrection plant correlates with its antioxidant status. *The Plant Journal* 31(1): 13-24
130. Kranner I., Cram W.J., Zorn M., Wornik S., Yoshimura I., Stabentheiner E., Pfeifhofer H.W. (2005) Antioxidants and photoprotection in a lichen as compared with its isolated symbiotic partners. *PNAS* 102(8): 3141-3146
131. Kristmundosdóttir T., Jónsdóttir E., Ögmundstóttir H.M. and Ingólfssdóttir K. (2005) Solubilization of poorly soluble lichen metabolites for biological testing on cell lines. *European Journal of Pharmaceutical Sciences* 24: 539-543
132. Kubo I., Lee Y.-W., Pettei M., Pilkiewicz F. and Nakanashi K. (1976) Potent army work antifeedants from the East African *Warburgia* plants. *J.C.S. Chemistry Communications* 1148: 1013-1014

133. Kubo I. and Taniguchi M. (1988) Polygodial, an antifungal potentiator. *Journal of Natural Products* 51 (1): 22-29
134. Kumar KC S. and Müller K. (1999a) Lichen metabolites 2: Antiproliferative and cytotoxic activity of gyrophoric, usnic and diffractic acid on human keratinocyte growth. *Journal of Natural Products* 62: 821-823
135. Kumar KC S. and Müller K. (1999b) Lichen metabolites 1: Inhibitory action against leukotriene B₄ biosynthesis by a non-redox mechanism. *Journal of Natural Products* 62: 817-820
136. Kunin C.M. (1993) Resistance to antimicrobial drugs – a worldwide calamity. *Annals of Internal Medicine* 118(7): 557-561
137. Lappin G., Kuhn W., Jochemsen R., Kneer J., Chaudhary A., Oosterhuis B., Drijfhout W.J., Rowland M. and Garner R.C. (2006) Use of microdosing to predict pharmacokinetics at the therapeutic dose: experience with 5 drugs. *Clinical Pharmacology and Therapeutics* 80(3): 203-215
138. Lauterwein M., Oethinger M., Belsner K., Peters T. and Marre R. (1995) *In vitro* activities of the lichen secondary metabolites vulpinic acid, (+)-usnic acid, and (-)-usnic acid against aerobic and anaerobic microorganisms. *Antimicrobial Agents and Chemotherapy* 39(11): 2541-2543
139. Lewis K. and Ausubel F.M. (2006) Prospects for plant-derived antibacterials. *Nature Biotechnology* 24(12): 1504-1507
140. Lipinski C.A., Lombardo F., Dominy B.W. and Feeney P.J. (2001) Experimental and computational approaches to estimate solubility and permeability in drug discovery and development settings. *Advanced Drug Delivery Reviews* 46: 3-26
141. Liu J.F., Xu P., Jiang D.J., Li F.S., Shen J., Zhou Y.J., Xu P.S., Tan B. and Tan G.S. (2009) A new flavonoid from *Selaginella tamariscina*. *Chinese Chemical Letters* 20(5): 595-597
142. Livermore D.M. and Woodford N. (2006) The β -lactamase threat in Enterobacteriaceae, *Pseudomonas* and *Acinetobacter*. *Trends in Microbiology* 14(9): 413-420

143. Lu C-H., Chang W-N., Chuang Y-C. and Chang H-W. (1999) Gram-negative bacillary meningitis in adult post-neurosurgical patients. *Surgical Neurology* 52: 438-444
144. Lunde C.S. and Kubo I. (2000) Effect of polygodial on the mitochondrial ATPase of *Saccharomyces cerevisiae*. *Antimicrobial Agents and Chemotherapy* 44(7): 1943-1953.
145. Madhi S.A., Petersen K., Madhi A., Khoosal M. and Klugman K.P. (2000) Increased disease burden and antibiotic resistance of bacteria causing severe community-acquired lower respiratory tract infections in human immunodeficiency virus type1-infected children. *Clinical Infectious Diseases* 31: 170-176
146. Madikane V.E., Bhakta S., Russel A.J., Campbell W.E., Claridge T.D.W., Elisha B.G., Davies S.G., Smith P. and Sim E. (2007) Inhibition of mycobacterial arylamine *N*-acetyltransferase contributes to antimycobacterial activity of *Warburgia salutaris*. *Bioorganic and Medicinal Chemistry* 15: 3579-3586
147. Madomombe I.T. and Afolayan A.J. (2003) Evaluation of antimicrobial activity of extracts from South African *Usnea barbata*. *Pharmaceutical Biology* 41(3): 199-202
148. Maes R.F. (1999) Tuberculosis II: the failure of the BCG vaccine. *Medical Hypotheses* 53(1): 32-39
149. Mahandru M.M. and Gilbert O.L. (1979) Chemical studies in *Fulgensia*: structures of two new chlorodepsidones. *The Bryologist* 82(2): 302-305
150. Makler M.T., Ries J.M., Williams J.A., Bancroft J.E., Piper R.C., Gibbins B.L. and Hinrichs D.J. (1993) Parasite lactate dehydrogenase as an assay for *Plasmodium falciparum* drug sensitivity. *The American Society of Tropical Medicine and Hygiene* 48, 739-741
151. Malhotra S., Subban R. and Singh A.P. (2008) Lichens- role in traditional medicine and drug discovery. *The Internet Journal of Alternative Medicine* 5(2)

152. Marra A.R., Wey S.B., Castelo A., Gales A.C., Cal R.G.R., Filho J.R.D.C., Edmond M.B. and Pereira C.A.P. (2006) Nosocomial bloodstream infections caused by *Klebsiella pneumoniae*: impact of extended-spectrum β -lactamase (ESBL) production on clinical outcome in a hospital with high ESBL prevalence. *BMC Infectious Diseases* 6: 24-31
153. Maschmeyer G. and Ruhnke M. (2004) Update on antifungal treatment of invasive *Candida* and *Aspergillus* infections. *Mycoses* 47: 263-276
154. Mashimbye M.J., Maumela M.C. and Drewes S.E. (1999) A drimane sesquiterpenoids lactone from *Warburgia salutaris*. *Phytochemistry* 51: 435-438
155. McDonald P., Mitchell E., Johnson H., Rossney A., Humphreys H., Glynn G., Burd M., Doyle D. and McDonnell R. (2003) Epidemiology of MRSA: the North/South study of MRSA in Ireland 1999. *Journal of Hospital Infection* 54: 130-134
156. McGaw L.J., Lall N., Meyer J.J.M. and Eloff J.N. (2008) The potential of South African plants against *Mycobacterium* infections. *Journal of Ethnopharmacology* 119: 482-500
157. Mdluli K. and Spigelman M. (2006) Novel targets for tuberculosis drug discovery. *Current Opinion in Pharmacology* 6: 459-467
158. Miller A.A., Bundy G.L., Mott J.E., Skepner J.E., Boyle T.P., Harris D.W., Hromochy A.E., Marotti K.R., Zurenko G.E., Munzner J.B., Sweeney M.T., Bammert G.F., Hamel J.C., Ford C.W., Zhong W-Z., Graber D.R., Martin G.E., Han F., Dolak L.A., Seest E.P., Ruble J.C., Kamilar G.M., Palmer J.R., Banitt L.S., Hurd A.R., Barbachyn M.R. (2008) Discovery and characterization of QPT-1, the progenitor of a new class of bacterial topoisomerase inhibitors. *Antimicrobial Agents and Chemotherapy* 52(8): 2806-2812
159. Moland E.S., Hong S.G., Thomson K.S., Larone D.H. and Hanson N.D. (2007) *Klebsiella pneumoniae* isolate producing at least eight different β -lactamases, including AmpC and KPC β -lactamases. *Antimicrobial Agents and Chemotherapy* 51(2): 800-801

160. Monnet F., Bordas F., Deluchat V., Chatenet P., Botineau M. and Baudu M. (2005) Use of aquatic lichen *Dermatocarpon luridum* as bioindicator of copper pollution: accumulation and cellular distribution tests. *Environmental Pollution* 138: 455-461
161. Mosmann T. (1983) Rapid colorimetric assay for cellular growth and survival: application to proliferation and cytotoxicity assays. *Journal of Immunological Methods* 65: 55-63
162. Mowla S.B., Thomson J.A., Farrant J.M. and Mundree S.G. (2002) A novel stress-inducible antioxidant enzyme identified from the resurrection plant *Xerophyta viscosa* Baker. *Planta* 215: 716-726
163. Muchuweti M., Nyamukonda L., Chagonda L.S., Ndhla la A.R., Mapure C. and Benhura M. (2006) Total phenolic content and antioxidant activity in selected medicinal plants of Zimbabwe. *International Journal of Food Science and Technology* 41 (Supplement 1): 33-38
164. Müller K. (2001) Pharmaceutically relevant metabolites from lichens. *Applied Microbiology and Biotechnology* 56:9-16
165. Mulvey M.R. and Simor A.E. (2009) Antimicrobial resistance in hospitals: how concerned should we be? *Canadian Medical Association Journal* 180(4): 408-415
166. Murray B.E. (1994) Can antibiotic resistance be controlled? *The New England Journal of Medicine* 330: 1229-1230
167. Muthaura C.N., Rukunga G.M., Chhabra S.C., Omar S.A., Guantai A.N., Gathirwa J.W., Tolo F.M., Mwitari P.G., Keter L.K., Kirira P.G., Kimani C.W., Mungai G.M. and Njagi E.N.M. (2007) Antimalarial activity of some plants traditionally used in treatment of malaria in Kwale district of Kenya. *Journal of Ethnopharmacology* 112: 545-551
168. Nash T.H. (1996) Lichen Biology. Cambridge University Press. ISBN 0521459745
169. Neu H.C. (1992) The crisis in antibiotic resistance 257: 1064-1073
170. Newman D.J., Cragg G.M., Snader K.M. (2000) The influence of natural products upon drug discovery. *Natural Product Reports* 17: 215-234

171. Newman D.J., Cragg G.M., Snader K.M. (2003) Natural products as sources of new drugs over the period 1981-2002. *Journal of Natural Products* 66: 1022-1037
172. Ngure P.K., Tonui W.K., Ingonga J., Mutai C., Kigundu E., Ng'ang'a Z., Rukunga G. and Kimutai A. (2009) *In vitro* antileishmanial activity of extracts of *Warburgia ugandensis* (Canellaceae), a Kenyan medicinal plant. *Journal of Medicinal Plants Research* 3(2): 61-66
173. Nguyen L. and Thompson C.J. (2006) Foundations of antibiotic resistance in bacterial physiology: the mycobacterial paradigm. *Trends in Microbiology* 14(7): 304-312
174. Nordmann P., Cusson G. and Naas T. (2009) The real threat of *Klebsiella pneumoniae* carbapenemase-producing bacteria. *Lancet Infectious Diseases* 9: 228-236
175. Nostro A., Germanò M.P., D'Angelo V., Marino A. and Cannatelli M.A. (2000) Extraction methods and bioautography for evaluation of medicinal plant antimicrobial activity. *Letters in Applied Microbiology* 30: 379-384
176. Núñez-Sellés A.J., Delgado-Hernández R., Garrido-Garrido G., García-Rivera D., Guevara-García M. and Pardo-Andreu G.L. (2007) The paradox of natural products as pharmaceuticals. Experimental evidences of a mango stem bark extract. *Pharmacological Research* 55: 351-358
177. O'Brien R.J. (2003) Development of fluoroquinolones as first-line drugs for tuberculosis – at long last! *American Journal of Respiratory and Critical Care Medicine* 168: 1266-1268
178. O'Brien R.J. and Nunn P.P. (2001) The need for new drugs against tuberculosis: obstacles, opportunities, and next steps. *American Journal of Respiratory and Critical Care Medicine* 162: 1055-1058
179. Okunade A.L., Elvin-Lewis M.P.F. and Lewis W.H. (2004) Natural antimycobacterial metabolites: current status. *Phytochemistry* 65: 1017-1032
180. Olila D., Olwa-Odyek and Opuda-Asibo J. (2001a) Antibacterial and antifungal activities of extracts of *Zanthoxylum chalybeum* and *Warburgia*

- ugandensis*, Ugandan medicinal plants. *African Health Sciences* 1(2): 66-72
181. Olila D., Opuda-Asibo J., Olwa-Odyek (2001b) Bioassay-guided studies on the cytotoxic and *in vitro* trypanocidal activities of a sesquiterpene (muzigadial) derived from a Ugandan medicinal plant (*Warburgia ugandensis*). *African Health Sciences* 1(1): 12-15
 182. Olila D., Olwa-Odyek and Opuda-Asibo J. (2002) Screening of *Zanthoxylum chalybeum* and *Warburgia ugandensis* for activity against measles virus (Swartz and Edmonston strains) *in vitro*. *African Health Sciences* 2(1): 2-10
 183. Orme I. (2001) Search for new drugs for treatment of tuberculosis: tuberculosis drug screening program. *Antimicrobial Agents and Chemotherapy* 45(7): 1943-1946
 184. Owens R.C. and Rice L. (2006) Hospital-based strategies for combating resistance. *Clinical Infectious Diseases* 42: S173-S181
 185. Patel D.V. and Gordon E.M. (1996) Applications of small-molecule combinatorial chemistry to drug discovery. *Drug Discovery Today* 1(4): 134-144
 186. Paterson D.L., Ko W-C., Von Gottberg A., Mohaptra S., Casellas J.M., Goossens H., Mulazimoglu L., Trenholme G., Klugman K.P., Bonomo R.A., Rice L.B., Wagener M.M., McCormack J.G. and Yu V.L. (2003) Antibiotic therapy for *Klebsiella pneumoniae* bacteremia: implications of production of extended-spectrum β -lactamases. *Clinical Infectious Diseases* 39: 31-37
 187. Paudel B., Bhattarai H.D., Lee J.S., Hong S.G., Shin H.W. and Yim J.H. (2008) Antibacterial potential of Antarctic lichens against human pathogenic Gram-positive bacteria. *Phytotherapy Research* 22: 1269-1270
 188. Paulsen I.T. (2003) Multidrug efflux pumps and resistance: regulation and evolution. *Current Opinion in Microbiology* 6: 446-451

189. Peláez F. (2006) The historical delivery of antibiotics from microbial naturally products – can history repeat? *Biochemical Pharmacology* 71: 981-990
190. Perry N.B., Benn M.H., Brennan N.J., Burgess E.J., Ellis G., Galloway D.J., Lorimer S.D. and Tangney R.S. (1999) Antimicrobial, antiviral and cytotoxic activity of New Zealand lichens. *Lichenologist* 31(6): 627-636
191. Petrikos G. and Skiada A. (2007) Recent advances in antifungal chemotherapy. *International Journal of Antimicrobial Agents* 30: 108-117
192. Piddock L.J.V. (2006) Clinically relevant chromosomally encoded multidrug resistance efflux pumps in bacteria. *Clinical Microbiology Reviews* 19(2): 382-402
193. Pieters L. and Vlietinck A.J. (2005) Bioguided isolation of pharmacologically active plant components, still a valuable strategy for the finding of new lead compounds? *Journal of Ethnopharmacology* 100: 57-60
194. Pinheiro C., Chaves M.M. and Ricardo C.P. (2001) Alterations in carbon and nitrogen metabolism induced by water deficit in the stems and leaves of *Lupinus albus* L. *Journal of Experimental Botany* 52(358): 1063-1070
195. Podterob A.P. (2008) Chemical composition of lichens and their medical applications. *Pharmaceutical Chemistry Journal* 42(10): 582-588
196. Porras O.N. (1996) Lower respiratory tract infections. *Current Therapeutic Research* 57(A): 36-40
197. Prinzing A.J. (1999) Wind-acclimated thallus morphogenesis in a lichen (*Evernia prunastri*, Parmeliaceae) probably favoured by grazing disturbances. *American Journal of Botany* 86(2): 173-183
198. Proctor M.C.F. and Tuba Z. (2002) Poikilohydry and homoihydry: antithesis or spectrum of possibilities? *New Phytologist* 156: 327-349
199. Projan S.J. (2003) Why is big pharma getting out of antibacterial drug discovery? *Current Opinion in Microbiology* 6: 427-430

200. Rabe T. and Van Staden J. (1997) Antibacterial activity of South African plants used for medicinal purposes. *Journal of Ethnopharmacology* 56: 81-87
201. Rabe T. and Van Staden J. (2000) Isolation of an antibacterial sesquiterpenoid from *Warburgia salutaris*. *Journal of Ethnopharmacology* 73: 171-174
202. Rahalison L., Hamburger M., Hostettmann K., Monod M. and Frenk E. (1991) A bioautographic agar overlay method for the detection of antifungal compounds from higher plants. *Phytochemical Analysis* 2(5): 199-203
203. Rates S.M.K. (2001) Plantst as a source of drugs. *Toxicon* 39: 603-613
204. Reis R.A., Tischer C.A., Gorin P.A.J. and Iacomini M. (2002) A new pullulan and a branched (1 \rightarrow 3)-, (1 \rightarrow 6)-linked β -glucan from the lichenised ascomycete *Teloschistes flavicans*. *FEMS Microbiology Letters* 210: 1-5
205. Reis R.A., Iacomini M., Gorin P.A.J., de Souza L.M., Grube M., Cordeiro L.M.C. and Sasaki G.L. (2005) Fatty acid composition of the tropical lichen *Teloschistes flavicans* and its cultivated symbionts. *FEMS Microbiology Letters* 247: 1-6
206. Rex J.H., Cooper Jr. C.R., Merz W.G., Galgiani J.N. and Anaissie E.J. (1995a) Detection of amphotericin B-resistant *Candida* isolates in a broth-based system. *Antimicrobial Agents and Chemotherapy* 39(4): 906-909
207. Rex J.H., Rinaldi M.G. and Pfaller M.A. (1995b) Resistance of *Candida* species to fluconazole. *Antimicrobial Agents and Chemotherapy* 39(1): 1-8
208. Rios J.L. and Recio M.C. (2005) Medicinal plants and antimicrobial activity. *Journal of Ethnopharmacology* 100: 80-84
209. Roach J.A.G., Musser S.M., Morehouse K. and Woo J.Y.J (2006) Determination of usnic acid in lichen toxic to elk by liquid chromatography with ultraviolet and tandem mass spectrometry detection. *Journal of Agricultural and Food Chemistry* 54: 2484-2490

210. Roberts M.S., Magnusson B.M., Burczynski F.J. and Weiss M. (2002) Enterohepatic circulation: physiological, pharmacokinetic and clinical implications. *Clinical Pharmacokinetics* 41(10): 751-790
211. Robicsek A., Jacoby G.A. and Hooper D.C. (2006) The worldwide emergence of plasmid-mediated quinolone resistance. *Lancet Infectious Diseases* 6: 629-640
212. Rosso M.L., Bertoni M.D., Adler M.T. and Maier M.S. (2003) Anthraquinones from the cultured lichen mycobionts of *Teloschistis exilis* and *Caloplaca erythrantha*. *Biochemical Systematics and Ecology* 31: 1197-1200
213. Scott P. (2000) Resurrection plants and the secrets of eternal leaf. *Annals of Botany* 85:159-166
214. Seaman T.A. (2005) MSc Dissertation. The antimicrobial and antimycobacterial activity of plants used for the treatment of respiratory ailment in Southern Africa and the isolation of anacardic acid from *Ozoroa paniculosa*. University of the Witwatersrand.
215. Sherwin H.W., Pammenter N.W., February E., Van Der Willigen C. and Farrant J.M. (1998) Xylem hydraulic characteristics, water relations and wood anatomy of the resurrection plant *Myrothamnus flabellifolius* Welw. *Annals of Botany* 81: 567-575
216. Shirtcliffe N.J., Pyatt F.B., Newton M.I., and McHale G. (2006) A lichen protected by a super-hydrophobic and breathable structure. *Journal of Plant Physiology* 163(11): 1193-1197
217. Singh S.B. and Barrett J.F. (2006) Empirical antibacterial drug discovery – foundation in natural products. *Biochemical Pharmacology* 71: 1006-1015
218. Smyth A., Martin M. and Cairns J. (1995) Traditional healers may cause dangerous delays. *British Medical Journal* 311: 948
219. Spellberg B., Powers J.H., Brass E.P., Miller L.G. and Edwards Jr. J.E. (2004) Trends in antimicrobial drug development: implications for the future. *Antimicrobial Research and Development* 38: 1279-1286

220. Sterner O. and Szallasi A. (1999) Novel natural vanilloid receptor agonists: new therapeutic targets for drug development. *Trends in Pharmacological Sciences* 20: 459-465
221. Strohl W.R. (2000) The role of natural products in a modern drug discovery program. *Drug Discovery Today* 5(2): 39-41
222. Stover C.K., Warrenner P., VanDevanter D.R., Sherman D.R., Arain T.M., Langhorne M.H., Anderson S.W., Towell J.A., Yuan Y., McMurray D.N., Krelswirth B.N., Barry C.E. and Baker W.R. (2000) A small-molecule nitroimidazole drug candidate for the treatment of tuberculosis. *Nature* 405: 962-966
223. Strahilevitz J., Engelstein D., Adler A., Temper V., Moses A.E., Block C. and Robicsek A. (2007) Changes in *qnr* prevalence and fluoroquinolone resistance in clinical isolates of *Klebsiella pneumoniae* and *Enterobacter* spp. collected from 1990 to 2005. *Antimicrobial Agents and Chemotherapy* 51(8): 3001-3003
224. Sumita Y., Nouda H., Kanazawa K. and Fukasawa M. (1995) Antimicrobial activity of SM-17466, a novel carbapenem antibiotic with potent activity against methicillin-resistant *Staphylococcus aureus*. *Antimicrobial Agents and Chemotherapy* 39(4): 910-916
225. Szallasi A., Bíró T., MÓdarres S., Garlaschelli L., Petersen M., Klusch A., Vidari G., Jonassohn M., De Rosa S., Sterner O., Blumberg P.M. and Krause J.E. (1998) Dialdehyde sesquiterpenes and other terpenoids as vanilloids. *European Journal of Pharmacology* 356: 81-89
226. Takhi M., Singh G., Murugan C., Thaplyyal N., Maitra S., Bhaskarreddy K.M., Amarnath P.V.S., Mallik A., Harisudan T., Trivedi R.K., Sreenivas K., Selvakumar N. and Iqbal J. (2008) Novel and potent oxazolidinone antibacterials featuring 3-indolylglyxamide substituents. *Bioorganic and Medicinal Chemistry Letters* 18: 5150-5155
227. Talbot G.H., Bradley J., Edwards J.E., Gilber D., Scheld M. and Bartlett J.G. (2006) Bad bugs need drugs: an update on the development pipeline

- from the antimicrobial availability task force of the Infectious Diseases Society of America. *Clinical Infectious Diseases* 42: 657-668
228. Tam C.M. (1998) Rifapentine: A viewpoint. *Drugs* 56(4): 617
 229. Taniguchi M., Adachi T., Oi S., Kimura A., Katsumara S., Isoe S. and Kubo I. (1984) Structure-activity relationship of the *Warburgia* sesquiterpene dialdehydes. *Agricultural and Biological Chemistry* 48(1): 73-78
 230. Taniguchi M., Yano Y., Tada E., Ikenishi K., Oi S., Haraguchi H., Hashimoto K. and Kubo I. (1988) Mode of action of polygodial, an antifungal sesquiterpene dialdehyde. *Agricultural and Biological Chemistry* 52(6): 1409-1414
 231. Taylor J.L.S., Rabe T., McGaw L.J, Jäger A.K. and Van Staden J. (2001) Towards the scientific validation of traditional medicinal plants. *Plant Growth Regulation* 34: 23-37
 232. Tenover F.C. (2001) Development and spread of bacterial resistance to antimicrobial agents: an overview. *Clinical Infectious Diseases* 33(Suppl 3): S108-S115
 233. Tenover F.C. and Hughes J.M. (1996) The challenges of emerging infectious diseases. Development and spread of multiply-resistant bacterial pathogens. *The Journal of the American Medical Association* 275(4): 300-304
 234. Thevissen K., Kristensen H.H., Thomma B.P.H.J., Cammue B.P.A. and François I.E.J.A. (2007) Therapeutic potential of antifungal plant and insect defensins. *Drug Discovery Today* 12(21/22): 966-971
 235. Trager W. and Jensen J.B. (1976). Human malaria parasite in continuous culture. *Science* 193(4254), 673-5
 236. Trébucq A. Revisiting sputum smear microscopy. *International Journal of Tuberculosis and Lung Disease* 8(7): 805
 237. Trouiller P., Olliaro P., Torreele E., Orbinski J., Laing R. and Ford N. (2002) Drug development for neglected diseases: a deficient market and a public-health policy failure. *Lancet* 359: 2188-2194

238. Türk A.Ö. Yilmaz M., Kivanç M. and Türk H. (2003) The antimicrobial activity of extracts of the lichen *Cetraria aculeate* and its protolichesterinic acid constituent. *Zeitschrift für Naturforschung* 58c: 850-854
239. Ueda Y. and Sunagawa M. (2003) *In vitro* and *in vivo* activities of novel 2-(thiazol-2-ylthio)-1 β -methylcarbapenems with potent activities against multiresistant Gram-positive bacteria. *Antimicrobial Agents and Chemotherapy* 47(8): 2471-2480
240. Van Dobben H.F., Wolterbeek H.Th., Wamelink G.W.W. and Ter Braak C.J.F. (2001) Relationship between epiphytic lichens, trace elements and gaseous atmospheric pollutants. *Environmental Pollution* 112: 163-169
241. Van Eeckhaut A., Lanckmans K., Sarre S., Smolders I. and Michotte Y. (2009) Validation of bioanalytical LC-MS/MS assays: evaluation of matrix effects. *Journal of Chromatography B*
242. Van Vuuren S.F. (2008) Antimicrobial activity of South African medicinal plants. *Journal of Ethnopharmacology* 119: 462-472
243. Van Wyk B-E., van Oudtshoorn B. and Gericke N. (2002). Medicinal Plants of South Africa. Briza Publications, Pretoria, South Africa.
244. Vatopoulos A.C., Kalapothaki V. and Legakis N.J., on behalf of the Hellenic Antibiotic Resistance Study Group (1996) Risk factors for nosocomial infections caused by Gram-negative bacilli. *Journal of Hospital Infection* 34: 11-22
245. Vedantam G. and Hecht D.W. (2003) Antibiotics and anaerobes of gut origin. *Current Opinion in Microbiology* 6: 457-461
246. Verhoef J. and Fluit A. (2006) Surveillance uncovers the smoking gun for resistance emergence. *Biochemical Pharmacology* 71: 1036-1041
247. Viljoen A.M., Klepser M.E., Ernst E.J., Keele D., Roling E., Van Vuuren S., Demirci B., Baser K.H.C. and Van Wyk B-E. (2002) The composition and antimicrobial activity of the essential oil of the resurrection plant *Myrothamnus flabellifolius*. *South African Journal of Botany* 68: 100-105
248. Von Köckritz-Blickwede M., Rohde M., Oehmcke S., Miller L.S., Cheung A.L., Herwald H., Foster S. and Medina E. (2008) Immunological

- mechanisms underlying the genetic predisposition to severe *Staphylococcus aureus* infection in the mouse model. *The American Journal of Pathology* 173(6): 1657-1668
249. Wallis R.S., Helfand M.S., Whalen C.C., Johnson J.L., Mugerwa R.D., Vjecha M., Okwera A. and Ellner J.J. (1996) Immune activation, allergic drug toxicity and mortality in HIV-positive tuberculosis. *Tubercle and Lung Disease* 77: 516-523
 250. Warner D.F. and Mizrahi V. (2004) Mycobacterial genetics in target validation. *Drug Discovery Today: Technologies* 1(2): 93-98
 251. Wegener H.C. (2003) Antibiotics in animal feed and their role in resistance development. *Current Opinion in Microbiology* 6: 439-445
 252. Weig M. and Brown A.J.P. (2007) Genomics and the development of new diagnostics and anti-*Candida* drugs. *Trends in Microbiology* 15(7): 310-317
 253. Weiss W.J., Murphy T., Lenoy E., Young M. (2004) *In vivo* efficacy and pharmacokinetics of AC98-6446, a novel cyclic glycopeptide, in experimental infection models. *Antimicrobial Agents and Chemotherapy* 48(5): 1708-1712
 254. Wheeler P.R. and Anderson P.M. (1996) Determination of the primary target for isoniazid in mycobacterial mycolic acid biosynthesis with *Mycobacterium aurum* A+. *Biochemical Journal* 318: 451-457
 255. White T.C., Marr K.A. and Bowden R.A. (1998) Clinical, cellular, and molecular factors that contribute to antifungal drug resistance. *Clinical Microbiology Reviews* 11(2): 382-402
 256. Whittaker A., Bochicchio A., Vazzana C., Lindsey G. and Farrant J. (2001) Changes in leaf hexokinase activity and metabolite levels in response to drying in the desiccation-tolerant species *Sporobolus stapfianus* and *Xerophyta viscosa*. *Journal of Experimental Botany* 52(358): 961-969
 257. WHO (2008). Anti-tuberculosis drug resistance in the world. Report number 4. The WHO/IUATLD Global Project on Anti-tuberculosis drug resistance surveillancen 2002-2007.

258. Wiesner J. (2008). Thesis dissertation. Isolation and Characterisation of Antiplasmodial Compounds from *Xerophyta* Species and the Bioavailability, Metabolic and Efficacy Evaluation of 9-O-acetylhydnocarpin in a Mouse Model. University of Cape Town.
 259. Wolfender J-L., Queiroz E.F. and Hostettmann K. (2005) Phytochemistry in the microgram domain – a LC-NMR perspective. *Magnetic Resonance in Chemistry* 43: 697-709
 260. Wube A.A., Bucar F., Gibbons S. and Asres K. (2005) Sesquiterpenes from *Warburgia ugandensis* and their antimycobacterial activity. *Phytochemistry* 66: 2309-2315
 261. Wunberg T., Hendrix ., Hillisch A., Lobell M., Meier H., Schmeck C., Wild H. and Hinzen B. (2006) Improving the hit-to-lead process: data-driven assessment of drug-like and lead-like screening hits. *Drug Discovery Today* 11(3/4): 175-180
 262. www.gaiaherbs.com
 263. Yamamoto Y., Miura Y., Higuchi M. and Kinoshita Y. (1993) Using lichen tissue cultures in modern biology. *The Bryologist* 96(3): 384-393
 264. Yamamoto Y., Mizuguchi R. and Yamada Y. (1985) Tissue cultures of *Usnea rubescens* and *Ramalina yasudae* and production of usnic acid in their cultures. *Agricultural and Biological Chemistry* 19(11): 3347-3348
 265. Yamamoto Y., Mizuguchi R., Takayama S. and Yamada Y. (1987) Effects of culture conditions on the growth of usneaceae lichen tissue cultures. *Plant Cell Physiology* 28(8): 1421-1426
 266. Ying B-P., Peiser G., Ji Y-Y., Mathias K., Tutko D. and Hwang Y-S. (1995) Phytotoxic sesquiterpenoids from *Canella winterana*. *Phytochemistry* 38(4): 909-915
 267. Yuan X., Xiao S. and Taylor T.N. (2005) Lichen-like symbiosis 600 million years ago. *Science* 308: 1017-1020
- Zetola N., Francis J.S., Nuermberger E.L. and Bishai W.R. (2005) Community-acquired meticillin-resistant *Staphylococcus aureus*: an emerging threat. *Lancet Infectious Diseases* 5: 275-286

Appendix

A. Extract yields

Table 33: The percentage yields of the acetone extracts of ten lichen species

	Lichen	Lichen mass (g)	Extract mass (g)	Percentage yield (%)
L1	<i>Xanthoria parietina</i>	0.761	0.014	1.827
L8	<i>Xanthoparmelia notata</i>	2.644	0.223	8.424
L11	<i>Xanthoparmelia semiviridis</i> (WC)	4.660	0.244	5.242
L14	*Unkown1 (<i>Parmotrema</i> sp.)	2.036	0.423	20.786
L15	<i>Xanthoparmelia semiviridis</i> (EC)	2.400	0.437	18.202
L16	<i>Flavoparmelia soredicans</i>	1.217	0.225	18.488
L17	<i>Teloschistes chrysophthalmum</i>	0.450	0.052	11.556
L18	Unknown 2 (foliose soil lichen)	2.550	0.099	3.864
L19	<i>Thamnolia subuliforme</i>	1.729	0.346	19.987
L20	<i>Usnea rubrotincta</i>	1.602	0.091	5.686

Table 34: The percentage yield of extracts of *Xanthoparmelia semiviridis* (L15) from the Eastern Cape

Extract	Sample mass (g)	Percentage yield (%)
Petroleum ether	0.592	0.311
Dichloromethane	3.21	1.687
Dichloromethane precipitate	0.996	0.523
Ethyl acetate	3.754	1.973
Ethyl acetate precipitate	1.343	0.706
Methanol	26.085	13.707
Methanol precipitate	2.736	1.438
Water	1.254	0.659
Total	12.631	6.637

Table 35: The percentage yields of desiccation-tolerant plants

Plant and mass	Extractant	Extract mass (g)	Percentage yield (%)
<i>Myrothamnus flabellifolius</i> 100.0g	petroleum ether	3.421	3.421
	dichloromethane	7.504	7.504
	ethyl acetate	3.299	3.299
	methanol	13.543	13.543
<i>Cheilanthes contracta</i> 21.5g	petroleum ether	0.164	0.764
	dichloromethane	0.392	1.820
	acetone	0.346	1.607
	methanol	2.494	11.580
	water	0.235	1.090
<i>Selaginella dregei</i> 206.9g	petroleum ether	0.280	0.135
	dichloromethane	0.992	0.479
	ethyl acetate	0.500	0.242
	methanol	1.877	0.907
	water	0.633	0.306
<i>Xerophyta retinervis</i> stems 100.0g	petroleum ether	1.283	1.283
	dichloromethane	0.79	0.79
	ethyl acetate	0.233	0.233
	methanol	2.025	2.025
<i>Xerophyta retinervis</i> leaves 72.5g	petroleum ether	0.390	0.537
	dichloromethane	0.803	1.108
	ethyl acetate	0.396	0.547
	methanol	3.785	5.221
	water	4.084	5.633
<i>Xerophyta retinervis</i> husks 118.0g	petroleum ether	1.400	1.186
	dichloromethane	0.682	0.578
	ethyl acetate	0.295	0.250
	methanol	2.390	2.025
	water	0.591	0.501

Table 36: The percentage yield of *Warburgia salutaris* dichloromethane and ethyl acetate extracts

Plant part and mass	Extractant	Extract mass (g)	Percentage yield (%)
Bark 151.2g	dichloromethane	4.43	2.9
	ethyl acetate	0.36	0.2
Leaves 497.4g	dichloromethane	34.05	6.8
	ethyl acetate	2.98	0.6
Twigs 153.0g	dichloromethane	4.21	2.7
	ethyl acetate	0.76	0.5
Stem 206.8g	dichloromethane	2.47	1.2
	ethyl acetate	0.42	0.2

B. HPLC chromatograms

Figure 59: The HPLC chromatogram of the liquid-liquid petroleum ether fraction of *W. salutaris* bark dichloromethane extract (WSBD1) at 229.9nm.

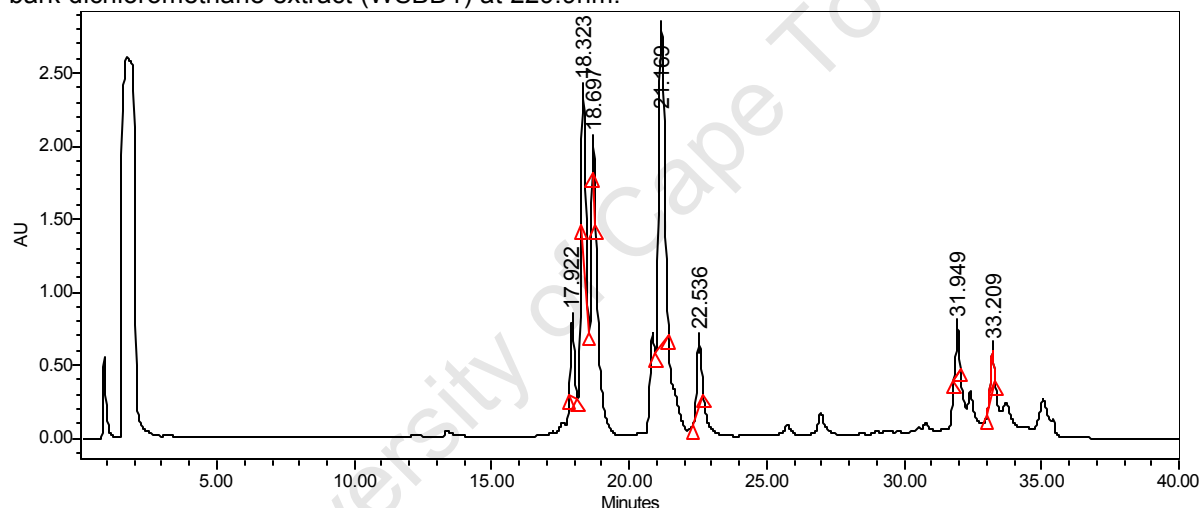
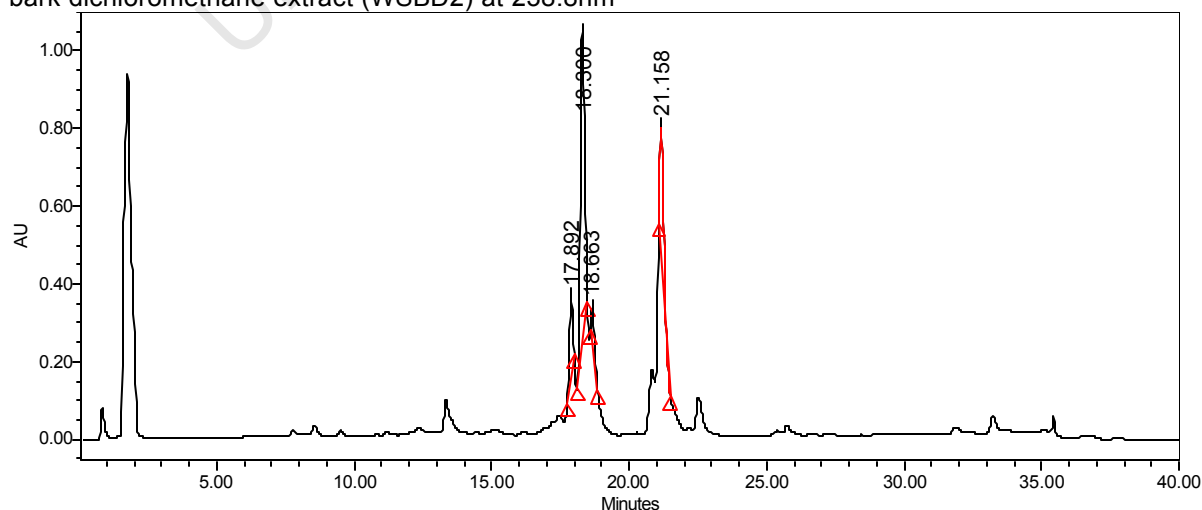


Figure 60: The HPLC chromatogram of the liquid-liquid petroleum ether fraction of *W. salutaris* bark dichloromethane extract (WSBD2) at 238.8nm



C. NMR spectra

Lichen NMR

Figure 61: The GHMBC spectrum from L17-1 isolated from *Teloschistas chrysaphthalmum*

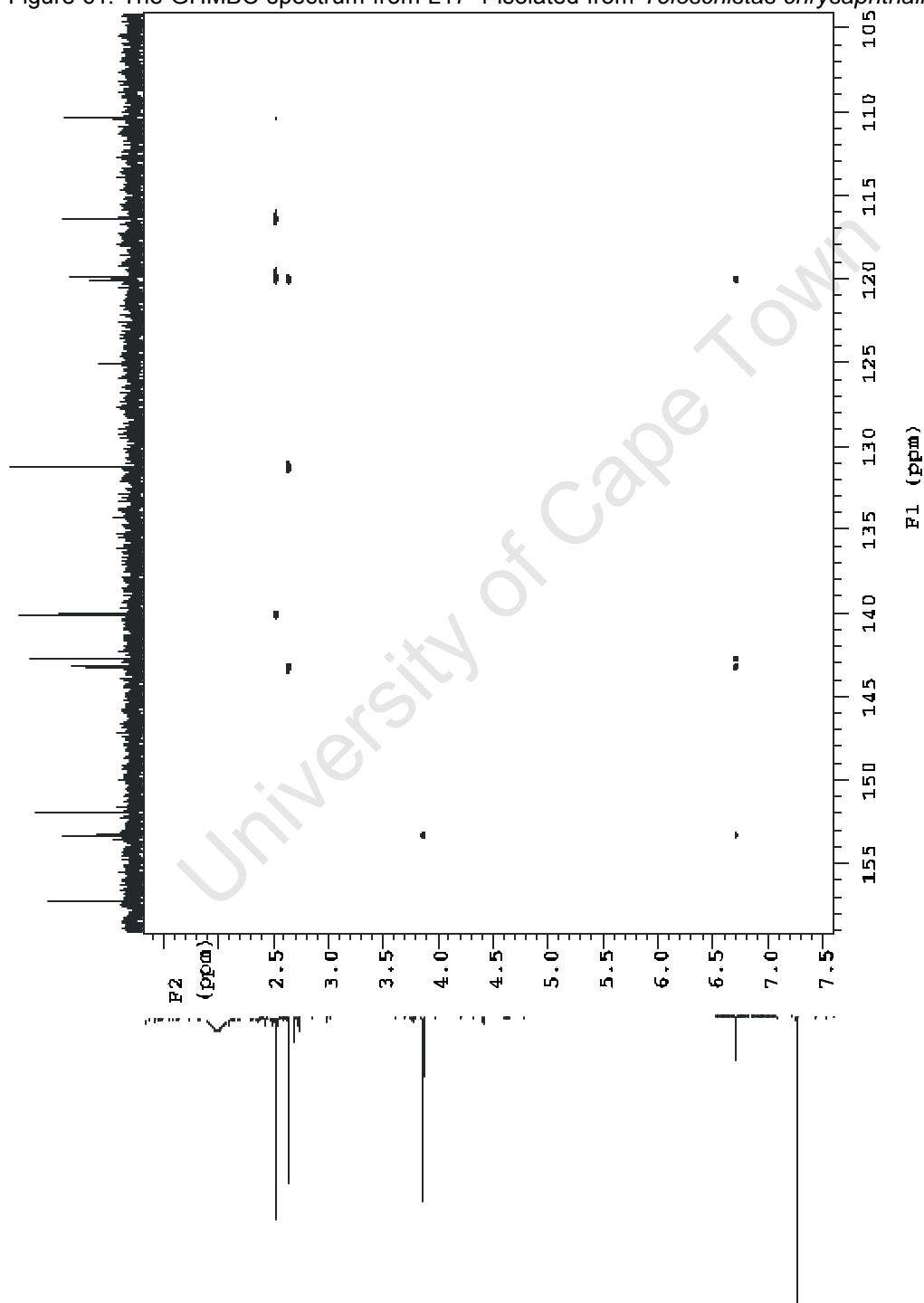


Figure 62: The GHMBC spectrum from L17- isolated from *Teloschistas chrysaphthalmum*

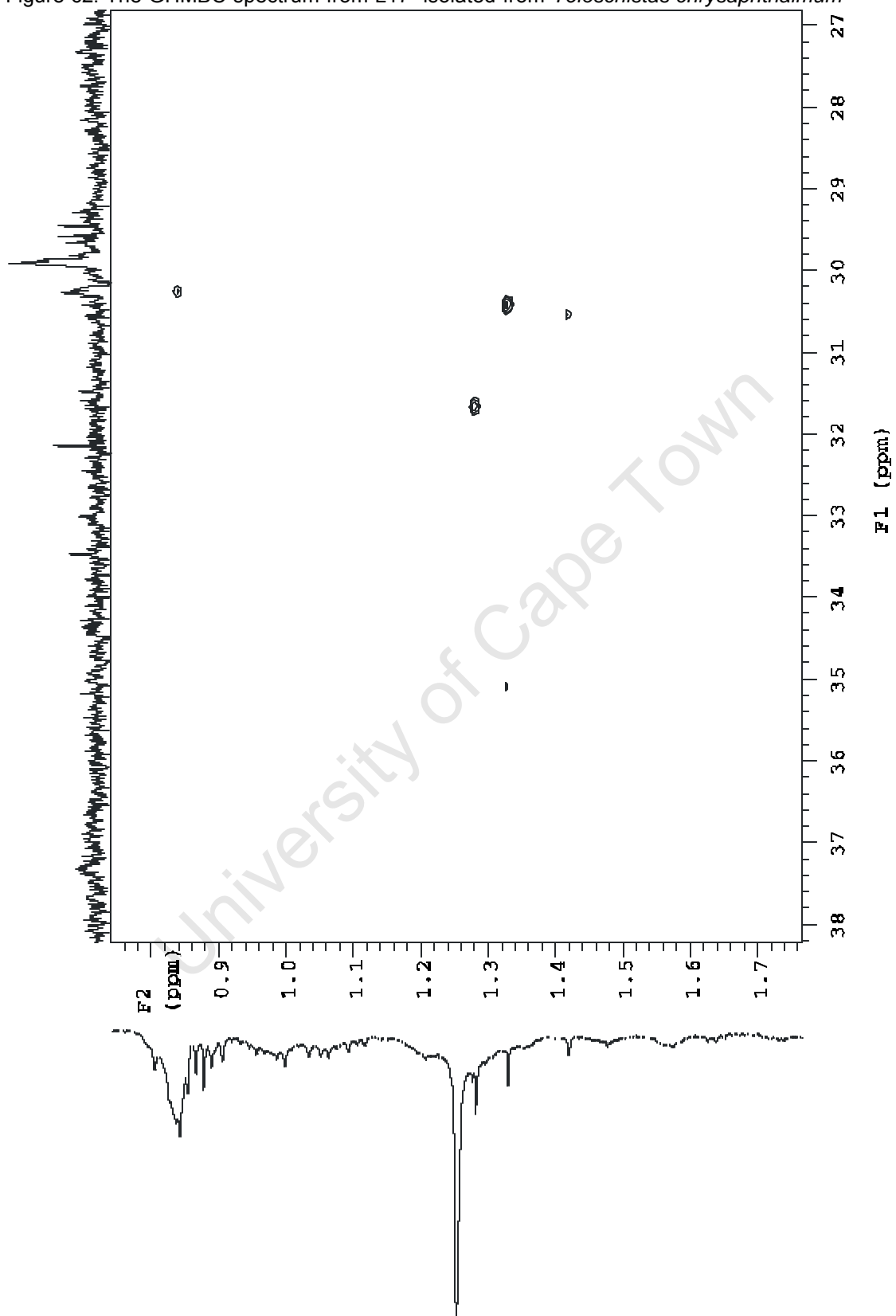


Figure 63: The GCOSY spectrum from L17-1 isolated from *Teloschistas chrysaphthalmum*

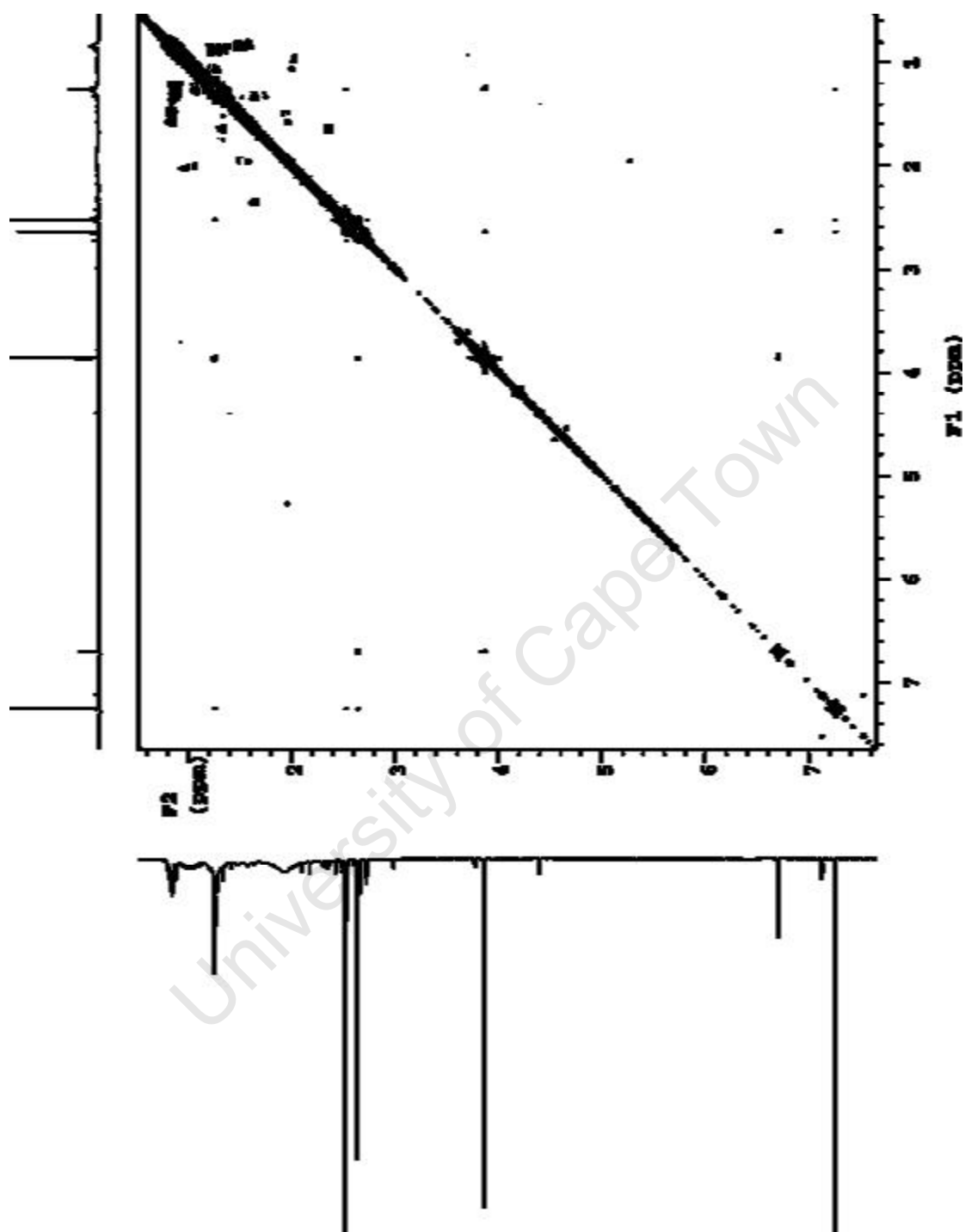


Figure 64: The GHSQC spectrum of L17-1 isolated from *Teloschistas chrysaphthalmum*

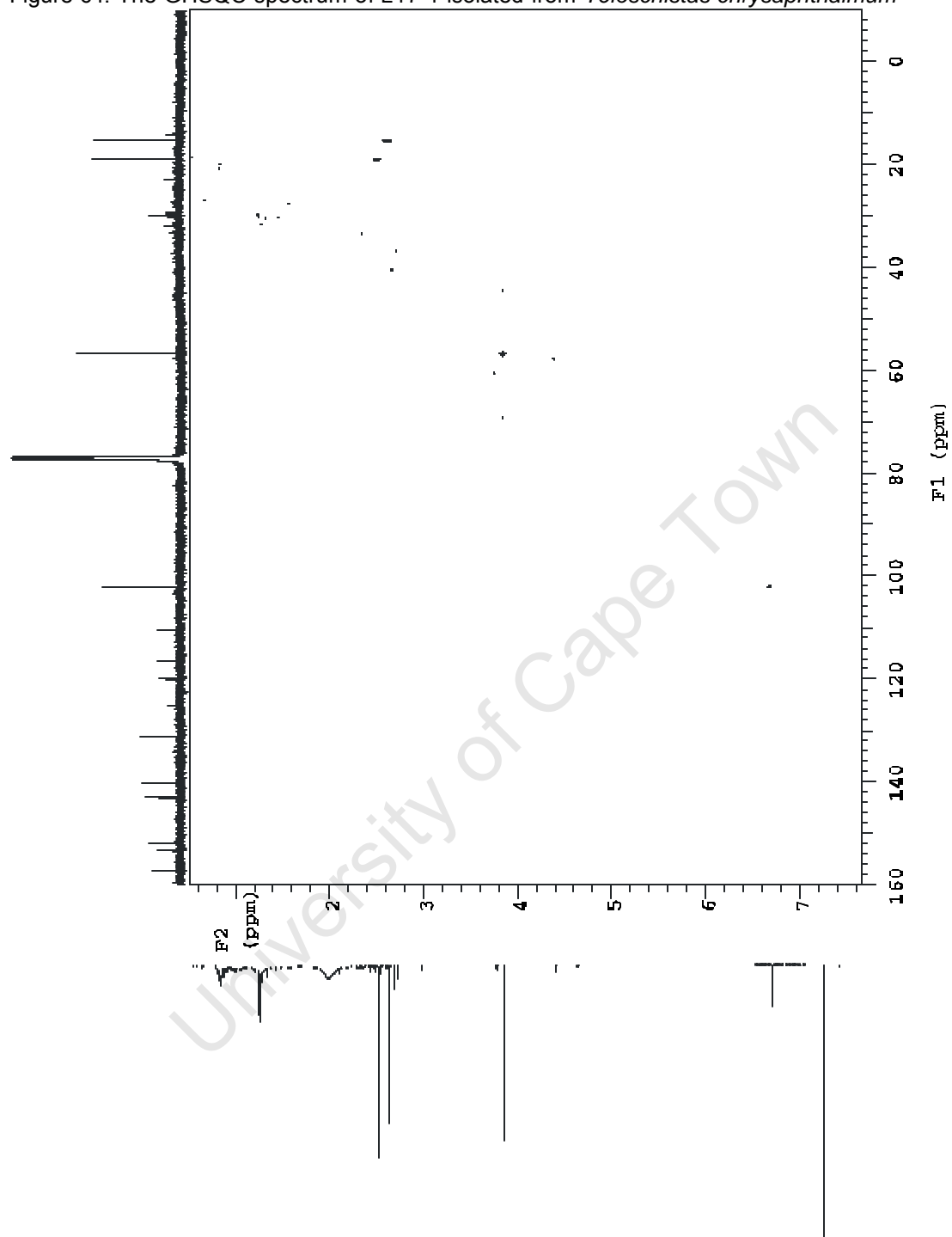


Figure 65: The DEPT spectrum of L17-1 isolated from *Teloschistas chrysaphthalmum*

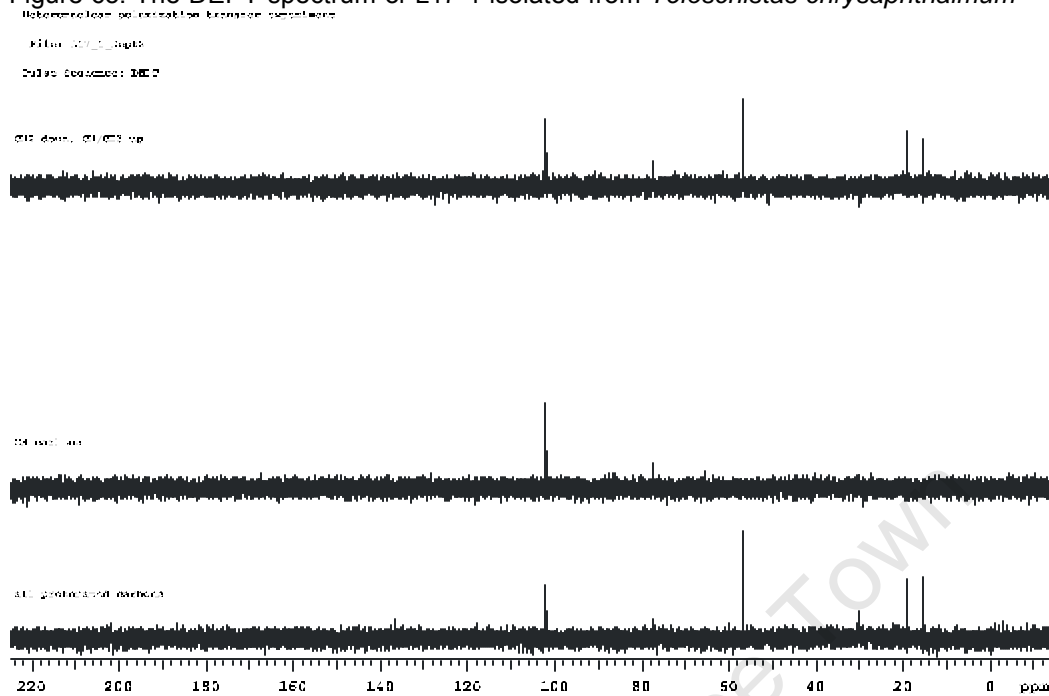


Figure 66: The ^1H NMR spectrum of L17-3 from *T. chrysophthalmum* obtained on a 900MHz instrument

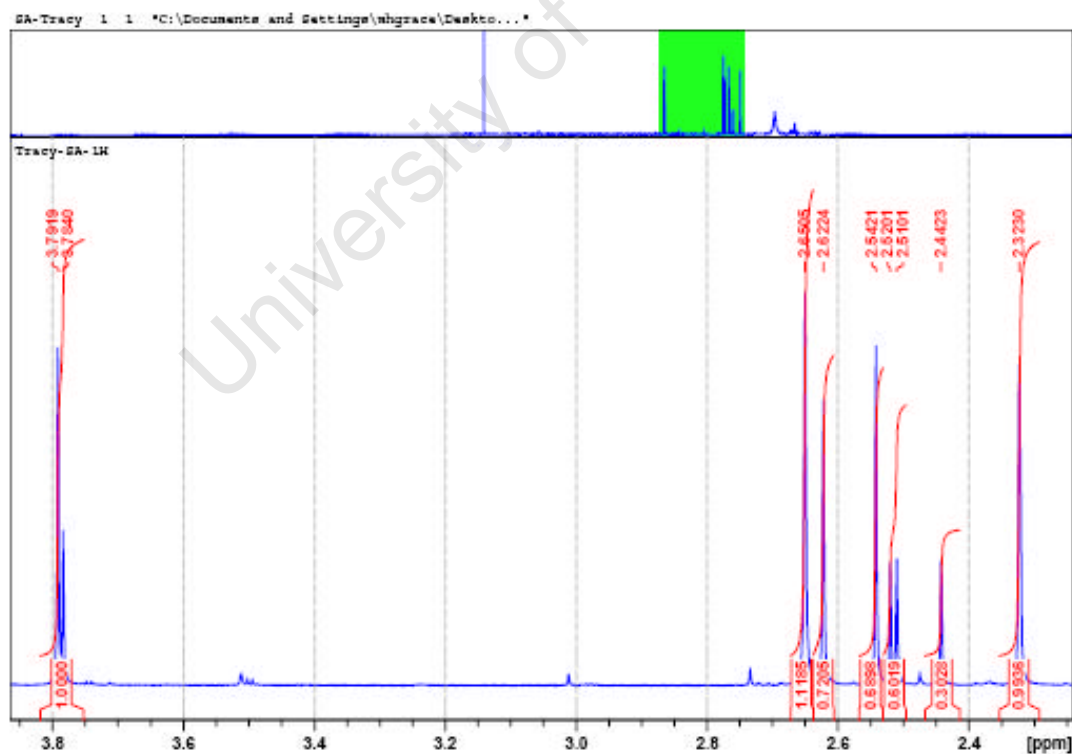


Figure 67: An expansion of the region from 2.25 to 2.7ppm on the ^1H NMR spectrum of L17-3 derived from *T. chrysophthalmum* obtained on a 900mHz instrument.

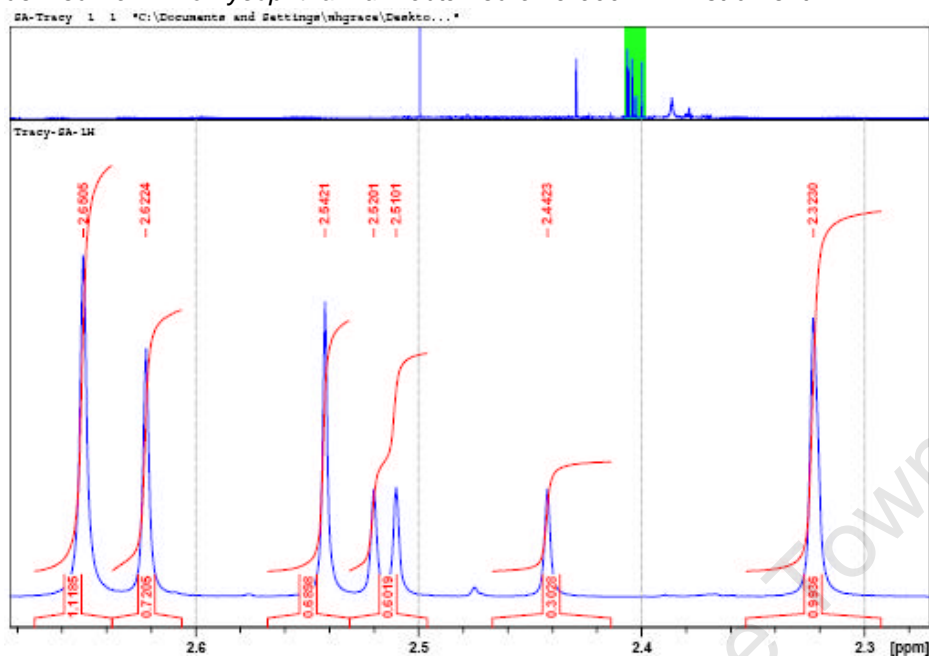


Figure 68: The ^{13}C spectrum of L17-3 derived from *T. chrysophthalmum*

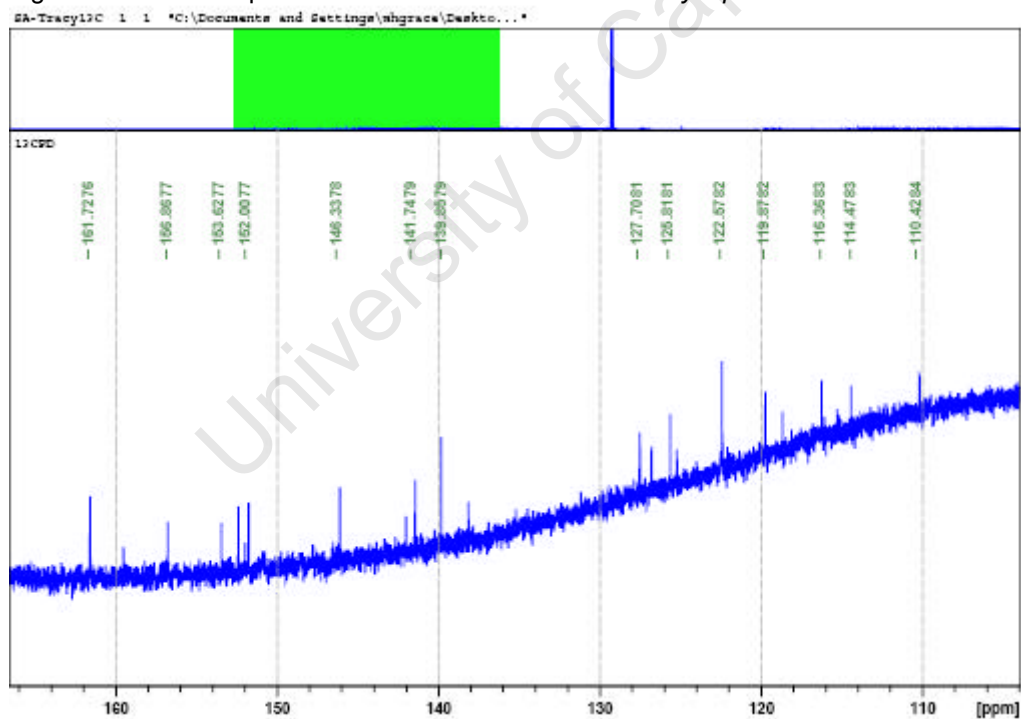


Figure 69: The ^{13}C spectrum of L17-3 derived from *T. chrysophthalmum*

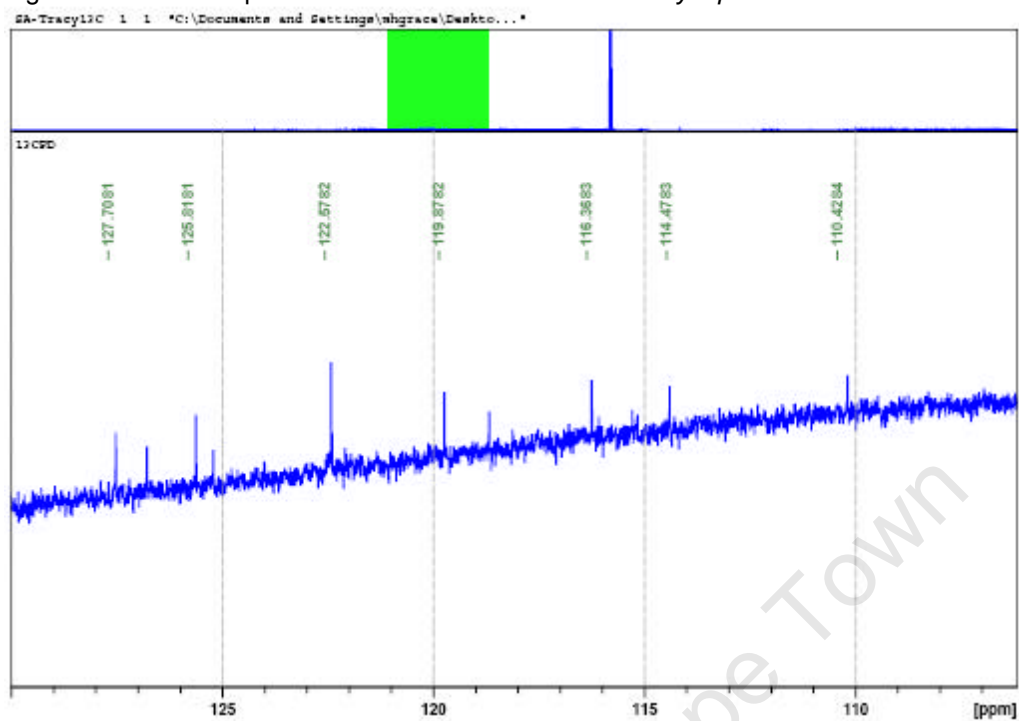


Figure 70: The ^{13}C spectrum of L17-3 derived from *T. chrysophthalmum*

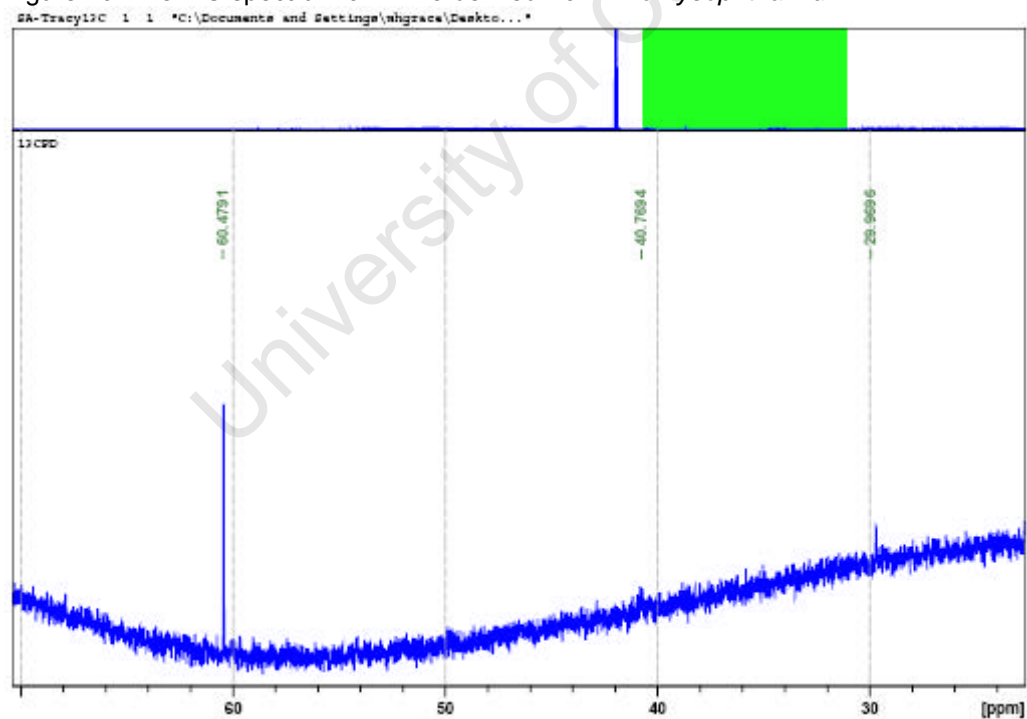


Figure 71: The ^{13}C spectrum of L17-3 derived from *T. chrysophthalmum*

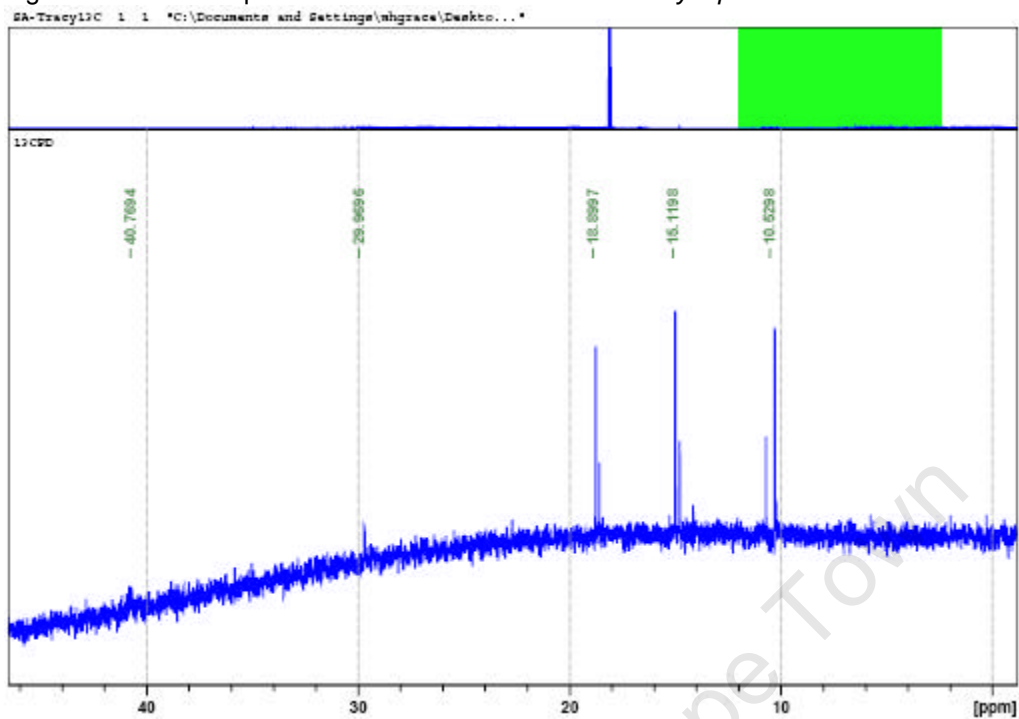


Figure 72: The GCOSY correlations of L17-3 derived from *T. chrysophthalmum*

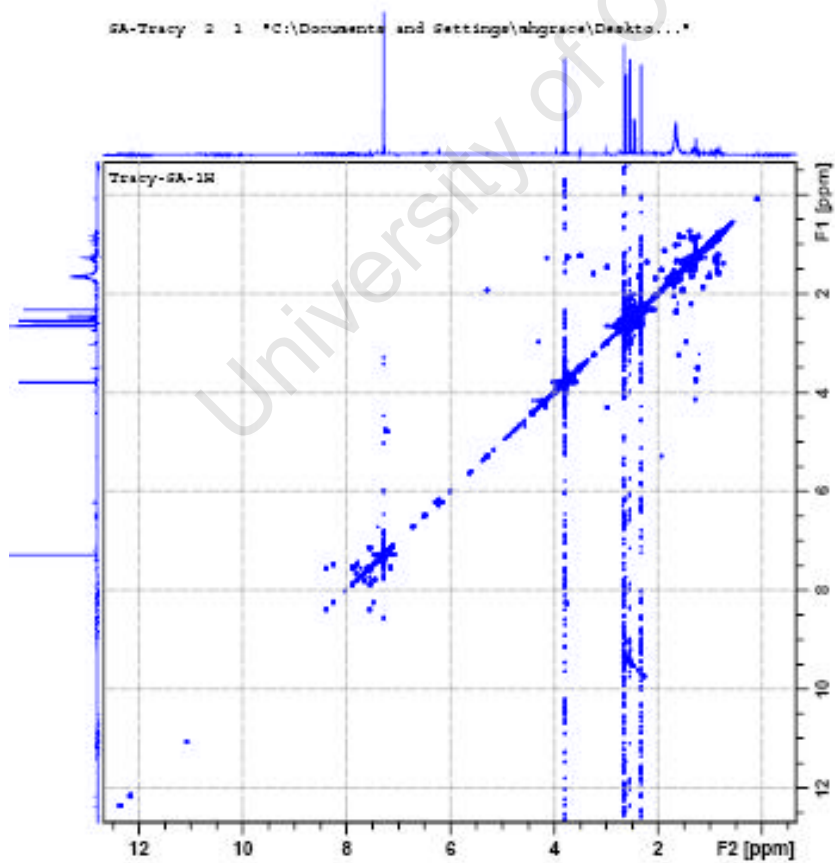


Figure 73: The GCOSY correlations of L17-3 derived from *T. chrysophthalmum*

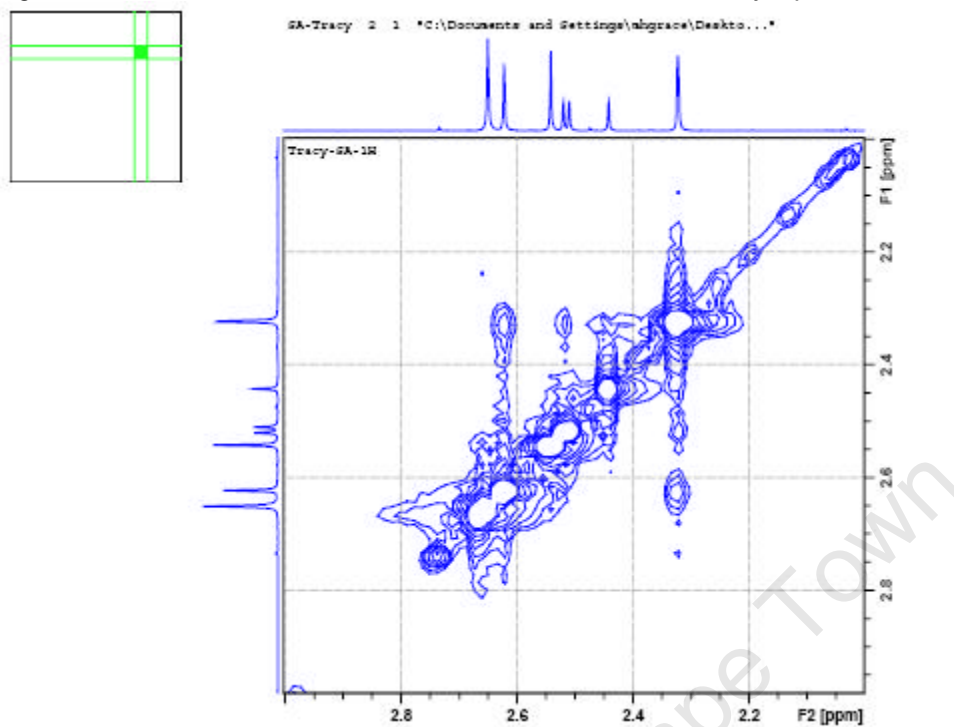


Figure 74: The GHMBC correlations of L17-3 derived from *T. chrysophthalmum*

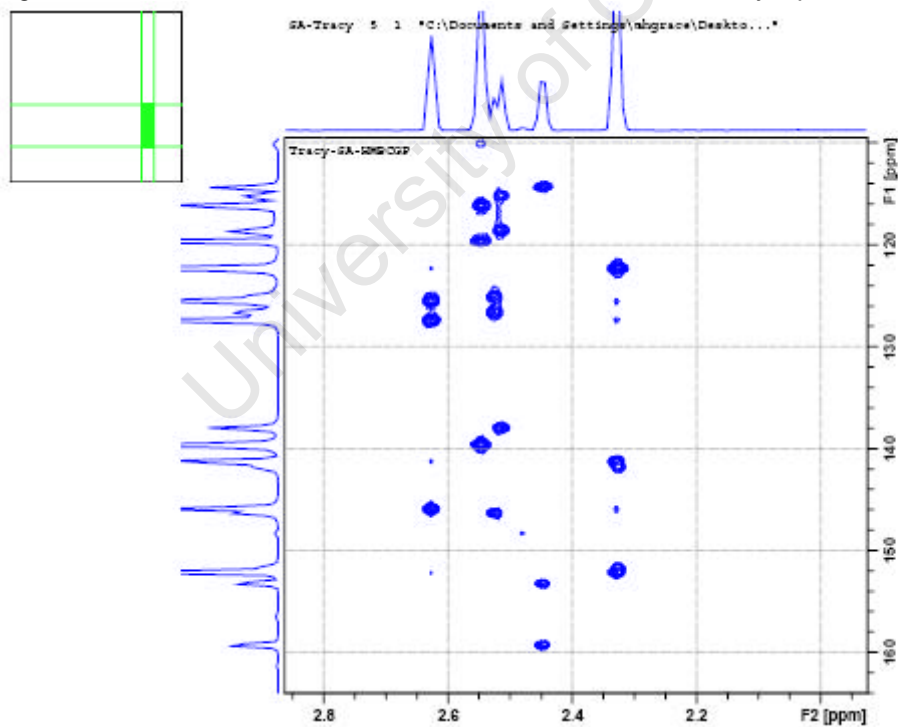


Figure 75: The GHMBC correlations of L17-3 derived from *T. chrysophthalmum*

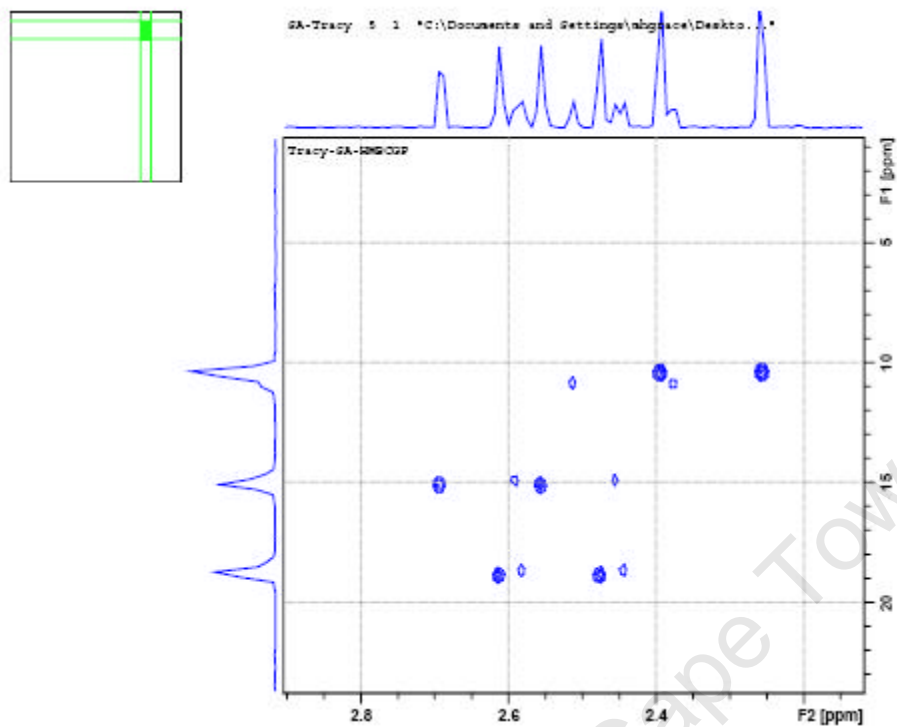


Figure 76: The GHMBC correlations of L17-3 derived from *T. chrysophthalmum*

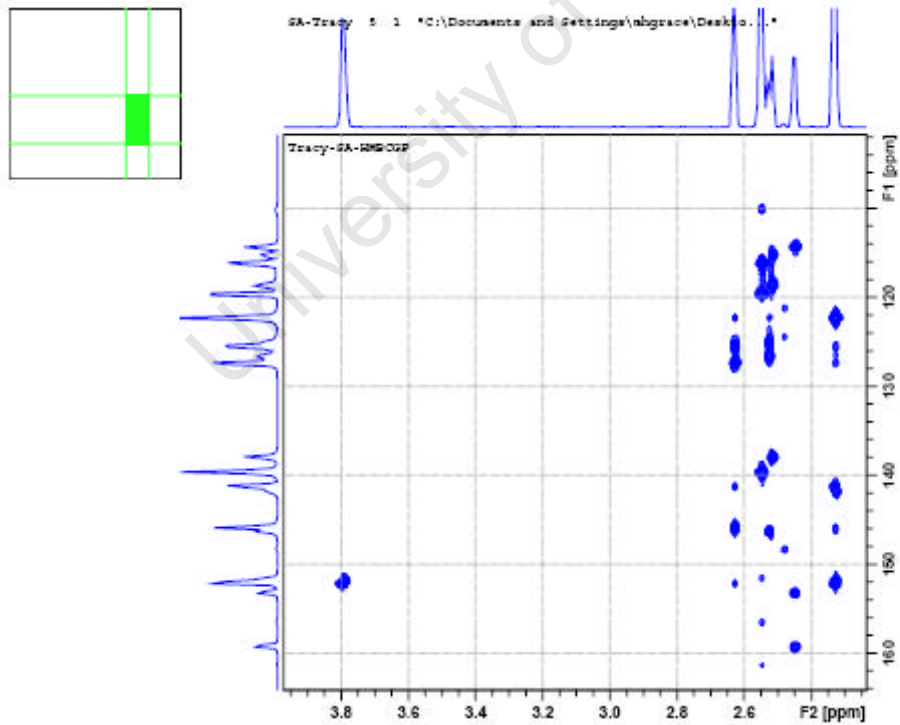


Figure 77: The GHMQC correlations of L17-3 derived from *T. chrysophthalmum*

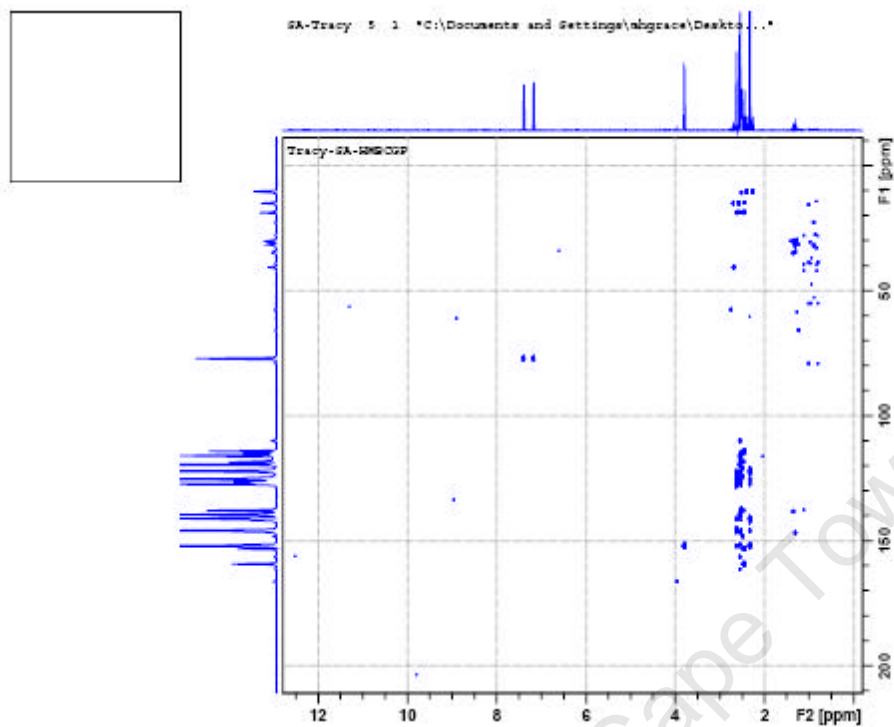


Figure 78: The GHMQC correlations of L17-3 derived from *T. chrysophthalmum*

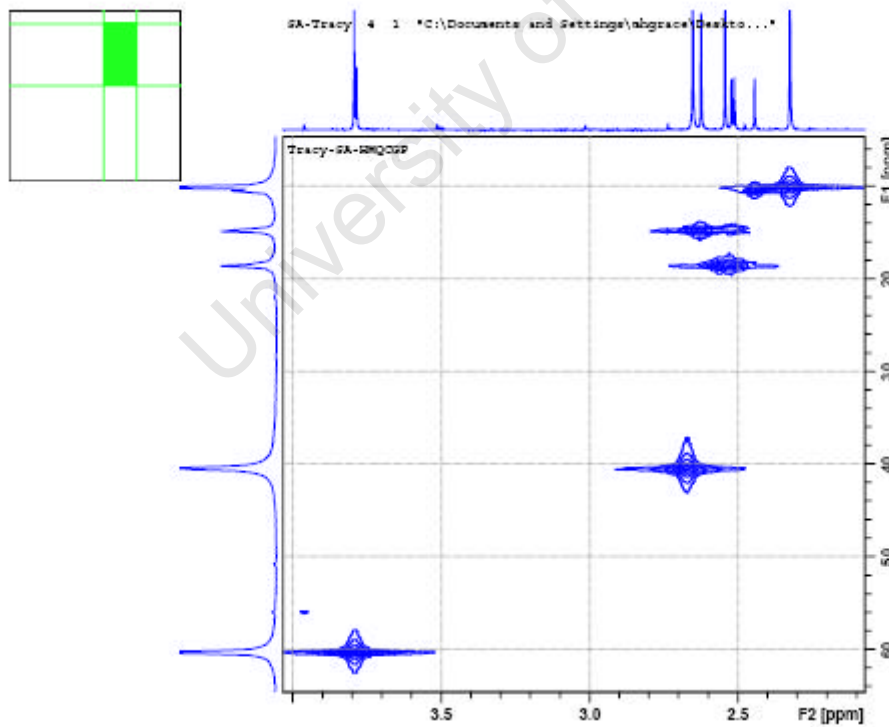


Figure 79: The DEPT spectra of L17-3 derived from *T. chrysophthalmum*
Heteronuclear polarization transfer experiment

File: home/vnmr1/vnmrdata/Data2009/March2009/T_Seaman/L17_3_DEPT.fid

Pulse Sequence: DEPT

CH3 carbons

CH2 carbons

CH carbons

all protonated carbons

220 200 180 160 140 120 100 80 60 40 20 0 ppm

***Warburgia salutaris* NMR**

Figure 80: The ^1H NMR spectrum of muzigadial isolated from the dichloromethane extract of the bark of *Warburgia salutaris*.

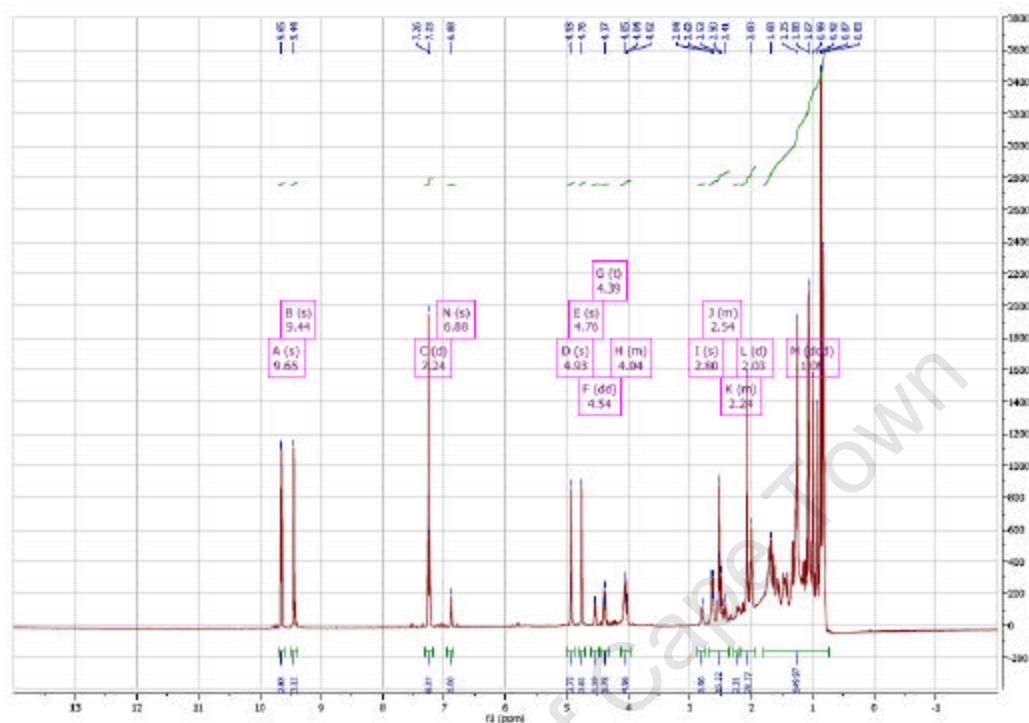


Figure 81: The ^{13}C spectrum of muzigadial isolated from the dichloromethane extract of the bark of *Warburgia salutaris*

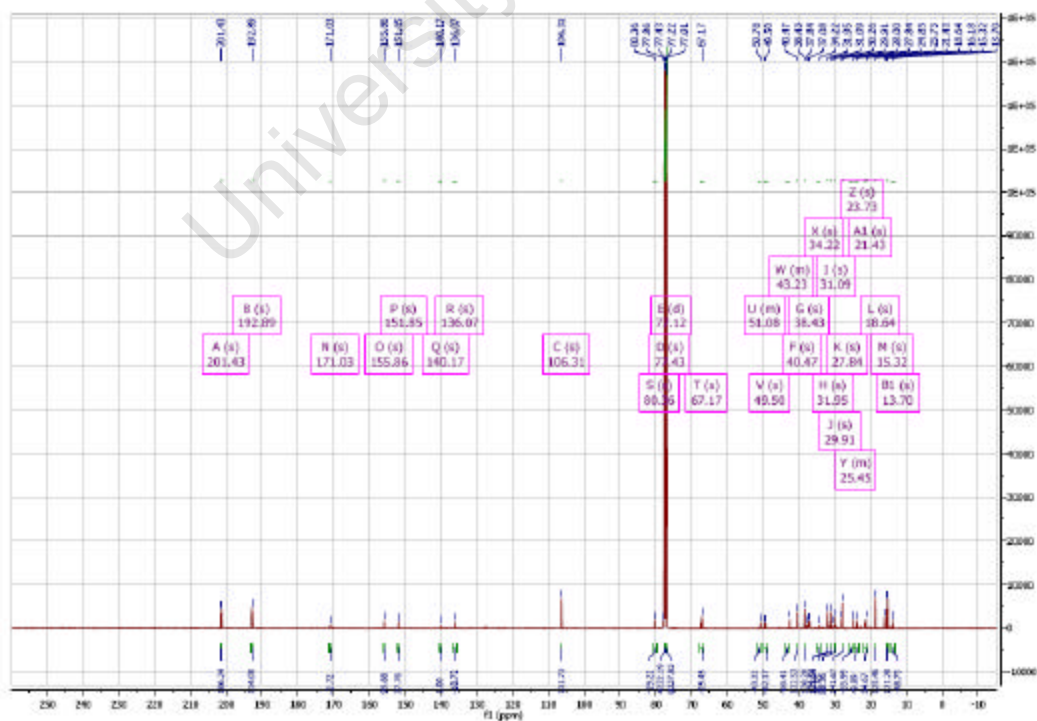


Figure 82: The ^1H NMR spectrum of warburganal isolated from the dichloromethane extract of the bark of *Warburgia salutaris*

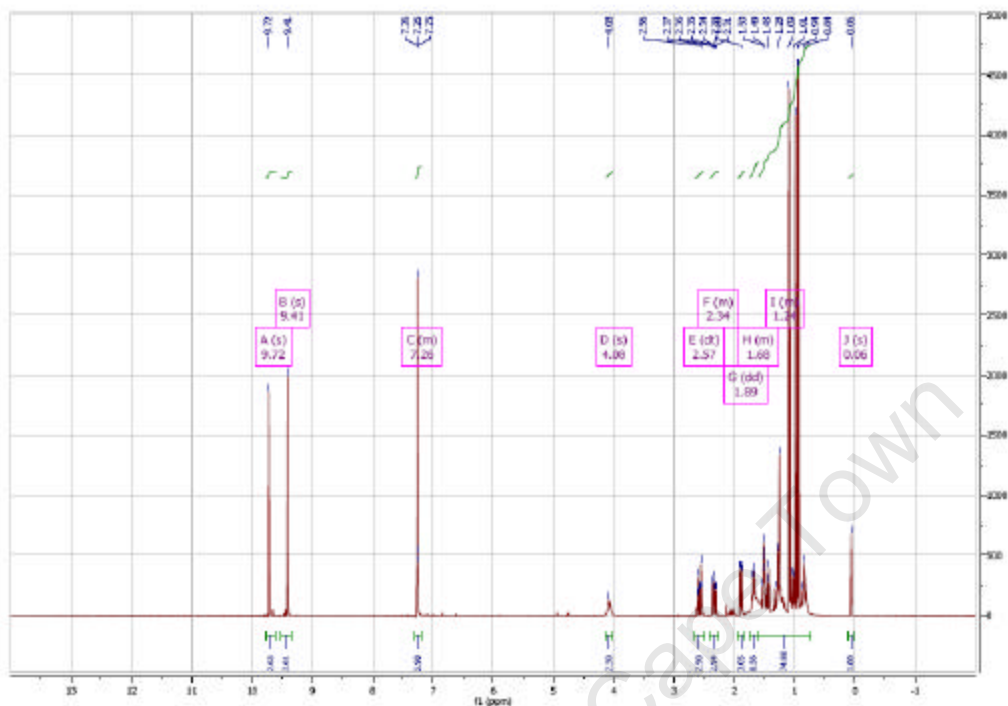


Figure 83: The ^{13}C NMR spectrum of warburganal isolated from the dichloromethane extract of the bark of *Warburgia salutaris*.



Figure 84: The ^1H NMR spectrum of ugandensidal isolated from the dichloromethane extract of the bark of *Warburgia salutaris*

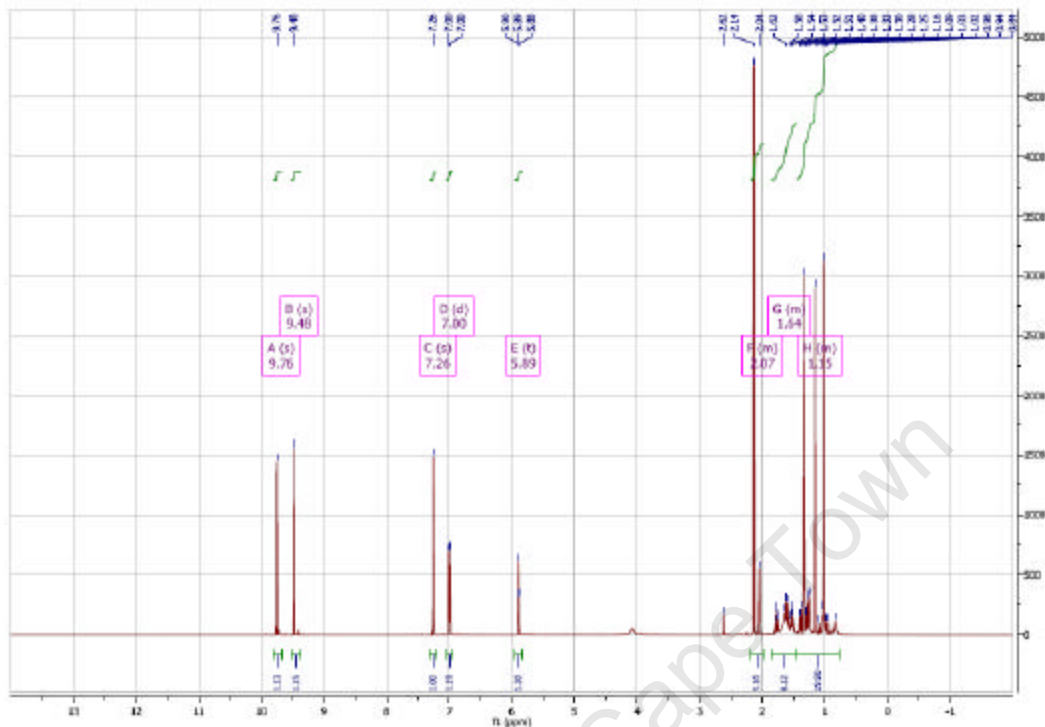


Figure 85: The ^{13}C NMR spectrum of ugandensidal isolated from the dichloromethane extract of the bark of *Warburgia salutaris*



D. In vivo bioavailability

Figure 86: The *in vivo* concentration of L17-1 in each of three mice after oral administration at 10mg/kg in combination with L17-3.

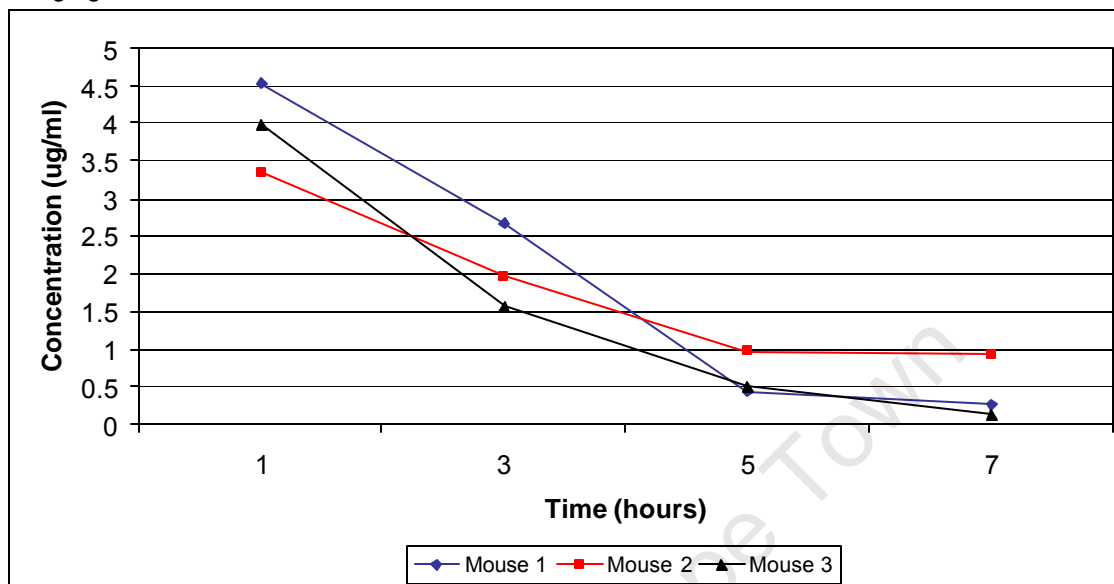


Figure 87: The *in vivo* concentration of L17-1 in each of three mice after subcutaneous administration at 10mg/kg in combination with L17-3.

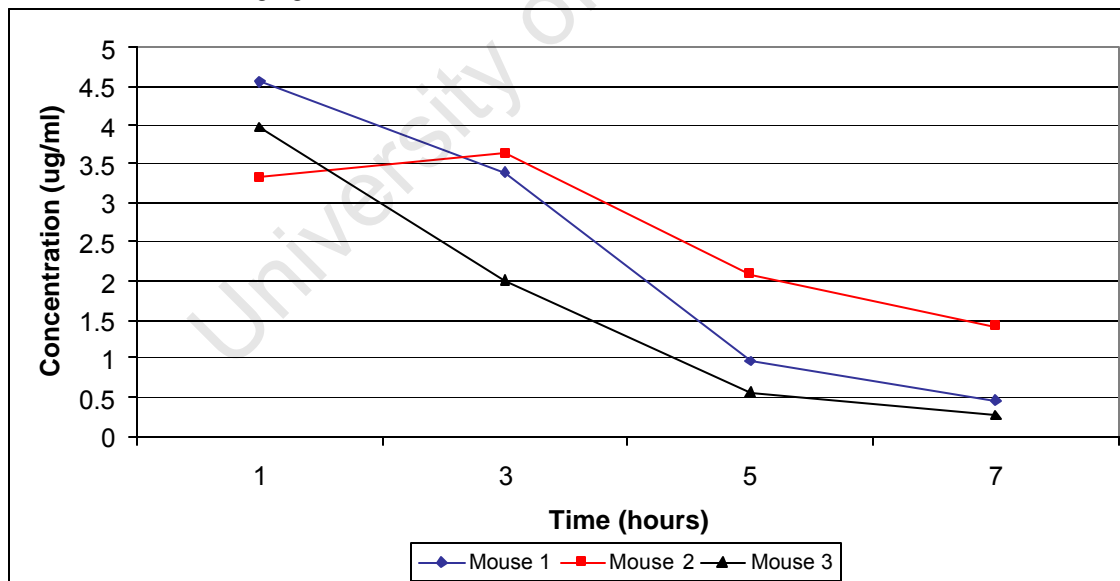


Figure 88: The *in vivo* concentration of L17-3 in each of three mice after oral administration at 10mg/kg in combination with L17-1.

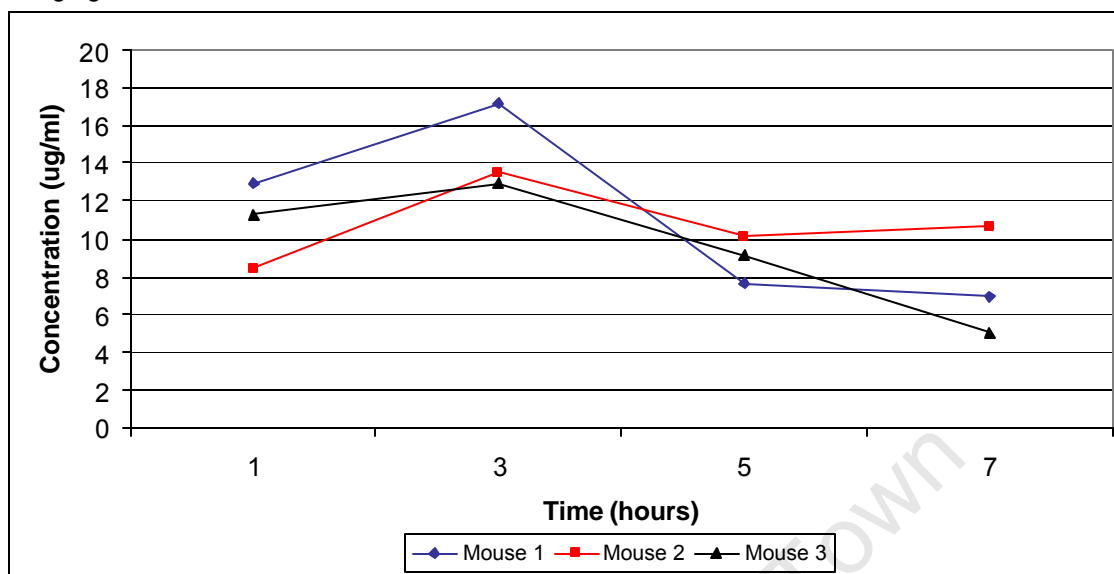


Figure 89: The *in vivo* concentration of L17-3 in each of three mice after subcutaneous administration at 10mg/kg in combination with L17-1.

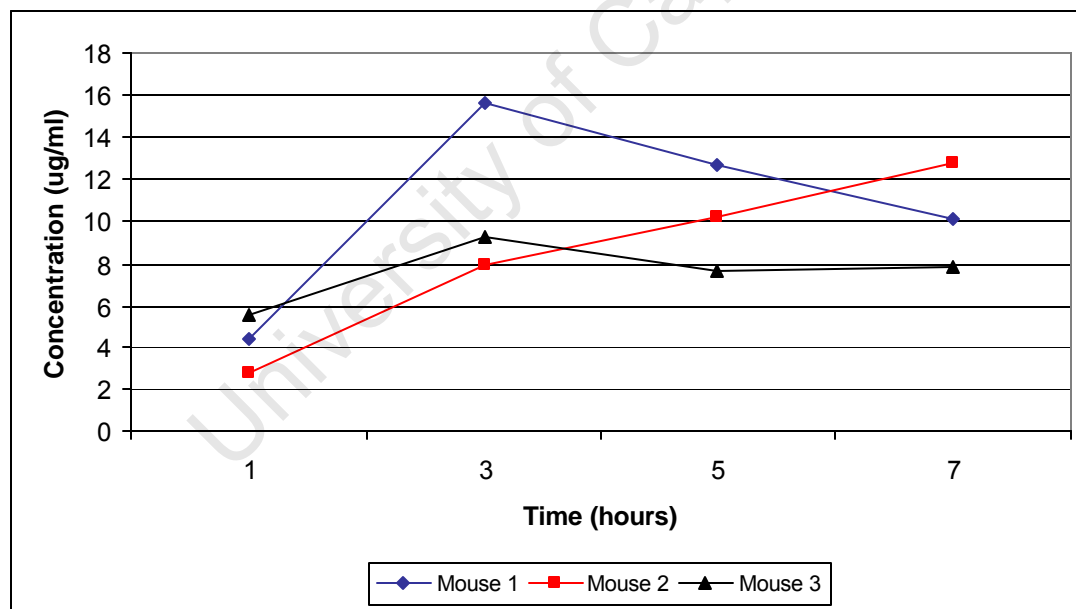


Table 37: The measured levels of L17-3 in five mice after oral administration at 5mg/kg. Values are in µg/ml. The LLOQ for L17-3 was determined to be 0.0244µg/ml.

Hours	Mouse 1	Mouse 2	Mouse 3	Mouse 4	Mouse 5	Ave	Std Dev
0	0	0	0	0	0	0	0
1	2.29	2.61	2.47	1.25	1.99	2.122	0.5397
3	2.85	3.02	3.22	N/A	3.26	3.0875	0.1900
5	2.3	1.82	2.37	1.57	2.82	2.176	0.4903
8	1.05	1.16	1.61	1.17	1.91	1.38	0.3658
12	0.625	0.458	0.975	0.794	0.992	0.7688	0.2293
24	0.00236	0	0.0288	0.0241	0.0151	0.014072	0.0128
48	0	0	0	0.00363	0	0.000726	0.0016
72	0	0	0	0	0	0	0
96	0	0	0	0	0	0	0

Abbreviations: N/A - not available; Std Dev – standard deviation; Ave - average

Table 38: The measured levels of L17-3 in five mice after subcutaneous administration at 5mg/kg. Values are in µg/ml. The LLOQ for L17-3 was determined to be 0.0244µg/ml.

Hours	Mouse 1	Mouse 2	Mouse 3	Mouse 4	Mouse 5	Ave	Std Dev
0	0	0	0	0	0	0	0
1	2.717	4.552	4.186	2.928	3.898	3.6562	0.7991
3	3.652	4.695	5.017	4.074	4.303	4.3482	0.5314
5	2.111	2.457	3.299	2.316	2.62	2.5606	0.4532
8	1.466	0.833	1.239	0.628	0.91	1.0152	0.3345
12	0.185	0.275	0.162	0.284	0.223	0.2258	0.0537
24	0.003	0	0.007	0.003	0	0.0043333	0.0023
48	0	0	0	0	0	0	0
72	0	0	0	0	0	0	0
96	0	0	0	0	0	0	0

Abbreviations: Std Dev – standard deviation; Ave - average

Table 39: The measured levels of L17-3 in five mice after intravenous administration at 5mg/kg. Values are in µg/ml. The LLOQ for L17-3 was determined to be 0.0244µg/ml.

Hours	Mouse 1	Mouse 2	Mouse 4	Mouse 5	Mouse 6	Ave	Std Dev
0	0	0	0	0	0	0	0
1	7.341	7.228	3.856	2.811	4.412	5.1296	2.0497857
3	7.452	4.515	5.191	5.856	7.081	6.019	1.2405142
5	4.139	4.817	5.222	5.927	4.838	4.9886	0.6536469
8	4.266	4.637	4.07	4.841	3.174	4.1976	0.6472544
12	1.827	1.663	1.671	2.409	1.446	1.8032	0.3647893
24	0.093	0	0.022	0.023	0.115	0.0506	0.0502125
48	0	0	0	0	0	0	0
72	0	0	0	0	0	0	0
96	0	0	0	0	0	0	0

Abbreviations: Std Dev – standard deviation; Ave - average

E. Lichen genetic sequences

Figure 90: The genetic sequence of *Xanthoria parietina* (L1)

```
CCGAGAGTGACGGACGCCCGCGGGCGCCGTCCCGGGGGCCCCGCCCGGAC
CTCTTCAACCCTGTGAATATTTGCCCTTGTGCTTCGGCGAGCGTCGAGG
CCTTTCGCGCCTCGGCCCGGCTCCGGCCGGTGAGCTCTCGCCCGAGGCC
CTCTCCATTGGCTCTACAGTGACGTCCGAGGATTTGCAATCAATATCAA
AACTTTCAACAACGGATCTCTTGGTTCTGGCATCGATGAAGAACGCAGCG
AAATGCGATAAGTAATGTGAATTGCAGAATTCAGTGAATCATCGAATCTT
TGAACGCACATTGCGCCCCCTGGTATTCCGGGGGGCATGCCTGTTGAGC
GTCATTGCAACCCTCAAGCTCTGCTTGGTATTGGGCGTTTCGTTCCAAGG
AGGCGCGCCCGCAAATCAGTGGCGGTCCAGGGAGACTTCAAGCGCAGTAG
AAACATTCCGCTATCGAGGTGTCGCCTGCGGCCNGGCCAGAAAACCCCA
AATCCAANNATNNACCTCGGNTCAGGTAGGGA
```

Figure 91: The genetic sequence of *Xanthoparmelia notata* (L8)

```
CTGAGAGAGGGGCTTCGTGCTCCCGGGGGTTTCGGCCCCCTGACTCTTAC
CCTTTGCGTACCTACCTTTGTTGCTTTGGCGGACCCGAGAATCCTCTCGC
GTGCACTCTTAGGCCGGCGAGTGTCCGTGAGAGGCCCA TTTAATTCTATT
CATTAGAGACGTCCGAGTCCACAATAACAATAAAAACTTTCAACAAC
GGATCTCTTGGTTCCAGCATCGATGAAGAACGCAGCGAAATGCGATAAGT
AATGTGAATTGCAGAATTCAGTGAATCATCGAATCTTTGAACGCACATTG
CGCCCCCTCGGCATTCCGGGGGGGCATGCCTGTTGAGCGTCATTGCACCCC
TCAAGCGTAGCTTGGTATTGGGCTCTCGCCCCCGCGGCGTGCCCGAAAAA
CAGTGGCGGTCCGGCGTGACTTTAAGCGTAGTAACATCTTCCCGCTCTGA
AGCACGCGTCGNGGCCNGGCCAAATAACCCCTATTTACTTCTATAANNNCCT
CGGATCAGGTAGGGA
```

Figure 92: The genetic sequence of *Xanthoparmelia semiviridis* (WC) (L11)

```
CCGAGAGAGGGGCTTGTACTCCCGGGGGCTTCGGCCCCCAACTCTTAC
CCTTTGCGTACCTACCTTTGTTGCTTTGGCGGACCCGGGAATTCTCCCGC
GCCGACCTTAGGCCTGCGAGTGTCCGTGAGAGGCCCATTCATTCTATTT
CTTAGTGATGTCCGAGTCCAAAAACACAATGATAAAAACTTTCAACAACG
GATCTCTTGGTTCCAGCATCGATGAAGAACGCAGCGAAATGCGATAAGTA
ATGTGAATTGCAGAATTCAGTGAATCATCGAATCTTTGAACGCACATTGC
GCCCCCTCGGCATTCCGGGGGGGCATGCCTGTTGAGCGTCATTGCACCCCT
CAAGCGCAGCTTGGTATTGGGCTCTCGCCCCCGTGCGGTGCCCGAAAAAC
AGTGGCGGTCCGGCGTGACTTTAAGCGTAGTAACATCTTCCCGCTCTAAA
GCTCTTGCCGNGGTCTGCCAGACAACCTCATTTACTTCTATAATNNACCT CG
GATCAGGTAGGGA
```

Figure 93: The genetic sequence of an unknown lichen species L14, possibly a *Parmotrema* sp.

```
ACTGAGAGAGGGGCTTCGCGCTCCCGGGGGCTTCGGCCCCCACTCTTAC
CCTGTGTGTACCTACCTTTGTTGCTTTGGCGGACCTCGGGGGTTCTCCTC
CGCGTCCGGCTTTCGGGTGATGAGCGTCCGTGAGGGGCCACTTACATTC
TGTTTATCAGTGTGCTCCGAGTATAAAATGAATAAATAAAAACTTTCAAC
AACGGATCTCTTGGTTCCAGCATCGATGAAGAACGCAGCGAAATGCGATA
AGTAATGTGAATTGCAGAATTCAGTGAATCATCGAATCTTTGAACGCACA
TTGCGCCCCCTCGGTATTCCGGGGGGGCATGCCTGTTGAGCGTCATTACAC
CTCTCAAGCTTCGCTTGGTATTGGGTCACTCGCCCCCGAGGCGTGCCCGA
AAAGCAGTGGCGGTCCGGCGTGACTTTAAGCGTAGTAATACCATCCCCG
CTTTGAAAGTTCCGCTTGTGGCTCGCCAGACAACCGTCATGTAGAAGGTT
TACCCGCTGTATGCTTCCAATATT
```

Figure 94: The genetic sequence of *Xanthoparmelia semiviridis* (EC) (L15)

```
CCGAGAGAGGGGCTTGTACTCCCGGGGCTTCGATCCCCAACTCTTCAC
CCTTTGCGTACCTACCTTTGTTGCTTTGGCGGACCCGGGAATCCTCTCGC
GCCGACCTTAGGCCTGCGAGCGTCCGTGAGAGGCCATTTAATCCTTTTT
ATTAGTGATGTCCGAGTCCAAACAATGATAAAAACTTTCAACAACGGATC
TCTTGTTCCAGCATCGATGAAGAACGCAGCGAAATGCGATAAGTAATGT
GAATTGCAGAATTCAGTGAATCATCGAATCTTTGAACGCACATTGCGCCC
CTCGGCATTCCGGGGGGCATGCCTGTTGAGCGTCATTGCACCCCTCAAG
CGCAGCTTGGTATTGGGCTCTCGTCCCCGTGGCGTGCCCGAAAAACAGTG
GCGGTCCGGCGTGACTTTGAGCGTAGTAACGTCTCCGCTCTAAAGCTCT
CGCTGTGTCCGGCCAAACAAACCTCATCTACTTCTATAANNNCCTCGGAT
CAGGTAGGGATAC
```

Figure 95: The genetic sequence of *Flavoparmelia soledicans* (L16)

```
CTGAGAGAGGGGCTTCGCGCTCCCGGGGCTTCGGCCCCCACTCTTCAC
CCCTTGTTACCGCTCCGCATTGCTTTGGCGGGCTTGGGCGCCCGTCAG
ATGCGCTTCTAAATCCTGTTTATCAGTGCCGTCCGAGTATCAACAAATA
TATAAAAACTTTCAACAACGGATCTCTTGGTTCAGCATCGATGAAGAAC
GCAGCGAAATGCGATAAGTAATGTGAATTGCAGAATTCAGTGAATCATCG
AATCTTTGAACGCACATTGCGCCCTCGGTATTCGGGGGGCATGCCTGT
TCGAGCGTCATTACACCCCTCAAGCGTAGCTTGGTATTGGGCCCTCGCCC
CCACGGCGTGCCCGGAAATCAGTGGCGGTCCGGCGTGACTTCGAGCGTAG
TAACTTATCCCGCTCTGAAACCCGCGTCAGGTGCGCCAGAACTTTATA
TGCTTCACTAATTGACCTCGGATCAGGTAGGGATAC
```

Figure 96: The genetic sequence of *Teloschistes chrysaphthalmum* (L17)

```
TCCGGCGCCACCGGAGGGTGACGCATCCTCACAGTGGCAAAGTGCTCGCG
GGTACAGGGCAAAGCAAACCCAGTATTTCTCTCGAGGANGAGGTATCCT
ATAAGGTATCCTCGGGGAAAGCTCACGAGAAATAAGGCATGACTCCGGCG
TCATCTTTAGAGATGGCGAACGCTCGTCAGTGGCCCGTAAACCTGTTGT
ACTAGTGCAGTCTGAGCTATAAAGCAAATTAATTAACCTTTCAACAACG
GATCTCTTGGTCTGGCATCGATGAAGAACGCAGCGAAATGCGATAAGTA
ATGTGAATTGCAGAATTCAGTGAATCATCGAATCTTTGAACGCATATTGC
GCCCTTGGTATTCCGAGGGGCATACCTGTTGAGCGTCATTACAACCT
CAAGCTTGTCTTGGTATTGAGCGTTCGCTCTTCCGTGCGAGGGAGTGGCG
TGCTTAAAAATAAGTGGCGGTCTCTGAGACTTCAAGCGCAGTAAAGCCG
TCGCTTCAGAAGCTTTTACCCGGGGATTAGCCATCGAAACCCTAATAT
CTCAANGANNNNCCTCGGATCAGGTAGGG
```

Figure 97: The genetic sequence of an unknown lichen (L18)

```
CTGAGAGAGGGGCTTGTGCTCCCGGGGTTTCGGCCCCCACTCTTAAC
CCTTTGCGTATCTACCTTTGTTGCTTTGGCGGACCCGAGAAACCTCTCGC
GCTGGCTCTTAGGTGCGTGAGCGTCCGTGAGAGGCCATTTCTTCTATT
GATCAGTGATGTCCGAGTTCAAACAATGAATAAAAACTTTCAACAACGGA
TCTCTTGGTTCAGCATCGATGAAGAACGCAGCGAAATGCGATAAGTAAT
GTGAATTGCAGAATTCAGTGAATCATCGAATCTTTGAACGCACATTGCGC
CCCTCGGTATTCCGGGGGGCATGCCTGTTGAGCGTCATTGCACCCCTCA
AGCGCAGCTTGGTATTGGGCTCTCGCCCCGTGGCGTGCCCGAAAAACAG
TGGCGGTCCGGCATGACTTTAAGCGTAGTAACATCTTCCGCTCTAAAGC
TCTCGCCGNGGCCGCAATNACCCTATATTTCTATAANNNCCTCGG
ATCAGGTAGGGA
```

Figure 98: The genetic sequence of *Thamnolia subuliforme* (L19)

ACAGAGATTGACCCCTTCAAGGGGTGGAACCTCCATCCCGTGTGAAGATT
ACCCGCTGTTGCTTCNNNNCTTTGTGCACCAATAGCATATCACAAAATTC
GTTGTAATTGTGACGTCTGAGTATACAAACAAAATAAACTTTCAACAAC
GGATCTCTTGTTCTGGCATCGATGAAGAACGCAGCGAAATGCGATAAGT
AATGCGAATTGCAGAATTCAGTGAATCATCGAATCTTTGAACGCACATTG
CACCTTCGGGCATTCCGGGAGGTATGCCTGTTGAGCGTCATTTACCTT
TCAAGCTTCTACTTTATGGCTTGGTCTTGGGCTGCCTGAATTTACAACAG
TCTCAAAATCAGTGGCAGTGGCAGCAGATCCCGAGCGTAGTGACACTTT
TTGCTCTGTTGATTTGTGCCGTGANGGCCAATAAGCTCCGTGTGCTTAGG
CACCCAACCTTCAANGANGNCCTCGGATCAGGTAGGGATNCNN

Figure 99: The genetic sequence of *Usnea rubrotincta* (L20)

CCGAGAGAGGGGCTTCGCGCTCCCGGGGGCTTCGGCCTCCACCTCTTCAC
CCATTGCGTACTTACCGTTGTTGCTTTGGCGAGCCATAGGGTCCGCCTAC
GCCGGCCTTGGGGCTGGTGAGCGCTCGTCAGGGGCCTTTCAAACTCTGT
TTTTAGTGACGTCCGAGTATAATAACAAATCGTAAAACTTTCAACAACGG
ATCTCTTGTTCCAGCATCGATGAAGAACGCAGCGAAATGCGATAAGTAA
TGTGAATTGCAGAATTCAGTGAATCATCGAATCTTTGAACGCACATTGCG
CCCCTCGGTATTCGGGGGGCATGCCTGTTGAGCGTCATTACACCCCTC
AAGCGTAGCTTGGTATTGGGTCTGCCCCCTTGGGTGTGCCCCAAAAGCAG
TGGCGGTCCGGAGCGACTTTGAGCGTAGTAAATTATCATCCCGCTTTGAA
AGATCGGCTTTGGGCTAGCCAGAAACCCCAATATTCTATAATNNACCTC
GGATCAGGTAGGGANNCC